

**COMBINED OZONE AND ULTRASOUND PROCESS FOR THE  
DESTRUCTION OF 1,4-DIOXANE IN CONTINUOUS  
FLOW REACTOR**

---

A Dissertation  
Submitted to  
the Temple University Graduate Board

---

In Partial Fulfillment  
of the Requirements for the Degree  
DOCTOR OF PHILOSOPHY

---

by  
Major Michael T. Dietrich, USAF, Biomedical Science Corps  
December 2016

Examining Committee Members:

Dr. Rominder Suri, Advisory Chair, Civil & Environmental Engineering  
Dr. Huichun (Judy) Zhang, Civil & Environmental Engineering  
Dr. Erica McKenzie, Civil & Environmental Engineering  
Dr. Parsaoran Hutapea, Mechanical Engineering

©  
Copyright  
2016

by

Michael Thomas Dietrich  
All Rights Reserved

## ABSTRACT

Clean water is essential to life. Growth in world population, changing diets, and a warming climate are driving an increase in the demand for water. Better management of water resources will help prevent scarcity, but in order to fully meet the future demand for safe, clean drinking water, new water treatment technologies are needed. This dissertation investigates a technology which is not well understood; the combination of ozone and ultrasound as potentially an efficient technology. Since nearly all previously published studies of combined ozone/ultrasound utilized batch reactors, a continuous flow reactor was constructed for this research. 1,4-Dioxane, henceforth referred to as dioxane, was chosen to evaluate the effectiveness of the combined ozone/ultrasound process. Dioxane is commonly detected in surface and groundwater and is a suspected human carcinogen. A recalcitrant contaminant, it resists direct oxidation by chlorine, oxygen, ozone, and biological treatment. It is miscible in water and doesn't sorb readily to organic matter, so it spreads rapidly in groundwater contamination plumes. It also resists air stripping and filtration, including reverse osmosis. For these reasons, dioxane makes an excellent candidate to measure the effectiveness of advanced oxidation processes, such as combined ozone/ultrasound. The treatment of dioxane by advanced oxidation processes has been studied extensively in the past. However, only one study has been published using combined ozone/ultrasound, and it was done in a batch reactor operating at a high ultrasonic frequency. The reactor built for this study also permitted reactor pressurization effects to be studied in a manner that has not been reported before for the combined ozone/ultrasound process.

In this study, the combination of ozone and ultrasound was found to cause synergistic removal of dioxane from drinking water; the removal achieved by the combination significantly exceeded the sum of the removal achieved by ozone and ultrasound separately. In fact, the combination of ozone and ultrasound was found to remove more than double the dioxane that would be removed by doing both treatment processes separately. Ultrasound (20 kHz) was ineffective in removing dioxane alone, achieving less than 20% removal. At 16 mg/L, ozone alone was found to achieve removal of up to 86% after a 16 minute treatment time, but appears sensitive to matrix effects, especially pH. When ultrasound was combined with just 1.2 mg/L of aqueous ozone, over 90% removal occurred after a 16 minute treatment. Removal of dioxane was found to be driven not by ozone itself, but by radicals, suggesting that the decomposition of ozone is responsible for the generation of radical species and subsequent removal of dioxane. Ultrasound was found to increase the decomposition of ozone and appeared to be driving increased mass transfer of ozone into the aqueous phase. Modest reactor pressure appears to aid dioxane removal, but further increases in pressure did not appear to further enhance removal.

An empirical model was constructed using a form similar to the Chick & Watson model for disinfection. Given inputs of initial aqueous ozone concentration, initial dioxane concentration, treatment time, and ultrasonic power, the model is able to predict effluent concentrations of dioxane with a relative root mean squared error of less than 5%. Additionally,  $R_{CT}$  and mass balance analyses were performed, and both analysis techniques suggested that the removal of dioxane is dependent on the consumption of aqueous ozone.

Spiked drinking water is representative of water that has undergone conventional treatment but requires a polishing step, and the combined ozone/ultrasound has shown promise as a polishing technology. Owing to its recalcitrance, prevalence, and mobility, dioxane represents a real and challenging groundwater contaminant, and combined ozone/ultrasound has shown promise as a groundwater treatment option. Additionally, the process is capable of dioxane removal in a pH range of 4-10. This pH independence, coupled with its ability to degrade recalcitrant contaminants, suggests that combined ozone/ultrasound holds promise as an industrial wastewater treatment option, too. The removal achieved by both ozone and combined ozone/ultrasound was an order of magnitude greater than what has been reported in previously published reports. However, a comparison of cost effectiveness relative to other advanced oxidation processes remains an area for future study. Finally, the combined ozone/ultrasound process holds promise as a drinking water treatment option in remote areas, since it requires only electricity. As a promising technology for polishing water for reuse, treating contaminated groundwater, treating industrial wastewater, and potentially improving access to safe drinking water in remote areas, combined ozone/ultrasound could aid in meeting global water demand in the future.

## ACKNOWLEDGEMENTS

I'd like to thank Dr. Rominder Suri, my advisor, for his guidance during my three years at Temple. When I met Dr. Suri and he showed me the Water and Environmental Technology (WET) Center, I knew that Temple was the school that I wanted to attend. I was immediately impressed by the wealth of experimental and analytical capabilities of the center as well as the wealth of experience of the researchers that I met. I have learned a great deal under his tutelage and these past years have been the best of my Air Force career to date.

I'd also like to thank my committee members for their wisdom and guidance throughout my dissertation process. I came to Temple with a mechanical engineering background, but little experience in water treatment research. However, in your courses, as well as those taught by your peers in the department, I learned the science behind water treatment. The physical, chemical and biological principles that I was taught in your classrooms gave me the tools necessary to pass my preliminary exam in time to meet the aggressive timeline that the Air Force had set for me. More importantly, the didactic courses gave me the understanding necessary to design the experiments, select and set up the instrumentation, and process, analyze, and interpret the results; the very tools needed to conduct the research contained herein.

I would also like to thank my fellow students in the Civil and Environmental Engineering Department, especially those who were a part of the WET Center. You

made me feel welcome from day one, and were always willing to lend a hand, share your experience, or teach me new things.

I'd like to thank Dr. Gangadhar Andaluri and Dr. Ryan Smith, fellow researchers at the WET Center. These two not only helped keep the analytical instruments in good working order, but as relatively recent PhD graduates themselves, they also gave me valuable mentorship me as I navigated this process.

I would like to thank the United States Air Force for selecting me for the Air Force Institute of Technology (AFIT) Civilian Institution Program (CIP). My time in the AFIT CIP has been an excellent opportunity to advance my education, gain valuable research experience, and learn new analytical techniques. I hope to apply what I have learned at Temple to protect the health of US servicewomen and servicemen as a Bioenvironmental Engineer.

I'd like to thank my parents, Tom and Kathy, for the lifetime of love and support they've given me. From a very early age, they instilled in me the importance of education and hard work, and most importantly, they showed me how a loving marriage should work and how parents can fill up a home with love.

I'd like to thank my son, John, for opening up a part of my heart that I hadn't even known was there. As I was finishing this dissertation, John arrived as an 8 pounds, 15 ounce bundle of love. He gives me a dose of joy and instant perspective whenever I look at him.

Lastly, I would like to thank my amazing wife, Jennifer, for her support, patience, and assistance throughout my time at Temple. In research, things are bound to go wrong

from time to time, chromatographs fail, ozone generators break, software crashes just before you click the save button; but every time I had a rough day, she was there to pick me up. She was also there to celebrate with me when things went right: when finals went well, when data matched the hypothesis, or when new instrumentation was brought online successfully. I could not have made it this far without her love and support.

***Disclaimer:***

*The views expressed in this article are those of the author and do not necessarily reflect the official policy or position of Temple University, the National Science Foundation, the Air Force, the Department of Defense or the U.S. Government.*

*This research was partially supported by the Water & Environmental Technology (WET) Center at Temple University, a National Science Foundation (NSF) Industry and University Cooperative Research Center (IUCRC).*

# TABLE OF CONTENTS

	Page
ABSTRACT.....	iii
ACKNOWLEDGEMENTS.....	vi
LIST OF TABLES.....	xiii
LIST OF FIGURES.....	xiv
LIST OF EQUATIONS.....	xvii
CHAPTERS	
1. INTRODUCTION.....	1
1.1. Background.....	1
1.1.1. Water Demand.....	1
1.1.2. 1,4-Dioxane.....	10
1.2. Literature Review.....	13
1.2.1. Treatment Technologies.....	13
1.2.2. 1,4-Dioxane Reaction Mechanism.....	27
1.2.3. Toxicity.....	29
1.3. Research Gap.....	31
2. PROBLEM STATEMENT.....	32
2.1. Goals and Objectives.....	32

2.2.	Significance.....	33
3.	EXPERIMENTAL .....	35
3.1.	Materials and Reagents .....	35
3.2.	Experimental Design.....	37
3.2.1.	Objective 1: Effects of Ozone Dose and Residence Time .....	37
3.2.2.	Objective 2: Effect of Pressure.....	39
3.2.3.	Objective 3: Effect of Ultrasonic Intensity .....	40
3.2.4.	Objective 4: Effect of Initial pH.....	40
3.2.5.	Objective 5: Effect of Radical Scavenging .....	41
3.2.6.	Objective 6: Reactor Modeling .....	42
3.3.	Data Collection .....	42
3.4.	Analytical Methods.....	47
3.4.1.	pH.....	47
3.4.2.	Conductivity .....	47
3.4.3.	Aqueous Ozone Concentration.....	47
3.4.4.	Gaseous Ozone Concentration .....	47
3.4.5.	TIC/TOC Concentration.....	48
3.4.6.	Temperature .....	48
3.4.7.	Reactor Pressure.....	48
3.4.8.	Water Flow Rate.....	48
3.4.9.	Gaseous Flow Rate.....	48

3.4.10. 1,4-Dioxane Concentration .....	48
4. RESULTS .....	51
4.1. Objective 1: Effect of Ozone Dose and Residence Time .....	51
4.1.1. Implications of Ozone Dose and Residence Time .....	60
4.2. Objective 2: Effect of Pressure .....	61
4.2.1. Constant Air Phase Ozone Dosage.....	61
4.2.2. Constant Aqueous Phase Ozone Dosage.....	68
4.2.3. Implications of Pressure Results .....	73
4.3. Objective 3: Effect of Initial pH .....	76
4.3.1. Implications of Initial pH Results .....	80
4.4. Objective 4: Effect of Ultrasonic Intensity .....	80
4.4.1. Implications of Ultrasonic Intensity Results .....	82
4.5. Objective 5: Effect of Scavenging .....	83
4.5.1. Implications of Scavenging Results .....	89
4.6. Objective 6: Reactor Modeling.....	91
4.6.1. Tracer Study .....	91
4.6.2. Development of Predictive Model .....	93
4.6.3. $R_{CT}$ Analysis .....	105
4.6.4. Mass Balance Analysis.....	109
4.6.5. Implications of Modeling Results .....	113
5. KEY CONTRIBUTIONS AND FUTURE WORK.....	114

5.1.	Key Contributions .....	114
5.2.	Future Work .....	115
5.2.1.	AOP Comparison .....	115
5.2.2.	Byproducts/Toxicity .....	127
5.2.3.	Additional Contaminants.....	128
5.2.4.	Model Refinement/Scalability.....	129
6.	CONCLUSION .....	131
	BIBLIOGRAPHY .....	136
	APPENDICES .....	158
A.	ARDUINO SKETCH.....	158
B.	GNUPLOT SCRIPT FOR 3D PLOTS .....	167
C.	THERMISTOR MANUFACTURER’S DATA.....	168
D.	PRESSURE TRANSDUCER MANUFACTURER’S DATA .....	169
E.	EXPERIMENTAL DATA .....	170
F.	RAW DATA FROM ARDUINO DATA COLLECTION DEVICE .....	184

## LIST OF TABLES

Table 3-1 Drinking Water Characteristics .....	35
Table 4-1 1,4-Dioxane Removal Pseudo-1st Order Rate Constants.....	53
Table 4-2 pH and Rate Constants for 2.5mg/L Ozone Dose .....	79
Table 4-3 Dispersion Characteristics of Continuous Flow Reactor.....	93
Table 4-4 Root Mean Squared Error Analysis of Model.....	102
Table 4-5 Applicability of Model to Pilot Scale Ozonation Study.....	104
Table 5-1 AOP Rate Constant Comparison .....	126
Table E1 Effects of Ozone Dose, Treatment Time, and Ultrasound Intensity .....	170
Table E2 Calibration Standards .....	174
Table E3 Effects of Reactor Pressure .....	175
Table E4 Effects of Matrix .....	176
Table E5 Ozone Concentration and Partial Pressure .....	177
Table E6 Effects of Mixing Zone .....	178
Table E7 Effect of pH.....	179
Table E8 Pressure/Flow/Ozone Concentration Data .....	180
Table E9 AOP Comparison Data.....	182
Table E10 Mass Balance Analysis.....	183

## LIST OF FIGURES

Figure 1-1 Delaware and Schuylkill River Watersheds.....	7
Figure 1-2 Acoustic Cavitation.....	22
Figure 3-1 Experimental Schematic.....	37
Figure 3-2 Experimental Data Monitor.....	43
Figure 3-3 Thermistor Circuit Diagram.....	45
Figure 3-4 GC/MS Calibration Curves.....	50
Figure 4-1 1,4-Dioxane Removal vs Ozone Dose.....	51
Figure 4-2 1,4-Dioxane Removal after A.) 2.5, B.) 5, C.) 7.2, and D.) 16 Minutes.....	52
Figure 4-3 1,4-Dioxane Removal Pseudo-1st Order Curves.....	53
Figure 4-4 1,4-Dioxane Removal By Location.....	57
Figure 4-5 Effect of Static Mixer.....	58
Figure 4-6 Aqueous Dose Pressure Response for Constant Air Phase Dose.....	62
Figure 4-7 Mass Transfer Pressurization Effects for Ozone System.....	63
Figure 4-8 Mass Transfer Pressurization Effects for Ozone/Ultrasound System.....	64
Figure 4-9 Pressure Effects on $[O_3]_{air}$ and $[O_3]_{aq}$ for A.) Ozone and B.) Ozone/US.....	66
Figure 4-10 Effect of Pressure on 1,4-Dioxane Removal ( $[O_3]_{air}=10$ mg/L).....	67
Figure 4-11 Confirmation of Henry's Constant.....	69
Figure 4-12 Ozone Weight Percentage and Reactor Pressures.....	70
Figure 4-13 Effect of System Pressurization.....	71
Figure 4-14 Influence of Initial pH.....	76
Figure 4-15 Influence of pH on Ozone System.....	77

Figure 4-16 Influence of pH on Combined Ozone/Ultrasound System.....	78
Figure 4-17 Influence of pH on Ultrasound System.....	79
Figure 4-18 Effect of Ultrasonic Intensity .....	81
Figure 4-19 Removal vs Ultrasonic Power.....	82
Figure 4-20 Effect of Added Scavenger on 1,4-Dioxane Removal.....	84
Figure 4-21 Apparent 1 <sup>st</sup> Order Rate Constant vs. Aqueous Ozone Dose.....	85
Figure 4-22 Deionized Water vs Drinking Water.....	87
Figure 4-23 Ultrasound Effect on Ozone Consumption in DI Matrix .....	88
Figure 4-24 Ozone Stability.....	88
Figure 4-25 Step-up Tracer Study.....	92
Figure 4-26 Fitting Experimental Results to Chick & Watson Model .....	95
Figure 4-27 Dioxane Removal from O <sub>3</sub> Alone Predicted by Model .....	98
Figure 4-28 Experimental Data for O <sub>3</sub> Alone with Model Overlay.....	99
Figure 4-29 Dioxane Removal from Combined O <sub>3</sub> /Ultrasound Predicted by Model.....	100
Figure 4-30 Experimental Data for Combined O <sub>3</sub> /Ultrasound with Model Overlay.....	101
Figure 4-31 Model Performance for A.) Ozone and B. Ozone/Ultrasound.....	103
Figure 4-32 R <sub>CT</sub> Determination.....	106
Figure 4-33 Mass Balance Schematic.....	109
Figure 4-34 Mass Balance Study .....	112
Figure 5-1 Schematic for Parallel Ultrasound and UV Treatment .....	117
Figure 5-2 CBD Calibration Curve.....	119
Figure 5-3 Continuous Flow UV Calibration Curve.....	120
Figure 5-4 Continuous Flow Reactor vs CBD for 1,4-Dioxane Removal.....	121

Figure 5-5 Ultrasound Treatment Combinations for 1,4-Dioxane Removal .....	122
Figure 5-6 UV Treatment Combinations for 1,4-Dioxane Removal .....	123
Figure 5-7 AOP Comparison .....	125
Figure F1 Ozone and Flow Rate Data from January 2016 .....	184
Figure F2 Ozone and Ultrasound Data from January 2016 .....	185
Figure F3 Temperature and Ultrasound Data from January 2016 .....	185
Figure F4 Ozone and Ultrasound Data from November 2015.....	187
Figure F5 Ozone and Flow Rate Data from November 2015.....	188

## LIST OF EQUATIONS

Equation 1-1 Sonication of Ozone Gas.....	24
Equation 1-2 Formation of Primary Intermediate-1 .....	27
Equation 1-3 Formation of Primary Intermediate-2 .....	27
Equation 1-4 Formation of Primary Intermediate-3 .....	27
Equation 1-5 Formation of Primary Intermediate-4 .....	28
Equation 1-6 Formation of Primary Intermediate-5 .....	28
Equation 1-7 Formation of Primary Intermediate-6 .....	28
Equation 1-8 Formation of Primary Intermediate-7 .....	28
Equation 1-9 Formation of Primary Intermediate-8 .....	28
Equation 3-1 Pressure Calculation.....	44
Equation 3-2 Steinhart-Hart.....	45
Equation 3-3 Thermistor Voltage .....	45
Equation 4-1 Empirical Ultrasound Rate Constant from Xu et al .....	54
Equation 4-2 Model Equation for Continuous Flow Reactor .....	74
Equation 4-3 Theoretical Transient Ozone Dose-1 .....	74
Equation 4-4 Theoretical Transient Ozone Dose-2 .....	74
Equation 4-5 General Rate Constants .....	83
Equation 4-6 Rate Constants.....	84
Equation 4-7 Synergy Calculation .....	85
Equation 4-8 Mean Reactor Residence Time .....	92
Equation 4-9 Variance .....	92
Equation 4-10 Vessel Dispersion Number, $D/uL$ .....	93

Equation 4-11 Chick & Watson Model for Pathogens .....	94
Equation 4-12 Modified Chick & Watson .....	94
Equation 4-13 Modified Chick & Watson-2.....	95
Equation 4-14 Rate Constant for Chick & Watson.....	95
Equation 4-15 Modified Chick & Watson for O <sub>3</sub> /US.....	96
Equation 4-16 Modified Chick & Watson for O <sub>3</sub> .....	96
Equation 4-17 Calculation of k <sub>0</sub> Using Linear Interpolation .....	96
Equation 4-18 Model Equation for Continuous Flow Reactor .....	97
Equation 4-19 Root Mean Squared Error .....	101
Equation 4-20 Reaction with Hydroxyl Radical.....	105
Equation 4-21 Integrated Reaction with Hydroxyl Radical.....	105
Equation 4-22 R <sub>CT</sub> Definition .....	105
Equation 4-23 1,4-Dioxane Removal Using R <sub>CT</sub> .....	105
Equation 4-24 R <sub>CT</sub> Calculation .....	107
Equation 4-25 Gas Compartment Mass Rate Balance .....	111
Equation 4-26 Water Compartment Mass Balance.....	111
Equation 4-27 Aqueous Ozone Consumption Estimate.....	111
Equation 4-28 Aqueous Ozone Consumption Estimate.....	112
Equation 5-1 Radiant Flux in Collimated Beam Device .....	119
Equation 5-2 Radiant Flux in Reactor .....	120

# CHAPTER 1. INTRODUCTION

## 1.1. Background

### *1.1.1. Water Demand*

The world uses over  $1194 \times 10^9 \text{ m}^3$  of fresh water and ground water annually, and the world is growing (Wang & Zimmerman, 2016). Since 1970, the population has grown by three billion people and it is projected to increase by another two billion by 2050. This increase is expected to cause a 55% increase in global fresh water demand (OECD, 2012). Agriculture demands more water than any other sector, and this means that the water supply will have to double by 2050 from its 2000 levels just to ensure that the world's projected population of nine billion has enough to drink and eat (Chartres & Varma, 2011).

A warming climate is also expected to impact water supplies across the globe, worsening water scarcity while also increasing food costs (US-DoD, 2014). Climate changes have a major impact on the hydrologic cycle (Hoffman, 2009), so water availability is extremely dependent on climate and weather. Water scarcity is typically thought of as an issue for the developing world. However, climate change is expected to cause unpredictable effects on water scarcity in both the developed and developing world (Fishman, 2011). Australia provides an excellent case study for how it affects, and will affect, the developed world. In 2010, the Australian government launched water initiatives with a total bill amounting to A\$1,500 per person (~US \$1,100 at current exchange rates) (Fishman, 2011). There is also growing concern that a warming climate may exacerbate the spread waterborne disease. This has been identified as a priority

research area by the US National Assessment on the Potential Health Impacts of Climate Variability and Change (Hoffman, 2009).

The United States government recognizes the challenge posed by future water scarcity and is taking steps to address this challenge. In May of 2015, the president signed Executive Order 13693 which set a number of Federal water management goals: reducing potable, landscaping, and agricultural use by 2% annually, for a total of 36% reduction by 2025, mandating increased water monitoring, installing storm water and wastewater management infrastructure on federal property, setting a goal for net-zero water use for federal buildings constructed after 2020, mandating newly constructed Federal buildings to achieve net-zero water, and identifying existing facilities for and implement actions to achieve net-zero water usage. “Net-zero” water use means that a building is designed, built, and operated in a manner to greatly reduce total water consumption (Obama, 2015). This is achieved through use of non-potable sources, water recycling, and water reuse in order to return an equivalent amount of water as the building demands (Obama, 2015).

Additionally, the future scarcity of water is projected to increase competition for water resources. This increased competition could worsen tensions and potentially cause the escalation of conflicts (US-DoD, 2014). In the developed world, water has been very dependable for a very long time. It’s notable that we have words for when we lose electricity service, we call it a “power failure”. When we lose cell phone service, we call it a “dead zone”. We even have a whole array of terms to describe less-than-ideal internet connectivity. However, water is so dependable in the United States that we don’t have an equivalent word or phrase for when water service is lost (Fishman, 2011). Due

to these dependable supplies, recent history has been relatively free from conflicts directly related to water disputes. In a study of 412 conflicts of the 20<sup>th</sup> century, water was noted as a partial cause in only seven of them, and only four of these involved actual fighting (Lomborg, 2001) (Bell, 2009). However, access to water has spawned conflict throughout human history and water scarcity has contributed to the fall of great civilizations. In fact, our word “rival” is derived from the Latin “rivalis”, which means to share a riverbed (Bell, 2009).

Water scarcity is already causing an impact to public health today. According to the World Health Organization, 4 out of every 10 people suffer from health effects such as cholera, typhoid, salmonellosis, and dysentery; conditions often caused by lack of access to clean drinking water (Chartres & Varma, 2011). A growing population will only exacerbate these adverse health effects. The United Nations general assembly has even recognized access to clean water as being a human right, citing the need of 884 million people who don't have access to safe drinking water and 2.6 billion people who don't have access to basic sanitation (Muruganandham, et al., 2014) (UN General Assembly, 2010). At environmentally relevant concentrations, a contaminant like dioxane poses primarily chronic health risks, while the diseases listed above pose primarily acute health risks. However, both chronic and acute health risks can cause death and both take a toll on the affected population. Given the many risks posed by water scarcity, such as hunger, disease, and conflict, there is a clear need to better manage water resources.

#### *1.1.1.1. Efficiency*

One of the best ways to stretch finite water resources is to use it more efficiently. In the United States, one of every six gallons of water leaks out of a water main before it ever reaches an end user, and water infrastructure is even leakier in Great Britain and France (Fishman, 2011). In areas where scarcity is already becoming an issue, efficient water practices are already being put into place. In Irvine, California, reclaimed water has been in use for over 25 years for crop irrigation and watering lawns (Hoffman, 2009). In Salisbury, Australia, storm water and waste water have become big business; it is used for flushing toilets, watering lawns, and even washing freshly shorn sheep's wool (Fishman, 2011). Since agriculture is responsible for approximately 70% of fresh water demand globally, inefficient irrigation practices present a ripe area for improvement (Bell, 2009). Not only is about 60% of irrigation water is lost to evaporation, but irrigation can cause soil salinity to increase, eventually leading to the loss of productive farmland (Bell, 2009). Additional improvement in agricultural water use efficiency may come from drought-resistant crop cultivars, which have the potential to increase food production without the subsequent increase in water demand (Chartres & Varma, 2011). However, while agricultural water efficiency is improving, a global trend towards increased meat consumption is having the opposite effect. As more people rise in income globally, their food consumption not only increases, but the type of food consumed changes as well. The global increase in income is causing a shift away from diets comprised primarily of cereals, towards diets incorporating more meat products. This dietary shift is causing an increase in water demand per capita because it requires significantly more water to produce meat than grains. For instance, growing enough to feed a person whose diet consists mostly of cereals requires about 528 gallons of water

per day. However, feeding that same person a diet rich in beef requires approximately 1320 gallons of water per day (Chartres & Varma, 2011).

#### *1.1.1.2. Water Reuse*

Another way to more efficiently manage water resources is through water reuse. Water reuse can occur directly, indirectly, or inadvertently (Hoffman, 2009). Direct Potable Reuse (DPR) is the “introduction of reclaimed water (with or without retention in an engineered storage buffer) directly into a drinking water treatment plant, either collocated or remote from the advanced wastewater treatment system” (US-EPA, 2012). This is the least common mode of water reuse, but it has been employed in places with water access challenges, such as the International Space Station and Windhoek, Namibia, (Chartres & Varma, 2011) and it is expanding as a reuse option. In 2010, the California passed a SB 918 which mandated the State Department of Public Health to adopt uniform water recycling criteria for indirect potable reuse by the end of 2013 and to adopt uniform water recycling criteria for direct potable reuse by the end of 2016 (California, 2010).

Indirect Potable Reuse (IPR) is the “augmentation of a drinking water source (surface or groundwater) with reclaimed water followed by an environmental buffer that precedes drinking water treatment” (US-EPA, 2012). Indirect potable water reuse is already being done across the United States, particularly in Florida and California. A reuse project serving Orlando and Orange County, Florida treats up to 65.5 million gallons per day (MGD), with approximately half being used for irrigation and half for ground water recharge. A 15 MGD project serving the Walt Disney World Resorts provides treated wastewater for five golf courses, five hotels, highway medians, a water park, and a tree farm, and still reserves about half the treated water for groundwater

recharge (Florida Department of Environmental Protection, 2011). In Southern California, the Orange County Groundwater Replenishment System is the world's largest system for indirect potable reuse. This system combines microfiltration, reverse osmosis, and UV/H<sub>2</sub>O<sub>2</sub> to treat up to 100 MGD to potable reuse standards, injecting the treated water to recharge the Orange County Groundwater Basin. Additional treated water has been injected to coastal barrier wells to prevent seawater from infiltrating this augmented ground water supply (Orange County Water District).

Inadvertent reuse, or de facto reuse, is the most common type of water reuse. This involves any “ situation where reuse of treated wastewater is, in fact, practiced but is not officially recognized (e.g., a drinking water supply intake located downstream from a wastewater treatment plant (WWTP) discharge point)” (US-EPA, 2012). The drinking water that was used in this this study is a good example of inadvertent reuse. This water was produced by the Philadelphia Water Department, which operates three large water treatment plants. Due to its central location in Philadelphia, the Water Environmental Technology (WET) Center at Temple University is served by a mixture of water from the Baxter treatment plant, which uses the Delaware River for its source, and the Queen Lane treatment plant, which uses the Schuylkill River (Philadelphia Water Department, 2014).

The following figure was created by the Philadelphia Water Department to illustrate the vast, multi-state watershed that influences the city's drinking water. While they are not shown in the figure, numerous community and industrial treatment plants discharge treated wastewater into the Delaware River, Schuylkill River, and many of their tributaries. Some fraction of the discharges from all of these wastewater plants eventually makes its way into the Baxter and Queen Lane water treatment plants, where it

is treated and sent to the community. Therefore, the water used for this study contains the same fraction of inadvertently reused wastewater from the watersheds of two large rivers which are under the influence of treated effluents from a region spanning across swaths of eastern Pennsylvania, western New Jersey, and southern New York.



*Figure 1-1 Delaware and Schuylkill River Watersheds*

(Philadelphia Water Department,

<http://www.phila.gov/water/wu/Water%20Quality%20Reports/2015WaterQuality.pdf>,

2014)

Surface waters like the rivers and streams in the previous figure pose some water treatment challenges. However, contamination to groundwater is particularly problematic. Groundwater is the source of potable water for approximately 40% of the US population and 93% of public water systems in our country rely on groundwater (Hoffman, 2009). Natural processes which rely on oxygen and sunlight, which can help treat surface waters, are not available to degrade contaminants in an aquifer (U.S. Department of the Interior, 1998).

Any reuse of water, whether direct, indirect, or inadvertent, poses the same challenge; the water must be adequately treated before it can be safely consumed. However, there are some contaminants which aren't adequately eliminated in conventional water and wastewater treatment plants. Most water treatment techniques and water management practices in wide use today were developed prior to 1970, for a much less populous world with more abundant surface and ground water resources. These techniques were developed before the health risks for a number of emerging contaminants were understood and before analytical instruments capable of detecting threshold health risk levels had been fielded.

As our understanding of health risks from emerging contaminants improves, and as analytical improvements continue to drive minimum levels of detection lower, regulatory and health guidelines will also change. More stringent treatment standards can also drive water scarcity, as water sources previously thought to be safe or treatment systems previously thought to be adequate fail to meet the new standards. As a very recent and local example of how regulatory changes affect potable water supplies, the US Environmental Protection Agency (EPA) released a new health advisory for

perfluorooctanoic acid (PFOA) and perfluorooctane sulfonate (PFOS) as this dissertation was being drafted. The updated EPA guidance created a new health advisory level of 70 parts-per-trillion (ng/L) for combined exposure to PFOA and PFOS, compounds were/are used in the production of carpet, clothing, fabric, furniture, packaging, and cookware, as well as fire-fighting foam (US-EPA, 2016). The new advisory level was enacted to protect the most at-risk populations (breast-feeding infants and fetuses) from developmental effects like: low birth weight, accelerated puberty, cancer, liver damage, and other effects to the thyroid and immune system (US-EPA, 2016). In response to the new health guidelines, two community water wells in a neighboring county were immediately shut down because they failed to meet the new, more stringent standard. The shutdown of these wells, coupled with several others that had been shut down earlier for exceeding previous EPA advisory levels, has left the community operating on just 9 of 14 of its wells (Bagenstose, 2016). These are only two emerging contaminants and only one community, but this example illustrates what can happen to water supplies when new understanding of health risks from emerging contaminants leads to more stringent regulations.

The demand created by a growing population and the supply constraints that will be imposed by increasingly stringent water treatment standards are going to severely strain current water treatment options. Investment in water resource management is needed now to address the scarcity of water today and the projected scarcity tomorrow. Investment in water has been shown to yield a strong return, too. The World Health Organization estimates that two dollars are returned for every dollar invested in

improving drinking water access. The return on investment in sanitation is even greater, with \$5.50 returned for every dollar invested (World Health Organization, 2012).

To prepare for the water-stressed world of the near future, advanced water treatment technologies are needed. The subject of this study is a water treatment process which holds potential for potable water treatment as well as treatment for reuse. To evaluate a treatment process's potential; a model contaminant(s) should be chosen which can be used as a yardstick to measure the effectiveness of the advanced oxidation process (AOP). For this study, 1,4-dioxane was chosen because it poses a number of treatment challenges. For instance, dioxane is:

1. Resistant to commonly used treatment technologies - (*advanced treatment is needed*)
2. Soluble in water and able to migrate within an aquifer; i.e. not readily sorbable to soil and/or organic matter - (*rapid spreading contaminant plumes create large and dilute plumes, putting greater areas at risk*)
3. Widely detected, both in surface water and groundwater - (*contaminant is commonly found*)
4. A health threat - (*health threat should drive treatment objectives*)

#### 1.1.2. 1,4-Dioxane

Recently, there has been increased concern and regulations regarding emerging contaminants (ECs) in water. 1,4-Dioxane is one of these ECs and has been detected in groundwater throughout the United States (Zenker, Borden, & Barlaz, 2003) (US-EPA, 2016). It has been classified as a known animal and probable human carcinogen (US-

EPA, 1,4-Dioxane (CASRN 123-91-1), 2005). 1,4-Dioxane is a solvent and stabilizer and more than 1.3 million pounds were disposed of or released within the US in 2013 (US-EPA, 2013). It is widely used as an additive for chlorinated solvents such as methyl chloroform degreasers (Mohr, 2010). It is used in the processing of dyes, oils, resins, and waxes (Adams, Scanlan, & Secrist, 1994), in the manufacture of small arms ammunition (US Army Environmental Command, 2010), and also in nuclear science for the scintillation detection of low-energy beta radiation (Chitra, Paramasivan, Cheralathan, & Sinha, 2012). The US-EPA has classified 1,4-dioxane as a priority hazardous pollutant, and the carcinogenic risk from oral exposure is  $11 \mu\text{g}\cdot\text{kg}^{-1}\cdot\text{day}^{-1}$  (US-EPA, 1,4-Dioxane (CASRN 123-91-1), 2005).

#### *1.1.2.1. Regulations*

A maximum contaminant limit (MCL) for drinking water has not been established, but the US-EPA has a health advisory limit of  $0.35 \mu\text{g}/\text{L}$  based on a 1 in  $10^6$  cancer risk. Additionally, the office of environmental health hazard assessment (OEHHA). 1,4-Dioxane has set a drinking water notification level of  $1 \mu\text{g}/\text{L}$  (California Environmental Protection Agency, 2016) and dioxane used as a measure of the effectiveness of advanced treatment processes. These treatment processes must show a 0.5 log reduction (69%) of 1,4-dioxane in order to meet water-recycling criteria (California Dept of Public Health, 2014) (Gerrity & Snyder, 2011).

#### *1.1.2.2. Properties*

The physical and chemical properties of 1,4-dioxane play a major role in its environmental fate and transport. It is miscible in water, making it highly mobile in contaminated groundwater and surface water. According to the US-EPA, it is one of the

most mobile organic contaminants and is able to travel long distances without degradation (US-EPA, Technical Fact Sheet - 1,4-Dioxane, 2012). Due to its low affinity for the vapor phase, it is a difficult organic contaminant to treat (US-EPA, 2006). Its low Henry's law constant ( $9.05 \times 10^{-6} \text{ atm} \cdot \text{m}^3/\text{mol}$ ) (Suh & Mohensi, 2004) (Son, Choi, Khan, & Zoh, 2006) and low octanol water partition coefficient ( $\log K_{OW} = -0.27$ ) make it unsuitable for removal via air stripping and carbon adsorption (Suh & Mohensi, 2004) (Son, Choi, Khan, & Zoh, 2006).

#### *1.1.2.3. Occurrence*

Occurrence of 1,4-dioxane has been studied and varies widely. In the United States, it has been found at over 50 EPA Superfund sites (Mohr, 2010). In 2012, 1,4-dioxane was included in the Third Unregulated Contaminant Monitoring Rule (UCMR 3). To comply with this rule, 35,856 samples were analyzed from 4,849 public water systems nationwide. Of these samples, 1,4-dioxane was detected in 4,145 samples (11.6%) and 1,069 (3.0%) exceeded the advisory limit of  $0.35 \mu\text{g/L}$  (0.35 parts-per-billion). Additionally, 1,4-dioxane was detected in 1,062 of the public water systems sampled (21.9%) and 336 (6.9%) of those systems had one or more samples which exceeded the advisory limit (US-EPA, 2016). In a Japanese study, 24 out of 27 sites had detectable concentrations of 1,4-dioxane, with results up to  $52 \mu\text{g/L}$  and  $0.1\text{-}16.0 \mu\text{g/L}$  were detected in river water (Abe, 1999). Common point sources for dioxane are 1,1,1-trichloroethane (TCA) spill sites and from landfill leachate (Zenker, Borden, & Barlaz, 2003). Due to the mobility and recalcitrance of 1,4-dioxane and its use as a solvent stabilizer, even sites where solvents had been spilled in the past can remain sources of 1,4-dioxane contamination.

## 1.2. Literature Review

### 1.2.1. Treatment Technologies

A number of treatment technologies, including physical processes, biological processes, and AOPs have been tested for the removal of 1,4-dioxane from water. Conventional water and wastewater treatment processes, such as chemical treatment, air stripping, carbon adsorption, and biological treatment, have all been ineffective (Zenker, Borden, & Barlaz, 2003). There have also been investigations into dioxane removal by reverse osmosis (Kegel, Rietman, & Verliefd, 2010), phytoremediation (Aitchison, Kelley, Alvarez, & Schnoor, 2000), anodic oxidation (Choi, Lee, Shin, & Yang, 2010), O<sub>3</sub>/UV (Peyton & Glaze, 1988) (Kwon, et al., 2012), H<sub>2</sub>O<sub>2</sub>/O<sub>3</sub> (Chitra, Paramasivan, Cheralathan, & Sinha, 2012), TiO<sub>2</sub> based photo-catalytic and H<sub>2</sub>O<sub>2</sub>/UV processes (Coleman, Vimonses, Leslie, & Amal, 2007) (Stefan & Bolton, 1998) (Maurino, Calza, Minero, Pelizzetti, & Vincenti, 1997), biodegradation (Klecka & Gonsior, 1986) (Zenker, Borden, & Barlaz, 2004), Fenton and Fenton-like processes (Son, Im, & Zoh, 2009) (Kishimoto & Sugimura, 2010) (Kitamura, Kishimoto, Okura, & Otsu, 2011), ultrasound (Son, Choi, Khan, & Zoh, 2006), ozone (Andaluri, Curran, & Suri, 2012), and persulfate (Felix-Navarro, Lin-Ho, Barrera-Diaz, & Perez-Sicairos, 2007). The most effective treatment technique is distillation, but it is extremely energy intensive since 1,4-dioxane has a boiling point of 101.1° C (Maurino, Calza, Minero, Pelizzetti, & Vincenti, 1997) (US-EPA, 2006).

#### 1.2.1.1. Conventional Treatment Processes

#### 1.2.1.1.1. Chlorination

Typical chlorine disinfection does not remove 1,4-dioxane (0%), nor does ferric chloride coagulation (0%) or potassium permanganate (0%) (McGuire, Suffet, & Radzuil, 1978). However, chlorination under slightly acidic pH (5.2) and high temperature conditions (75°C) has been shown to remove dioxane where hypochlorous acid is twelve times in molar excess (Klecka & Gonsior, 1986) (Zenker, Borden, & Barlaz, 2003). Unfortunately, other studies have shown that chlorinated analogs of 1,4-dioxane are three orders of magnitude more toxic than 1,4-dioxane itself (Woo, et al., 1980) (Zenker, Borden, & Barlaz, 2003).

#### 1.2.1.1.2. Air Stripping

Air stripping takes advantage of the principal of vapor-liquid equilibrium, by exposing contaminated water to ambient air. The concentration gradient between the contaminated liquid and the clean air drives volatile contaminants out of the water (US-EPA, 1987). Although 1,4-dioxane is characterized as a semi-volatile compound, it is extremely resistant to air stripping (Zenker, Borden, & Barlaz, 2003) (Mohr, 2010). In fact, aeration for 2.4 hours at an 80 to 1 air to water ratio was demonstrated to remove only 3% of 1,4-dioxane (McGuire, Suffet, & Radzuil, 1978).

#### 1.2.1.1.3. Activated Carbon

Activated carbon adsorption is a treatment technique which removes hydrophobic water contaminants. This works by van der Waals attraction between the contaminant and the highly porous activated carbon (Kegel, Rietman, & Verliefde, 2010). Powdered activated carbon is ineffective at removing 1,4-dioxane (0%) and granular activated

carbon has been shown to only remove 50-67% (Zenker, Borden, & Barlaz, 2003) (Johns, Marshall, & Toles, 1998) (McGuire, Suffet, & Radzvil, 1978).

#### 1.2.1.1.4. Biological

Biological treatment is the exploitation of organisms, typically bacteria, for the removal of contaminants from water. This type of treatment has shown promise for the removal of 1,4-dioxane. Bacteria have been discovered which are capable of metabolizing 1,4-dioxane directly (Parales, Adamus, White, & May, 1994) (Mahendra & Alvarez-Cohen, 2005) or as a co-contaminant (Zenker, Borden, & Barlaz, 2000) (Mahendra, Grostern, & Alvarez-Cohen, 2013) (Zenker, Borden, & Barlaz, 2004). However, dioxane is poorly removed by the conventional activated sludge process (Abe, 1999). Manipulating sludge by pre-seeding it with 150 mg/L of dioxane can improve the activated sludge process. In fact, such pre-seeded sludge was found to be capable of removal to below detection limits. At initial concentrations above 150 mg/L, however, the pre-seeded sludge was incapable of complete removal of dioxane (Roy, Anagnostu, & Chaphalkar, 1995) (Zenker, Borden, & Barlaz, 2003). Also, a trickling bio-filter was found to remove 93-97% of 1,4-dioxane, but the removal was dependent upon the spiking the influent water with tetrahydrofuran (THF) as a growth substrate (Zenker, Borden, & Barlaz, 2004)

#### *1.2.1.2. Phytoremediation*

Phytoremediation is the use of plants to partially or substantially remediate selected contaminants in contaminated soil, sludge, sediment, ground water, surface water, or waste water. It can be carried out within the plant, both above and below the soil, or it can occur in the rhizosphere, the sub-surface soil zone within 1mm of the root.

This can involve degradation of contaminants, dissipation of contaminants into the atmosphere, accumulation of contaminants by the plants, or the immobilization of a contaminant plume (Pivetz, 2001). Hybrid poplar trees have been tested for the treatment of contaminated soil and water. The trees were found to be capable of transpiring 76-83% of the dioxane contamination into the atmosphere, where it has a much shorter chemical half-life due to photodegradation (Aitchison, Kelley, Alvarez, & Schnoor, 2000). While phytoremediation removes a significant percentage of dioxane, it is not able to address water scarcity since it relies on the vaporization of the water.

#### *1.2.1.3. Reverse Osmosis*

Reverse osmosis is a treatment technique in which high pressure is used to force water through a semi-permeable membrane. Results for the removal of 1,4-dioxane by reverse osmosis vary, but have been reported in the range of 50-80% (Kegel, Rietman, & Verliefde, 2010) (Chakraborti, et al., 2009). Since reverse osmosis does not completely remove 1,4-dioxane, less intensive filtration processes using sand or mixed media are ineffective as well.

#### *1.2.1.4. Advanced Oxidation Processes*

Advanced Oxidative Processes (AOPs), which are those processes that generate hydroxyl radicals, are useful in the degradation of a wide variety of organic contaminants in water. Due to the high ionization potential of the hydroxyl radical (2.86 eV), AOPs are useful in the degradation of a wide variety of recalcitrant organic contaminants in water (Muruganandham, et al., 2014). Several AOPs have shown promise for the removal of 1,4-dioxane (Choi, Lee, Shin, & Yang, 2010) (Suh & Mohensi, 2004)

(Kishimoto, et al., 2008) (Xu, Mochida, Naito, & Yasuda, 2012) (Even-Ezra, et al., 2009) (Chitra, Paramasivan, Cheralathan, & Sinha, 2012) (Adams, Scanlan, & Secrist, 1994).

#### 1.2.1.4.1. Anodic Oxidation

Anodic oxidation is an electrochemical AOP in which dioxane combines with water in the anode to form carbon dioxide, hydroxide ions, and protons. This process has been shown to be relatively unaffected by pH between 1.7 and 12.4. Over 95% removal was achieved, but the rate of dioxane removal was driven primarily by electrical current density. However, electrode material selection is critically important. Boron-doped diamond electrodes were found to be much more effective for dioxane removal than platinum-coated steel (Choi, Lee, Shin, & Yang, 2010).

#### 1.2.1.4.2. Photocatalysis

Titanium dioxide as a photocatalyst has been tested for 1,4-dioxane removal. In this process, photons striking the titanium dioxide create electron-hole pairs. These holes react with water or hydroxide ions at the surface to form hydroxyl radicals, which are then capable of degrading a wide variety of contaminants. At pH 5.5, this treatment process is capable of complete dioxane removal, with a first order rate constant of  $0.17 \text{ min}^{-1}$ . Interestingly, the addition of 100mM bicarbonate, a scavenger of radicals, didn't alter the rate constant (Maurino, Calza, Minero, Pelizzetti, & Vincenti, 1997). The size of the photocatalyst appears to play a major role. In another photocatalyst study, nano-sized titanium dioxide (Degussa P25) was found to remove dioxane 13 times faster than magnetic particles that had been coated with titanium dioxide, which had a radius 5 times as large (Coleman, Vimonses, Leslie, & Amal, 2007).

#### 1.2.1.4.3. Ozone/Peroxide

Ozone/peroxide is an advanced oxidation process in which hydroxyl radicals are formed by a radical chain mechanism between ozone and hydrogen peroxide (Acero & Von Gunten, 2001) (Muruganandham, et al., 2014). The O<sub>3</sub>/H<sub>2</sub>O<sub>2</sub> combination has been shown to oxidize 1,4-dioxane following first order kinetics with a rate constant of 0.059 min<sup>-1</sup> (Takahashi, et al., 2013) . While this process was capable of complete dioxane removal, it was also found to be susceptible bicarbonate alkalinity (Adams, Scanlan, & Secrist, 1994) (Suh & Mohensi, 2004).

#### 1.2.1.4.4. Ozone/Ultraviolet

In the ozone/UV process, hydroxyl radicals can be created by the breakdown of ozone, by direct UV photolysis, or through a reaction whereby water and ozone combine under UV to create hydrogen peroxide (Muruganandham, et al., 2014). The peroxide molecules formed in this manner can subsequently be split into two hydroxyl radical by another photon, or can form radicals by combining with another ozone molecule, as in the O<sub>3</sub>/H<sub>2</sub>O<sub>2</sub> process outlined above (Beltran, 2003) (Peyton & Glaze, 1988). Combined UV (120W) and bubbled ozone (~35mg/L air phase) was shown to cause first order degradation of dioxane following with a rate constant of 0.0225 min<sup>-1</sup> (Takahashi, et al., 2013). Another study varied ozone bubble size and found that it had a significant impact on kinetics, with first order rate constants varying from 0.019 min<sup>-1</sup> to 0.343 min<sup>-1</sup> when ~43 mg/L air phase ozone was supplied (Kishimoto & Nakamura, 2011).

#### 1.2.1.4.5. Peroxide/Ultraviolet

The photolysis of hydrogen peroxide by ultraviolet radiation generates hydroxyl radicals, which are capable of degrading a variety of contaminants. The relative dose of

UV light and peroxide is important since excess peroxide can serve to scavenge some of the produced hydroxyl radicals (Muruganandham, et al., 2014). Under UV photolysis, 100mM of hydrogen peroxide has been shown to remove dioxane with a first order rate constant of  $0.040 \text{ min}^{-1}$ . The addition of 100mM bicarbonate as a hydroxyl radical scavenger reduced that rate to  $0.0047 \text{ min}^{-1}$  (Maurino, Calza, Minero, Pelizzetti, & Vincenti, 1997).

#### 1.2.1.4.6. Fenton and Fenton-Like Processes

The Fenton process is an AOP which combines ferrous iron ( $\text{Fe}^{2+}$ ) and hydrogen peroxide. When ferrous iron and peroxide are combined, they form a hydroxide ion, a hydroxyl radical, and ferric iron ( $\text{Fe}^{3+}$ ). This process is capable of 97-99% removal of 1,4-dioxane (Ghosh, Samanta, & Ray, 2010).

Other studies have used electrochemical processes to improve the Fenton-like processes. One such study involved combining ferrous iron with hypochlorous acid, which has been reported to create hydroxyl radicals in a Fenton-like process (Candeias, Stanford, & Wardman, 1994). The hypochlorous acid was made by the oxidation of chloride ions at an anode, while the ferrous iron was created by reduction of ferric iron at the cathode. Under acidic conditions (pH 2-3), 1,4-dioxane was removed at a rate of 0.03 to 0.04 mmol/min as the current density of the electrodes increased from 1.4 to 21  $\text{mA/cm}^2$  (Kitamura, Kishimoto, Okura, & Otsu, 2011) (Kishimoto & Sugimura, 2010). One potential issue with this system which was not addressed in the published study was the toxicity of byproducts. While the hydroxyl radical is the primary oxidant, the presence of chlorine could be problematic as chlorinated analogs of 1,4-dioxane are

believed to be significantly more toxic than the dioxane itself (Woo, et al., 1980) (Mohr, 2010).

Another Fenton-like process has also been studied involving the combination of zero-valence iron with UV light for the removal of 1,4-dioxane. This combination was found to degrade dioxane at a first order rate constant of  $0.0019 \text{ min}^{-1}$  (Son, Im, & Zoh, 2009).

#### 1.2.1.4.7. Persulfate

Persulfate is used to oxidize contaminants either through heating or with a catalyst. Hydroxyl radicals and sulfate radicals are generated by the photolysis or thermal decomposition of persulfate in aqueous solution. Persulfate treatment relies on these radicals for contaminant degradation. At neutral pH, persulfate degrades dioxane with a first order rate constant of  $0.0108 \text{ min}^{-1}$  at  $25^{\circ}\text{C}$ , but that value increase to  $0.159 \text{ min}^{-1}$  at  $50^{\circ}\text{C}$  (Felix-Navarro, Lin-Ho, Barrera-Diaz, & Perez-Sicairos, 2007). The addition of a metallic catalyst can further increase degradation rates (Felix-Navarro, et al., 2013). Persulfate in combination with UV light has been used as well, and was found to degrade dioxane faster than hydrogen peroxide combined with UV light, with removal by 0.01 M persulfate and full spectrum UV occurring at a rate of  $0.44 \text{ min}^{-1}$  (Maurino, Calza, Minero, Pelizzetti, & Vincenti, 1997).

#### 1.2.1.5. Ozone

Ozone is commonly used as an oxidant in water treatment. With an oxidation potential of 2.07V, ozone can react directly with many contaminants in water. In solution, ozone can also be transformed into a number of important secondary oxidants,

including hydrogen peroxide and the hydroxyl radical (Hoigne J. , 1998). Ozone consumption can occur either by reacting directly with a solute in the water, it can be initiated by reacting with hydroxyl radical, or it can be initiated by reacting with the hydroxide ion. Therefore the consumption rate of ozone is very dependent on the solutes present and the pH of the solution. In the absence of compounds which promote or inhibit the consumption of ozone, the ratio of  $O_3/\cdot OH$  at neutral pH is approximately  $10^{7.9}$  (Westerhoff, Song, Amy, & Minear, 1997). Since ozone can form hydroxyl radicals by reacting with hydroxide ions, ozone has been studied for the removal of 1,4-dioxane at various pH conditions. The reaction rate constant for wastewater conditions where ozone was in excess was found to be  $1.2 \text{ min}^{-1}$  at neutral pH, but 20 times greater ( $24 \text{ min}^{-1}$ ) at pH 9 (Barndok, Cortijo, Hermosilla, Negro, & Blanco, 2014).

#### *1.2.1.6. Ultrasound*

Ultrasound is process which relies on pressure waves through the aqueous medium. These waves are capable of causing bubbles to form, grow, and eventually collapse. This process of bubble formation and collapse is known as acoustic cavitation (Franc & Michel, 2006).

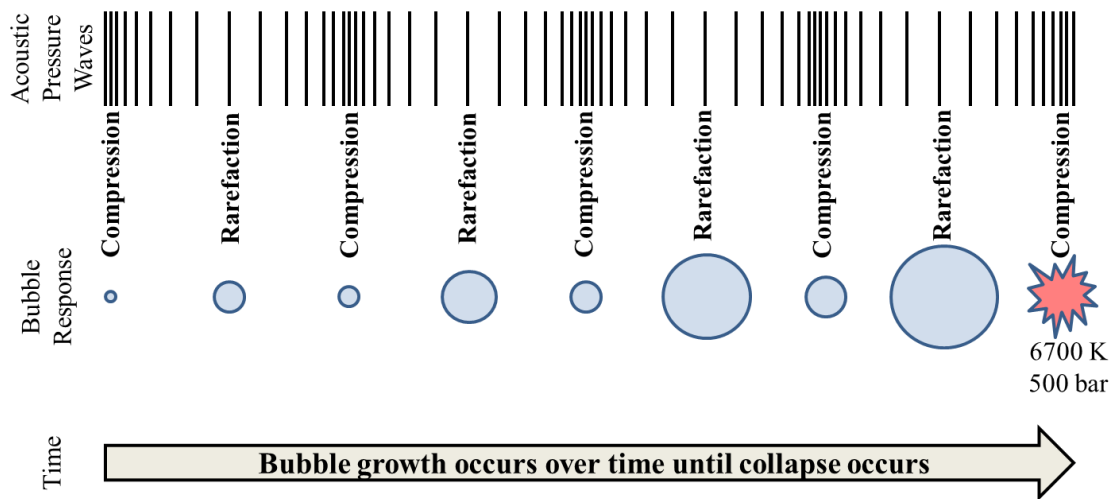


*Figure 1-2 Acoustic Cavitation*

Removal of contaminants by ultrasound can occur in three ways: thermal degradation at cavitation sites, supercritical oxidation, and hydroxyl radical oxidation in gas/liquid interfacial or bulk liquid regions (Cyr, Paraskewich, & Suri, 1999) (Suri, Andaluri, Abburi, & Velicu, 2008). As gas bubbles collapse under sonication, short term (<1  $\mu\text{sec}$ ) spikes of up to 6700 K and pressures of about 500 atmospheres can occur at the cavitation sites, enabling localized thermal degradation (Fujikawa & Akamatsu, 1980) (Brennen, 2014) (Suslick, 1990). Supercritical oxidation is the process by which organic contaminant are oxidized in water at temperatures and pressures above the critical point, a temperature and pressure condition above which a fluid becomes a supercritical fluid. In the supercritical state, water behaves with both liquid and gaseous traits, permitting the oxidation of organic contaminants. For water, this critical point is 647.096 K and 22.064 MPa (International Association for the Properties of Water and Steam, 2007). Since temperatures of 6700 K and pressures of 84.8 bar can be achieved at the cavitation sites,

localized supercritical oxidation is also possible (Fujikawa & Akamatsu, 1980). Finally, hydroxyl radicals can be generated by the violent collapse of bubbles, which can act at the interfacial region, or in the bulk liquid. However, these radicals are short lived and degradation is most likely to occur near the cavitation sites.

In literature, ultrasound has been studied for the treatment of: domestic wastewater (Madge & Jensen, 2002), estrogens (Suri, Andaluri, Abburi, & Velicu, 2008), aryl-azo-naphthol dyes (Gultekin & Ince, 2006), reactive dyes (Lall, Mutharasan, Shah, & Dhurjati, 2003) (Ince & Tezcanli, 2001), methyl tert-butyl ether (Kang & Hoffmann, 1998), and many others. Treatment of 1,4-dioxane by sonication has been studied as well. At 358 kHz, dioxane degradation followed first order kinetics with a rate constant of  $0.025 \text{ min}^{-1}$  (Beckett & Hua, 2000) and the addition of 100mM ferrous iron increased that rate constant to  $0.049 \text{ min}^{-1}$  (Beckett & Hua, 2003). At 490 kHz, degradation followed first order kinetics with a rate constant of  $0.0024 \text{ min}^{-1}$ . In another study at 20 kHz, the same ultrasonic frequency to be employed in the current study, the first order rate constant was found to be  $0.0132 \text{ min}^{-1}$  (Son, Choi, Khan, & Zoh, 2006). The wide variety of rate constants reported for the sonication of dioxane is likely due to the use of different frequencies and different power densities.

Combined ozone/ultrasound is another type advanced oxidation process, and one that hasn't been studied as extensively as others. Combined ozone/ultrasound holds promise for water treatment due to its ability to degrade a number of contaminants. It also has some operational advantages. With the proper equipment ozone can be generated from the air and ultrasound waves can be generated using only electricity, enabling water treatment without any additional chemical inputs.

### 1.2.1.7. Combined Ozone/Ultrasound Process

The behavior of aqueous ozone under sonication has been investigated. When ozone gas undergoes cavitation, it has been theorized that a thermal process converts the ozone to molecular oxygen and an oxygen atom, which is then free to react with water molecules to form a hydroxyl radicals (Kang & Hoffmann, 1998) (Weavers & Hoffmann, 1998) (Hart & Henglein, 1986).



Weavers and Hoffmann found that 20 kHz ultrasound served to increase mass transfer of ozone by measuring the mass transfer coefficient,  $k_L a$ . Additionally, they've suggested that while increased turbulence may be partially responsible for the increased mass transfer, the majority of the effect is due to the increased ozone degradation creating a larger concentration gradient (Weavers & Hoffmann, 1998). In a study of the decolorization of reactive dye, blue 19, the addition of ultrasound to ozone served to increase both the mass transfer coefficient of ozone as well as the apparent first order rate constant of decolorization, with both values increasing with ultrasonic power (Lall, Mutharasan, Shah, & Dhurjati, 2003). Guo et al noted that the combined ozone/ultrasound process boosted removal of sulfamethoxazole in water, attributing the improvement to the increased production of hydroxyl radicals in the combined process (Guo, et al., 2015).

The effects of ultrasound on mass transfer in a gas-liquid system have been studied extensively in a pressurized reactor using nitrogen in deionized water. The study found that 20 kHz ultrasound coupled with gas bubbles serves to increase the mass

transfer coefficient up to one-hundred fold (Laugier, Andrianstsiferana, Wilhelm, & Delmas, 2008). The study found that the improvement in the mass transfer under sonication was a function of ultrasonic power. It was one of very few studies to explore the effect of reactor pressure. However, a pressure range typical of an organic synthesis reactor was utilized. These pressures ranged from 43.5 to 145 pounds-per-square-inch (PSI), which was significantly higher than the 8 to 75 PSI range employed in the current study (Laugier, Andrianstsiferana, Wilhelm, & Delmas, 2008).

The combined ozone/ultrasound process has been shown to improve mineralization rates of phenol, azo dyes, reactive dyes, humics, and methyl tert-butyl ether (MTBE) (Kindak & Ince, 2007) (Lesko, Hoffmann, & Colussi, 2006) (Lall, Mutharasan, Shah, & Dhurjati, 2003) (Gultekin & Ince, 2006) (Ince & Tezcanli, 2001) (Stepniak, Stanczyk-Mazanek, & Kusiak, 2012) (Kang & Hoffmann, 1998). It has been theorized that this effect is due to the creation and subsequent migration of volatile intermediates into the cavitation bubbles, where direct pyrolysis can occur (Olson & Barbier, 1993). Xu, Shi, and Wang studied the combined ozone/ultrasound process for the removal of p-nitrophenol and a synergistic enhancement was observed. They also noted that the combined ozone/ultrasound process was less developed than other AOPs (Xu, Shi, & Wang, 2005).

Al Hashimi et al studied the combined ozone/ultrasound process for the treatment of bacteria, using a commercial  $USO_3$  system from USS GmbH. This study found that the ultrasound enhanced the treatment of bacteria by declumping of cell clusters, ultrasound-induced cellular membrane damage, enhanced ozone decomposition, and

increased production of free radicals and hydrogen peroxide (Al-Hashimi, Mason, & Joyce, 2015).

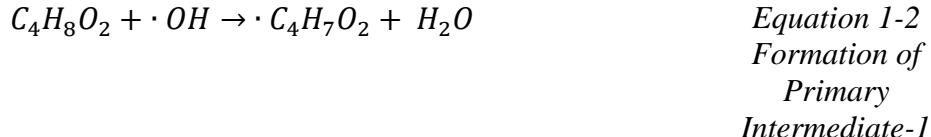
In another study, combined ozone and ultrasound was studied for the removal of 1,4-dioxane in a semi-batch reactor. The study compared the contributions from ozone millibubbles, microbubbles, and ultrasonic intensity to overall removal. A synergistic enhancement of removal was noted with increasing ozone concentration and ultrasonic intensity (Xu, Mochida, Naito, & Yasuda, 2012).

Several commercial products have been created which utilize the combined ozone/ultrasound process. These include the  $USO_3$  system from USS GmbH, the ASMR Series from Aquasonic Management International, and the OZONIX system from Ecosphere (Gogate, et al., 2014). The OZONIX system is the only one that specifically notes using pressurization to boost performance. The Ozonix system has been patented and targeted for water treatment in the energy sector, and includes an anti-fouling electro-precipitation process, in addition to ozone and ultrasound. It is touted for its ability to prevent bio-fouling (bacterial growth) and for potential savings for the disposal and treatment of flow-back water produced by the fracking process (Ecosphere Technologies, 2016). The combined ozone/ultrasound process has also been touted for use in treating the coal ash that is generated by coal gasification power plants (McGuire D. , 2015). These commercial products indicate that the combined ozone/ultrasound process is suitable for industrial wastewater treatment. The process is also capable of treating groundwater, and is capable of treating a variety of contaminants.

### 1.2.2. 1,4-Dioxane Reaction Mechanism

The reaction mechanism of 1,4-dioxane has been extensively studied for H<sub>2</sub>O<sub>2</sub>/UV process. Upon reaction with the hydroxyl radical, 1,4-dioxane was theorized to form four major intermediates: 1,2-ethanediol monoformate, 1,2-ethanediol diformate (ethylene glycol), formic acid, and methoxyacetic acid (Stefan & Bolton, 1998). In a study heterogeneous photocatalytization of hydrogen peroxide and peroxydisulfate in the presence of titanium dioxide, Maurino et al also found 1,2-ethanediol diformate to be the primary intermediate (Maurino, Calza, Minero, Pelizzetti, & Vincenti, 1997).

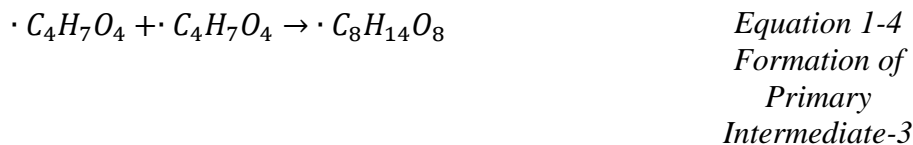
According to Stefan and Boltan, the predominant reaction pathway is initiated by a hydroxyl radical causing an H-abstraction of the 1,4-dioxane, forming a 1,4-dioxanyl radical:



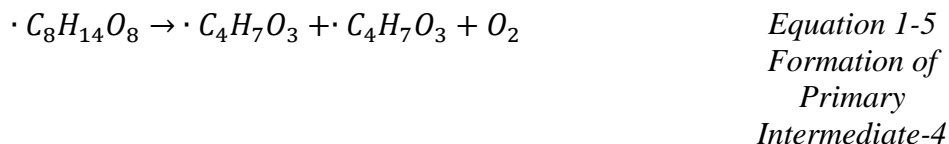
Next, the 1,4-dioxanyl radical combines with dissolved oxygen to form peroxy radicals:



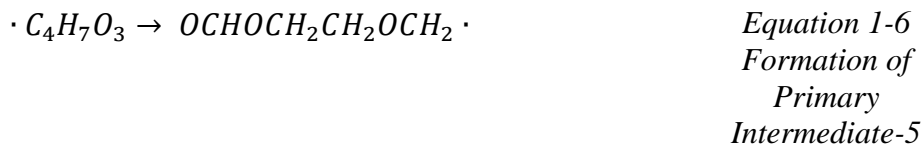
Then, two of the peroxy radicals combine to form tetroxide compound:



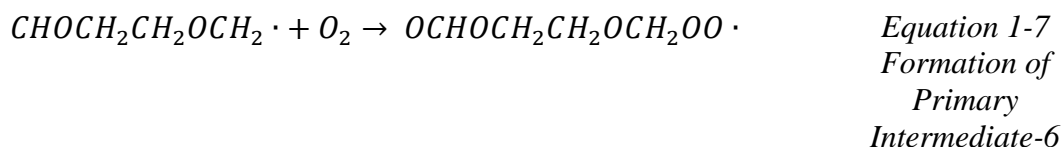
Next, the tetroxide decomposes to form oxygen and two  $\alpha$ -oxyl radicals:



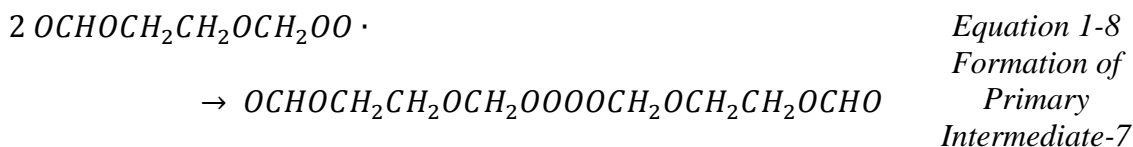
Then, the  $\alpha$ -oxyl radicals undergo carbon-carbon splitting to form a radical:



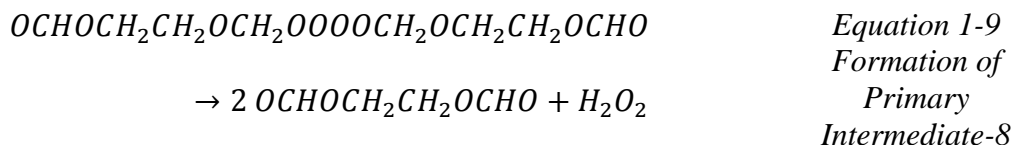
Next, this radical reacts with dissolved oxygen to form another peroxy radical:



Then, two peroxy radicals undergo dimerization:



Finally, this dimerized compound decomposes into two molecules of 1,2-ethanediol diformate and a hydrogen peroxide, or through a chain of reactions requiring oxygen, to 1,2-ethanediol monoformate and formaldehyde. However, the branching ratio favors the formation of 1,2-ethanediol diformate over monoformate 3:1 (Stefan & Bolton, 1998). This primary reaction is given by:



The last intermediates prior to mineralization are: glycolic acid, formic acid, glyoxalic acid, and oxalic acid (Stefan & Bolton, 1998).

The reaction mechanism has also been studied for the ultrasound process. While specific intermediates were not reported, Son et al found the hydroxyl radical to be responsible for 1,4-dioxane degradation and that the degradation followed a sigmoidal model. They also reported that the degradation was suppressed by the addition of bicarbonate as a radical scavenger (Son, Choi, Khan, & Zoh, 2006).

### *1.2.3. Toxicity*

The carcinogenicity of 1,4-dioxane has been demonstrated in a number of animal studies via inhalation, ingestion, and dermal exposure (Hoch-Ligeti, Argus, & Arcos, 1970) (Argus, Arcos, & Hoch-Ligeti, 1965) (King, Shefner, & Bates, 1973). However, direct evidence of causing tumors in humans is limited (US Army Environmental Command, 2010). In an inhalation toxicity study on humans, the half-life of 1,4-dioxane was determined to be  $59 \pm 7$  minutes. Over 99% is excreted as the metabolite 2-hydroxyethoxyacetic acid (HEAA) and only 0.3% is excreted as 1,4-dioxane (Young, Braun, Rampy, & Chenoweth, 1977). This metabolite is not considered to cause cancer, so the carcinogenicity is believed to be due to 1,4-dioxane directly, rather than its metabolic products (US Army Environmental Command, 2010).

There is currently a gap in knowledge regarding the mode by which 1,4-dioxane causes cancer. Until more is known about how 1,4-dioxane causes cancer in humans, it is not possible to compare the risk from the intermediate byproducts with the risk from 1,4-dioxane directly. However, the most prevalent intermediate byproducts are considered less toxic than 1,4-dioxane.

The primary intermediate byproducts are the most worrisome from a toxicological standpoint and include: 1,2-ethandiol diformate, 1,2-ethandiol monoformate, methoxyacetic acid and formaldehyde (Beckett & Hua, 2000). 1,2-Ethandiol diformate (ethylene glycol diformate) carries a health rating of one, so it should not present any significant risk as a byproduct of 1,4-dioxane treatment (US National Center for Biotechnology Information, 2015). 1,2 Ethandiol monoformate (ethylene glycol monoformate) does not carry any health rating. However, formaldehyde exhibits both acute and carcinogenic risks (US National Center for Biotechnology Information, 2015). Both 1,4-dioxane and formaldehyde are probable human carcinogens, and methoxyacetic acid is an endocrine disruptor, which complicates the risk analysis (Henley & Korach, 2005). Formaldehyde has a minimum risk level of 0.2 mg/kg/day. This means that doses below this are not believed to cause an appreciable risk of non-cancer health effects (Agency for Toxic Substances and Disease Registry, 2012). However, formaldehyde appears to be only a minor byproduct of 1,4-dioxane degradation, with maximum detected formaldehyde <15% of 1,4-dioxane destroyed. Methoxyacetic acid, the other intermediate thought pose a significant health risk, exhibited a relatively low conversion (~10%) as well (Stefan & Bolton, 1998).

The final intermediates prior to mineralization are: oxalic acid, formic acid, glycolic acid, and glyoxylic acid. Dilute formic acid is approved as a food additive (US Food and Drug Administration, 2015). Oxalic acid is a naturally occurring nutrient and is present in a variety of vegetables in the 0.1-1.5% range (Agriculture, 2015). However, oxalate is also a leading cause of kidney stones (calcium oxalate) and glycolic and glyoxylic acid are metabolized into oxalate in the liver. While these final intermediates

are toxic at high doses, any contribution from the oxidization of dilute (parts-per-billion range) 1,4-dioxane in water could not reach harmful levels (Richardson, 1973).

While direct studies linking 1,4-dioxane to human carcinogenicity are lacking, it is still a suspected human carcinogen, so the need to remove it from water is apparent. However, it is important to investigate the intermediate byproducts of 1,4-dioxane degradation, as complete mineralization may not be feasible in an actual treatment system. Though it seems unlikely that the toxicity of the intermediate byproducts could exceed that of dioxane, a toxicity analysis remains an important area for future study.

### **1.3. Research Gap**

Most of the published studies on the removal of 1,4-dioxane utilized batch or semi-batch reactors, most using spiked deionized water, and most analyzed the effect of inhibitors. To the best of my knowledge, only one published study has investigated combine ozone/ultrasound for the treatment of 1,4-dioxane, and it utilized batch testing. Very few dioxane studies have been performed in a continuous flow reactor. For the combined ozone/ultrasound process, I believe a continuous flow system is a better representation of a practical treatment system than batch. The continuous flow reactor also permits the study of reactor pressurization. To the best of my knowledge, pressure effects have not been previously reported for this treatment process/contaminant combination. Also, I believe the use of spiked drinking water is a better real-world matrix representation than spiked deionized water, especially when considering a treatment process with the potential for water reuse. For these reasons, this study utilizes a continuous flow reactor and drinking water spiked with 1,4-dioxane.

## **CHAPTER 2. PROBLEM STATEMENT**

### **2.1. Goals and Objectives**

The overall objective is to investigate the combined ozone and ultrasound process for the removal of 1,4-dioxane in drinking water in a continuous flow reactor. The following operational parameters, as listed below, were investigated and the findings were used to build an empirical model for the reactor:

#### 1. Effects of Ozone Dose and Residence Time

The effects of ozone dose and reactor residence time was evaluated to determine if environmentally relevant concentrations of 1,4-dioxane can be removed by ozone dosages and treatment times that could have be practically achievable in a real treatment system.

#### 2. Effect of Pressure

Reactor pressure effects were studied because pressure is clearly an important parameter in any system utilizing a gas/liquid mixture, and because no previously published studies could be found which adequately explained how pressure affects the combined ozone/ultrasound process.

#### 3. Effect of Ultrasonic Intensity

Ultrasonic intensity effects were studied to determine how ozone/ultrasound process effectiveness is affected by power input. Since ultrasonic power input represents an operating cost, the effect of ultrasonic intensity is a qualitative indicator of the economics of the combined ozone/ultrasound process.

#### 4. Effects of Initial pH

The effect of initial pH was studied to determine the relative pH sensitivity of ozone alone versus combined ozone/ultrasound. The pH sensitivity of ozone and combined ozone/ultrasound gives an indication of what source waters may be more amenable to either treatment process.

#### 5. Effects of Radical Scavenging

The effect of the presence of radical scavenging compounds was studied to determine the relative contribution to dioxane removal from radical generation as opposed to direct interaction with ozone or removal from thermal ultrasonic effects. This effect was studied by comparing results obtained in drinking water with results obtained in drinking water with added bicarbonate (a hydroxyl radical scavenger) and results obtained in deionized water (no scavengers present).

#### 6. Model Combined Ozone/Ultrasound Process

A model for the combined ozone/ultrasound process was created to provide a tool for predicting the removal of 1,4-dioxane. While little data exists in published literature for 1,4-dioxane removal by combined ozone/ultrasound, attempts were made to compare other studies in other reactors to determine if the model could be expanded to other systems.

## **2.2. Significance**

This research is significant because it explored a treatment process that hasn't been well studied and because it centered on an emerging contaminant which is prevalent, harmful, and very difficult to treat. The contaminant 1,4-dioxane was chosen

because it is a good yardstick to measure the potential of an AOP for water reuse. Additionally, by utilizing a continuous flow reactor and a representative water reuse matrix (i.e. spiked drinking water), the results of this research are more easily translatable into real-world applications of the treatment technology. Finally, an empirical model was created and some preliminary work was done to evaluate the scalability of this model. It is hoped that this model, coupled the improved understanding of the ozone/ultrasound process gained from this research, will aid water operators looking to create optimized water treatment solutions. It is also hoped that this research could someday be used to meet the water needs of the future, either through a polishing treatment for water use/reuse or by providing safe drinking water in remote areas.

## CHAPTER 3. EXPERIMENTAL

### 3.1. Materials and Reagents

For this research, 1,4-dioxane (99.9%), 1,4-dioxane  $d_8$  (99%), methylene chloride (99%), sodium bicarbonate (ACS grade), and sodium chloride (ACS grade) were purchased from Sigma Aldrich. Sodium thiosulfate (ACS grade) used for ozone quenching was purchased from Fisher Scientific. To adjust pH, concentrated hydrochloric acid from Fisher Scientific and sodium hydroxide ( $\geq 97.0$ ) from Sigma Aldrich were used. Deionized water was obtained from a Barnstead NANOpure Diamond ultrapure water system. This system utilizes a four stage deionization process, combining UV, ultrafiltration, and a 0.2  $\mu\text{m}$  filter, capable of producing water with resistivity of up to 18.2  $\text{M}\Omega/\text{cm}$  (Barnstead Thermolyne, 2000).

Drinking water from the Philadelphia Water Department (mixture of water from Baxter Treatment Plant and Queen Lane Treatment Plant) was used for the majority of experiments. Spiked drinking water was chosen because it simulates water meant for human consumption, either as direct or indirect potable reuse, which has been through a conventional water treatment train (settling, coagulation, filtration, disinfection), yet still contains 1,4-dioxane, necessitating some subsequent or “polishing” treatment by an AOP. Average characteristics for this water are given in the table below:

*Table 3-1 Drinking Water Characteristics*

<b>Total Organic Carbon</b>	1.95 $\pm$ 0.32 ppm
<b>Total Inorganic Carbon</b>	7.85 $\pm$ 1.22 ppm
<b>pH</b>	7.01 $\pm$ 0.39 (Philadelphia)

	Water Department, 2014)
<b>Total Chlorine Residual</b>	1.26-3.55 ppm at treatment plant (degassed prior to experimentation)  (Philadelphia Water Department, 2014)
<b>1,4-Dioxane</b>	0.10 (0-0.16 range) ppb  (Philadelphia Water Department, 2014)

A suitable reactor was constructed in order to study the combined effects of ozone and ultrasound in a flow through system. This reactor is comprised of: two high density polyethylene (HDPE) tanks (1,000 liters each), one each for storing the untreated and treated water, two pumps, the first for adjusting flow and the second for providing pressurization for the reactor, a Wedeco ozone generator, a one-way valve for ozone injection, a static mixer, an Orbisphere aqueous ozone measurement system, a 2.57 L stainless steel sonication chamber, a 20 kHz Telsonic ultrasound generator and longitudinal probe, a cooling system, a throttle valve to provide controllable water pressure within the system, a degassing column, stainless steel tubing for water, a three way valve for sampling, as well as various stainless steel fittings.

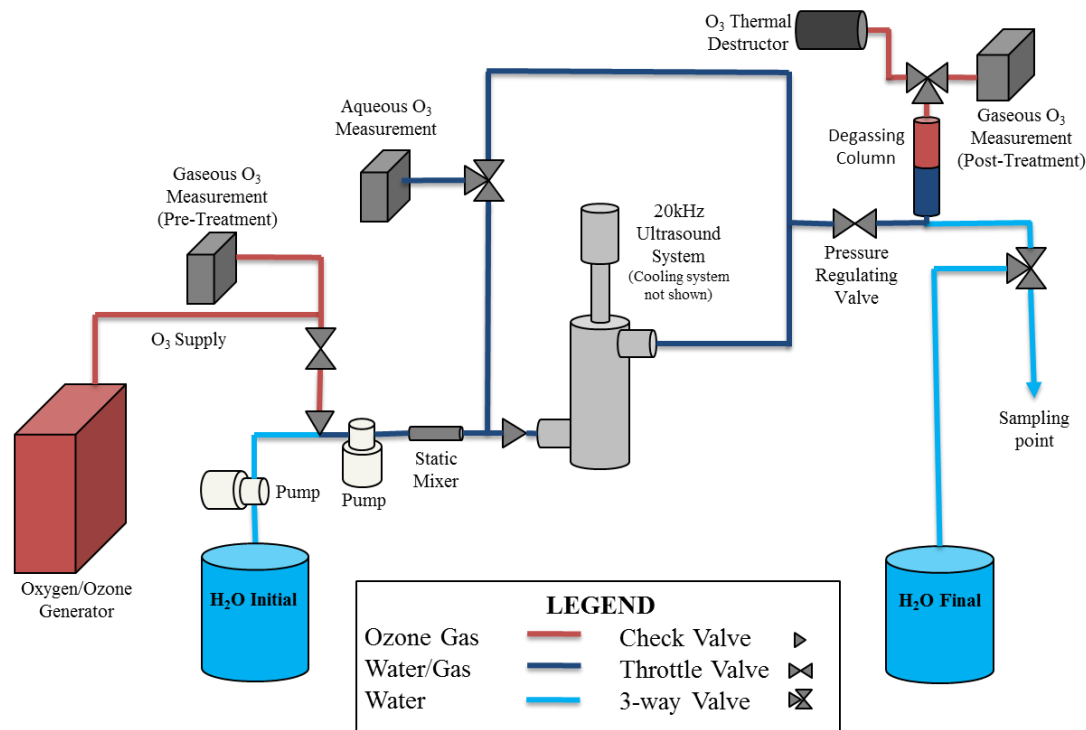


Figure 3-1 Experimental Schematic

## 3.2. Experimental Design

### 3.2.1. Objective 1: Effects of Ozone Dose and Residence Time

Testing the effects of varied ozone dosages and varied treatment times was conducted via a suite of experiments with treatment times spanning 2.5 to 16 minutes and aqueous ozone dosages from 1 to 15 mg/L. For this and other objectives, an initial concentration of 20 µg/L (parts-per-billion) 1,4-dioxane was chosen because it was high enough to permit quantification, yet low enough to be environmentally relevant for water reuse applicability (Zenker, Borden, & Barlaz, 2003). The experimental procedure is detailed in the following paragraph.

Prior to beginning the experiment, cleaned and labelled glassware was prepared by injecting 0.1 N sodium thiosulfate solution into glassware, to quench any ozone remaining in the samples. The sodium thiosulfate (0.1 M) was added in a ratio of 1  $\mu$ L for each 1 mL of sample. The system was flushed with the 1,4-dioxane/tap water mixture from the influent tank. During flushing, the flow rate was set by making adjustments to the first of two pumps in series. The flow rate was determined by weight using a Hanhart timepiece and an Ohaus digital scale. Once the flow rate was set, the system was flushed for at least two additional chamber retention times, to ensure that any residual water from prior test was flushed. Additionally, the ozone generator was turned on and allowed to warm up during the initial flush. The ozone generator stabilized in about 15 minutes, typically. While warming up, the ozone generated was diverted by a valve to a thermal destructor unit (not shown in figure). After flushing was complete, the initial, untreated, samples were drawn from the sample point. After initial water samples had been drawn, ozone was injected into the water stream between the two pumps. The ozone generator manometer was adjusted to maintain a constant 0.5 bar reading, and the generator's rotameter was adjusted to maintain constant volumetric gas flow into the water. The Orbisphere display was used to adjust the ozone levels in the water, and all subsequent ozone adjustments were made by changing only the weight percentage setting. This ensured a constant gas injection rate and only the ozone/oxygen ratio would change. Once the desired aqueous ozone level was achieved, the system was monitored and data recorded for at least twice the chamber retention time to ensure a quasi-steady-state was reached prior to sampling. A tracer study was used to confirm that quasi-steady-state was reached after two retention times. This study is outlined in section 4.6.1. After achieving

quasi-steady state, the ozonated samples were drawn, and the Telsonic ultrasound generator was turned on. Again, the system parameters, including ultrasonic power output, were monitored and recorded for at least twice the chamber retention time. After again reaching quasi-steady state, samples were drawn for the combined ozone/ultrasound process. Next, the Telsonic ultrasound generator was turned off and adjustments to the ozone generator weight percentage were made to prepare for the next set of experimental conditions. This process was completed for each of the desired aqueous ozone conditions. Samples were also taken using only ultrasonic treatment. These were done in much the same way, with ultrasound being applied for at least two chamber retention times prior to sampling. However, these samples were taken either before the ozone was applied, or after the ozone generator had been turned off and the measured aqueous ozone had returned to zero  $\mu\text{g/L}$ .

### 3.2.2. *Objective 2: Effect of Pressure*

Pressure effects were tested in two separate sets of experiments. In the first set, constant aqueous ozone concentration was maintained as pressure increased. In the second set, constant air phase ozone concentration was maintained. For the constant aqueous phase concentration tests, a pressure control valve was adjusted to the desired level while monitoring the analog and digital pressure readings. For a given input of air phase ozone, the aqueous ozone readings increased predictably at the higher pressures. So, to compare the effect of just pressurization, the weight percentage was reduced on the ozone generator until the desired aqueous ozone level was achieved. Once the desired pressure and ozone levels stabilized, the system was allowed to run for a minimum of two retention times prior to sampling.

For the constant aqueous phase concentration tests, the ozone generator was set to provide the desired aqueous ozone concentration for the unpressurized condition. Air phase ozone concentrations were noted throughout the experiment. For higher pressure tests, adjustments were made to the pressure control valve, but no changes were made to the ozone generator. As before, the reactor was allowed to reach quasi-steady state before each sample was taken. These tests were aimed at learning the net operational advantages of a pressurized combined ozone/ultrasound reactor.

### *3.2.3. Objective 3: Effect of Ultrasonic Intensity*

Experiments were made to determine the effect of ultrasound power. A control set of tests was performed at 100% ultrasonic intensity and another set of experiments was carried out at 25% intensity. The 25% value was chosen because the power output did not vary linearly with the intensity on the ultrasonic generator. For both intensity conditions, samples were taken for initial, ultrasound-only, ozone-only, and combined ozone/ultrasound conditions.

### *3.2.4. Objective 4: Effect of Initial pH*

The effect of the pH of the water to be treated was studied, as well. An aqueous ozone concentration of 2.5 mg/L was chosen for this set of experiments. A suite of experiments was performed at pH 4 and pH 10 to compare with previous results at neutral pH. No additional reactor pressure was employed. Drinking water was spiked with 20 ppb of 1,4-dioxane, and adjustments were made by adding sodium hydroxide or hydrochloric acid. Samples were taken for ultrasound alone, ozone alone, and combined ozone/ultrasound and multiple treatment times were used. Prior to sampling, the reactor

was allowed to reach quasi-steady state. The pH of effluent was also measured when each sample was drawn.

### 3.2.5. *Objective 5: Effect of Radical Scavenging*

To test the effects of radical scavenging, experiments were carried out with varied doses of bicarbonate (100 mM, 10 mM, 1 mM, 0 mM). Bicarbonate acts as a radical scavenger, reacting quickly with hydroxyl radicals,  $k_{\text{OH}\cdot/1,4\text{-dioxane}}=8.5\times 10^6 \text{ M}^{-1}\text{s}^{-1}$ , slowly with ozone,  $k_{\text{O}_3/\text{HCO}_3}\ll 0.1 \text{ M}^{-1}\text{s}^{-1}$ , and acting to retard the breakdown of ozone (Glaze & Kang, 1989) (Glaze W. H., 1987) (Staehelin & Hoigne, 1982) (Elovitz & von Gunten, 1999) (Buxton, Greenstock, & Helman, 1988). Bicarbonate was not expected to significantly affect removal by direct ozone attack or by pyrolysis or other non-radical consequences of ultrasonic cavitation. Therefore, any changes in removal after the addition of bicarbonate were assumed to be the result of increased competition for radicals in the matrix.

These experiments evaluated the removal of 1,4-dioxane by ultrasound alone, ozone alone, and combined ozone/ultrasound. As mentioned in an earlier section, ultrasound can remove organic contaminants in three ways: thermal destruction at cavitation sites, supercritical oxidation near the cavitation sites, and hydroxyl radical oxidation in the bulk liquid or bubble interfacial region. Under ultrasonic radiation, ozone molecules break down into oxygen molecules and oxygen radicals. These oxygen radicals, in turn, can react with a water molecule to form two hydroxyl radicals (Kang & Hoffmann, 1998) (Weavers & Hoffmann, 1998). Testing the effect of radical scavenging helped determine the relative contribution of hydroxyl radical oxidation to the overall removal of 1,4-dioxane.

Drinking water was used for the vast majority of experiments in this study. The drinking water matrix contains inorganic carbon already, acting as a scavenger. It also contains organic carbon, which acts to speed up the breakdown of ozone (Staehelin & Hoigne, 1985). To test how the systems perform in a scavenger-free matrix, sets of experiments using ultrasound, ozone, and combined ozone/ultrasound were done using deionized water that had been spiked with 20 parts-per-billion 1,4-dioxane.

#### *3.2.6. Objective 6: Reactor Modeling*

The system was modeled as a plug-flow reactor. Prior to modeling, the reactor was analyzed using a step-up tracer study. This was done early to verify that assumption that quasi-steady state would be reached by twice the retention time. Additionally, this study examined 1,4-dioxane removal using the  $R_{CT}$  concept that was developed by Elovitz and von Gunten. This analysis is useful simplification for exploring the removal mechanism for compounds which are removed by the hydroxyl radical by not by ozone itself (Elovitz & von Gunten, 1999). Finally, this study attempted a mass balance comparing the mass of 1,4-dioxane removed with the mass of aqueous ozone consumed.

### **3.3. Data Collection**

Data collection was aided by a custom Arduino UNO-based data collection device. This system writes elapsed time and sensor data to an SD card in a comma-separated-value text file. The system also displays current sensor conditions on a 16 X 2 liquid crystal display (LCD). See the figure below for a detailed schematic of this device, and Appendix A for the Arduino sketch (programming code). The system was

configured to read, display and record data for six experimental parameters and was powered by either USB, or a 9V, 750mA DC power converter.

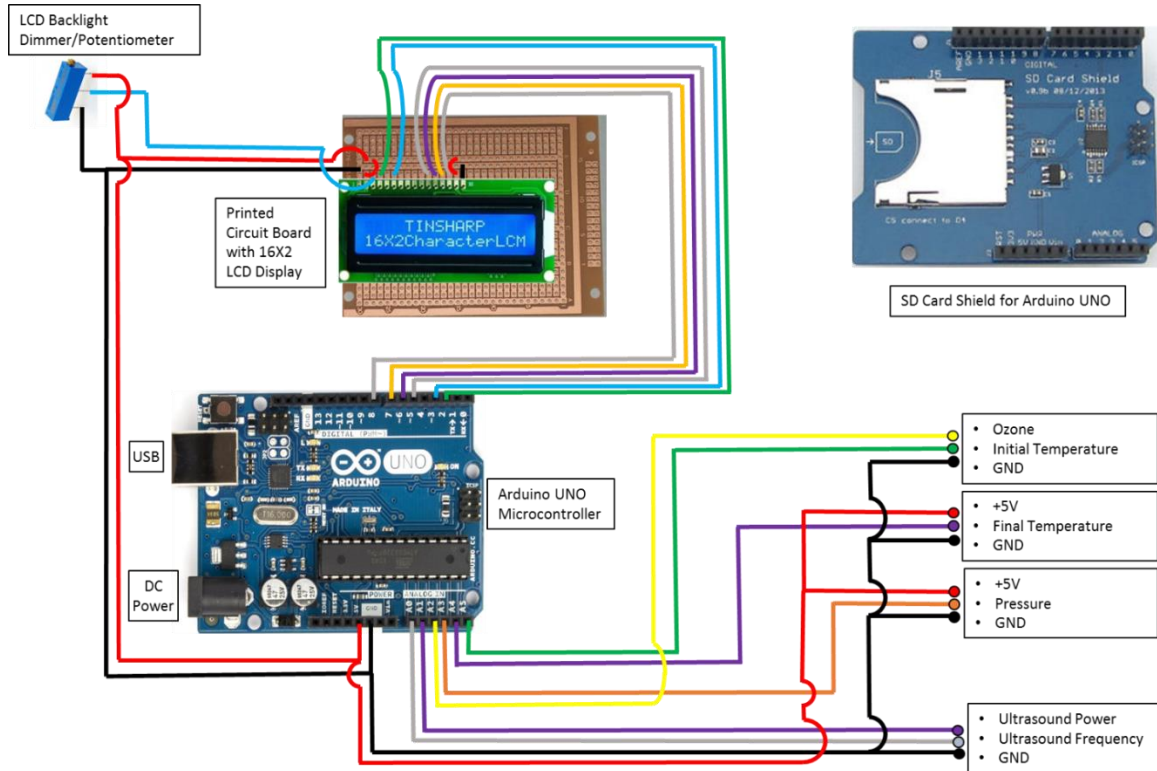


*Figure 3-2 Experimental Data Monitor*

The first channel measured the ultrasound power output of the Telsonic generator. The Telsonic generator outputs a 0-10 volt signal for current power output, with 10 volts corresponding to 2000 watts. This signal voltage is measured between pin 13 and pin 15 on the 25-pin D-Sub interface (Telsonic AG, 2006). To protect from circuit overload and to ensure compatibility with the Arduino UNO analog-to-digital converter (ADC), the 0-10 volt signal had to first be converted to a 0-5 volt signal. This was accomplished using a voltage divider with two matched resistors of 1 kΩ each.

The second channel measured the ultrasonic frequency output of the Telsonic generator. This signal voltage is given as a 5 volt waveform between pin 13 and pin 20

on the 25-pin D-Sub interface (Telsonic AG, 2006). The ADC was not needed to interpret this signal, so code was written to directly measure the period of the waveform. The period measured was then used to calculate the frequency of the signal.

The third channel measured the aqueous ozone content in the water, as measured by the Orbisphere 410. The Orbisphere has three user-configurable analog outputs, and aqueous ozone concentration was chosen for one of these outputs. The analog outputs were configured to output a 0-20 mA signal in tri-linear mode, to allow for the widest measurement range. A 0-1000  $\Omega$  potentiometer was adjusted to 250  $\Omega$ , and was used to create a current loop which converts the 0-20 mA output into a 0-5 volt signal. Tri-linear mode setup parameters were as follows: 0-1 volt was mapped to 0-1000  $\mu\text{g/L}$  aqueous ozone, 1-4 volts was mapped to 1000-10000  $\mu\text{g/L}$ , and 4-5 volts was mapped to 10000-15000  $\mu\text{g/L}$  (Hach Lange, 2009).

The fourth channel was used to measure water pressure in the sonication chamber. This was accomplished utilizing a Wells PS401 pressure transducer. This transducer requires a 5 volt supply, which was provided by the Arduino 5V output pin. The pressure transducer outputs a signal voltage that is linearly proportional to the pressure measured. Based on the manufacturer's data, the governing equation is given below.

$$Pressure (PSI) = \frac{(Volts - 4.5)}{0.0402} \qquad \begin{array}{l} \text{Equation 3-1} \\ \text{Pressure} \\ \text{Calculation} \end{array}$$

The fifth channel was used to measure the temperature of the water as it leaves the sonication chamber. This was accomplished using a TH44004 thermistor from

Omega. This thermistor has Steinhart-Hart constants of  $A=1.468*10^{-3}$ ,  $B=2.383*10^{-4}$ , and  $C=1.007*10^{-7}$ . The governing equation is given below (Steinhart & Hart, 1968).

$$\frac{1}{T(K)} = A + B \log R + C \log R(\Omega)^3 \quad \text{Equation 3-2} \\ \text{Steinhart-Hart}$$

With the Steinhart-Hart constants, the only independent variable required to calculate the temperature is the resistance of the thermistor (R in the above). To measure the resistance across the thermistor, a voltage divider was used, as depicted in the figure below.

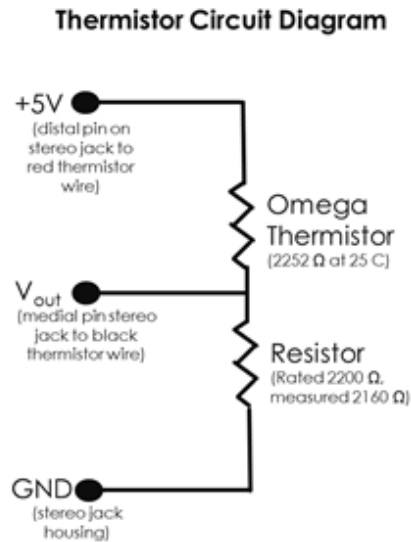


Figure 3-3 Thermistor Circuit Diagram

Using Ohm's law,  $V_{out}$  will be given by the following equation:

$$V_{out} = V_{in} * \frac{R_1}{R_1 + R_2} = 5V * \frac{R_1}{R_1 + 2160\Omega} \quad \text{Equation 3-3} \\ \text{Thermistor} \\ \text{Voltage}$$

The Arduino ADC is used to calculate  $V_{out}$ , and then the software solves for the unknown thermistor resistance ( $R_1$  in Eq. 2.3). Once the resistance is calculated, the

software uses the Steinhart-Hart equation to solve for the temperature, and convert that value into Celsius.

The sixth and final channel was used to record the influent water temperature, as measured by the Orbisphere 410. A second analog channel was configured to output a linear 0-20 mA signal for temperatures between 15 and 35 Celsius. A 0-1000  $\Omega$  potentiometer was adjusted to 250  $\Omega$ , and was used to create a current loop to convert the 0-20 mA signal into a 0-5 volt signal.

The data from each of these measurement channels was processed and displayed onto a 16 X 2 character LCD display. Due to the limited size of the display, the measurements were displayed on a cycle. Elapsed time, ultrasonic power, and aqueous ozone were displayed constantly, while one field cycled between initial and final temperature, and another field cycled between pressure and ultrasonic frequency. The cycles were controlled using software delays to be three seconds each, so that all available data was displayed and refreshed every six seconds, or 0.1 minutes. Every 0.1 minutes, data was also appended to a text file as comma-separated-values on an SD card. The SD card writer was part of a SD Card Shield attached directly to the Arduino UNO.

Throughout each experiment, data was also recorded manually using instantaneous readings from the various pieces of equipment and from analog pressure gauges. This was done both to ensure the accuracy of the digital readings, and to protect against data corruption or the loss of the SD card.

### **3.4. Analytical Methods**

#### *3.4.1. pH*

Initial and final pH measurements were obtained using either a Metler Toledo AT261 Delta Range pH meter or an Oakton 11 Series pH meter.

#### *3.4.2. Conductivity*

Conductivity for tracer studies were measured using an Oakton Multi-Parameter PCS Testr 35.

#### *3.4.3. Aqueous Ozone Concentration*

Aqueous ozone concentrations were measured using a Hach Orbisphere Model 410 Analyzer with a C1100 Ozone Sensor. This system uses an anode and cathode in an electrolytic solution, which is separated from the sample by a gas permeable membrane. Ozone penetrating through this membrane reacts at the cathode, causing an electrical current proportional to the partial pressure of the gas in the fluid being sampled (Hach Lange, 2010). The sensor and controller will be calibrated using the air calibration method, as per the manufacturer's recommendation.

#### *3.4.4. Gaseous Ozone Concentration*

Gaseous ozone concentrations were measured using a pair of identical BMT 964C Ozone Analyzers. The first analyzer measured the ozone/oxygen gas mixture before it was injected and the second measured the gas that was exiting from the degassing column.

#### *3.4.5. TIC/TOC Concentration*

Total inorganic carbon and total organic carbon were analyzed using an OI Analytical TOC 1030.

#### *3.4.6. Temperature*

The temperature of water entering the reactor was measured by a Hach Orbisphere Model 410 Analyzer with a C1100 Ozone Sensor. Temperature of water exiting the reactor was measured using a TH44004 thermistor from Omega.

#### *3.4.7. Reactor Pressure*

Pressure measurements were made using a PS401 pressure transducer as well as Dynamic Fluid Components analog dial gauges.

#### *3.4.8. Water Flow Rate*

Flow rates were measured in real time using a Hall effect flow meter with an Arduino controller. The measured flow rates displayed on the Arduino were used when making flow adjustments. Due to measurement fluctuations inherent to the Hall effect sensor and Arduino combination, all flow rates were confirmed by weight, using an Ohaus digital scale and Hanhart timepiece.

#### *3.4.9. Gaseous Flow Rate*

The flow rate for the ozone/oxygen mixture being injected into the reactor was measured and adjusted using an FM-6-2 ozone-compatible rotameter.

#### *3.4.10. 1,4-Dioxane Concentration*

Quantitative analysis of 1,4-dioxane was performed using liquid-liquid-extraction (LLE), followed by gas chromatography/mass spectrometry (GC/MS) analysis. A

100mL sample was spiked with a known amount of labeled internal standard (1,4-dioxane  $d_8$ ) and mixed with 25mL of methylene chloride in a 150mL separatory funnel. The aqueous phase was discarded and organic phase was used for analysis. The GC/MS analysis was performed using an Agilent 6890N GC coupled with a 5973N MS in Electron Ionization (EI+) mode. An SPB-624 fused silica capillary column (30 m X 0.25 mm x 1.4  $\mu$ m film thickness) was used. High purity helium was used as a carrier gas with a flow rate of 1 mL/min. Auto injections were made using splitless mode, with an injection volume of 3  $\mu$ L. Injection temperature was 250°C and the head pressure was 60 kPa of helium. Initial oven temperature was 45°C, held for 1 minute, and then ramped to 90°C at a rate of 7°C/min. Finally, the oven temperature was ramped to 200°C at 30°C·min<sup>-1</sup> and held for 5 minutes. Transfer line temperature to the MS was maintained at 230°C, electron energy was 70 eV, and ion source temperature was 250°C.

The mass-to-charge (m/z) ratio of the labeled internal standard (1,4-dioxane  $d_8$ ) is 96, while 1,4-dioxane mass-to-charge ratio is 88. The heavier internal standard also elutes slightly faster than non-deuterated 1,4-dioxane, creating two distinct peaks in the chromatogram. The known concentration of internal standard is represented by the earlier-eluting peak at m/z=96 and the unknown concentration of 1,4-dioxane is represented by the later-eluting peak at m/z=88. Therefore, to calculate the concentration of 1,4-dioxane, the integrated area under the peak at m/z=88 was divided by the integrated area under the peak at m/z=96, and this value was compared to a calibration curve. The calibration curve was created using extracted standards. To create these standards, water was first spiked with a known aliquots of 1,4-dioxane. Next, a known aliquot of internal standard (1,4-dioxane  $d_8$ ) was added. Finally, liquid-liquid-extraction

using dichloromethane was performed exactly as described above. Calibration was quite consistent throughout all experiments, as noted in the figure below.

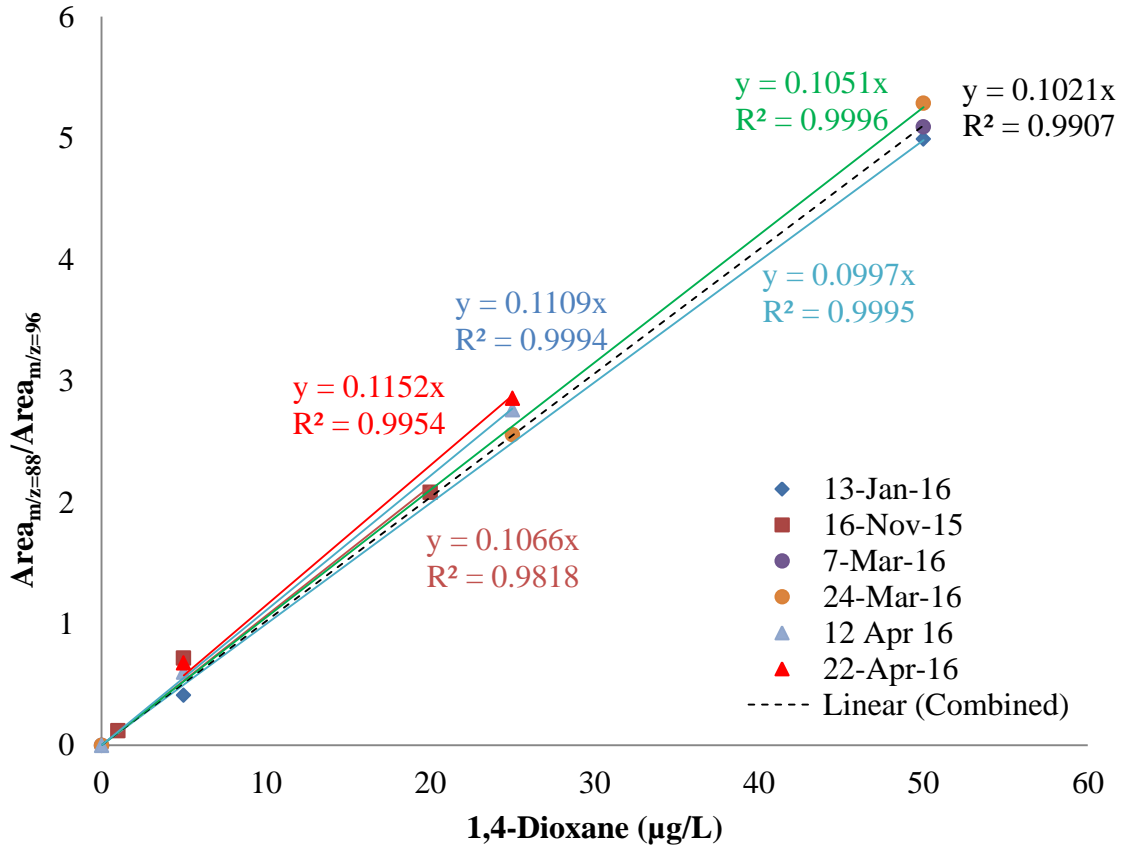


Figure 3-4 GC/MS Calibration Curves

Source Data in Table E2

## CHAPTER 4. RESULTS

### 4.1. Objective 1: Effect of Ozone Dose and Residence Time

A suite of tests were conducted to evaluate the effect of ozone dosage and residence time in the ozone/ultrasound system. For these tests, four chamber retention times were used (2.5, 5, 7.2, and 16 minutes), and five ozone concentrations were selected (1, 2.5, 5, 11, and 16 mg/L). The results of these tests are shown in Figures 4-1, 4-2, and 4-3.

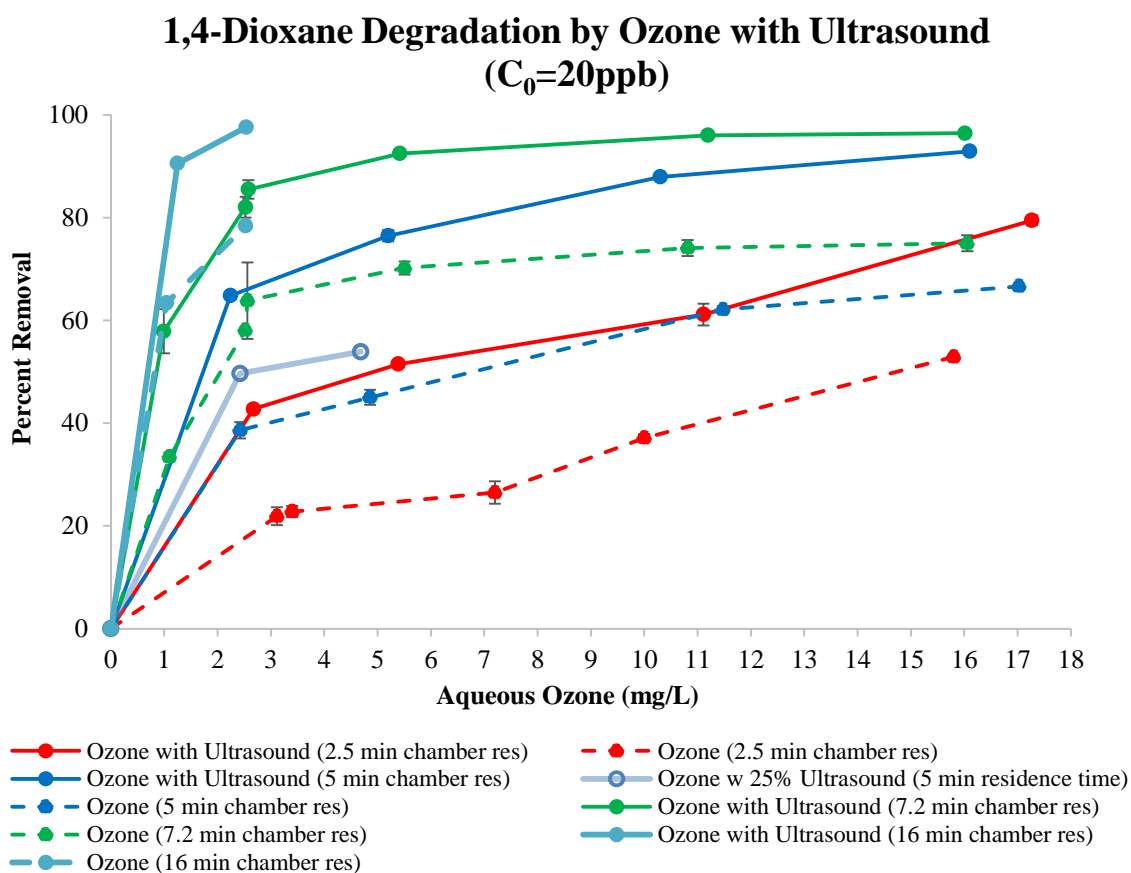


Figure 4-1 1,4-Dioxane Removal vs Ozone Dose

Source Data in Table E1

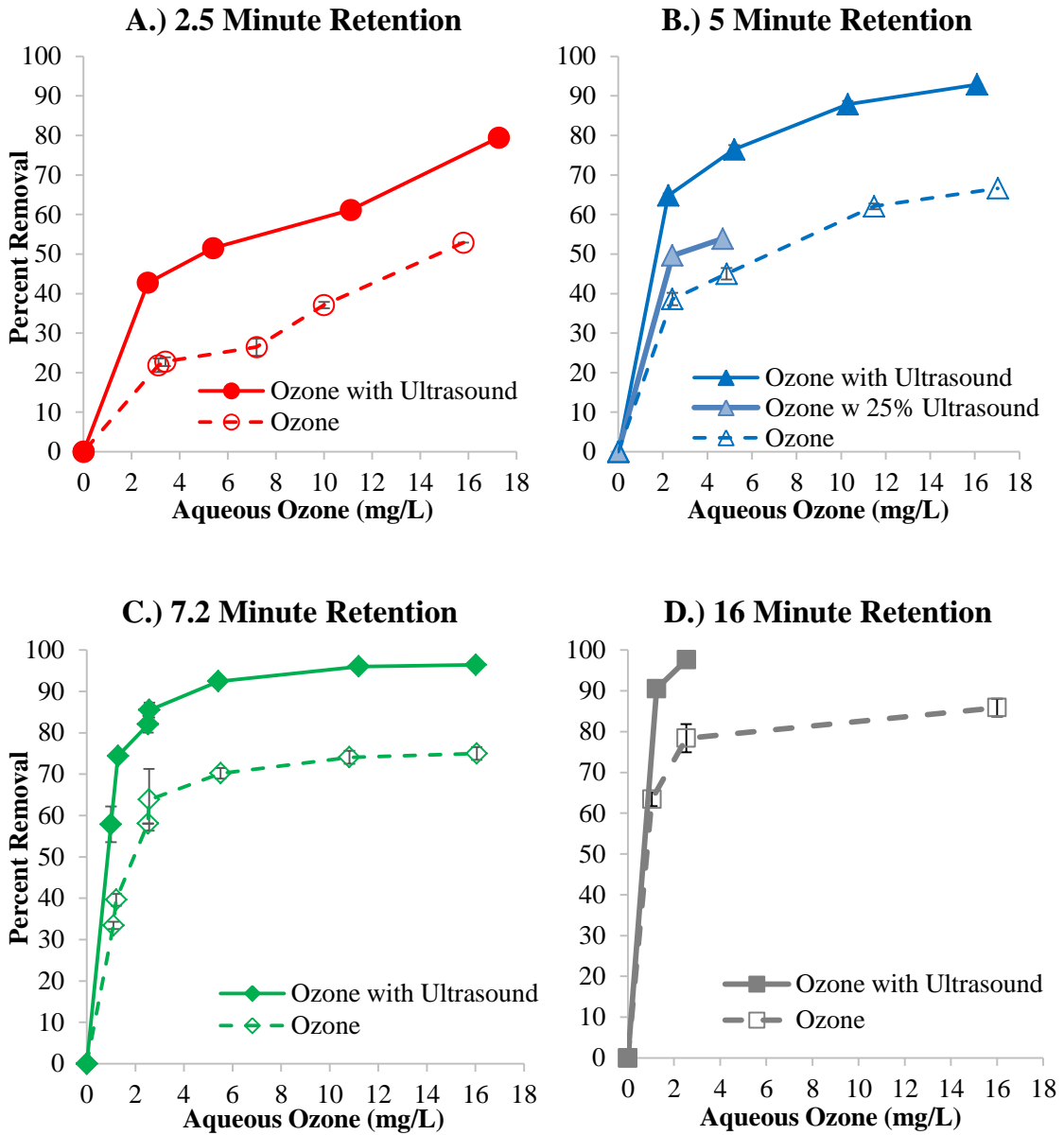


Figure 4-2 1,4-Dioxane Removal after A.) 2.5, B.) 5, C.) 7.2, and D.) 16 Minutes

Source Data in Table E1

These results can be sorted by aqueous ozone concentration and plotted as a collection of  $\ln(C/C_0)$  versus residence time curves, as shown in the following figure.

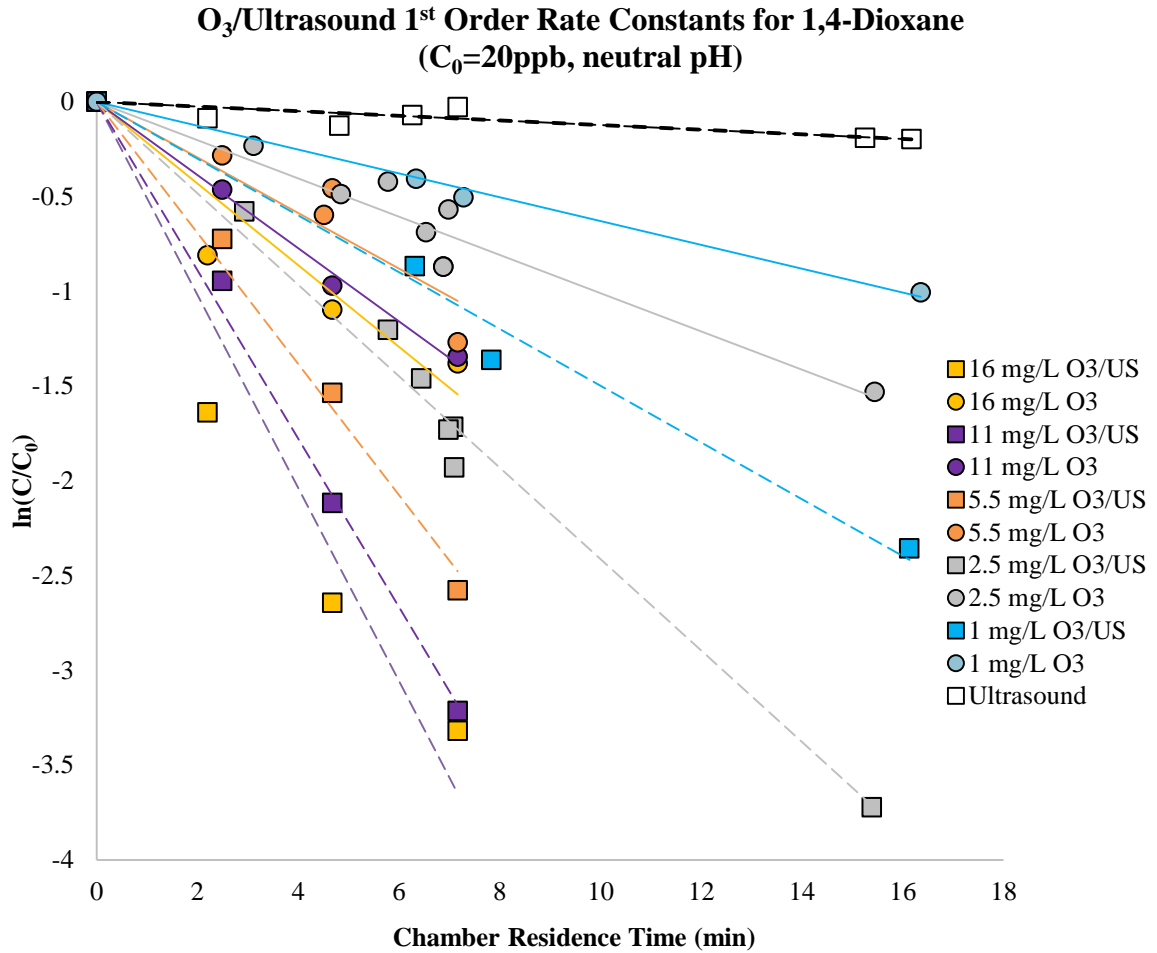


Figure 4-3 1,4-Dioxane Removal Pseudo-1st Order Curves

Source Data in Table E1

For a plug-flow reactor, the slope of the  $\ln(C/C_0)$  vs. time curve corresponds to the first order rate constant. These pseudo-1<sup>st</sup> order rate constants and their corresponding R-squared values are given in the table below.

Table 4-1 1,4-Dioxane Removal Pseudo-1st Order Rate Constants

Sample Set	k (min <sup>-1</sup> )	R <sup>2</sup>	Sample Set	k (min <sup>-1</sup> )	R <sup>2</sup>
0 mg/L O <sub>3</sub>	0	n/a	Ultrasound	0.0123	0.6396
1 mg/L O <sub>3</sub>	0.0618	0.9995	1 mg/L O <sub>3</sub> /Ultrasound	0.1449	0.9991
2.5 mg/L O <sub>3</sub>	0.1	0.9552	2.5 mg/L O <sub>3</sub> /Ultrasound	0.2402	0.9822
5.5 mg/L O <sub>3</sub>	0.1467	0.8766	5.5 mg/L O <sub>3</sub> /Ultrasound	0.3457	0.9904

11 mg/L O <sub>3</sub>	0.1931	0.9939	11 mg/L O <sub>3</sub> /Ultrasound	0.4442	0.9952
16 mg/L O <sub>3</sub>	0.2154	0.8616	16 mg/L O <sub>3</sub> /Ultrasound	0.5092	0.9284

The results from the tests of ultrasound alone yield results that are comparable to those published in the literature. Xu et al conducted the only other known study of combined ozone/ultrasound for the removal of 1,4-dioxane, and they found the ultrasound removal followed pseudo-first order reaction kinetics, where the rate constant,  $k$ , was a function of the ultrasonic power (Xu, Mochida, Naito, & Yasuda, 2012). Denoting  $P$  as the ultrasonic power input, in Watts, the rate constant, in  $\text{min}^{-1}$ , was found to vary as:

$$k = 2.6 * 10^{-5} * (P - 58)$$

*Equation 4-1  
Empirical  
Ultrasound Rate  
Constant from Xu  
et al*

The experimental setup was quite different in Xu et al, as a 16 cm long X 10 cm wide X 60 cm tall (9.6 L) batch reactor was used, along with an array of ultrasonic transducers placed on the vertical wall, operating at 490 kHz. This research utilized a continuous flow vertical cylinder (2.57 L) with a cylindrical ultrasonic probe mounted longitudinally within the reactor, operating at 20 kHz. However, applying the mean power from ultrasound-only tests (713 W) into the equation from Xu et al yields a first order rate constant of  $0.017 \text{ min}^{-1}$ . Considering the many differences in experimental setup, the estimate using the equation developed by Xu et al. compares reasonably well with the  $0.013 \text{ min}^{-1}$  obtained experimentally in this study. However, the comparisons for the ozone system and the combined ozone/ultrasound system are dissimilar. In Xu et al., the first order rate constant for ozone alone was just  $0.0025 \text{ min}^{-1}$  for a 2.5 mg/L aqueous ozone concentration (Xu, Mochida, Naito, & Yasuda, 2012).

Barndok et al reported a first order rate constant of  $1.2 \text{ min}^{-1}$  for 1,4-dioxane removal by ozonation in wastewater. In their study, ozone was pumped into a semi-batch reactor continuously to ensure that the ozone was always in excess, permitting a simplified estimation of the first order rate constant calculation. The synthetic wastewater solution used in the Barndok et al study contained 247.8 mg/L of 1,4-dioxane<sub>0</sub> and 450 mg/L COD<sub>0</sub>, however the ozone dosage was not reported (Barndok, Cortijo, Hermosilla, Negro, & Blanco, 2014). In the current study using spike drinking water, the rate obtained experimentally was  $0.24 \text{ min}^{-1}$ , an increase of two orders of magnitude over that reported by Xu et al ( $0.0025 \text{ min}^{-1}$ ), but only 20% of Barndok et al ( $1.2 \text{ min}^{-1}$ ).

There are three suspected causes for this discrepancy across these studies: matrix differences, mass transfer advantage in the continuous flow reactor, and differences in kinetics for continuously mixed flow versus plug flow reactors. Xu et al reported neither the type of water used nor the experimental pH. Assuming it was neutral, pH fails to account for the dramatic difference. Additionally, Xu et al didn't report the matrix which was used, so that may have differed from the drinking water used in this study. Different matrices can contain different promotor and scavenging compounds. The results of the current study for the removal of 1,4-dioxane by ozonation fall between the results obtained by Barndok et al and Xu et al (Barndok, Cortijo, Hermosilla, Negro, & Blanco, 2014) (Xu, Mochida, Naito, & Yasuda, 2012). Matrix differences likely explain some of discrepancy in reported ozonation rate constants since the current study used a drinking water matrix, with characteristics falling between the unreported, but presumably deionized, water used by Xu et al and the simulated wastewater used by Barndok et al.

Mass transfer differences offer another possible explanation for the discrepancy with Xu et al and Barndok et al. The mass transfer coefficient,  $k_La$ , was not reported for either study. Additionally, Barndok et did not report ozone concentration, only that ozone was considered “in excess” throughout the experiment, so no direct comparisons can be made. However, there was certainly more efficient mass transfer occurring in the continuous flow reactor than the batch reactor in the Xu et al study. The flow through reactor had an ozone injector just upstream of a high speed pump and a static mixer, while Xu et al utilized a bubble column. Qualitative differences in mass transfer coefficient ( $k_La$ ) values become evident when comparing the relative concentrations of air phase and water ozone in both systems. Xu et al injected 101.5 mg/L ozone (air phase) to achieve 2.5 mg/L ozone in the water phase, only reaching steady state after approximately 40 minutes. In this study, a mere 11 mg/L ozone (air phase) was found to raise the aqueous phase concentration to 2.5 mg/L under typical experimental conditions. Given the intense mixing and pressure effects from the pump and static mixer, it is possible that aqueous ozone concentrations in the flowing water locally exceeded the concentrations that were measured just downstream of the static mixer. This possibility could not be fully tested in the reactor used for this study. However, if  $k_La$  differences arising from the pump and static mixer were causing a hundred-fold increase in first order rate constant, it would imply that the majority of 1,4-dioxane removal was occurring before the water reaches the sonication chamber. This chamber is where the water spends the vast majority of its time during experiments, owing to the relatively large volume of the reactor in comparison to the small volume of the associated plumbing. To test the degree to which 1,4-dioxane degrades before entering the ultrasound reactor, a set

of tests was run using identical flow rates and ozone doses. In the first case, the water was sent through the reactor, as is done in typical experiments. In the second case, the water was diverted to sample port located between the static mixer and the reactor, bypassing the sonication chamber completely. The results for these tests can be found in the figure below (results for ultrasound alone can't be reported if the chamber is bypassed).

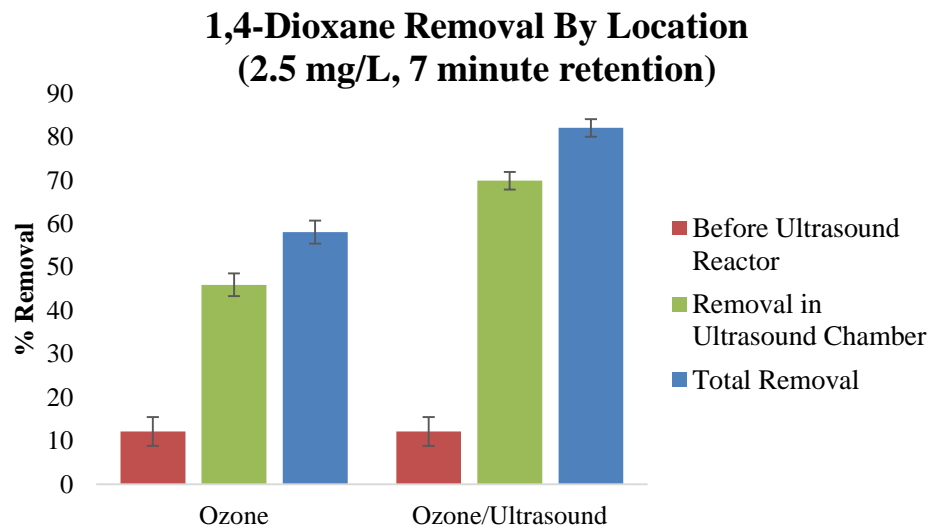


*Figure 4-4 1,4-Dioxane Removal By Location*

*Source Data in Table E6*

In the experiment depicted above, 12.2% of 58.1% total removal in the ozone system and 12.2% of 82.0% total removal in the combined ozone/ultrasound system was found to be occurring before the ozone/water mixture entered the ultrasonic reactor vessel. Since the mixing zone comprised only 88 mL (3.4%) of the total reactor volume, such a significant percentage of removal was not expected to occur in the mixing zone. So an additional set of experiments was performed to compare the relative removal

contributions from the injection site and piping with those contributions from the static mixer. To test this, ozonation tests were run at neutral pH. The first set of tests measured total 1,4-dioxane removal from ozonation at the reactor exit. The second set of tests bypassed the reactor and measured the removal occurring in the mixing zone, i.e. gas injection site and static mixer. For the third set of tests, the static mixer was removed and replaced by a section of steel tubing of equivalent internal diameter and volume, and total 1,4-dioxane removal was measured at the reactor exit. The last set of tests bypassed the reactor and measured the removal occurring in the mixing zone, but this time without the static mixer. The results of these are below.

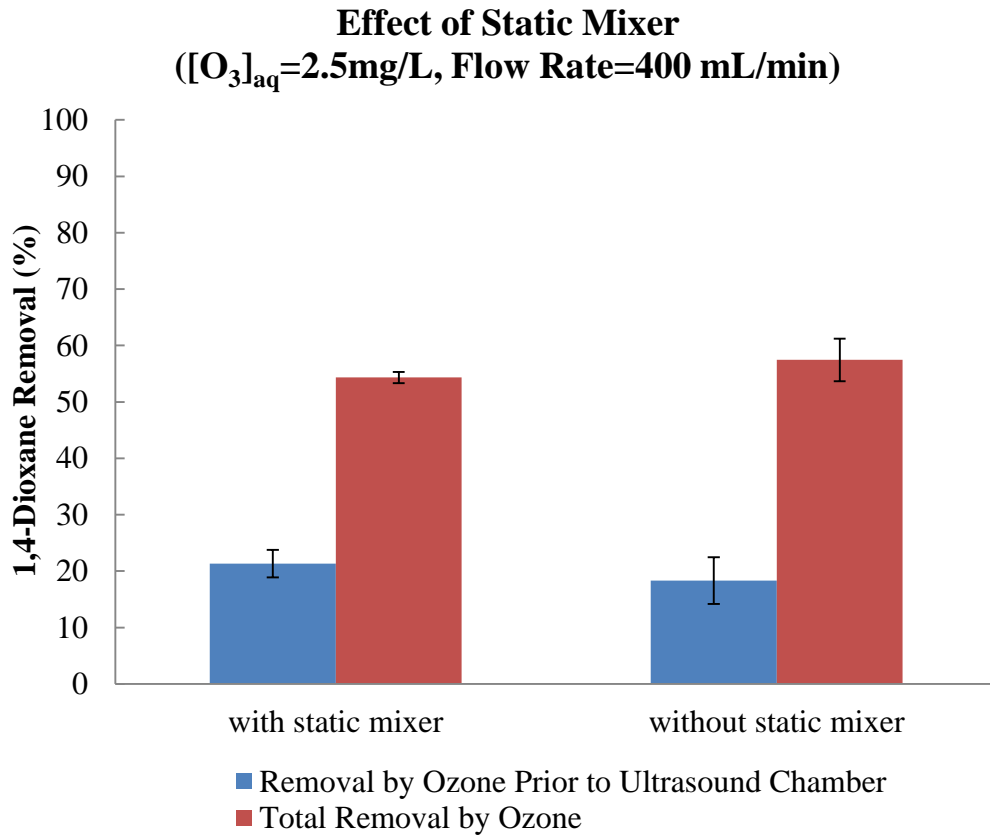


Figure 4-5 Effect of Static Mixer

Source Data in Table E6

For these tests, the measured aqueous ozone concentration was unchanged when the static mixer was replaced with an equivalent piece of ordinary pipe. Additionally, the change in measured flow rate and pressure was negligible after static mixer removal. Based on the standard deviation for the results depicted the figure above (shown as error bars), it appears that the effect of the static mixer on the removal of 1,4-dioxane is negligible.

While the removal occurring in the mixing section was found to make up a meaningful percentage of total removal in the ozone system ( $12.2/58.1=21\%$ ) and combined ozone/ultrasound system ( $12.2/82.0=14.9\%$ ), it is not large enough to account for the two order of magnitude difference in rate constants noted in this study compared to those in Xu et al.

The final likely cause for the greater dioxane removal observed in this study over that reported Xu et al. is the difference in kinetics between continuously mixed flow reactor and continuous flow/plug flow reactors. The reactor used by Xu et al. was a continuously stirred semi-batch reactor. While the water in the reactor was mixed and recirculated, the ozone was pumped in at the bottom, and exited at the top of the stirred tank. In this study, the water and ozone both entered at the inlet and exited at the outlet, as in a plug flow reactor. This has implications on the reaction kinetics for the ozone. For an ideal plug flow reactor, kinetics are dependent on the initial concentration of ozone. However, the kinetics of a continuously mixed flow reactor depend on the final, or in-tank, concentration of ozone, which is lower than the initial concentration. While the reactor used in this study was not behaving as an ideal plug flow reactor (please refer to section 4.6.1 for more on this), it was not a continuously mixed flow reactor either.

Therefore, inasmuch as the continuous flow reactor used for this study approached the performance of a plug flow reactor, it would have an advantage over the continuously mixed flow reactor employed in Xu et al.

#### *4.1.1. Implications of Ozone Dose and Residence Time*

The results showed that the removal of 1,4-dioxane by both ozonation and combined ozone/ultrasound was highly dependent on the applied ozone dose and residence time. For the combined ozone/ultrasound system, synergistic effects were observed; i.e. removal of 1,4-dioxane exceeded the sum of removal that would be expected by ozone and ultrasound alone. Ultrasonic cavitation is a complicated process, with associated thermal and pressure effects, which also have the potential to cause radical formation. Ozonation is more easily understood, but the propensity of ozone to break down into hydroxyl radicals is dependent on interactions with other aqueous compounds, the most notable of which is the hydroxide ion. When ozone and ultrasound are combined, the complexity is multiplied. Rather than examine all of the myriad possible outcomes of this combination, this study focused on the outcomes which drive 1,4-dioxane removal, which is the formation of hydroxyl radicals. The concept of  $R_{CT}$  describes the yield of hydroxyl radical per unit of ozone consumption, and will be expanded upon in chapter 4. This tool was used to simplify the combined ozone/ultrasound system into a value which was found to be predictive of 1,4-dioxane removal across all pH conditions, pressure conditions, ozone concentrations, treatment times, and ultrasonic intensities which were investigated in this study.

The findings of this study indicate that increased removal of 1,4-dioxane can be achieved through increasing ozone dosage, increasing residence time, or increasing both.

In a real-world application of the combined ozone/ultrasound system, the size of the reactor would determine the treatment time for a chosen flow rate, and reactor size is primarily a capital expense. There is a capital cost associated with achieving a desired ozone dose, but ozone dosage can primarily be thought of as an operating expense. The results of this study indicate that if the influent concentration of 1,4-dioxane and target effluent concentration are known, a reactor could be designed to balance capital and operating expenses to adequately treat the water.

## **4.2. Objective 2: Effect of Pressure**

Two sets of experiments have been made to explore the effect of reactor pressure on 1,4-dioxane removal. In one set, constant air phase ozone dosage was maintained as pressure was increased, while in the other constant aqueous phase ozone dosage was maintained.

### *4.2.1. Constant Air Phase Ozone Dosage*

Constant air phase ozone dosage was maintained by monitoring the influent air phase ozone dosage and flow rate, as displayed on the influent BMT 846C ozone meter and Labcorp 0.2-2.0 L/min rotameter, respectively. As reactor pressure was increased, the aqueous ozone dosage was allowed to increase as well.

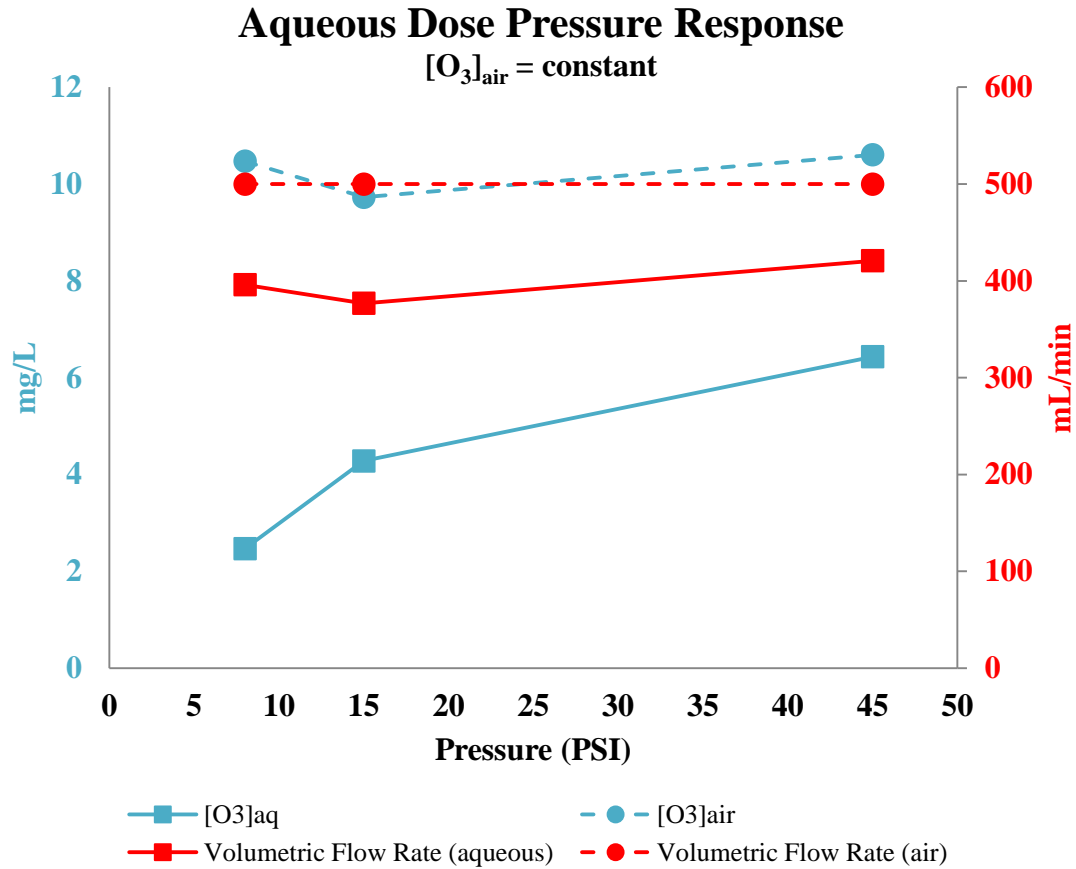


*Figure 4-6 Aqueous Dose Pressure Response for Constant Air Phase Dose*

*Source Data in Table E3, E8*

The figure above shows that constant air phase dosage was maintained while pressure was increased from 8, to 15, and finally 45 pounds per square inch (PSI). The aqueous ozone dose responded by increasing from 2.5 mg/L at 8 PSI, to 4.3 mg/L at 15 PSI and 6.4 mg/L at 45 PSI.

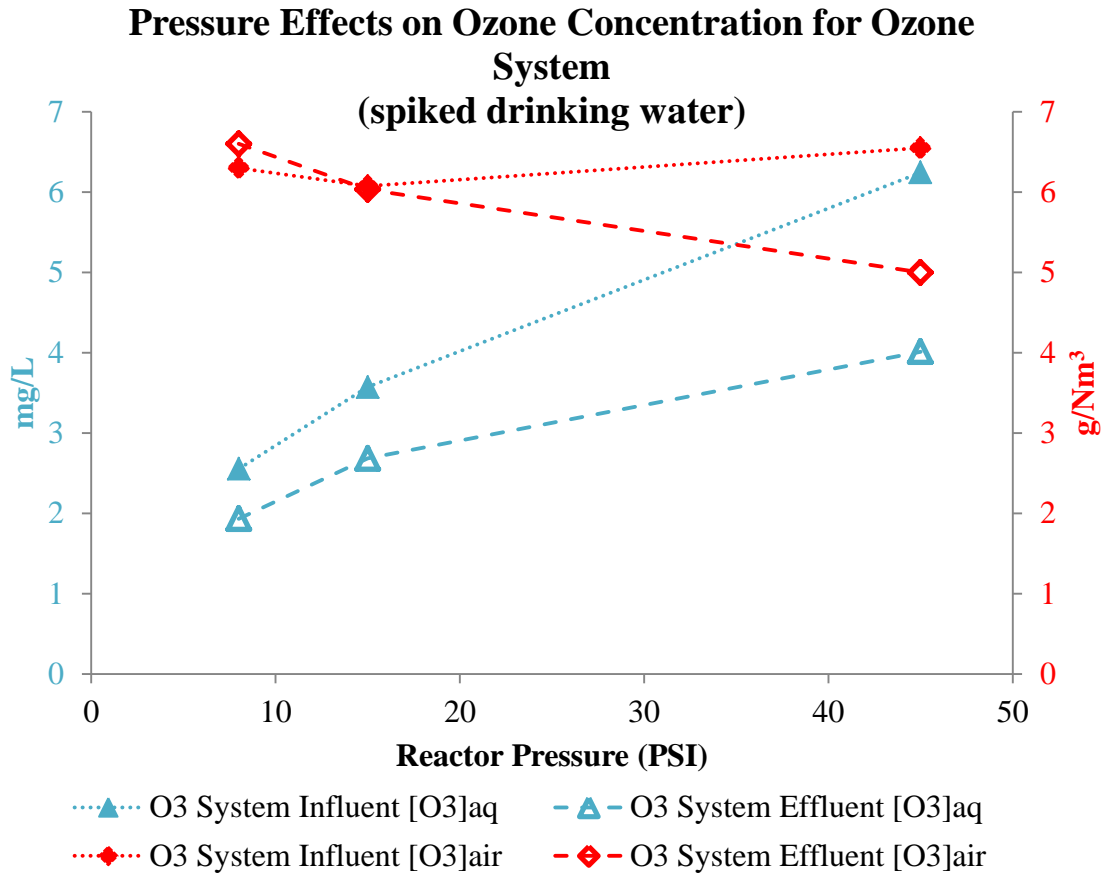


Figure 4-7 Mass Transfer Pressurization Effects for Ozone System

Source Data in Table E3

The figure above shows the changes to effluent ozone concentration in both air and aqueous phases as pressure is increased. For these tests, influent air phase ozone concentration was held constant (shown as solid red diamonds). The additional pressure has the greatest effect on influent water phase concentration, and modest effects on effluent concentrations in both air and water phases. At 8 PSI, it appears that the effluent air phase concentration is slightly higher than influent, but this is believed to be due to analytical error. Examining the water phase concentrations (blue triangles), it is clear that the additional pressure increasing the gap between influent and effluent

concentrations. Both influent and effluent aqueous ozone concentrations increase, but the effluent concentration increases more slowly, suggesting increased ozone consumption at higher pressures. Also, while the influent air phase concentration is roughly the same, the effluent concentration is showing a clear decline. This suggests that mass transfer is increasing with pressure.

The next figures show the pressure effects on air and aqueous phase ozone concentrations for the combined ozone/ultrasound system.

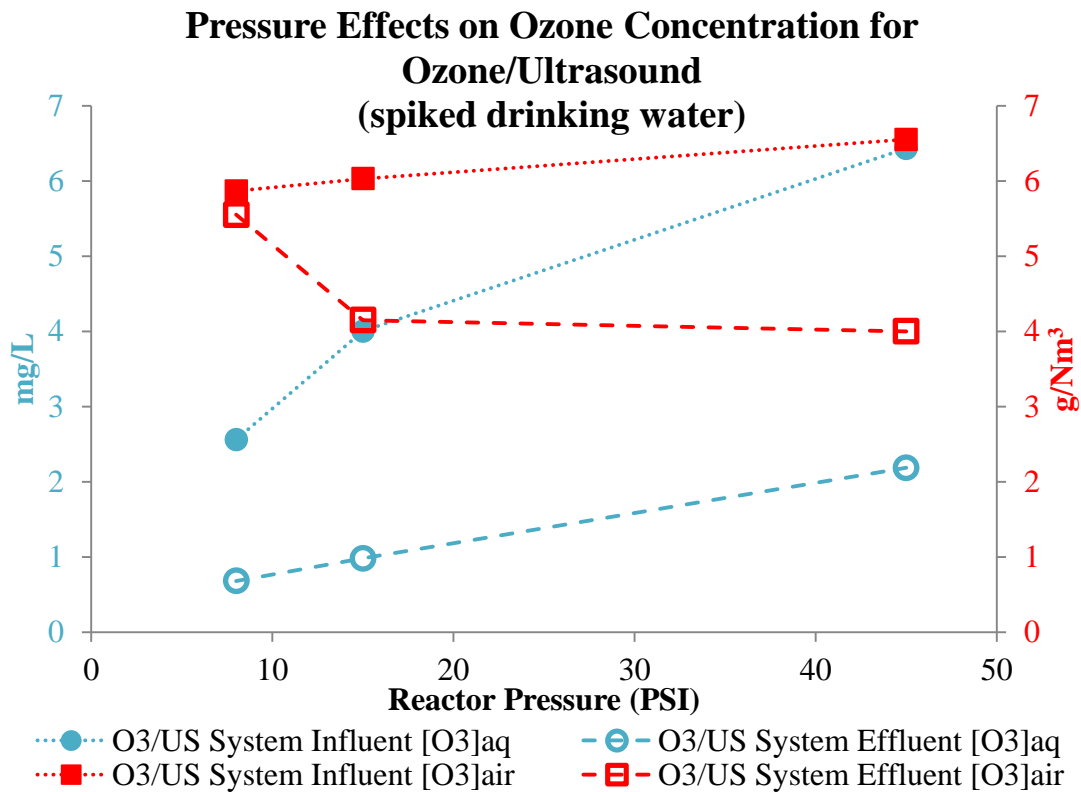


Figure 4-8 Mass Transfer Pressurization Effects for Ozone/Ultrasound System

Source Data in Table E3

This figure also suggests that increased pressure is increasing the ozone consumption. However, the consumption (represented by the span between solid and

hollow blue circles) is much greater at each pressure for the combined ozone/ultrasound system than it is for ozone alone. The span between influent and effluent air phase concentrations (solid and hollow red squares) also suggest that mass transfer is increasing with increased pressure as well, although this appears to flatten between 15 and 45 PSI.

In the figures above, it is clear that both influent and effluent aqueous phase concentrations increase with increasing pressure. The span between influent and effluent aqueous ozone concentrations (the distance between the dotted blue line and the dash blue line) increases with increasing pressure as well. This span denotes the aqueous ozone consumed during treatment. It is also evident in the figures above that this span is greater for the ozone/ultrasound system than it is for ozone alone, suggesting greater ozone consumption during sonication. This ozone consumption theory will be explored in more depth later as part of the  $R_{CT}$  analysis and discussion.

For the air phase concentrations, the trend is not as obvious as it is for aqueous phase, but the trend is still there. The air phase influent concentrations (red dotted lines) remain essentially the same as pressure is increased, as they should since that was the intent of the experiment. However, effluent air phase concentrations decrease with increasing pressure, as noted in the red dashed lines in both ozone and ozone/ultrasound systems. This, too, is expected, as increasing pressure is expected to drive more ozone gas into solution, leaving less ozone in the air phase. The spans between the red dotted and red dashed lines seem to support the hypothesis that sonication is driving mass transfer. This span increases with increasing pressure for both the ozone and ozone/ultrasound systems. However, at each pressure, the span for the ozone/ultrasound

system is greater than that for ozone alone. This ozone concentration data has also been plotted as percent change in Figure 4-9.

Increased ozone consumption during sonication in the aqueous phase explains the greater difference between influent and effluent aqueous concentrations. But, if sonication were only causing consumption in the aqueous phase, the air phase concentration would be unaffected. The only way air phase concentrations would change is if: sonication is decomposing gaseous ozone directly, sonication is causing mass transfer of ozone into aqueous phase, or some combination of the two. The constant aqueous phase ozone dosage experiments outlined in the next section yield further clues to the cause of this phenomenon.

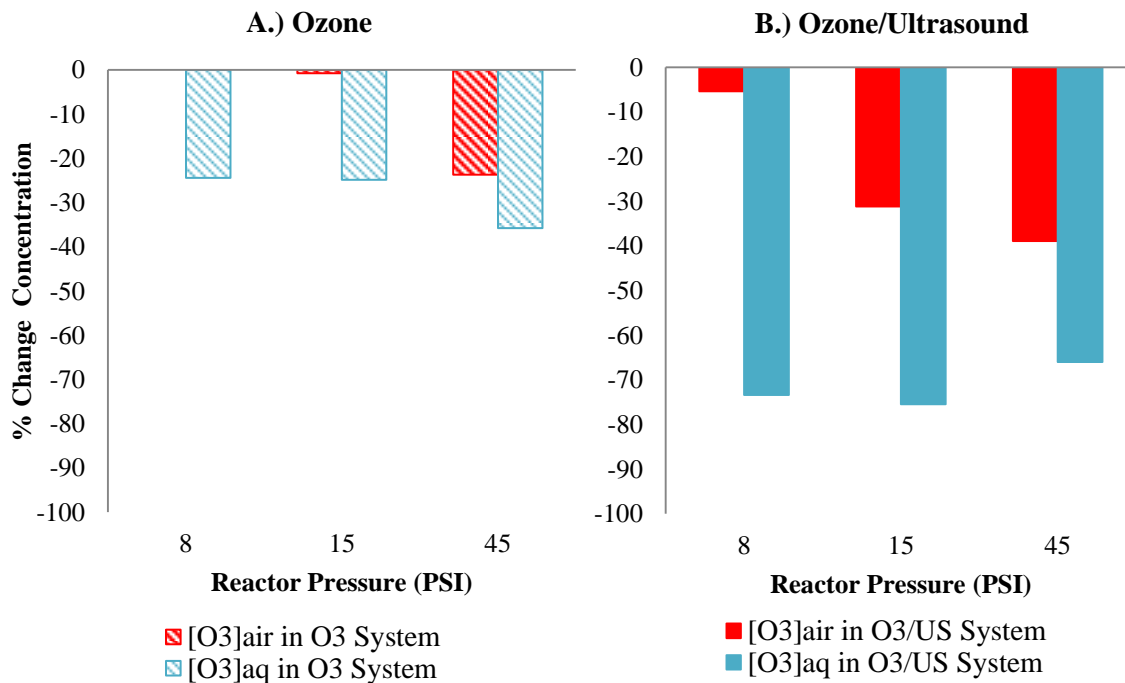


Figure 4-9 Pressure Effects on  $[O_3]_{air}$  and  $[O_3]_{aq}$  for A.) Ozone and B.) Ozone/US

Source Data in Table E3

Removal of 1,4-dioxane also responded to the increase in reactor pressure, with greater removal observed at 15 PSI and 45 PSI than that obtained at 8 PSI.

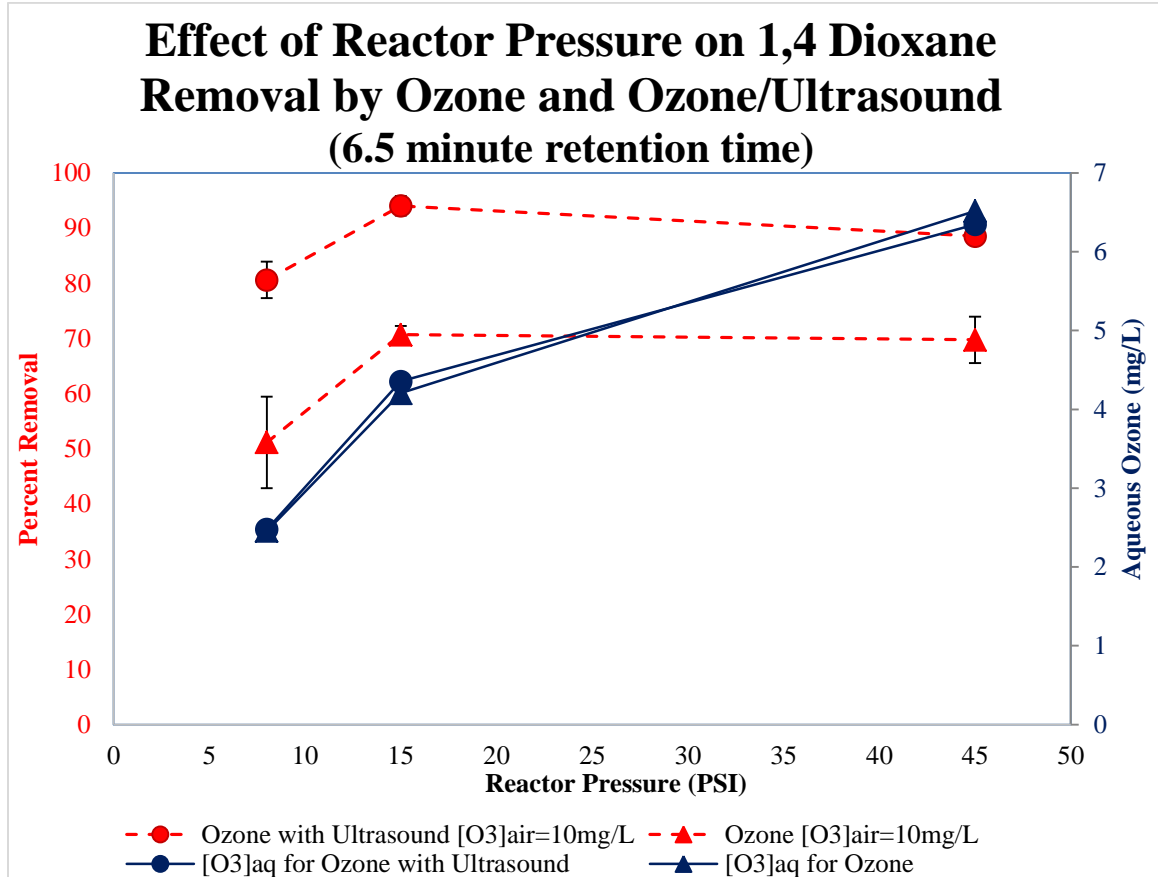


Figure 4-10 Effect of Pressure on 1,4-Dioxane Removal ( $[O_3]_{air} = 10 \text{ mg/L}$ )

Source Data in Table E3

In the figure above, it appears that there is a significant improvement in dioxane removal from increasing reactor pressure from 8 to 15 PSI. However, further increasing reactor pressure to 45 PSI was not found to yield additional improvement. This could be the result of elevated vapor pressure within the cavities causing a cushioning effect on the cavity implosion (Alliger, 1975).

#### 4.2.2. *Constant Aqueous Phase Ozone Dosage*

For the constant aqueous ozone dose experiments, constant aqueous ozone concentration was maintained while increasing pressure within the reactor. Water flow rate, i.e. reactor residence time, was held constant, as was the mass flow rate of the ozone/oxygen gas mixture. As pressure was increased, the weight percentage setting of the ozone generator was reduced until the desired aqueous ozone level was reached. Given the same water and gas flow rates through the reactor for each condition, it was assumed that any variance of the mass transfer coefficient,  $k_{La}$ , would be negligible throughout the experiment set, and any changes in dissolved ozone would be a function of the partial pressure of ozone. To confirm this assumption, the weight percentage of ozone was recorded. This weight percentage was first converted to a molar percentage. Then, the molar percentage was converted to a partial pressure for ozone using the measured reactor pressure and temperature and applying the ideal gas law. Finally, these calculated partial pressures were plotted versus the measured ozone concentrations, and the resulting slope was compared with published Henry's constant for ozone in water.

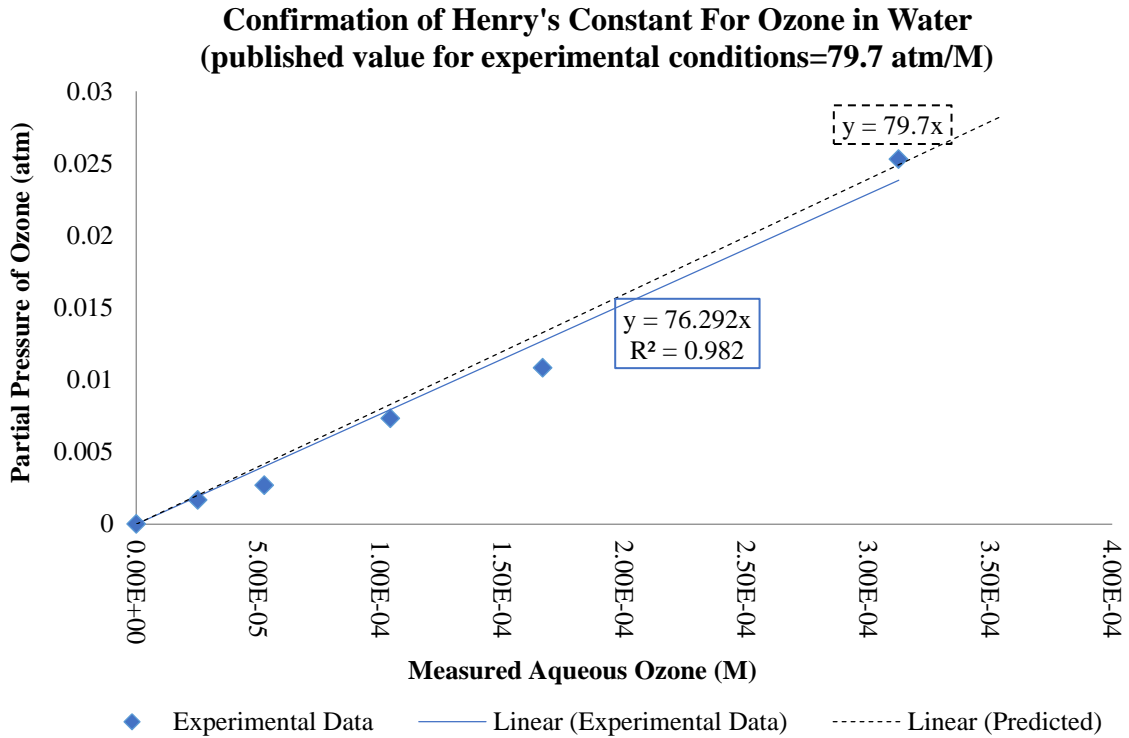


*Figure 4-11 Confirmation of Henry's Constant*

*Source Data in Table E4*

The results in the figure above support the assumption that any changes in the mass transfer coefficient,  $k_{L,a}$ , are negligible for constant flow rates. Additionally, there do not appear to be significant mass transfer limitations arising from the reactor mixing section.

## Ozone Wt % and Pressure Relationship

$$[\text{O}_3]_{\text{aq}} = \text{constant}$$

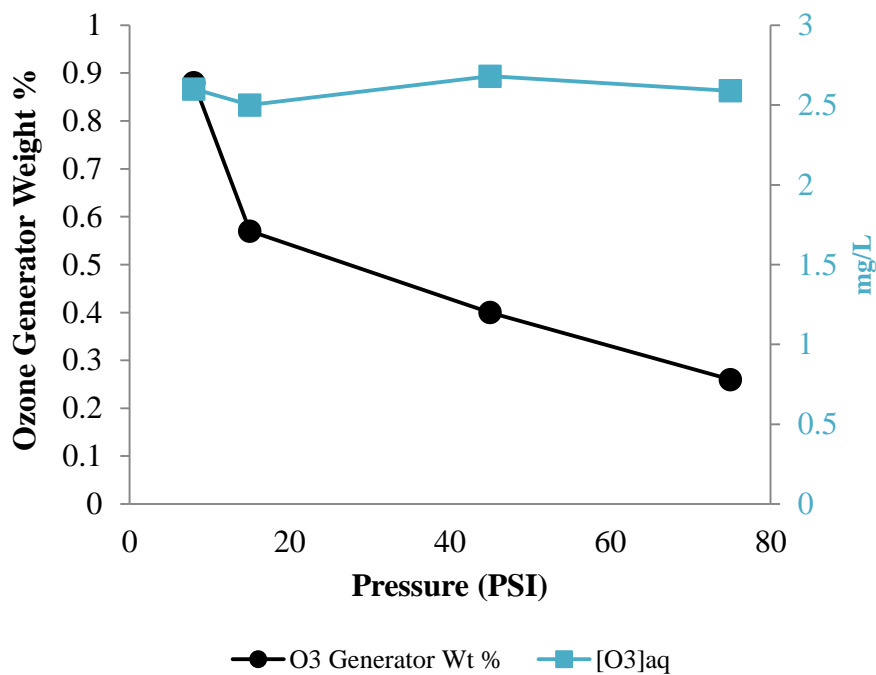


Figure 4-12 Ozone Weight Percentage and Reactor Pressures

Source Data in Table E3

The figure above depicts the relationship between the ozone generator weight percentage setting (black circles, primary y-axis) and the aqueous ozone (blue squares, secondary y-axis) as pressure is increased. The aqueous ozone concentration was able to be maintained at ~2.5 mg/L even as pressure was increased.

### 1,4 Dioxane Removal by Ozone and Ozone/Ultrasound Under Pressure (6.5 minute retention time)

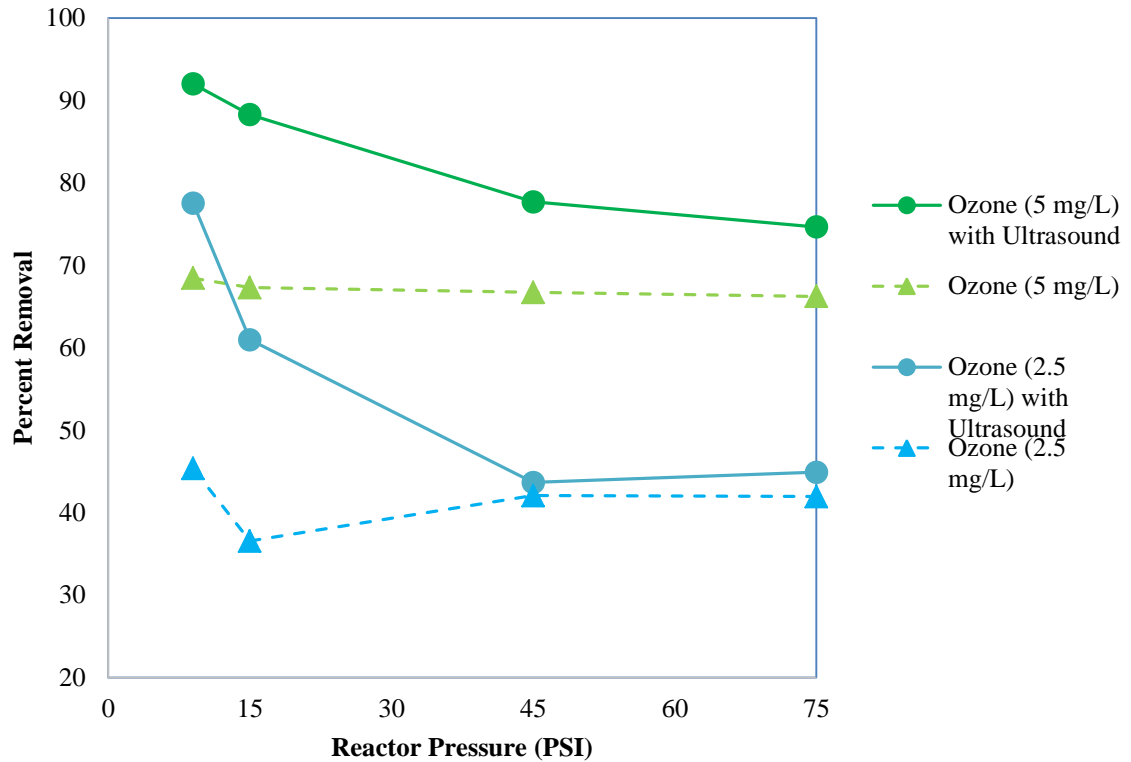


Figure 4-13 Effect of System Pressurization

Source Data in Table E3

As can be seen graphically in the figure above, the removal of 1,4-dioxane by the combined ozone/ultrasound system tends to approach the removal via ozone alone as reactor pressure is increased. In other words, the synergistic improvement from combined ozone/ultrasound is reduced as pressure increases. Two hypotheses are proposed to explain this:

- 1.) Ultrasonic decomposition of ozone decreases as pressure increases.

2.) Ultrasound facilitates additional mass transfer of ozone into aqueous phase (at higher pressure, there is less ozone in the air phase available for such mass transfer)

For the first case, if increased pressure were responsible for reducing the ability of ultrasound to decompose ozone that could certainly cause the reduction in synergy that was observed at higher pressures. Cushioning could account for some of this, as higher vapor pressures within the cavity can cushion the implosion (Alliger, 1975). It would also imply the synergy reduction would be proportional to ozone dose. However, this synergy, represented by gap between removal from combined ozone/ultrasound and that of ozone alone, appears to reduce more rapidly 2.5 mg/L than at 5 mg/L aqueous ozone. Such a dose-dependence of synergy would be an expected outcome of the second hypothesis; that mass transfer is responsible for the synergy. While there is increasingly less air phase ozone for a given aqueous ozone concentration as pressures are increased, there will still be a greater mass of gaseous ozone available for mass transfer for a 5 mg/L aqueous dose than at 2.5 mg/L, regardless of pressure.

Removal from ozone alone appears to be unaffected by the reactor pressure or reduced air phase ozone concentration, as evidenced by the relatively constant removal at 5 and 2.5 mg/L aqueous ozone concentrations. This suggests that dioxane removal by ozone alone is dictated by ozone decomposition, which has been shown in the literature to matrix dependent. The results of the constant aqueous phase tests, coupled with the results from the constant air phase tests, suggest that additional mass transfer is occurring as the result of sonication. These results support the theory advanced in previously published studies that ultrasound serves to increase mass transfer from air phase to water

phase, primarily due to the concentration gradient caused by ultrasonic ozone decomposition (Weavers & Hoffmann, 1998). To the best of my knowledge, the use of a pressurized reactor to demonstrate the mass transfer effect of combined ozone/ultrasound has not been done prior to this study.

#### *4.2.3. Implications of Pressure Results*

The results of the pressure study show the performance of both the ozone and ozone/ultrasound systems is sensitive to system pressure. The constant air phase concentration tests showed that improved removal of 1,4-dioxane could be achieved with only a few additional PSI of reactor pressure, but there didn't appear to be a significant benefit beyond that. The constant aqueous phase concentration tests hinted at mass transfer of ozone from air to water phase during sonication.

Additionally, the study of 1,4-dioxane removal in various locations of the reactor also hinted at a pressure dependence. A significant portion of 1,4-dioxane removal (21% for the ozone system and 15% for the combined ozone/ultrasound system) was found to be occurring before the water enters the ultrasonic chamber. This, too, is theorized to be due to the strong pressure dependence. It is theorized that transient ozone concentrations are achieved the region between the pressurization pump and the ultrasonic chamber which are much higher than those realized in the bulk of the ultrasonic chamber.

However, the time spent by the flowing water in this region between pump and chamber is negligible compared to that spent in the chamber. The total volume of the tubing, pump, static mixer, fittings, and valves that lie between the ozone gas injection port and the entrance to the reactor was measured to be 88 mL. The total volume of

water between the ozone injector and the static mixer's exit, where the pressure should be greatest, is only 44 mL. If it is assumed that the reaction kinetics within this region are the same as those in the ultrasound chamber, the only way for significant removal to occur would be for this transient ozone concentration to be much higher than what is entering the ultrasound chamber. Calculations were made to determine theoretical mean transient ozone dosages in this 88 mL region. For these calculations, it was assumed that the reaction would follow the Chick-Watson model that was outlined in the previous section. For a 2.5 mg/L aqueous ozone dose, the mean transient ozone dose was estimated to reach 182.4 mg/L and for a 1 mg/L aqueous ozone dose, the mean transient dose was estimated to be 84.9 mg/L. These calculations below were developed from the model that is discussed in Chapter 4.6.2:

$$\frac{d[1,4 \text{ diox}]}{dt} = -\left(0.07 + 0.1 \frac{0 \text{ W}}{940 \text{ W}}\right) [O_3]^{0.39} [1,4 \text{ diox}]$$

*Equation 4-2  
Model Equation  
for Continuous  
Flow Reactor*

$$\int \frac{d[1,4 \text{ diox}]}{dt[1,4 \text{ diox}]_0} = \int (-0.07)[O_3]^{0.39} dt$$

*Equation 4-3  
Theoretical  
Transient Ozone  
Dose-1*

$$\ln \frac{[1,4 \text{ diox}]}{[1,4 \text{ diox}]_0} = t(-0.07)[O_3]^{0.39}$$

*Equation 4-4  
Theoretical  
Transient Ozone  
Dose-2*

For these theoretical calculations,  $[O_3]$  represents the mean transient aqueous ozone concentration in mixing zone, i.e. the 88 mL of conveyance between the ozone gas injection point and the ultrasound reaction chamber entrance. For the first case, the initial

ozone concentration was  $2.5 \text{ mg/L}$ ,  $\frac{[1,4 \text{ diox}]_{\text{bypass}}}{[1,4 \text{ diox}]_0} = 0.878$ , and  $t = \frac{88 \text{ mL}}{360 \text{ mL/min}} = 0.244$  minutes. When equation 4-5 is solved for these conditions, it yields a mean transient ozone concentration of  $182.4 \text{ mg/L}$ . For the second case, the initial ozone concentration entering the reactor was  $1 \text{ mg/L}$ ,  $\frac{[1,4 \text{ diox}]_{\text{bypass}}}{[1,4 \text{ diox}]_0} = 0.904$ , and  $t = \frac{88 \text{ mL}}{345 \text{ mL/min}} = 0.255$  minutes. When equation 4-4 is solved for this set of conditions, it yields a mean transient ozone concentration of  $84.9 \text{ mg/L}$ .

While the removal noted in the mixing zone of the reactor does not account for the large variance with the results published by Xu et al., they do point to a potential explanation. The theoretical ozone concentrations achieved in this mixing zone were 73-85 times greater than those measured in the ultrasonic reactor, where the bulk of the 1,4-dioxane removal is occurring. The interphase dynamics in the continuous flow reactor used in this study are very different than those of the bubble column employed in the Xu et al study (Xu, Mochida, Naito, & Yasuda, 2012). In the batch experiment, micro bubbles of oxygen/ozone rise in a vessel with a rectangular cross section. In the flow through reactor used in this study, the bubbles travel alongside a plug of water as it moves through the reactor. The time it takes for a bubble to travel from the injection port to the degassing column was measured during several experiments. These times were calculated by starting the timer when the ozone gas injection valve was opened, and stopping the timer when the stream of bubbles emerged from the degassing column. Based on these tests, it takes an average of 24 seconds for the ozone/oxygen bubbles to transit the reactor. A batch reactor would have to be quite tall or bubbles quite tiny to achieve a comparable bubble contact time in a batch system.

### 4.3. Objective 3: Effect of Initial pH

To test the effect of initial pH, tests were run at pH 10 and pH 4 and compared with results previously obtained at neutral pH. For the pH 10 experiments, 0.1 M sodium hydroxide was added to 1,4-dioxane-spiked drinking water until the desired pH was reached. For the pH 4 experiments, concentrated hydrochloric acid was added to 1,4-dioxane-spiked drinking water until the desired pH was reached. For the neutral condition, no pH adjustment had been made to the drinking water. The results for ultrasound alone, ozone alone, and combined ozone/ultrasound are depicted in the following figure, in  $\ln(C/C_0)$  vs. time.

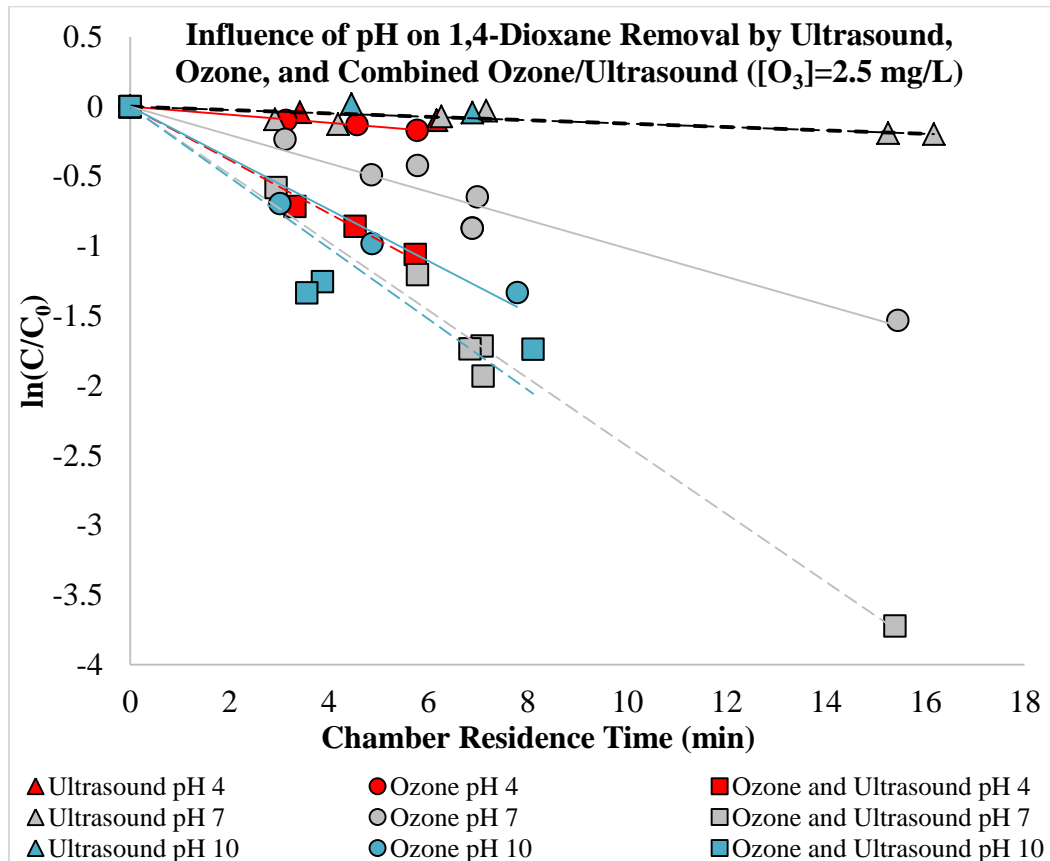


Figure 4-14 Influence of Initial pH

Source Data in Table E7

The results for treatment by ozone alone have been broken out for the following figure.

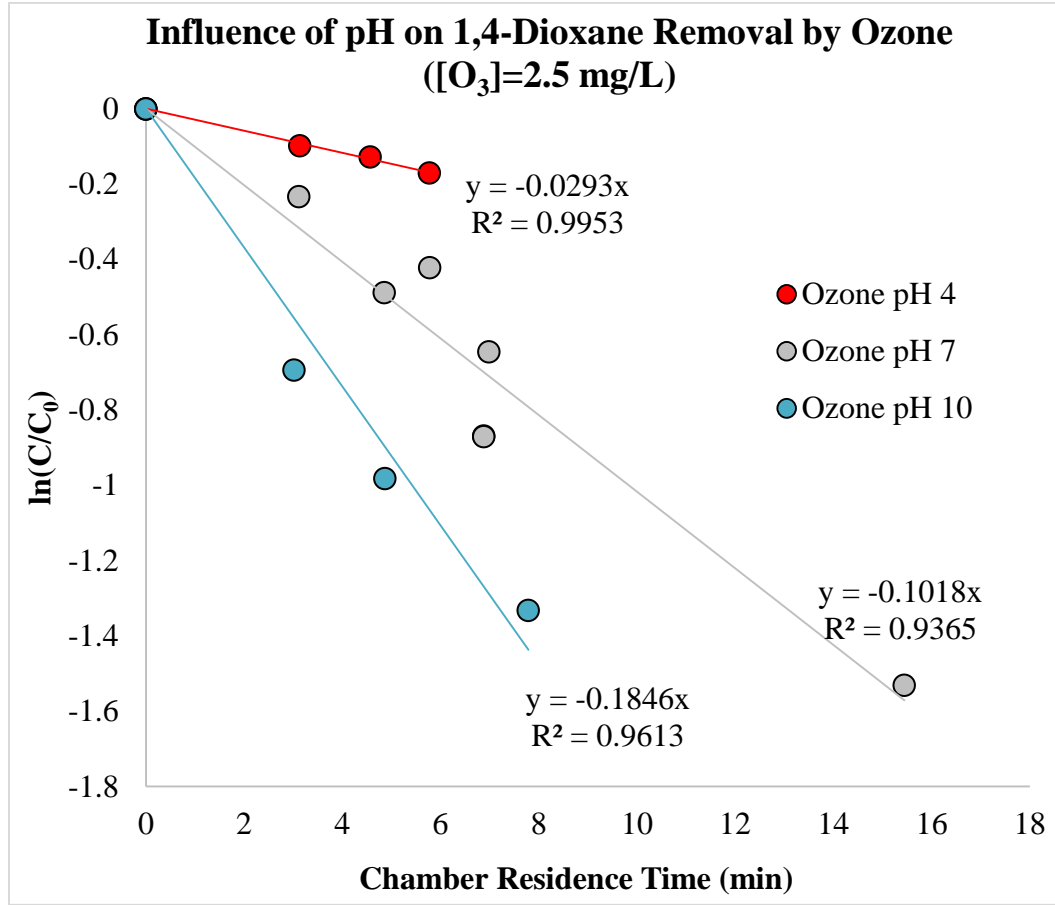


Figure 4-15 Influence of pH on Ozone System

Source Data in Table E7

It is worth noting the variation in first order rate constants for the ozone system, depicted by the slopes of the lines in the figure above. The combined ozone/ultrasound results have been broken out in the following figure.

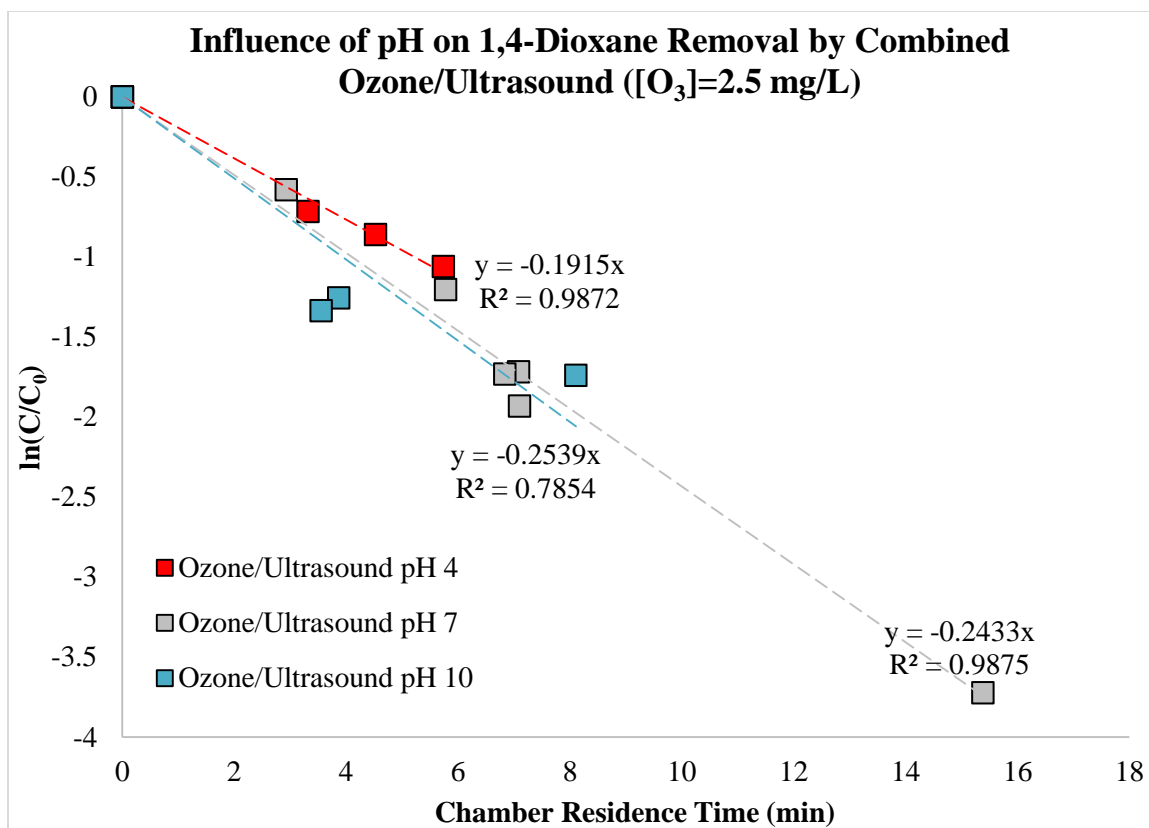


Figure 4-16 Influence of pH on Combined Ozone/Ultrasonnd System

Source Data in Table E7

It is worth noting the variation in first order rate constants for the combined ozone/ultrasonnd system, again depicted by the slopes of the lines in the figure above. Finally, the results for the ultrasonnd system are given below.

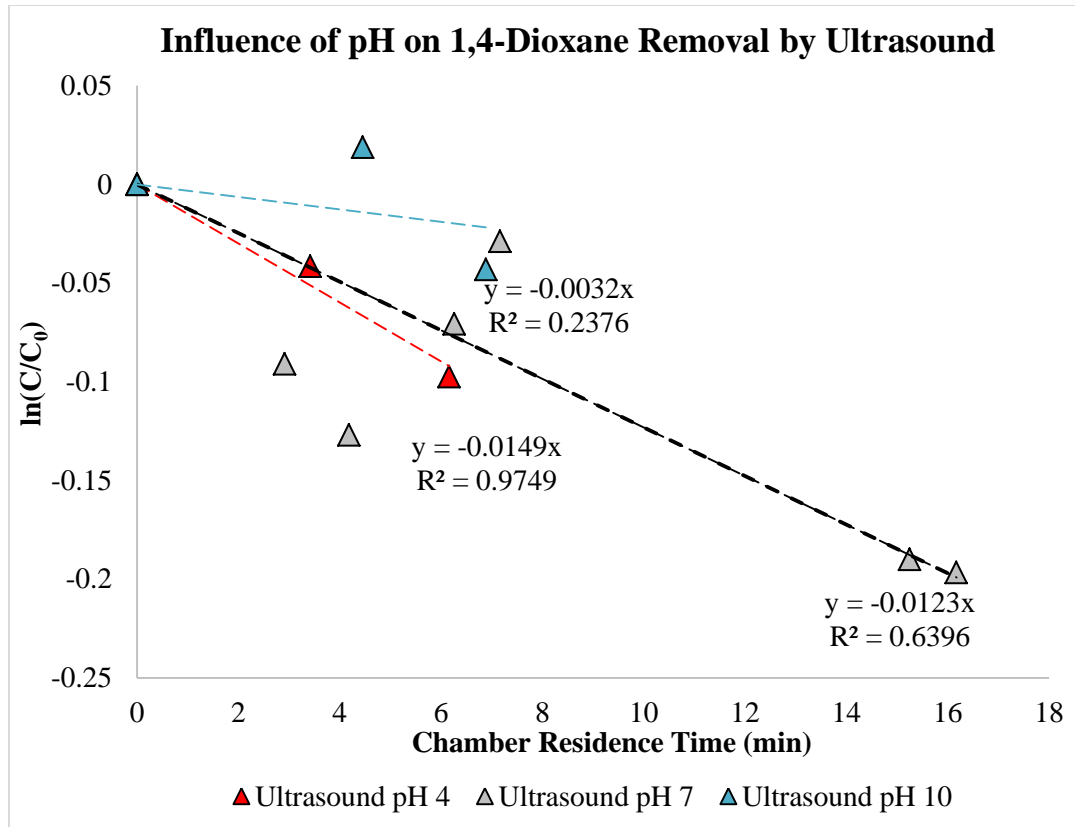


Figure 4-17 Influence of pH on Ultrasound System

Source Data in Table E7

Removal by ultrasound alone was minimal for all conditions, which makes it difficult to determine the influence of pH on this system. However, it appears that dioxane removal by full-power 20 kHz ultrasound is minimal in drinking water for pH from 4 to 10. The first order rate constants have been summarized in the table below.

Table 4-2 pH and Rate Constants for 2.5mg/L Ozone Dose

pH	$k_{\text{Ultrasound}}$ in $\text{min}^{-1}$ ( $R^2$ )	$k_{\text{Ozone}}$ in $\text{min}^{-1}$ ( $R^2$ )	$k_{\text{Ozone/Ultrasound}}$ in $\text{min}^{-1}$ ( $R^2$ )
4	0.015 (0.97)	0.029 (0.99)	0.19 (0.99)
7	0.012 (0.64)	0.10 (0.94)	0.24 (0.99)
10	0.0032 (0.24)	0.18 (0.96)	0.25 (0.79)

#### *4.3.1. Implications of Initial pH Results*

To evaluate the effect of the pH of the influent water, tests were conducted at pH 4 and pH 10, and the results were compared with the results at neutral pH. From the results of these tests, it appears that removal of 1,4-dioxane increases for the ozone system as pH increases. This is supported by the theory that ozone consumption is increased as pH is increased, as initiated by hydroxide ions (Staehelin & Hoigne, 1982) (Elovitz, von Gunten, & Kaiser, 2000) and agrees with the ozonation experiments conducted on 1,4-dioxane in simulated wastewater (Barndok, Cortijo, Hermosilla, Negro, & Blanco, 2014). In the combined ozone/ultrasound system, there appears to be a slight improvement in 1,4-dioxane removal as pH increases. Because ultrasound also increases ozone consumption, it is theorized that ozone consumption from ultrasound competes with consumption that is initiated by hydroxide ions, leading to a muted effect of ultrasound relative to pH. To put it another way, the addition of high power ultrasound to ozone tends to mute the influence of pH on hydroxyl radical production and 1,4-dioxane removal. This finding suggests that the addition of ultrasound could overcome the hindrance to contaminant removal noted in source waters with acidic, or less than optimal, pH conditions for ozonation.

#### **4.4. Objective 4: Effect of Ultrasonic Intensity**

The rate constant for the 20 kHz ultrasound at full power was determined to be  $0.012 \text{ min}^{-1}$ . While this is very modest in comparison to those obtained for ozone and ozone/ultrasound systems, it is very similar to the  $0.013 \text{ min}^{-1}$  rate constant which was obtained in an earlier 20 kHz study (Son, Choi, Khan, & Zoh, 2006). Additional tests

were conducted at 25% intensity for two ozone concentrations (2.5 mg/L and 5 mg/L) and compared with results at 100% intensity to determine the effect that ultrasonic intensity has on the removal of 1,4-dioxane. The 25% value was chosen because power output from the ultrasound generator did not vary linearly with intensity setting, and 25% intensity was found to yield approximately 50% of the power output. The results of these tests are in the figures below.

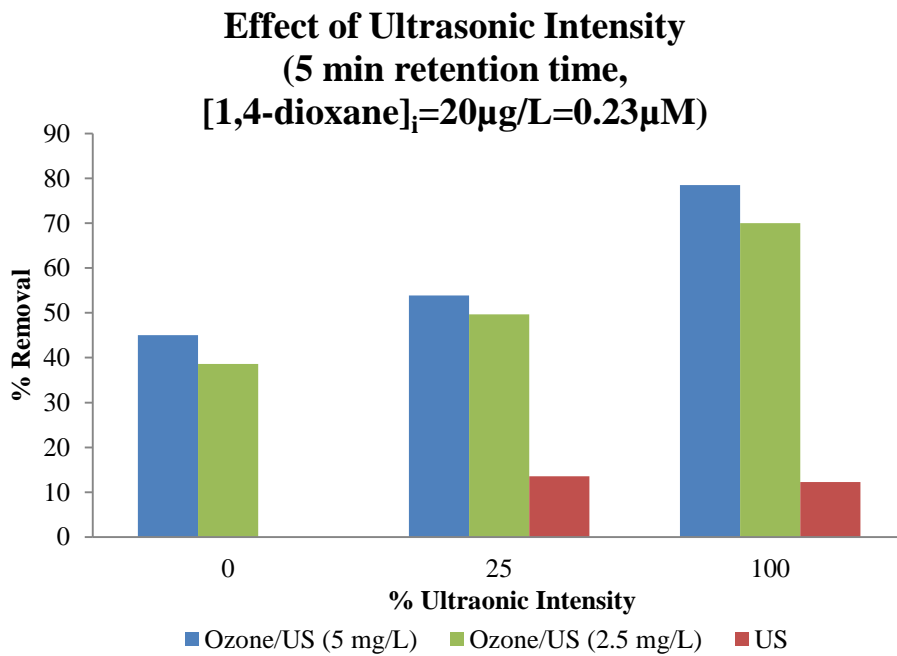


*Figure 4-18 Effect of Ultrasonic Intensity*

*Source Data in Table E1*

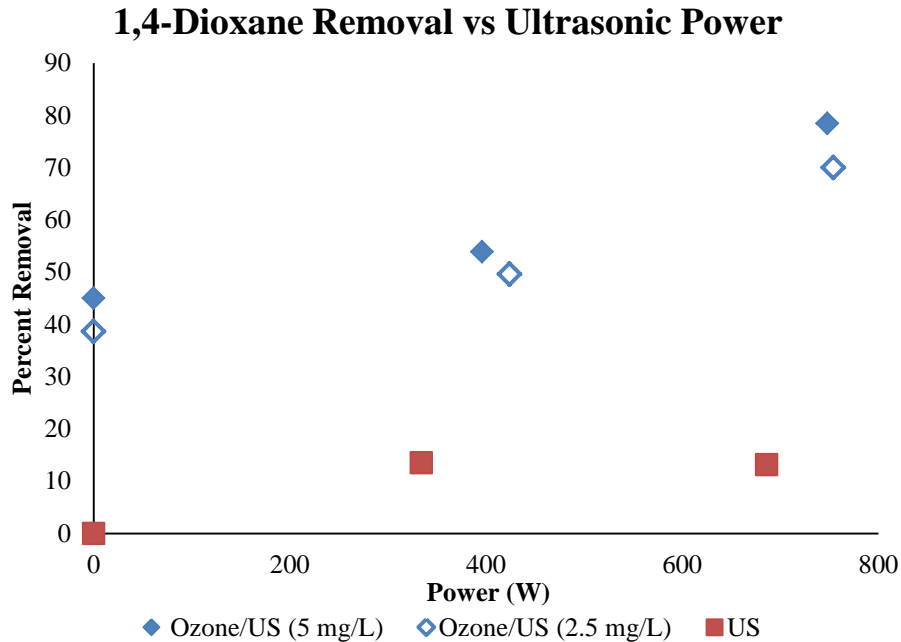


Figure 4-19 Removal vs Ultrasonic Power

Source Data in Table E1

#### 4.4.1. Implications of Ultrasonic Intensity Results

Ultrasound has been shown to be capable of removing contaminants in water (Kindak & Ince, 2007) (Lall, Mutharasan, Shah, & Dhurjati, 2003) (Son, Choi, Khan, & Zoh, 2006) (Stepniak, Stanczyk-Mazanek, & Kusiak, 2012) (Suri, Andaluri, Abburi, & Velicu, 2008) (Cyr, Paraskewich, & Suri, 1999). In this study, 20kHz ultrasound was not found to be particularly effective for removing 1,4-dioxane. However, in the combined ozone/ultrasound system, it was found to provide a significant enhancement to removal. At full power, the addition of ultrasound more than doubled the pseudo-first order rate constant obtained using a similar dose of ozone in the absence of sonication. While higher power ultrasound was shown to remove more 1,4-dioxane, a meaningful boost to removal was noted even at 25% intensity. It is believed that this enhancement is due to

an increase in the decomposition of ozone, causing a subsequent boost in the production of hydroxyl radicals. A similar phenomenon has been noted in study of the combined ozone/ultrasound treatment process for the removal of sulfamethoxazole (Guo, et al., 2015)

#### 4.5. Objective 5: Effect of Scavenging

Hydroxyl radical scavenging tests were conducted to tease out the reaction mechanism at work. Examining the combined ozone/ultrasound system yields a number of possible mechanisms that could be responsible for removing 1,4-dioxane: hydroxyl radicals generated by ultrasonic cavitation in the bulk water or at the water/air interface, cavitation induced pyrolysis within the bubbles, hydroxyl radicals generated by the decay of ozone, direct reaction of ozone with 1,4-dioxane, hydroxyl radicals generated by ozone/ultrasound synergy, or synergistic direct reaction by ozone. Assuming the total reaction rate constant to be a sum of rate constants for each of the components listed yields the equation below.

$$k_{total} = k_{US/\cdot OH} + k_{US/other} + k_{O_3/\cdot OH} + k_{O_3/O_3} + k_{synergy/\cdot OH} + k_{synergy/O_3}$$

*Equation 4-5  
General Rate  
Constants*

The data in Figure 4-19 suggests that when bicarbonate is present sufficiently in excess of 1,4-dioxane, removal is completely stopped.

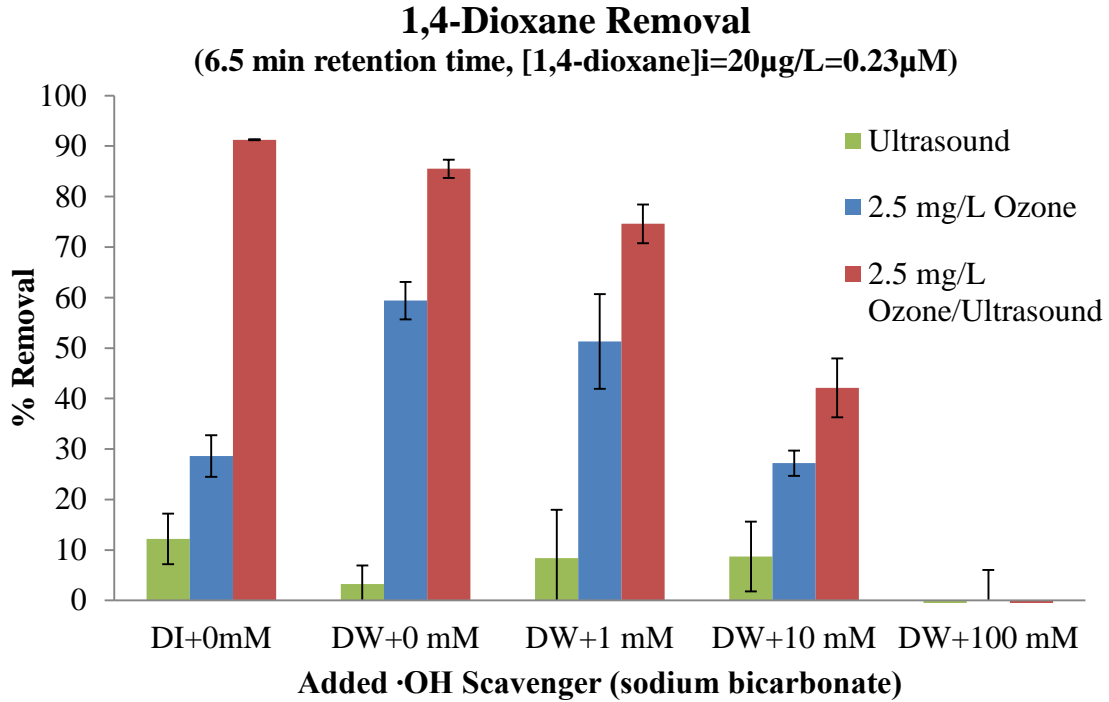


Figure 4-20 Effect of Added Scavenger on 1,4-Dioxane Removal

Source Data in Table E1, E4

The implication from Figure 4-18 is that removal by anything other than hydroxyl radicals is negligible. By neglecting those terms, Equation 4-5 simplifies to:

$$k_{total} = k_{US/\cdot OH} + k_{O_3/\cdot OH} + k_{synergy/\cdot OH} \quad \text{Equation 4-6}$$

Rate Constants

The individual k terms from this equation can therefore be determined by comparing the data from ultrasound-only experiments ( $k_{US/\cdot OH}$ ), ozone-only experiments ( $k_{O_3/\cdot OH}$ ), and combined ozone/ultrasound experiments ( $k_{total}$ ). Subtracting  $k_{O_3/\cdot OH}$  and  $k_{US/\cdot OH}$  from  $k_{total}$  yields  $k_{synergy/\cdot OH}$ . This is developed further in the modeling section.

## 1,4-Dioxane Rate Constants

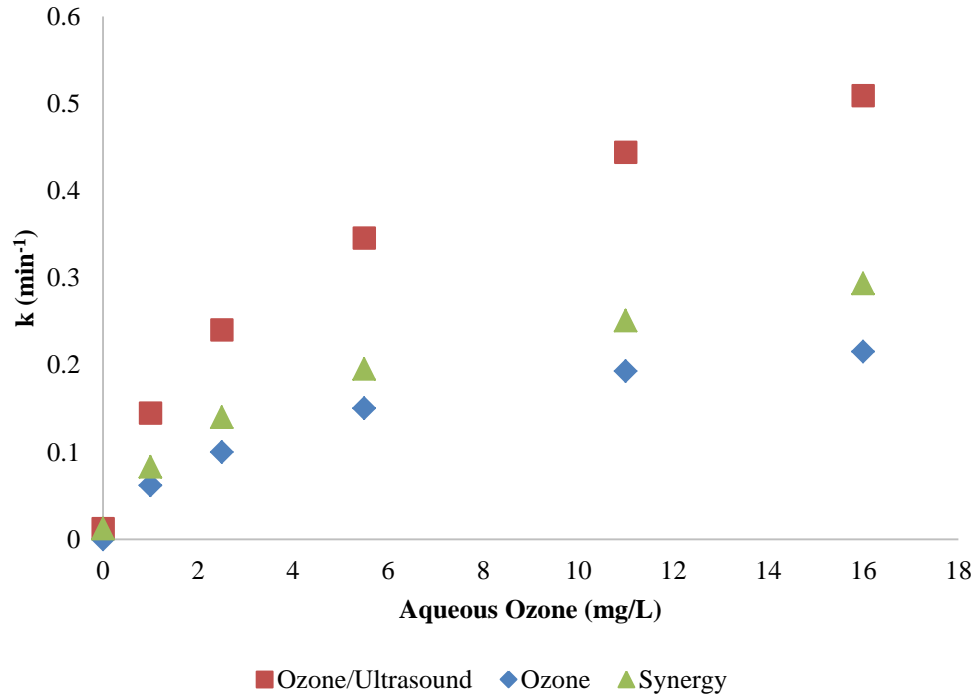


Figure 4-21 Apparent 1<sup>st</sup> Order Rate Constant vs. Aqueous Ozone Dose

Source Data in Table E1

In this figure, the ozone and ozone/ultrasound rate constants were obtained directly from the Table 3-1, while the “synergy” rate constants were obtained by subtracting the ozone rate constant and the ultrasound rate constant from each ozone/ultrasound rate constant. This becomes a simple rearrangement of Equation 3-3.

$$k_{synergy} = k_{synergy/OH} = k_{total} - k_{O_3/OH} - k_{US/OH} \quad \begin{array}{l} \text{Equation 4-7} \\ \text{Synergy} \\ \text{Calculation} \end{array}$$

A set of experiments was conducted using the same procedures outlined in section 3.1. However, the water was spiked with both 20 ppb (20 µg/L) of 1,4-dioxane and

sodium bicarbonate ( $\text{NaHCO}_3$ ). The addition of bicarbonate in sufficient excess should scavenge any hydroxyl radicals being created, without reacting with ozone directly (Cyr, Paraskewich, & Suri, 1999). So any 1,4-dioxane removal noted would have to come from other effects, like ultrasonic pyrolysis or direct reaction with ozone. A bicarbonate concentration of 100 mM (6100 mg/L) was the first condition tested. An initial sample was taken, along with a sonicated sample, an ozonated sample, and a sample exposed to combined ozone/ultrasound. No removal was observed in any of the samples, which supports the hypothesis that all 1,4-dioxane removal observed has been due to hydroxyl radical production. This was expected based on previously published studies which indicated a relatively slow reaction coefficient for 1,4-dioxane with ozone ( $k_{\text{O}_3/1,4\text{-dioxane}} = 0.32 \text{ M}^{-1}\text{s}^{-1}$ ) (Hoigne & Bader, 1983) and a very fast reaction coefficient for 1,4-dioxane with the hydroxyl radical ( $k_{\text{OH}/1,4\text{-dioxane}} = 2.4 \times 10^9 \text{ M}^{-1}\text{s}^{-1}$ ) (Suthersan & Payne, 2004). Additional experiments were run with 1 and 10mM added bicarbonate and the results are given below.

The addition of bicarbonate as a hydroxyl radical scavenger caused a significant effect on the removal of 1,4-dioxane by ozone and combined ozone/ultrasound. In these tests, the bicarbonate was added to dioxane-spiked drinking water. However, the drinking water matrix contains some inorganic carbon naturally (mean TIC was 7.85 ppm). To evaluate the performance of ultrasound, ozone, and combined ozone/ultrasound for a matrix without any naturally present scavenging compounds, a parallel series of experiments was conducted using dioxane-spiked deionized water. The results of those experiments are in the figure below.

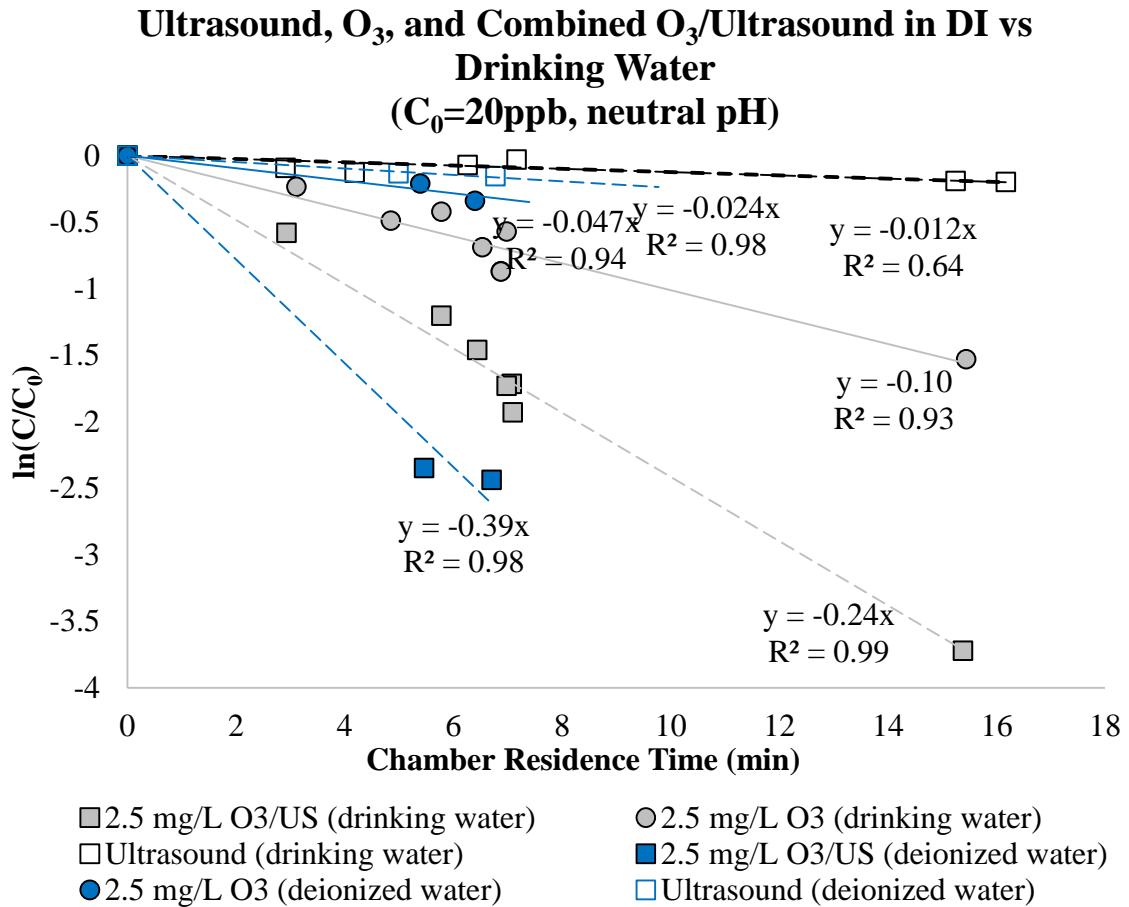


Figure 4-22 Deionized Water vs Drinking Water

Source Data in Tables E1, E4

As evidenced in the slopes of the figure above, faster rates of removal were achieved in deionized water for the ultrasound and combined ozone/ultrasound processes. However, the rate of removal from ozone alone decreased significantly.

Also, aqueous ozone showed much greater stability in the deionized matrix, as measured by the difference noted in the measured influent and effluent ozone concentrations. Organic carbon has been shown to increase ozone decomposition in previous work, so the absence of organic carbon in the deionized water is suspected to be

the cause of the greater ozone stability (Staelin & Hoigne, 1985). The addition of ultrasound serves to increase decomposition, as depicted in the following figures.

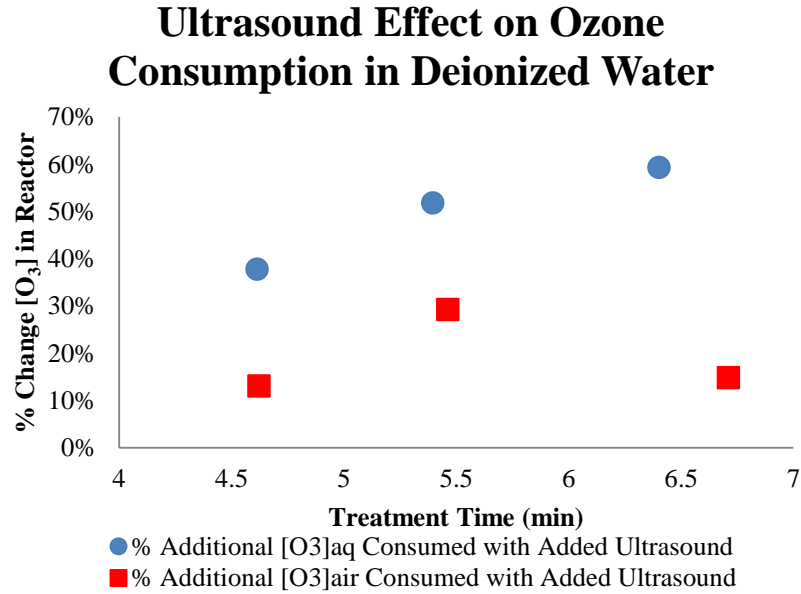


Figure 4-23 Ultrasound Effect on Ozone Consumption in DI Matrix

Source Data in Tables E1, E4, E8

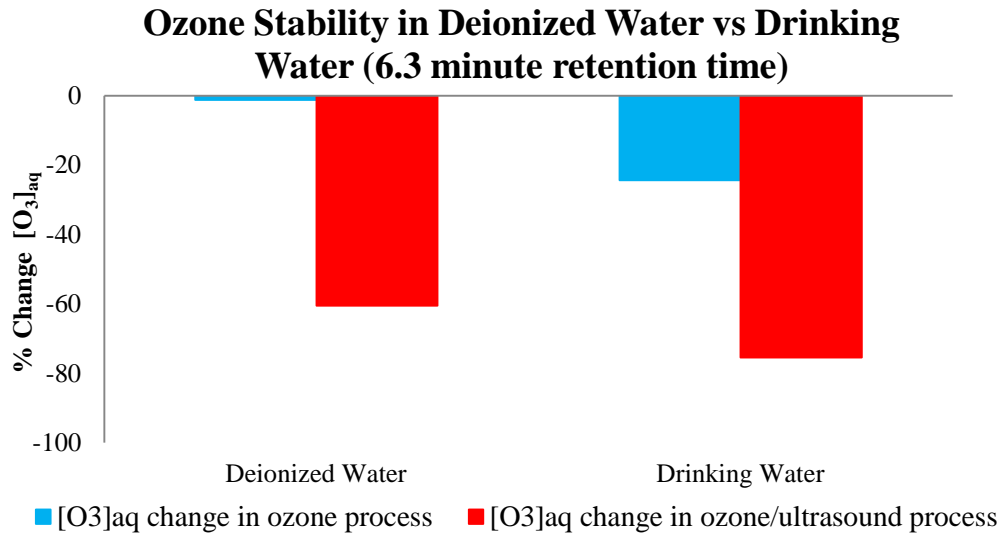


Figure 4-24 Ozone Stability

Source Data in Tables E4, E8

This ozone stability is also believed to be responsible for the substantial drop noted in the first order rate constant for dioxane removal. For example an aqueous dose of 2.5 mg/L, the first order rate constant dropped from 0.10 min<sup>-1</sup> in drinking water to 0.047 min<sup>-1</sup> in deionized water. Conversely, 1,4-dioxane removal in the combined ozone/ultrasound system improved. For an aqueous ozone dose of 2.5 mg/L, the rate constant increased from 0.24 min<sup>-1</sup> in spiked drinking water to 0.39 min<sup>-1</sup> in spiked deionized water. This will be discussed further in Chapters 4 and 6.

#### *4.5.1. Implications of Scavenging Results*

The results of the scavenging study indicate that 1,4-dioxane treatment will be highly dependent on the matrix being treated. Since 1,4-dioxane is dependent upon the hydroxyl radical, other compounds present in the water can compete for the radicals generated by this system. The degree to which these compounds inhibit the removal of 1,4-dioxane will depend on their concentration and their hydroxyl radical reaction rate constant, relative to 1,4-dioxane. While it was beyond the scope of this study to investigate all potential scavenging compounds, bicarbonate was chosen over *tert*-butanol, acetate, and other scavengers commonly mentioned in the literature because of its environmental relevance. In the results section, the addition of modest levels of sodium bicarbonate was shown to diminish the removal of 1,4-dioxane in both the ozone and the combined ozone/ultrasound systems, reducing removal by roughly half at a 10mM concentration and preventing any removal at all at 100mM concentration.

The results of the scavenging study suggest that only a negligible fraction of 1,4-dioxane removal is attributable to direct interaction with ozone, since ozone doesn't react with bicarbonate directly (Stahelin & Hoigne, 1982) and negligible removal was

measured after the addition of 100mM bicarbonate for both ozone and combined ozone/ultrasound processes. Additionally, the relatively low rate at which 1,4-dioxane is removed via ultrasound alone ( $k_{US}=0.012 \text{ min}^{-1}$ ) suggests that sonication at 20kHz does not produce hydroxyl radicals efficiently.

The tests in deionized water also point towards hydroxyl radical dependence for both the ozone and combined ozone/ultrasound processes. Ozone in deionized water showed excellent stability, but in the drinking water matrix there were measureable differences in the influent and effluent aqueous concentrations. In an earlier study, ozone stability in wastewater was shown to be a function of organic carbon and ozone dosages (Staehelin & Hoigne, 1985) (Nothe, Fahlenkamp, & Von Sonntag, 2009). In deionized water, TOC content was negligible, but the drinking water used for this study averaged 1.95 ppm. This organic carbon is believed to be responsible for the faster breakdown of ozone, concurrent production of hydroxyl radical, and the removal of 1,4-dioxane. It is believed that the increased rate of radical production in the drinking water matrix more than made up for the increase in scavenging compounds in the drinking water (7.85 ppm mean TIC).

In the combined ozone/ultrasound process, the performance edge went to the deionized water matrix. It is believed that the ultrasound drove the breakdown of ozone, and its concurrent hydroxyl radical production, in the absence of organic carbon. The ultrasound negated the need for organic carbon to provide for ozone consumption. Therefore, it is believed that the deionized matrix gained an advantage because there were no scavenging compounds present, freeing more of the generated hydroxyl radicals to attack the dioxane instead.

## 4.6. Objective 6: Reactor Modeling

### 4.6.1. Tracer Study

In order to create a model for the combined ozone/ultrasound reactor, its dispersion characteristics were measured first, using a conservative step-up tracer study. To accomplish this, two 30 liter carboys were filled, the first with drinking water, the second with 10 g/L NaCl in drinking water. Initial conductivity measurements were taken of the water in each tank. The system was turned on and the conductivity probe was positioned to measure the conductivity of the effluent stream. Initially, the carboy containing plain drinking water was used to flush the reactor. At time zero, the feed water was switched to the 10 g/L saline solution. Conductivity measurements were made every 15 seconds until the measurements stabilized at the same conductivity level as the 10 g/L carboy. These conductivity readings were plotted and the  $dC/dt$  values were computed for each point.

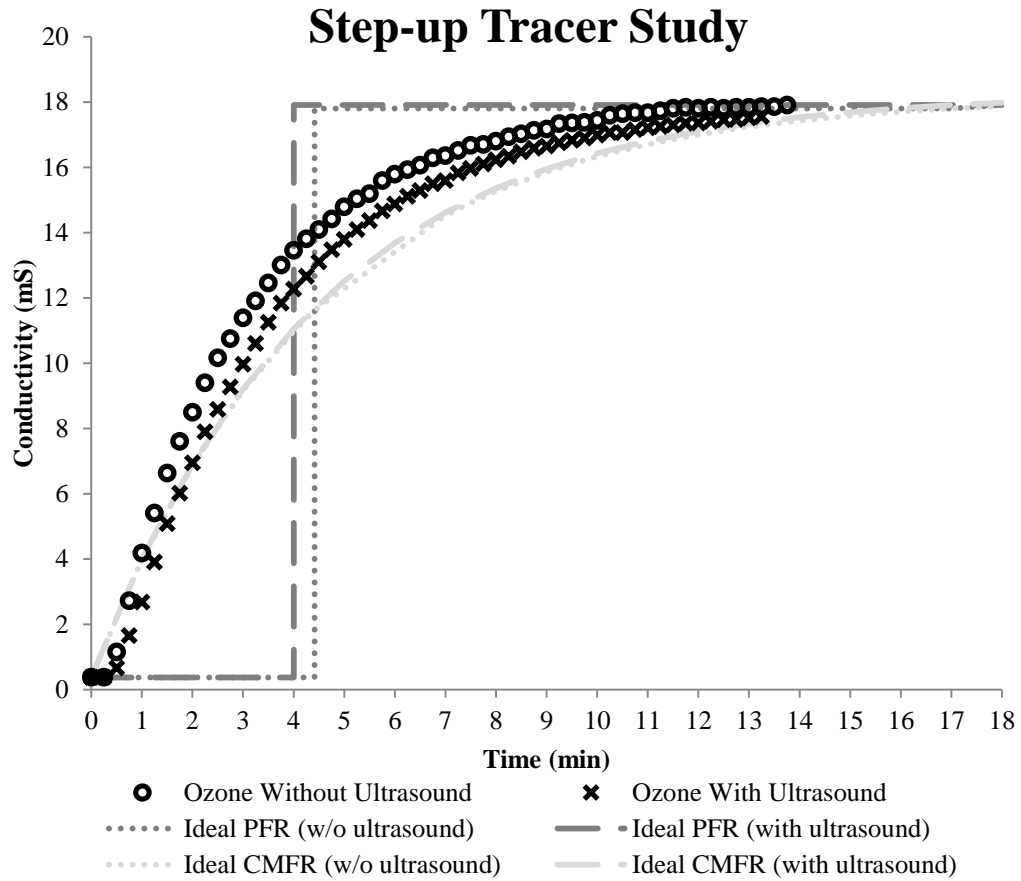


Figure 4-25 Step-up Tracer Study

This information was plugged into the equations below to compute the D/uL value for the reactor (Fogler, 1992) (Levenspiel, 1999).

$$\bar{t} = \frac{\sum t_i C_i \Delta t_i}{\sum C_i \Delta t_i} \quad \begin{array}{l} \text{Equation 4-8} \\ \text{Mean Reactor} \\ \text{Residence Time} \end{array}$$

$$\sigma^2 \cong \frac{\sum t_i^2 C_i \Delta t_i}{\sum C_i \Delta t_i} - \bar{t}^2 \quad \begin{array}{l} \text{Equation 4-9} \\ \text{Variance} \end{array}$$

$$\sigma_{\theta}^2 = \frac{\sigma_t^2}{\bar{t}^2} = 2 \left( \frac{D}{uL} \right) - 2 \left( \frac{D}{uL} \right)^2 [1 - e^{-uL/D}]$$

Equation 4-10  
Vessel Dispersion  
Number,  $D/uL$

This step-up tracer study was repeated three times: without ozone or ultrasound, with ozone (10 L/hr flow rate), and with ozone (10 L/hr flow rate) and ultrasound (100% intensity). The results of the tracer tests are below.

Table 4-3 Dispersion Characteristics of Continuous Flow Reactor

Reactor Condition	D/uL
No O <sub>3</sub> or Ultrasound	0.139
O <sub>3</sub> alone	0.142
O <sub>3</sub> with Ultrasound	0.187

The results of this tracer study were used to confirm that quasi-steady state would be achieved after more than two retention times had passed. In the following sections a plug-flow model will be developed. From the tracer study results, it is clear that the actual reactor is not an ideal plug flow reactor. Based on the calculated dispersion characteristics, the reactor can be thought of as a plug flow reactor with short circuiting is occurring. Because of this short circuiting, the 2.57 liter reactor has an effective volume of 2 liters. If the reactor were behaving as in a more ideal true plug flow fashion, the treatment performance would be expected to improve in proportion to the increase in effective volume.

#### 4.6.2. Development of Predictive Model

The results from the previous research objectives were used to build a predictive model of the combined ozone/ultrasound reactor. From the results found in Table 3-1 and Figure 3-2, it is clear that removal by ozone or combined ozone/ultrasound is sensitive to concentrations of both 1,4-dioxane and aqueous ozone. Therefore, modeling

as a simple first order reaction in a plug-flow reactor is inadequate. Attempts were made to model it as a second order reaction of the form:  $d[1,4\text{-dioxane}]/dt = -k[O_3][1,4\text{-dioxane}]$ . However, these attempts failed to adequately predict the outcome of some of the preliminary experiments. Next, an attempt was made to model the reactor using the finite volume technique, and a number of models using second order reaction kinetics were tried. Again, none proved capable of predicting all of the observed experimental outcomes. Finally, the reactor was modeled in the same form as the model described by Chick & Watson to predict the disinfectant dose required to achieve the desired inactivation of a pathogen. This same form of model has also been used for the disinfection of wastewater using a 20kHz ultrasound reactor (Madge & Jensen, 2002). This Chick & Watson model uses a reaction of the form:

$$\frac{d[\textit{pathogen}]}{dt} = -k_0[\textit{disinfectant}]^\eta[\textit{pathogen}]$$

*Equation 4-11  
Chick & Watson  
Model for  
Pathogens*

This reactor was modeled using the same structure, but after customizing the terms to fit the ozone and ozone/ultrasound systems, it becomes:

$$\frac{d[1,4 \textit{dioxane}]}{dt} = -k_0[O_3]^\eta[1,4 \textit{dioxane}]$$

*Equation 4-12  
Modified Chick &  
Watson*

To calculate the  $k_0$  and  $\eta$  terms, the rate constants from Table 3-1 were plotted with respect to aqueous ozone dose, yielding:

Fitting a power function curve to Figure 3-6 yields a rate constant equations in the same form as Chick & Watson:

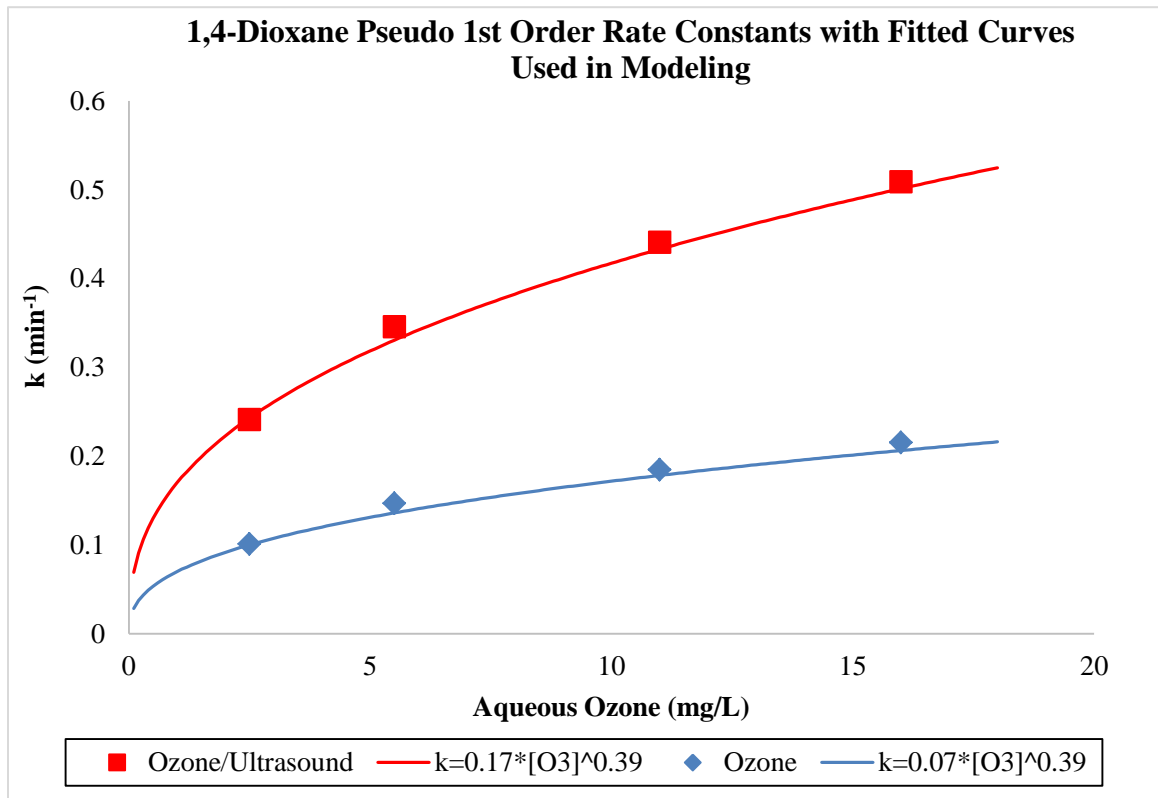


Figure 4-26 Fitting Experimental Results to Chick & Watson Model

Source Data in Table E1

The power trend line equations in Figure 3-7 can be used to solve for  $k_0$  and  $\eta$ , in the manner developed below:

$$\frac{d[1,4 \text{ dioxane}]}{dt} = -k_0[O_3]^\eta [1,4 \text{ dioxane}] = -k[1,4 \text{ dioxane}] \quad \begin{array}{l} \text{Equation 4-13} \\ \text{Modified Chick \&} \\ \text{Watson-2} \end{array}$$

Simplifying equation 4-13 yields:

$$-k_0[O_3]^\eta = -k \quad \begin{array}{l} \text{Equation 4-14} \\ \text{Rate Constant for} \\ \text{Chick \& Watson} \end{array}$$

From Figure 3-7, the rate constant equation for the ozone/ultrasound system is:

$$k = 0.17[O_3]^{0.39}$$

*Equation 4-15  
Modified Chick &  
Watson for O<sub>3</sub>/US*

Similarly, the rate constant equation for the ozone system is:

$$k = 0.07[O_3]^{0.39}$$

*Equation 4-16  
Modified Chick &  
Watson for O<sub>3</sub>*

After putting the experimentally obtained equations into the modified Chick and Watson form, it was noted that both exponent terms,  $\eta$ , are approximately equal to 0.39. This suggests that the addition of ultrasound to the ozone only changes the  $k_0$  term. It also suggests that it could be possible to compress both ozone and ozone/ultrasound systems into a single model if  $k_0$  was given as a function of ultrasonic power. To test this hypothesis, the mean  $k_0$  value of each experiment utilizing 100% intensity (~850 W) was first computed. Then, this value was compared to the  $k_0$  value computed for the ozone system (0% intensity, or 0 W). Next, a simple linear interpolation was used to predict the removal rate constant for 1,4-dioxane at an intermediate power level (25% intensity).

$$k_0 = 0.07 + (0.17 - 0.07) \frac{\text{Power (W)}}{940 \text{ W}}$$

*Equation 4-17  
Calculation of  $k_0$   
Using Linear  
Interpolation*

Using Equation 4-17 to calculate  $k_0$ , the results predicted by the model were compared with experimental data obtained at 25% intensity. These predictions were found to be in good agreement with the results obtained from 5 minute retention experiments using 2.5 and 5 mg/L aqueous ozone doses, and 25% ultrasonic intensity, corresponding to 424 and 396 W, respectively.

Substituting this 0.39 for  $\eta$  and Equation 4-17 for  $k_0$  into Equation 4-13 yields a single equation, where [1,4 diox] is in  $\mu\text{g/L}$ ,  $[\text{O}_3]$  is the aqueous dose in mg/L, and ultrasonic power is in W:

$$\frac{d[1,4 \text{ diox}]}{dt} = - \left( 0.07 + 0.1 \frac{\text{Power}}{940 \text{ W}} \right) [\text{O}_3]^{0.39} [1,4 \text{ diox}]$$

*Equation 4-18  
Model Equation  
for Continuous  
Flow Reactor*

This single equation has been found to give accurate predictions for ozone and ozone/ultrasound systems for ozone dosages from 0-16 mg/L, treatment times from 2.5-16 minutes, and ultrasonic power inputs from 0-1200 W.

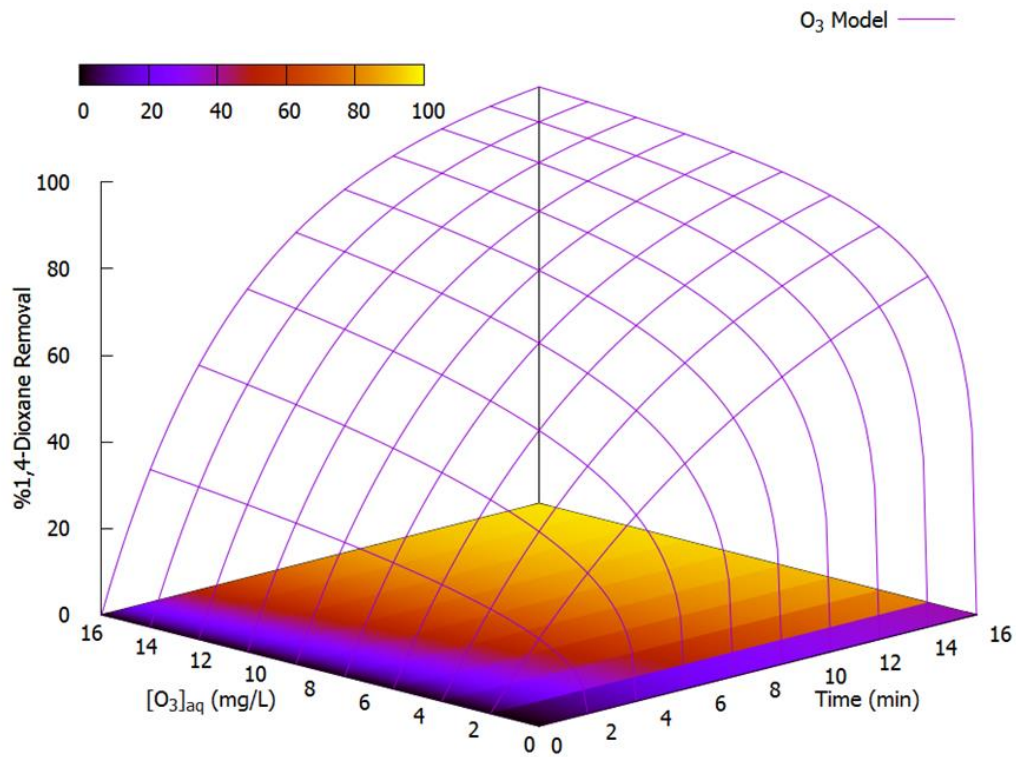


*Figure 4-27 Dioxane Removal from O<sub>3</sub> Alone Predicted by Model*

*Source Data in Table E1*

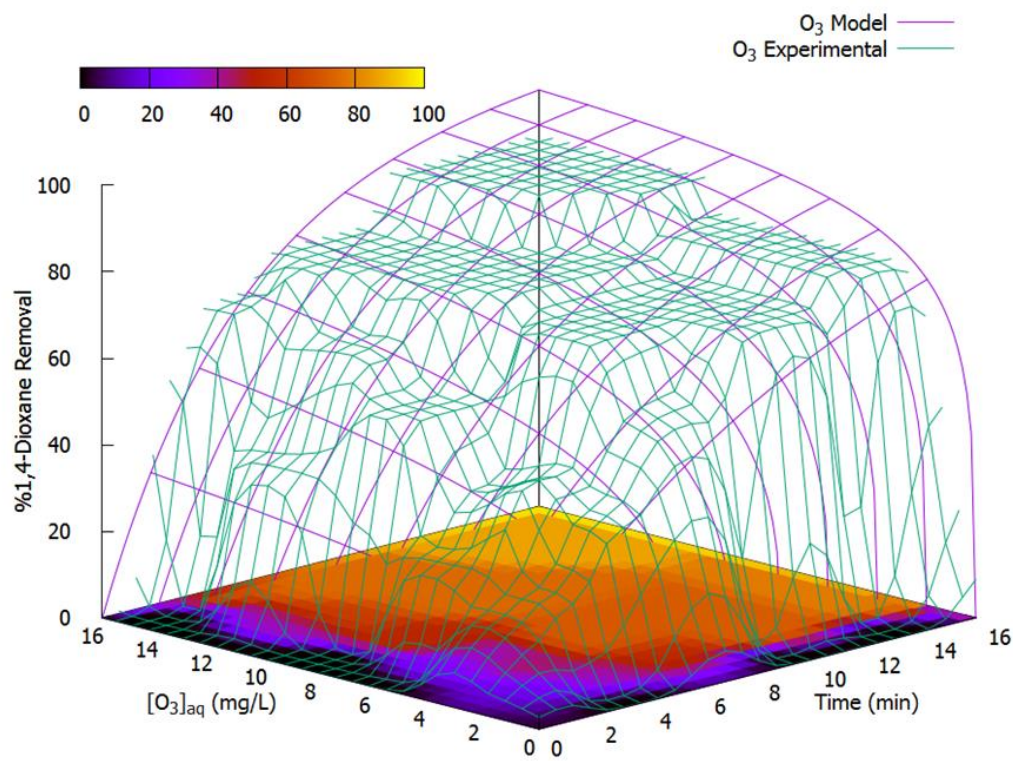


*Figure 4-28 Experimental Data for O<sub>3</sub> Alone with Model Overlay*

*Source Data in Table E1*

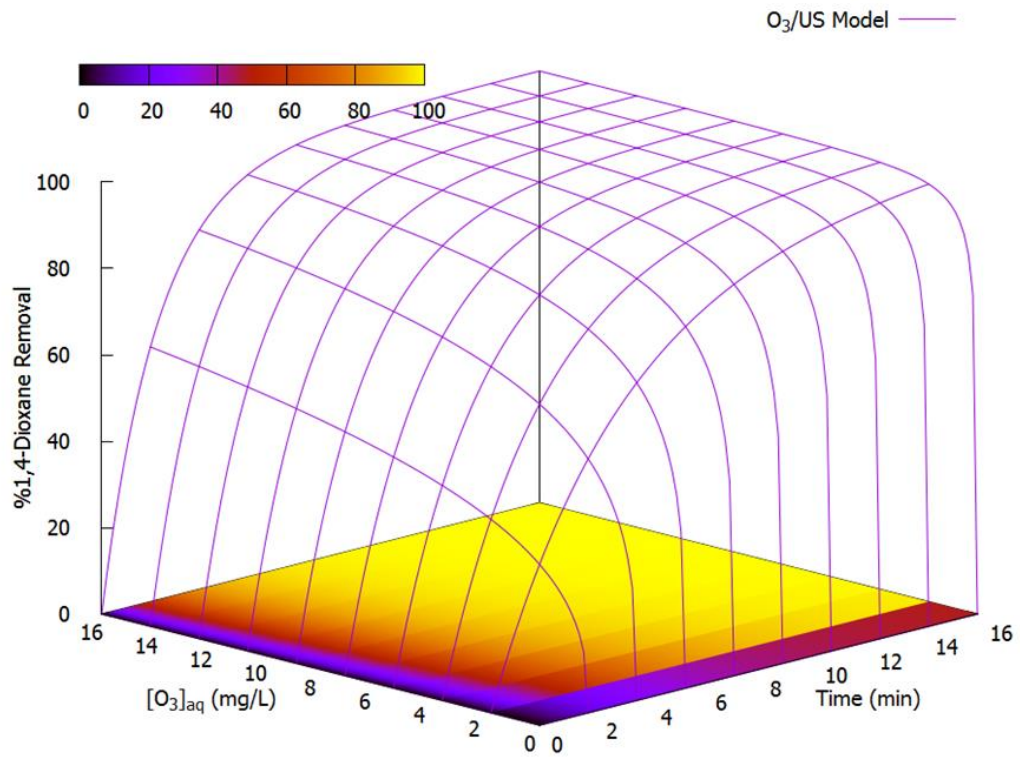


*Figure 4-29 Dioxane Removal from Combined O<sub>3</sub>/Ultrasound Predicted by Model*

*Source Data in Table E1*

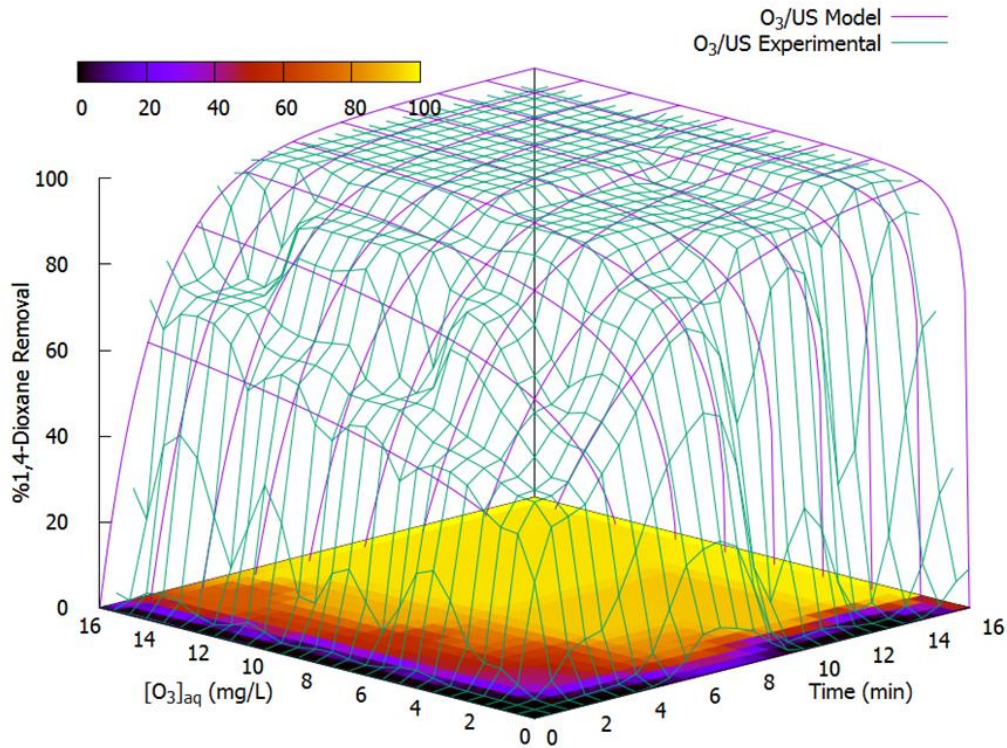


Figure 4-30 Experimental Data for Combined  $O_3$ /Ultrasound with Model Overlay

Source Data in Table E1

To evaluate the performance of this model, the root mean squared error (RMSE) was calculated for  $[1,4 \text{ diox}]/[1,4 \text{ diox}]_0$ , comparing those obtained experimentally with those predicted by the model (Unluturk, Atilgan, Baysal, & Unluturk, 2010). The equation used was:

$$RMSE = \sqrt{\frac{1}{n} \sum \left( \frac{[1,4 \text{ diox}]_{model} - [1,4 \text{ diox}]_{exp}}{[1,4 \text{ diox}]_{init}} \right)^2} \quad \begin{array}{l} \text{Equation 4-19} \\ \text{Root Mean} \\ \text{Squared Error} \end{array}$$

The RMSE data has been compiled in the table below:

Table 4-4 Root Mean Squared Error Analysis of Model

Time (min)	[O <sub>3</sub> ] <sub>aq</sub> init (mg/L)	[1,4-Dioxane] <sub>init</sub> (µg/L)	Power (W)	[1,4-Dioxane] <sub>final</sub> (µg/L)		rRMSE
				Experimental	Model Predicted	
6.89	2.52	17.01	0	7.13	8.36	0.005191
4.82	9.02	19.35	0	9.13	8.45	0.00121
7.10	2.56	22.51	0	10.18	10.77	0.000684
5.78	2.52	22.51	0	14.76	12.40	0.01102
3.12	2.50	25.86	0	20.48	18.77	0.004377
7.17	5.51	20.35	0	6.09	7.40	0.004131
4.68	5.79	20.45	0	12.94	10.43	0.015103
4.51	4.86	20.91	0	11.50	11.42	1.44E-05
2.49	5.83	19.35	0	14.58	13.51	0.003068
7.17	10.82	20.35	0	5.30	5.41	2.92E-05
4.68	11.48	20.45	0	7.75	8.44	0.001136
6.34	1.10	15.75	0	10.39	9.85	0.001188
15.45	2.53	16.02	0	3.47	3.25	0.000192
6.54	2.46	19.76	0	9.14	10.13	0.002499
7.65	2.47	13.46	0	6.15	6.15	8.31E-08
2.49	11.88	19.35	0	12.17	12.00	7.59E-05
7.17	16.06	20.35	0	5.11	4.31	0.00155
4.68	17.03	20.45	0	6.82	7.25	0.000443
16.36	1.04	16.32	0	5.98	4.98	0.003696
Ozone rRMSE						0.0541
7.09	2.54	17.01	940	3.06	3.14	2.27E-05
4.82	10.34	19.35	714	2.43	3.40	0.002495
6.42	12.87	18.89	600	2.58	1.84	0.001538
7.10	2.58	21.65	730	4.20	4.89	0.001027
5.78	2.46	22.51	754	6.76	6.73	1.6E-06
2.93	2.67	25.86	848	14.48	13.19	0.002511
7.17	5.42	20.35	709	1.55	2.78	0.003644
4.68	5.67	20.45	748	4.40	5.25	0.001724
2.49	5.39	19.35	750	9.39	9.51	4.32E-05
7.17	11.19	20.35	698	0.82	1.45	0.000959
4.68	11.33	20.45	739	2.46	3.44	0.002287
2.49	11.11	19.35	720	7.52	7.64	4.12E-05
15.39	2.54	16.02	869	0.39	0.48	3.1E-05
4.64	4.69	20.91	396	9.64	8.08	0.005544
4.85	2.42	20.91	424	10.53	9.56	0.002137
6.44	2.48	21.30	745	4.30	5.57	0.003542
7.17	16.02	20.35	721	0.74	0.92	7.89E-05

4.68	17.66	20.45	726	1.45	2.48	0.002516
16.13	1.25	16.32	788	1.55	1.18	0.000512
6.30	0.99	15.75	869	6.58	5.87	0.00203
Ozone/Ultrasound rRMSE						0.040425
Overall rRMSE						0.047581

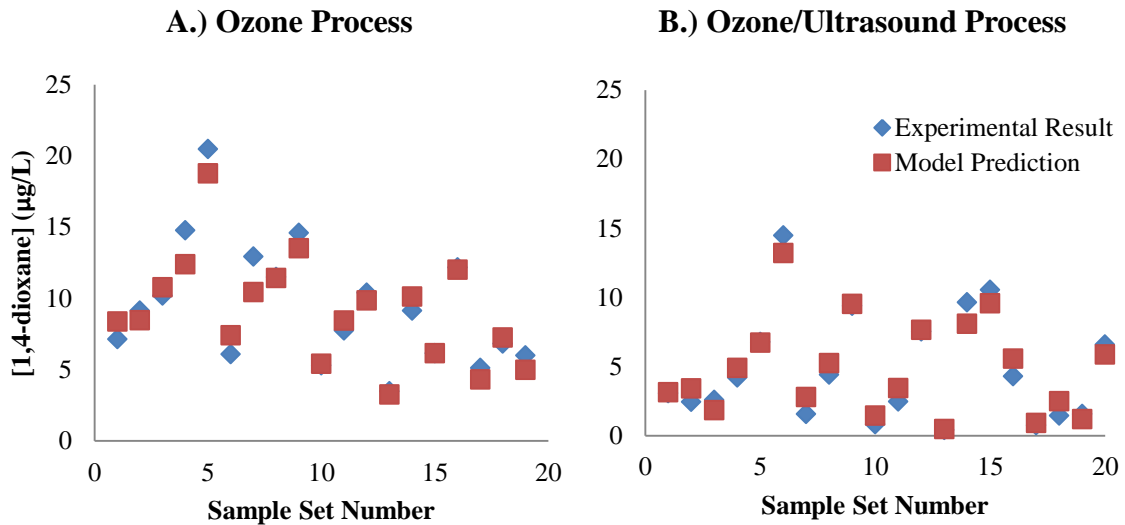


Figure 4-31 Model Performance for A.) Ozone and B. Ozone/Ultrasound

Source Data in Tables E4, E1

#### 4.6.2.1. Scalability of Model

The model defined in Equation 3-15 was developed in a 2.6 L reactor using flow rates that varied from 0.16 to 1.2 L/min. It was found to effectively predict 1,4-dioxane removal in this particular treatment system, but the model would be much more useful if it could be applicable to larger systems of similar designs. Therefore, the model was compared with previous experimental results from a pilot-scale reactor. This reactor had a 20 L volume and was operated at flow rates from 23 to 67 L/min (Andaluri G. , 2016). Unfortunately this pilot scale system did not allow for the combination of ozone and ultrasound. However, it did allow for comparison for treatment by ozone alone, and the

model was found to give reasonable, albeit conservative, estimates of the experimental results. The results of this set of experiments are tabulated below.

*Table 4-5 Applicability of Model to Pilot Scale Ozonation Study*

Retention Time (min)	[O <sub>3</sub> ] <sub>aq</sub> (mg/L)	[1,4-Dioxane] <sub>init</sub> (µg/L)	Experimental [1,4-Dioxane] <sub>final</sub> (µg/L)	Model Predicted [1,4-Dioxane] <sub>final</sub> (µg/L)
0.3	0.27	10	9.5 ± 0.39	9.87
0.35	0.35	10	9.5 ± 0.39	9.84
0.4	0.425	10	8.7 ± 0.39	9.80
0.85	0.9	10	8.8 ± 0.38	9.44
0.85	0.8	10	8.8 ± 0.47	9.47
0.85	1.2	10	8.6 ± 0.47	9.38
0.85	2.6	10	8.3 ± 0.46	9.17
0.85	3	10	8.1 ± 0.46	9.13
0.85	3.5	10	7.9 ± 0.45	9.08

(Andaluri G. , 2016)

Despite the reactor scale differing 10-fold and the flow rates differing 50-fold, the model still gives reasonable predictions for 1,4-dioxane removal, with several predictions falling within the reported experimental error and several other predictions falling just outside the experimental error bands.. The pilot scale system achieved ozone/water mixing with a venturi, while the smaller reactor used to build the model employed a static mixer in addition to the venturi effect. Both studies used spiked drinking water obtained from the Philadelphia Water Department. While comparisons to other published data showed less removal than what would be predicted by this model (Xu, Mochida, Naito, & Yasuda, 2012) (Kwon , et al., 2012), greater removal was achieved in the study involving spiked drinking water (Andaluri G. , 2016).

### 4.6.3. $R_{CT}$ Analysis

The reactor was also analyzed using the RCT concept, first developed by Elovitz and von Gunten. This concept will be outlined below. In order to use the RCT analysis on a contaminant, it must react very quickly with the hydroxyl radical and very slowly with ozone directly. Dioxane meets this criteria since  $k_{O_3, 1,4 \text{ dioxane}}=0.32 \text{ M}^{-1}\text{s}^{-1}$  and  $k_{OH\cdot, 1,4 \text{ dioxane}}=2.4 \times 10^9 \text{ M}^{-1}\text{s}^{-1}$  (Suthersan & Payne, 2004). Therefore, by ignoring the direct influence of ozone on the removal of 1,4-dioxane, the following rate equation emerges (Elovitz & von Gunten, 1999):

$$\frac{d[1,4 \text{ dioxane}]}{dt} = -k_{OH\cdot, 1,4 \text{ dioxane}} [1,4 \text{ dioxane}][OH\cdot] \quad \begin{array}{l} \text{Equation 4-20} \\ \text{Reaction with} \\ \text{Hydroxyl Radical} \end{array}$$

Rearranging and integrating the equation above yields:

$$\ln\left(\frac{[1,4 \text{ dioxane}]}{[1,4 \text{ dioxane}]_0}\right) = -k_{OH\cdot, 1,4 \text{ dioxane}} \int [OH\cdot] dt \quad \begin{array}{l} \text{Equation 4-21} \\ \text{Integrated} \\ \text{Reaction with} \\ \text{Hydroxyl Radical} \end{array}$$

Next,  $R_{CT}$  is defined as the ratio of hydroxyl radical exposure and ozone exposure:

$$R_{CT} = \frac{\int [OH\cdot] dt}{\int [O_3] dt} \quad \begin{array}{l} \text{Equation 4-22} \\ R_{CT} \text{ Definition} \end{array}$$

Substituting  $R_{CT}$  into the integrated equation:

$$\ln\left(\frac{[1,4 \text{ dioxane}]}{[1,4 \text{ dioxane}]_0}\right) = -k_{OH\cdot, 1,4 \text{ dioxane}} R_{CT} \int [O_3] dt \quad \begin{array}{l} \text{Equation 4-23} \\ 1,4\text{-Dioxane} \\ \text{Removal Using} \\ R_{CT} \end{array}$$

The influent and effluent aqueous ozone concentrations were measured in this study. One of the challenges posed by using a continuous flow reactor is that it didn't

permit aqueous ozone concentrations at any intermediate times. Therefore, to estimate the integration of ozone concentration over time, a simple linear interpolation from influent to effluent concentrations was employed. The left hand side of Equation 3-20 is determined by taking the natural logarithm of final 1,4-dioxane concentration divided by initial concentration. Plotting these natural logarithms versus the integrated ozone data yields the following figure.

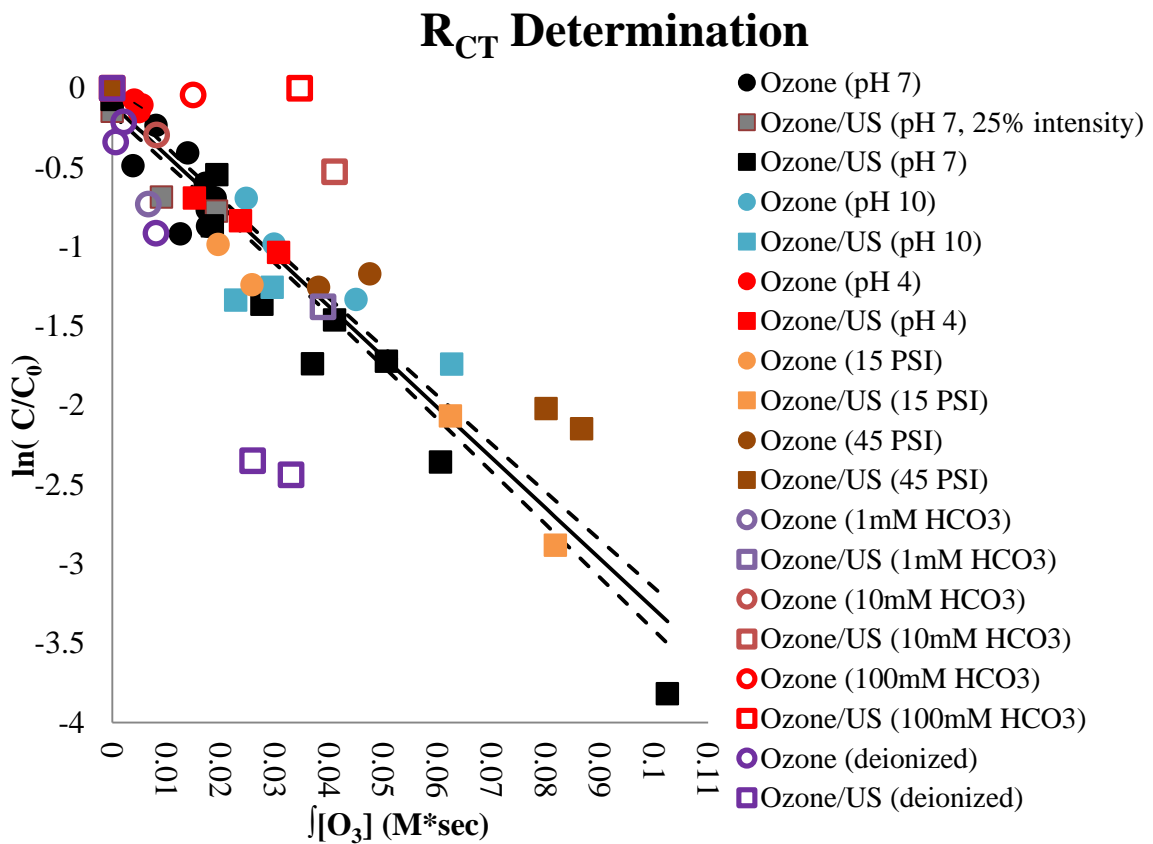


Figure 4-32 R<sub>CT</sub> Determination

Source Data in Table E3, E4, E8

The slopes depicted in the figure above represent the 95% confidence interval for the R<sub>CT</sub> of the spiked drinking water. The outlying data points are those hollow squares and circles which represent matrices other than spiked drinking water (i.e. deionized

water or drinking water with >10mM added bicarbonate), which were excluded from the confidence limit calculation. This slope can be traced back Equation 4-23, where it represents  $R_{CT}$  multiplied by the rate constant for 1,4-dioxane reacting with the hydroxyl radical. With this slope, it is possible to solve for the  $R_{CT}$  term using published data for the reaction rate constant,  $k_{OH \cdot 1,4 \text{ dioxane}}$ , is  $2.4 \times 10^9 \text{ M}^{-1}\text{s}^{-1}$  (Thomas, 1965) (Suthersan & Payne, 2004).

$$\text{slope} = -k_{OH \cdot 1,4 \text{ dioxane}} R_{CT} = (-2.4 \times 10^9 \text{ M}^{-1}\text{s}^{-1}) \times R_{CT} \quad \begin{array}{l} \text{Equation 4-24} \\ R_{CT} \text{ Calculation} \end{array}$$

The slope from Figure 4-30 can be used to solve Equation 3-21 for  $R_{CT}$ , yielding  $1.33 \times 10^{-8}$  for the spiked drinking water. This value is comparable to those published using para-chlorobenzoic acid as a hydroxyl radical probe. In a study of twelve natural surface and ground waters in Switzerland, the average  $R_{CT}$  was determined to be  $1.56 (\pm 1.6) \times 10^{-8}$  (Elovitz & von Gunten, 1999) (Acero, Stemmler, & Von Gunten, 2000).

The  $R_{CT}$  analysis also helps illuminate the mechanism at work in the combined ozone/ultrasound system. From Figure 4-31, the data for ozone, combined ozone/ultrasound (100% intensity), and combined ozone/ultrasound (25% intensity) all appear to fall near the confidence limit lines. The results of the pressurization study appear to fall near the confidence limits, as well, as do those of the pH study. Therefore, the mechanism behind the synergies noted in the combined ozone/ultrasound system is inferred to be a result of increased ozone consumption. If there were some other mechanisms at work in the combined ozone/ultrasound system, the ozone data points (filled circles) would be expected to follow a markedly different trend than the combined ozone/ultrasound data points (filled squares). Since the data for all experimental

conditions in drinking water appears to follow the same trend, and since the reaction rate constant doesn't change, the yield of hydroxyl radical per ozone consumed ( $R_{CT}$ ) appears to be the same for all pH, pressure, ozone, and ultrasound conditions. What is changing as a result of these experimental conditions, however, is the consumption of ozone. In short, the removal of dioxane requires hydroxyl radicals. Hydroxyl radicals require ozone consumption. Therefore, ozone consumption drives dioxane removal. This finding implies that treatment optimization strategies should be aimed at efficient consumption of aqueous ozone within the reactor.

The outlying data points (i.e. deionized experiments and the experiments using added bicarbonate) also indicate this same ozone consumption mechanism. The presence of compounds which compete with 1,4-dioxane for hydroxyl radicals (sodium bicarbonate, in this case) was shown to depress 1,4-dioxane removal. This competition serves to flatten the slope of the  $R_{CT}$  curve shown above, i.e. competition from scavengers would require the more ozone consumption and more hydroxyl radical production in order to remove an equivalent percentage of 1,4-dioxane. In deionized water, there is no such competition for hydroxyl radicals, so more dioxane removal is achieved per unit ozone consumed. The lack of competition serves to steepen the  $R_{CT}$  curve. Less dioxane removal was achieved by ozone alone in deionized water than in drinking water. The lack of scavenging compounds in deionized water was not enough to make up for the reduced ozone consumption. The strategy of maximizing ozone consumption to maximize dioxane removal would still apply, no matter what scavenging compounds are present in the matrix.

#### 4.6.4. Mass Balance Analysis

A mass balance analysis was conducted on the experimental data obtained from the previous objectives. A schematic for the reactor is given in Figure 4-33. Because the process involves both aqueous and gaseous phases, the reactor has been divided into two equal compartments for the graphic. This division is purely for simplicity and graphical clarity, since the gas compartment would be myriad bubbles dispersed throughout the reactor.

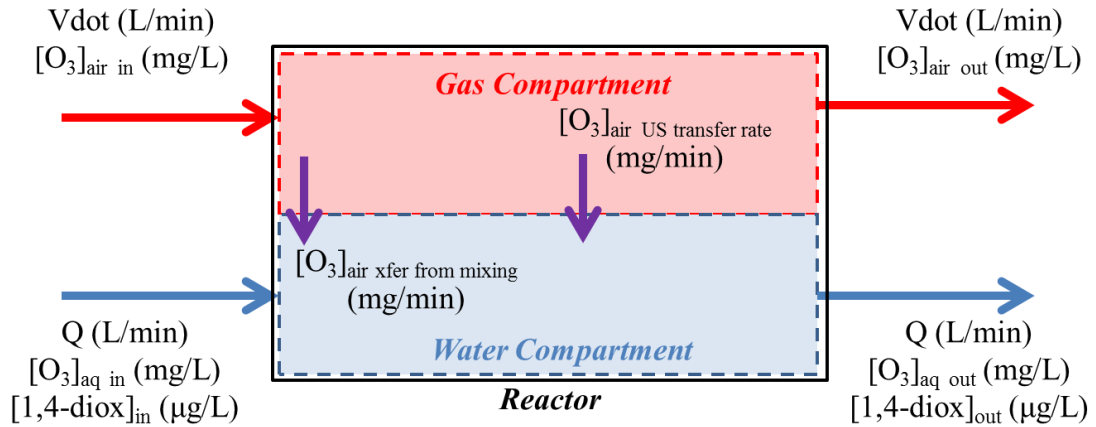


Figure 4-33 Mass Balance Schematic

The flow rates and concentrations outside the reactor are the values that were measured during experiments. Note that  $[O_3]_{aq\ in}$  is measured after the reactor mixing section, while  $[O_3]_{air\ in}$  is measured prior to the mixing section. This is why there is no  $[O_3]_{air\ xfer\ from\ mixing}$  term in Equation 4-26. The two arrows within the reactor, ozone transfer from gas to water in the reactor mixing section and ozone transfer from ultrasound, were not measureable. Therefore, to make an estimate of the mass balance, a number of assumptions were needed:

1. Quasi steady state condition

*Justification: Quasi steady state was ensured by waiting multiple retention times between samples and verified with a tracer study.*

2. Changes in  $[O_3]_{air}$  during ozonation (no ultrasound) were solely due to the reactor mixing section (i.e. negligible mass transfer or air phase ozone decay without sonication)

*Justification: The results of the constant  $[O_3]_{aq}$  pressure study support this, since removal of 1,4-dioxane was unaffected by lower  $[O_3]_{air}$  conditions at higher pressures.*

3. Net ozone mass transfer is from gas to liquid during sonication

*Justification: This assumption is supported by Figure 4-7.*

4. Changes in  $[O_3]_{air}$  during combined ozone/ultrasound were due to the reactor mixing section and mass transfer from ultrasound (i.e.  $[O_3]_{air}$  breakdown from sonication is considered transferred)

*Justification: If  $[O_3]_{air}$  is broken down as a result of cavitation, it could be considered to be simultaneously transferred since the gas bubble has collapsed.*

5. Given equivalent flow conditions, mass transfer in the reactor mixing section is equivalent for ozone and ozone/ultrasound.

*Justification: A reasonable assumption which is required in order to isolate and estimate the mass transfer due to ultrasound.*

Given these assumptions, the mass rate balance over the gas compartment is given in the equation below.

$$\begin{aligned}
V \dot{\left( \frac{L}{min} \right)} & \left( [O_3]_{air\ in} \left( \frac{mg}{L} \right) - [O_3]_{air\ out} \left( \frac{mg}{L} \right) \right) \\
& - [O_3]_{air\ US\ transfer\ rate} \left( \frac{mg}{min} \right) \\
& = [O_3]_{air\ xfer\ from\ mixing} \left( \frac{mg}{min} \right)
\end{aligned}$$

*Equation 4-25  
Gas Compartment  
Mass Rate  
Balance*

The mass rate balance over the water compartment is given below.

$$\begin{aligned}
[O_3]_{air\ US\ transfer\ rate} & \left( \frac{mg}{min} \right) \\
+ Q & \left( \frac{L}{min} \right) \left( [O_3]_{aq\ in} \left( \frac{mg}{L} \right) - [O_3]_{aq\ out} \left( \frac{mg}{L} \right) \right) - \\
& = [O_3]_{aq\ consumption\ rate} \left( \frac{mg}{L} \right)
\end{aligned}$$

*Equation 4-26  
Water  
Compartment  
Mass Balance*

The results from the ozone experiments were used to solve for  $[O_3]_{air\ US\ transfer\ rate}$  using Equation 4-25. Then, the  $[O_3]_{aq\ consumption\ rate}$  could be solved for as in Equation 4-27.

$$\begin{aligned}
V \dot{\left( \frac{L}{min} \right)} & \left( [O_3]_{air\ in} \left( \frac{mg}{L} \right) - [O_3]_{air\ out} \left( \frac{mg}{L} \right) \right) \\
+ Q & \left( \frac{L}{min} \right) \left( [O_3]_{aq\ in} \left( \frac{mg}{L} \right) - [O_3]_{aq\ out} \left( \frac{mg}{L} \right) \right) \\
& = [O_3]_{aq\ consumption\ rate} \left( \frac{mg}{min} \right)
\end{aligned}$$

*Equation 4-27  
Aqueous Ozone  
Consumption  
Estimate*

This aqueous ozone consumption rate was then compared with the removal rate for 1,4-dioxane.

$$\begin{aligned}
 [1,4 \text{ dioxane}]_{\text{removal rate}} \left( \frac{\mu\text{g}}{\text{min}} \right) &= Q \left( \frac{\text{L}}{\text{min}} \right) \left( [1,4 \text{ dioxane}]_{\text{in}} \left( \frac{\mu\text{g}}{\text{L}} \right) \right. \\
 &\quad \left. - [1,4 \text{ dioxane}]_{\text{out}} \left( \frac{\mu\text{g}}{\text{L}} \right) \right)
 \end{aligned}$$

Equation 4-28  
Aqueous Ozone  
Consumption  
Estimate

Finally, these mass rates for dioxane and aqueous ozone were normalized to compare mass of ozone to mass of dioxane. The results of this are given in Figure 4-33.

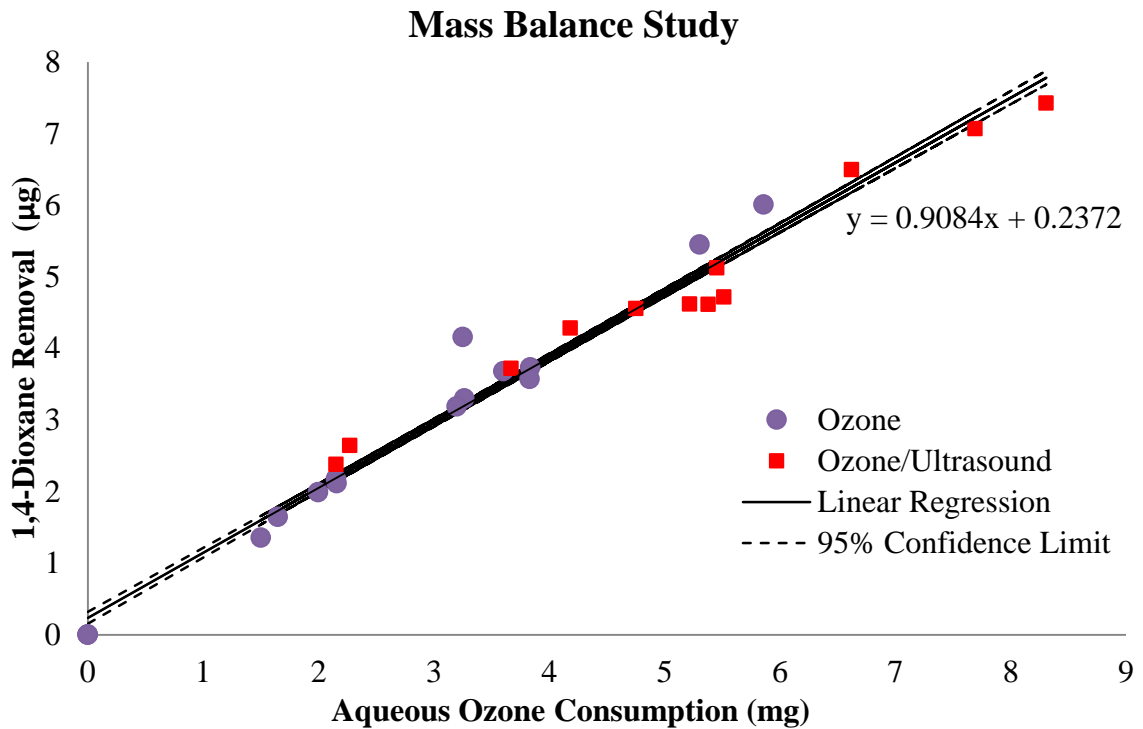


Figure 4-34 Mass Balance Study

Source Data in Table E10

This mass balance analysis gives support to the theory that the removal of 1,4-dioxane is dependent on the consumption of aqueous ozone. The data used for Figure 4-33 was obtained from ozone and combined ozone/ultrasound experiments conducted using a range of pressures (8-45 PSI), retention times (6-15 minutes), aqueous ozone

concentrations (1-16 mg/L). The linearity of the data suggests that dioxane removal is proportional to total aqueous ozone consumption (including air phase mass transfer), where (mass 1,4-dioxane removed) : (mass aqueous ozone consumed) is given by 0.91:1000 or 0.00091:1.

#### *4.6.5. Implications of Modeling Results*

The Chick & Watson-style model developed is capable of predicting 1,4-dioxane removal for a wide range of ozone dosages, ultrasound dosages, and treatment times. Since the removal of 1,4-dioxane is predicated on hydroxyl radical generation, an  $R_{CT}$  analysis could also be used for prediction. Each approach has its limitations. The use of  $R_{CT}$  requires the ability to measure both influent and effluent aqueous ozone concentrations, while the Chick & Watson-style model requires ultrasonic intensity measurements. Both models were found to be susceptible to matrix effects. The addition of bicarbonate as a hydroxyl radical scavenger will cause the Chick & Watson-style model to underestimate effluent concentrations of 1,4-dioxane. The  $R_{CT}$  same model is also sensitive to changes in the matrix since the data from the deionized and bicarbonate tests were shown to lie well outside the  $R_{CT}$  trend noted in drinking water tests. The  $R_{CT}$  analysis could be used to predict effluent concentration of 1,4-dioxane, if the  $R_{CT}$  value for the source water was known. If the matrix being treated is consistent, either model can work, but the Chick & Watson-style model is recommended in situations where ultrasonic intensity can be measured, and the  $R_{CT}$  analysis should be recommended for systems where influent and effluent aqueous ozone concentrations can be measured.

## CHAPTER 5. KEY CONTRIBUTIONS AND FUTURE WORK

### 5.1. Key Contributions

To the best of my knowledge, this is the first time that the combined ozone/ultrasound process has been studied for the removal 1,4-dioxane in a continuous flow reactor. It is also only the second published study for this AOP and this contaminant. Interestingly, this study achieved far faster dioxane removal kinetics than the previous study (Xu, Mochida, Naito, & Yasuda, 2012). It is believed that the faster kinetics are due to a mass transfer advantage of a continuous flow reactor over a batch system and to the use of spiked drinking water rather than deionized water. It is the first such study to explore the effects of reactor pressurization using constant aqueous ozone dose and constant air phase ozone dose approaches. This pressurization study yielded new evidence supporting the theory that ultrasound serves to increase ozone mass transfer to the water phase. It is the first such study to investigate the effects of pH. It is the first study to apply the  $R_{CT}$  concept to 1,4-dioxane removal by ozone/ultrasound. It is the first study to construct a Chick & Watson style empirical model for combined ozone/ultrasound. It is the first to create such a model capable of describing treatment by ozone alone, as well as combined ozone/ultrasound with varied ultrasonic power inputs.

Overall, the use of combined ozone and ultrasound shows promise as a treatment option for 1,4-dioxane. Based on the results of this study, the use of combined ozone and ultrasound in a pressurized reactor can effectively remove 1,4-dioxane. Based on the mass balance analysis, the key to dioxane removal appears to be the consumption of aqueous ozone, and the addition of ultrasound is one way to increase this consumption. It

is unknown if this treatment technology can be done in manner that makes it cost effective relative to other AOPs. However, even if it is found to be more costly, combined ozone and ultrasound could provide a useful alternative treatment technique in situations where the other benefits of ultrasound, such as direct thermal destruction and supercritical oxidation, are desirable, or for source waters and locations that are unsuitable for other AOPs.

## **5.2. Future Work**

Removal of 1,4-dioxane is highly dependent upon the generation of hydroxyl radicals. A comparison study of the O<sub>3</sub>/Ultrasound system with other AOPs, such as UV, UV/H<sub>2</sub>O<sub>2</sub>, UV/O<sub>3</sub>, UV/O<sub>3</sub>/H<sub>2</sub>O<sub>2</sub>, Ultrasound/O<sub>3</sub>/H<sub>2</sub>O<sub>2</sub> in a continuous flow reactor would be useful for water treatment operators looking to optimize treatment system selection given a particular influent water stream. Additionally, a detailed side-by-side comparison would aid greatly a cost comparison analysis, which would also enable operators to choose cost effective solutions. To this end, some preliminary work has been done, but a full comparative study was beyond the scope of this study.

### *5.2.1. AOP Comparison*

Based on the successful removal of 1,4-dioxane using combined ozone/ultrasound, the experimental reactor was redesigned to permit the testing of combined ozone/liquid oxidant/ultrasound as well as ozone/liquid oxidant/UV. To permit UV treatment combinations, a 1.8L Wedeco CHI-2 Ultraviolet Water Disinfection Unit was added in parallel to the existing ultrasound reactor. A three way valve permitted easy switching to send the water to either the ultrasound reactor or ultraviolet reactor. The effluent lines from both reactors rejoined at a T-fitting, and one-way valves

were placed at the exit of both the ultrasonic and UV reactor to prevent backflow. The arrangement of valves permitted pre and post chamber ozone measurements to be obtained in the same manner as done previously. The arrangement also permitted the same pressurization valve to be used. The maximum pressure in the UV reactor was limited to 150 PSI due to the limits of the quartz sleeve, but this far exceeded any of the pressures tested in this study (Wedeco, 2004). To permit the combination of both gaseous oxidant (ozone) and liquid oxidant, a peristaltic pump (Pharmacia Fine Chemicals Model P-1) was plumbed into the influent water feed line. This allowed controllable and metered injection of liquid just after the ozone injection point and just before the ultrasonic or UV reactor. A schematic for this experimental setup is shown below:

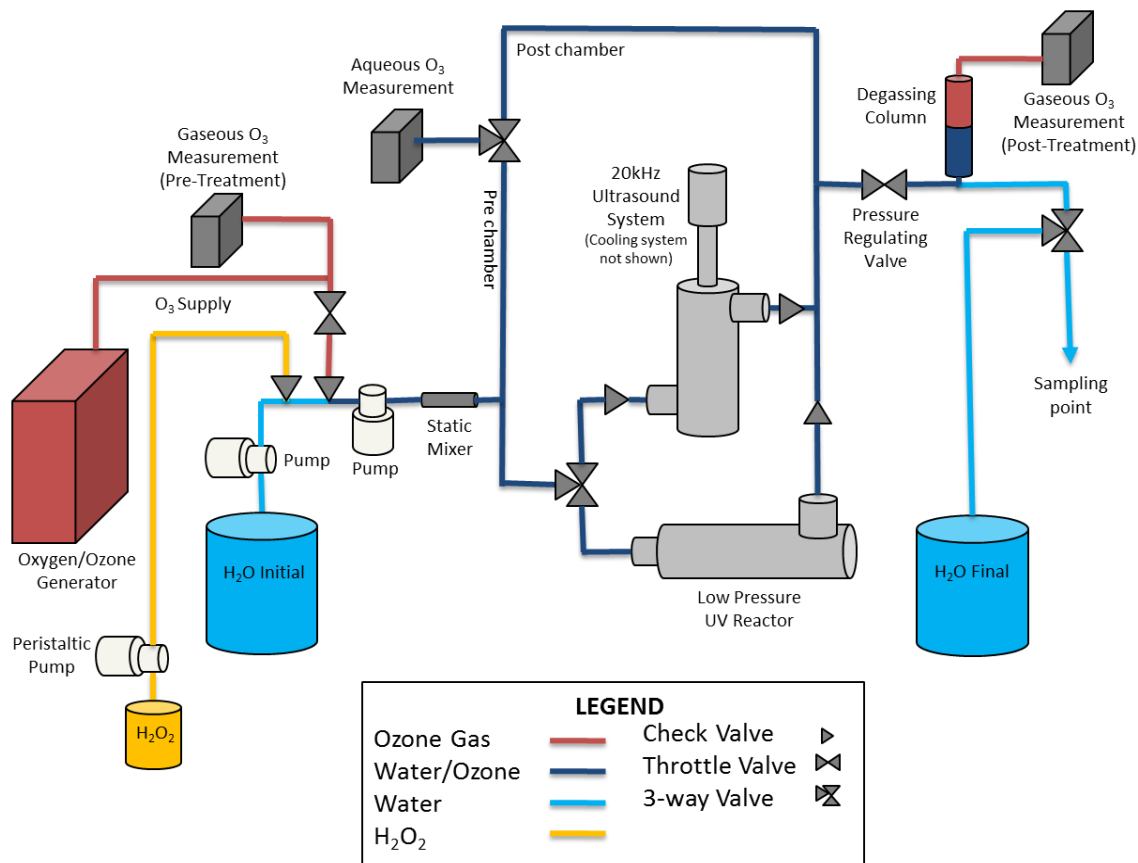


Figure 5-1 Schematic for Parallel Ultrasound and UV Treatment

The AOP comparison tests were done using drinking water that had been spiked with 20 ppb of 1,4-dioxane. Dioxane was chosen for a preliminary AOP comparison for the same reasons as it was chosen for the rest of this study: it is recalcitrant, requiring a powerful oxidant like the hydroxyl radical to treat, it is prevalent, having been detected in ground water in the US and abroad, and 1,4-dioxane removal is used by government regulators to evaluate AOP effectiveness (Zenker, Borden, & Barlaz, 2003) (Abe, 1999) (California Dept of Public Health, 2014). Spiked drinking water was chosen because it simulates water meant for human consumption, which has been through a conventional water treatment train (settling, coagulation, filtration, disinfection), yet still contains 1,4-dioxane, necessitating post-treatment by an AOP.

In batch tests of the combined ozone/peroxide system for the removal of 1,4-dioxane, the optimum molar dose ratio of ozone:peroxide was found to lie between 0.5 and 1.0 (Adams, Scanlan, & Secrist, 1994). However, the mole ratio in the previous study was based on moles of hydrogen peroxide compared to moles of air phase ozone. For this preliminary comparison, oxidant dosages of 2.5 mg/L for aqueous ozone and 10 mg/L for hydrogen peroxide were chosen as a starting point. In terms of molarity, this ratio works out to be 5.6:1 H<sub>2</sub>O<sub>2</sub>:O<sub>3</sub>, which appears significantly higher than what is recommended for the ozone/peroxide AOP. However, the air phase concentration is always higher than that of the aqueous phase. The high ratio was selected for two reasons. The first was that it was only a starting point, and the second was because the results of the continuous flow ozone and combined ozone/ultrasound tests suggest that ozone mass transfer plays a major role during sonication. Therefore, the optimum H<sub>2</sub>O<sub>2</sub>:O<sub>3</sub> ratio for a batch reactor may differ significantly from the optimum ratio in a continuous flow reactor.

The Wedeco UV reactor is fitted with a type UCS UV sensor. This sensor automatically calibrates, measures UV intensity at the 254nm wavelength with 99% selectivity, and is accurate to ±4% (Wedeco, 2004). To verify sensor operation, a uridine actinometry test was performed in the flow through reactor and compared with results from a collimated beam device (CBD). Experiments using the CBD were carried out similarly to other published studies (Linden & Darby, 1997). To test the UV intensity, 0.1M uridine solution was made in water (Sigma Aldrich). The radiant flux from the CBD is then characterized by:

$$D_{abs} = \frac{\Delta\alpha_{10}V}{\Phi_{\lambda}\varepsilon A_{CS}} \cdot C$$

*Equation 5-1  
Radiant Flux in  
Collimated Beam  
Device*

where  $D_{abs}$  is the absorbed dose, given in  $\text{mJ}/\text{cm}^2$ ,  $\Delta\alpha_{10}$  is the change in absorbance at 262nm as measured by a Hach DR5000,  $V$  is the sample volume in  $\text{cm}^3$ ,  $\Phi_{\lambda}$  is the quantum yield of uridine (estimated to be 0.02 mol/Einstein for 254nm) (Swenson & Setlow, 1962)),  $\varepsilon$  is the uridine extinction coefficient (estimated to be 8200  $\text{L}/\text{mol}\cdot\text{cm}$  (Wang S. Y., 1976)),  $A_{CS}$  is the cross sectional area of the sample dish, and  $C$  is a unit conversion constant (474591 J/Einstein). The calibration curve for the CBD tests is given in the following figure.

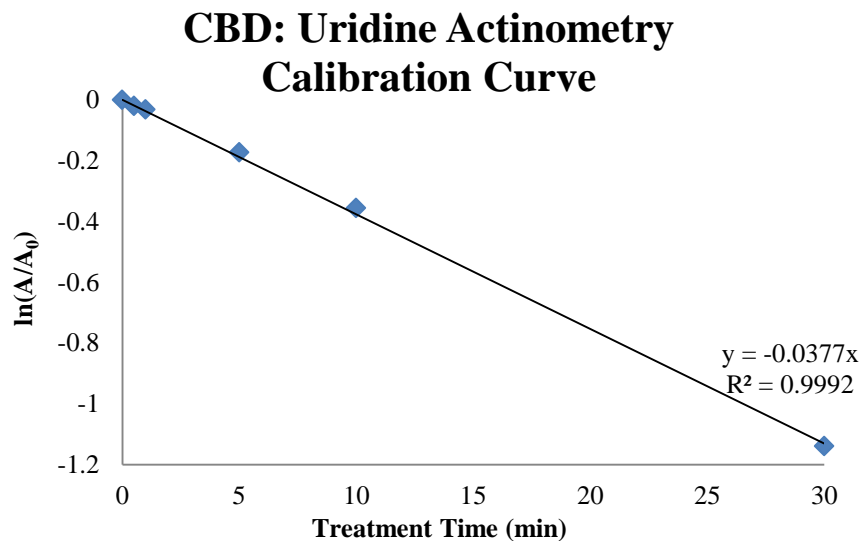


*Figure 5-2 CBD Calibration Curve*

*Source Data in Table E9*

To measure the UV intensity in the flow through reactor, the equation is modified to account for the different orientation of the reactor. In the CBD, a collimated beam of UV photons strike the sample uniformly on the surfaced. In the equation above, volume is divided by cross sectional area, which gives the depth of water in the petri dish. This

depth describes the photon path through the sample, which is the characteristic length for the CBD system. In the continuous flow reactor, the sample can be thought of as a donut-shaped plug of water. The center of the donut holds a quartz tube in which resides a low-pressure UV lamp. Photons travel radially from the quartz sleeve, so the analogous characteristic length is given by the difference between the radius of the inner edge of the reactor,  $R$ , and that of the outer edge of the quartz glass tube,  $r$  ( $3.5 - 1.225 = 2.275$  cm).

$$D_{abs} = \frac{\Delta\alpha_{10}(R - r)}{\Phi_{\lambda}\epsilon} \cdot C \quad \begin{array}{l} \text{Equation 5-2} \\ \text{Radiant Flux in} \\ \text{Reactor} \end{array}$$

A calibration curve was made using the continuous flow reactor by varying the pump speed, which in turn varies the treatment time, i.e. UV dose.

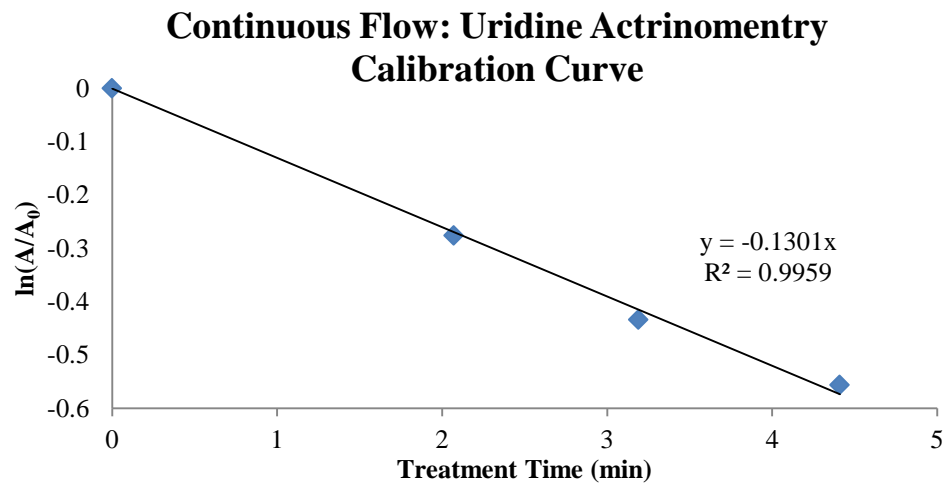


*Figure 5-3 Continuous Flow UV Calibration Curve*

*Source Data in Table E9*

Once the UV intensity of the continuous flow reactor had been confirmed with the uridine actinometry, another comparison set of tests was completed to verify the function of the peristaltic pump. The peristaltic pump flow rate was determined by timed weighing of the hydrogen peroxide supply bottle. Then, the pump flow rate was set to

meter out a flow of 10ppm of hydrogen peroxide to the feed water prior to UV irradiation. Continuous flow samples were exposed to different UV doses by varying the retention time. Then, the removal of 1,4-dioxane using combined H<sub>2</sub>O<sub>2</sub>/UV in a continuous flow reactor was compared with that in the CBD. Those results are given in the following figure. The slopes are nearly identical in both the continuous flow reactor and the CBD, indicating that both UV and H<sub>2</sub>O<sub>2</sub> dosing systems in the continuous flow reactor were functioning as expected.

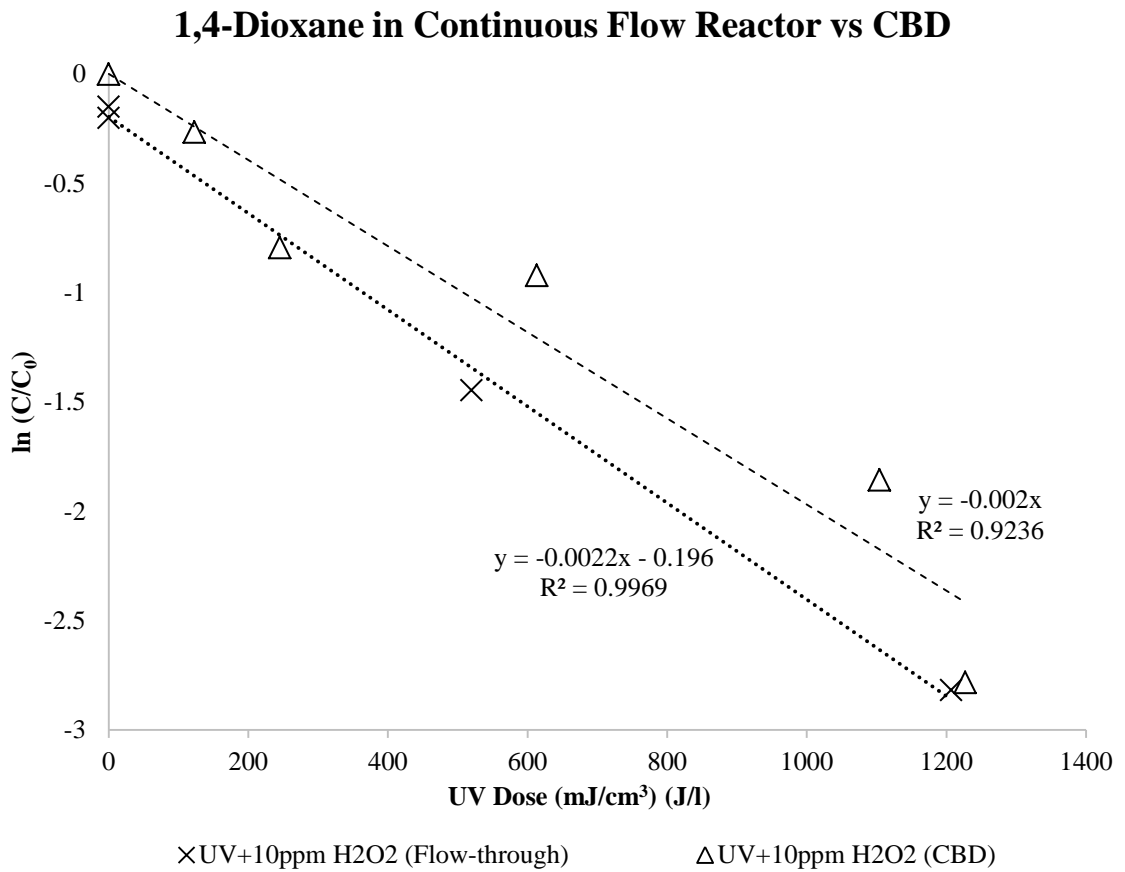


Figure 5-4 Continuous Flow Reactor vs CBD for 1,4-Dioxane Removal

Source Data in Table E9

The dose rate for the continuous flow UV reactor was calculated to 11.26 mW · s/cm<sup>2</sup>.

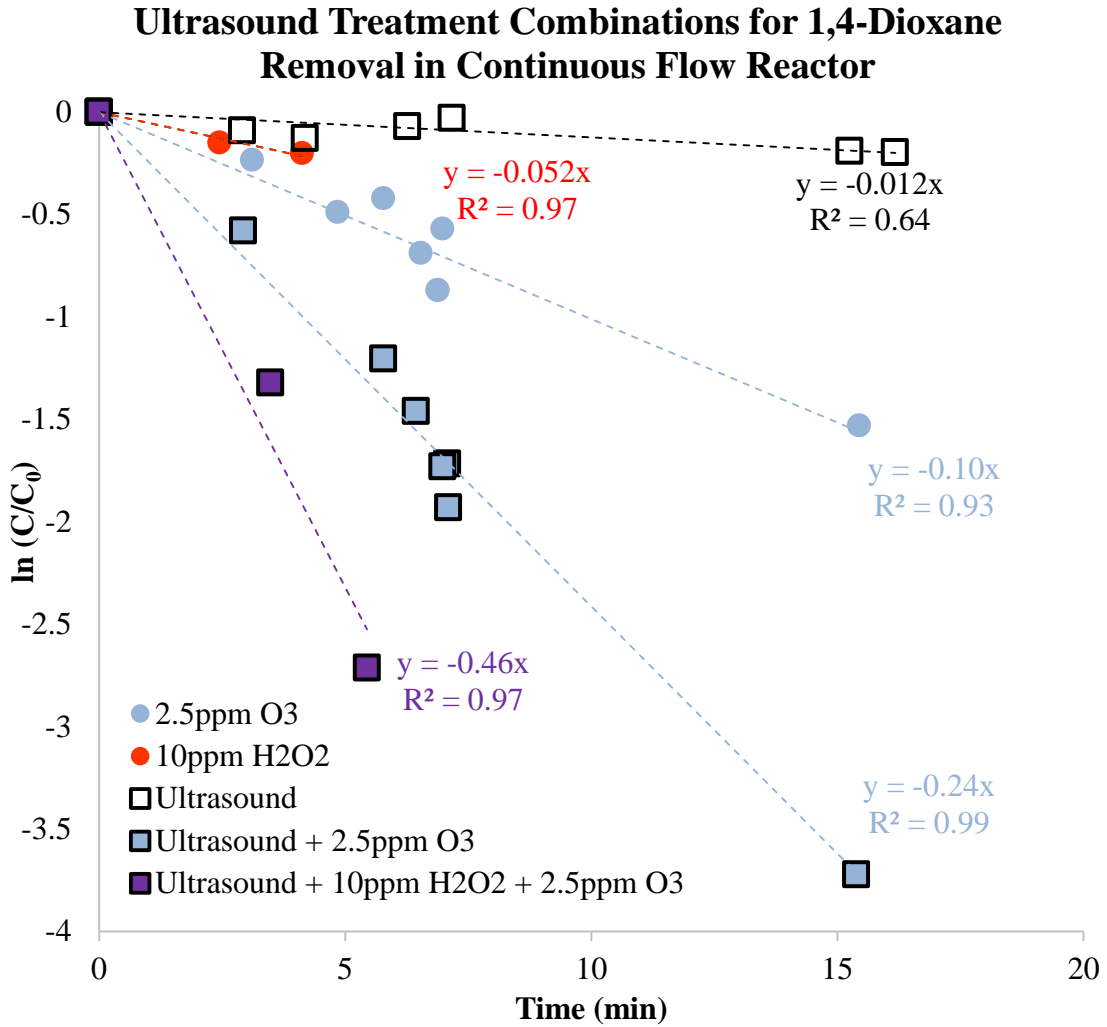


Figure 5-5 Ultrasound Treatment Combinations for 1,4-Dioxane Removal

Source Data in Table E9

In the figure above, the addition of 10ppm hydrogen peroxide to the combined ozone/ultrasound system appears to boost the rate of dioxane removal by 1.9X.

## Ultraviolet Treatment Combinations for 1,4-Dioxane Removal in Continuous Flow Reactor

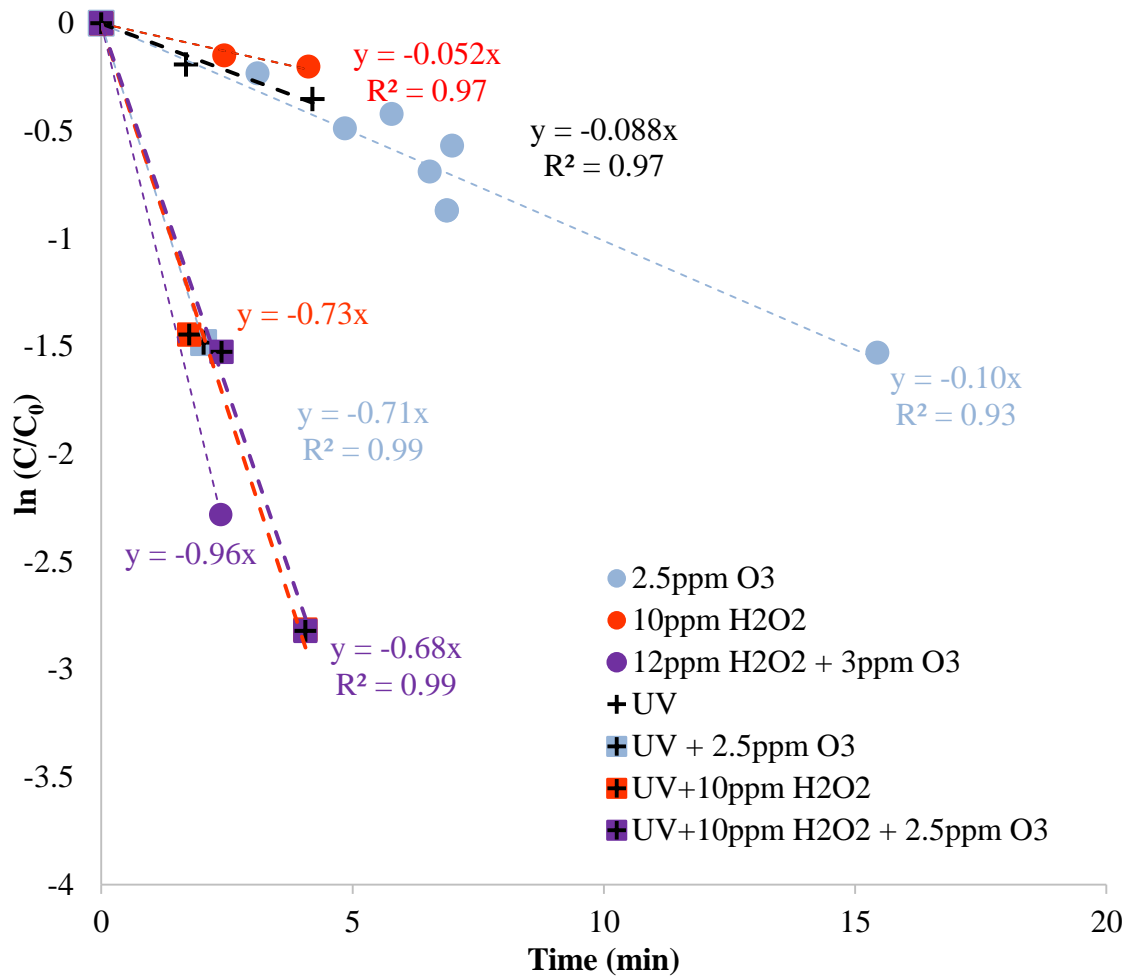


Figure 5-6 UV Treatment Combinations for 1,4-Dioxane Removal

Source Data in Table E9

In the figure above, the addition of UV to either ozone or hydrogen peroxide appears to reach a max rate of dioxane removal of  $\sim 0.7 \text{ min}^{-1}$ . No additional boost was noted from the combination of all three. The doses for the ozone/peroxide sample were slightly higher than the other conditions. This is likely the reason that this combination appears to have a slightly higher rate constant ( $0.96 \text{ min}^{-1}$ ). In a previous study, the rate constant for  $\text{O}_3/\text{H}_2\text{O}_2$  was calculated to be  $0.59 \text{ min}^{-1}$  (Takahashi, et al., 2013). The same

study obtained a rate constant of  $0.0038 \text{ min}^{-1}$  for ozonation and  $0.0018 \text{ min}^{-1}$  for UV, which were also lower than the preliminary results obtained here. In another previous study, 15mM of  $\text{H}_2\text{O}_2$  (510 mg/L) combined with UV was found to remove dioxane with a first order rate constant of  $0.52 \text{ min}^{-1}$ , comparable to the  $0.73 \text{ min}^{-1}$  obtained in this initial test (Stefan & Bolton, 1998).

The rate constant obtained with the  $\text{O}_3/\text{UV}$  combination was  $0.72 \text{ min}^{-1}$ , which is significantly higher than the  $0.0225 \text{ min}^{-1}$  reported in a previous batch study (Takahashi, et al., 2013). However, the previous study reported only air phase ozone dosage, which was  $\sim 35 \text{ mg/L}$  with a  $0.5 \text{ L/min}$  flow rate. Another study varied ozone bubble size and found that it had a significant impact on kinetics, with first order rate constants varying from  $0.019 \text{ min}^{-1}$  to  $0.343 \text{ min}^{-1}$  when  $\sim 43 \text{ mg/L}$  air phase ozone was supplied at  $0.5 \text{ L/min}$  with a 20W UV lamp, suggesting a strong dependence on mass transfer (Kishimoto & Nakamura, 2011). The apparent performance advantage of the continuous flow reactor for the  $\text{O}_3/\text{UV}$  process in the current study is similar to apparent advantage that was observed in comparing the flow through  $\text{O}_3/\text{Ultrasound}$  results with those of Xu et al, suggesting that perhaps batch studies are not reflective of ozonated continuous flow systems.

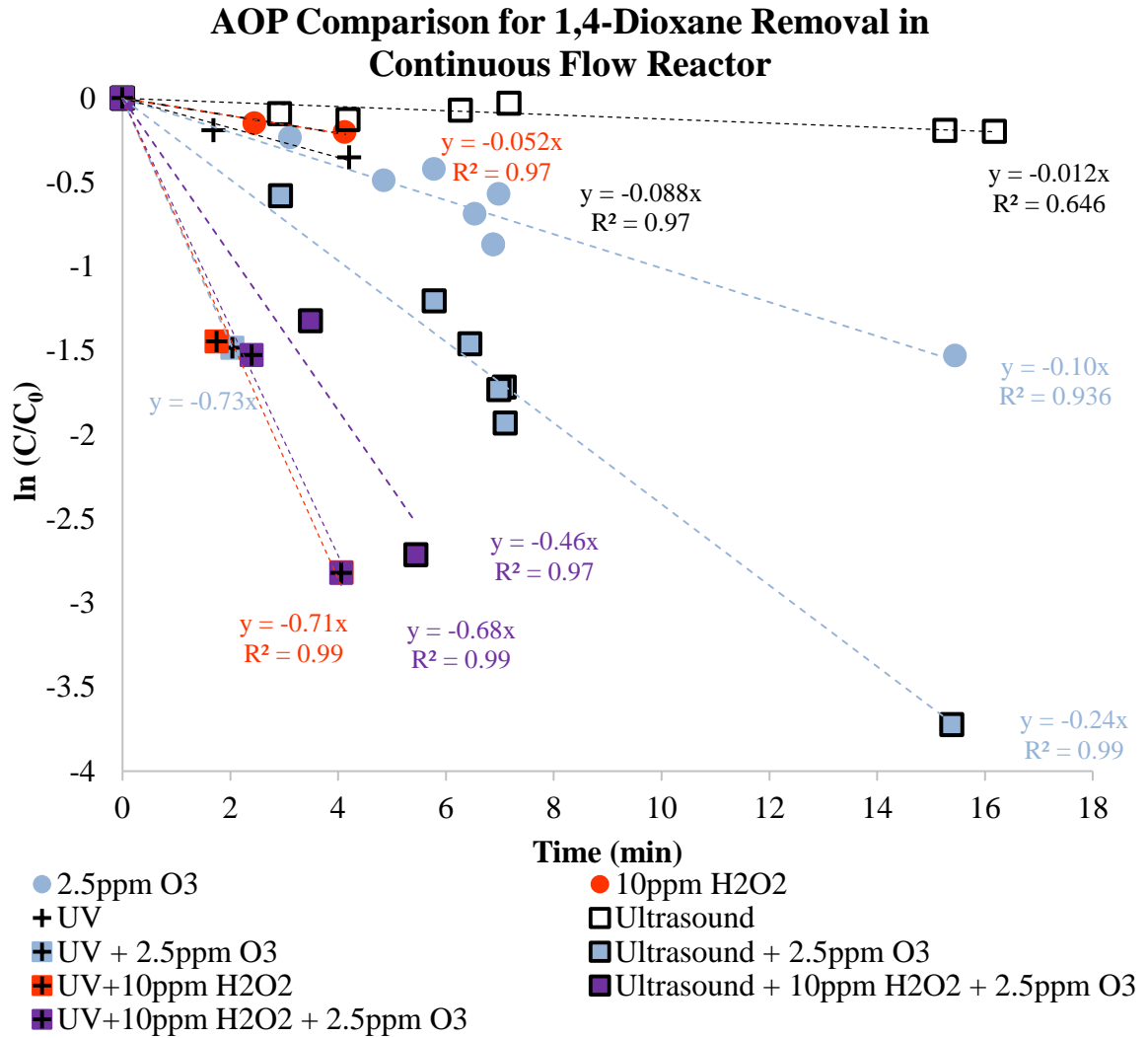


Figure 5-7 AOP Comparison

Source Data in Table E9

The figure above gives a visual comparison of a number of AOP combinations which were selected for initial testing. Based on the apparent first order rate constants, UV/H<sub>2</sub>O<sub>2</sub> and UV/O<sub>3</sub> show the most promise. The triple combination of UV/O<sub>3</sub>/H<sub>2</sub>O<sub>2</sub> didn't appear to be an improvement over either pairing. However, for the sonicated samples, the triple combination of US/O<sub>3</sub>/H<sub>2</sub>O<sub>2</sub> was the most promising of those tested.

Table 5-1 AOP Rate Constant Comparison

$[O_3]_{aq}$ (mg/L)	$[H_2O_2]$ (mg/L)	UV Intensity (mW/cm <sup>2</sup> )	Ultrasound Intensity (W)	Pseudo 1 <sup>st</sup> Order Rate Constant for 1,4-Dioxane Removal (min <sup>-1</sup> )	Published Results at neutral pH (min <sup>-1</sup> )
			800	0.012 <i>0.024 in DI</i>	0.018 (using empirical relationship from 490kHz data) (Xu, Mochida, Naito, & Yasuda, 2012) 0.0132 (600W @20kHz in DI) (Son, Choi, Khan, & Zoh, 2006)
		11		0.088	0.0038 (5.59x10 <sup>-4</sup> einstein/sec in DI) (Stefan & Bolton, 1998) 0.018 (13.3 and 18.6 mW/cm <sup>2</sup> in DI) (Takahashi, et al., 2013) 0.0019 (Kwon , et al., 2012)
2.5				0.1 <i>0.047 in DI</i>	0.0025 (Xu, Mochida, Naito, & Yasuda, 2012) 0.0038 (in DI) (Takahashi, et al., 2013) 0.0036 (Kwon , et al., 2012) 1.2 (industrial wastewater) (Barndok, Cortijo, Hermosilla, Negro, & Blanco, 2014)
2.5			800	0.24 <i>0.39 in DI</i>	0.0063 (150W @ 490kHz) (Xu, Mochida, Naito, & Yasuda, 2012)

3	12			0.96	0.059 (in DI) (Takahashi, et al., 2013) 24 (industrial wastewater) (Barndok, Cortijo, Hermosilla, Negro, & Blanco, 2014)
2.5		11		0.73	0.0225 (13.3 and 18.6 mW/cm <sup>2</sup> in DI) (Takahashi, et al., 2013) 0.0059 (Kwon , et al., 2012)
2.5	10		800	0.46	Not found reported in literature
2.5	10	11		0.68	0.01 (0.25<H <sub>2</sub> O <sub>2</sub> /O <sub>3</sub> (wt/wt)<0.75) (Kwon , et al., 2012)
	10	11		0.71	0.52 (H <sub>2</sub> O <sub>2</sub> 15x in excess, 5.59x10 <sup>-4</sup> einstein/sec in DI) (Stefan & Bolton, 1998) 0.02 (1M H <sub>2</sub> O <sub>2</sub> , 3.5x10 <sup>-3</sup> einsteins/cm <sup>2</sup> ) (Chitra, Paramasivan, Cheralathan, & Sinha, 2012)

### 5.2.2. Byproducts/Toxicity

In Chapter 1, the toxicity of 1,4-dioxane and some of its intermediate byproducts was discussed. However, the present study was conducted using water that had been spiked with 20 ppb of 1,4-dioxane, because it is an environmentally relevant concentration which was still within analytical capability. Using such a low initial concentration eliminates the possibility to explore intermediate byproducts. Future testing should include experiments with much higher initial concentrations of 1,4-

dioxane. This would enable an examination of intermediate byproducts as well as toxicity screening tests using treated and untreated water.

### 5.2.3. *Additional Contaminants*

Combined ozone/ultrasound was shown to not only remove 1,4-dioxane, it was shown to do so at a significantly faster rate than the only other published study on the subject (Xu, Mochida, Naito, & Yasuda, 2012). As such, the combined ozone/ultrasound process should be evaluated for additional contaminants. There were three key differences between this study and the previous study: the previous was a batch study with spiked deionized water (assumed, but not reported) and utilizing 490 kHz ultrasound, while this study was done in a continuous flow reactor with spiked drinking water and utilizing 20 kHz sonication. The primary cause of the improved performance noted in this study is believed to be the difference in batch reactor versus continuous flow. If a comparison of continuous flow and batch study results for other contaminants indicated a similar performance edge in the continuous flow reactor performance, it could suggest that batch studies are not ideal models for combined ozone/ultrasound process.

Contaminants or co-contaminants which might be more amenable to treatment from ultrasound or ozone directly would also be of interest to study in the future. In the literature, studies have shown ozone, ultrasound, and the combined ozone/ultrasound process to be effective at treating bacteria (*e Coli*) (Al-Hashimi, Mason, & Joyce, 2015) (Joyce & Mason, 2008). It would be interesting to study potential synergistic effects for treating spore-forming bacteria, which pose challenges for conventional water treatment processes. In addition to plate counts, the al-Hashimi study utilized flow-cytometry and TEM analysis to measure cellular damage and fragmentation from the ozone, ultrasound,

and combined ozone/ultrasound. The combined ozone/ultrasound process showed fast disinfection properties in *e Coli*. It would be interesting to study the effects of combined ozone/ultrasound on hardier, spore-forming microbes. A study by Joyce et al evaluated ultrasound for the treatment of spores showed that low frequency ultrasound (20kHz) functions to declump spores more than it does to kill them directly (Joyce, Phull, Lorimer, & Mason, 2003). In the combined ozone/ultrasound system, such ultrasonic declumping might make the spores more vulnerable to disinfection from the ozone.

#### 5.2.4. Model Refinement/Scalability

Based on the results of the pilot-scale ozonation study, the Chick & Watson style model appears to be scalable. However, more work is needed here since the pilot-scale reactor did not have the capability of testing combined ozone/ultrasound. A larger scale study of the combined ozone/ultrasound process may enable further refinement of the model. A model that could be applied to large-scale, continuous-flow reactor would obviously be very useful to planners and operators wishing to incorporate this treatment process into a real world treatment system.

Additionally, one of the causes for the improved dioxane removal noted in this study relative to previously published studies is believed to be the result of differences in reactor design. In previously published studies, ozone was injected into a stirred reactor, as in a continuous mixed flow reactor. In this study, ozone was injected at the reactor inlet and exited at the outlet, as in a plug flow reactor, albeit not an ideal plug flow reactor. Since plug flow reactor kinetics depend on the ozone concentration at the inlet and continuous mixed flow reactor kinetics depend on the lower in-tank ozone concentration, dioxane removal is expected to improve as reactor design becomes more

plug-flow-like. Another area of future work would be to verify this theory, possibly using reactor dispersion characteristics to predict relative reactor performance.

## CHAPTER 6. CONCLUSION

The world population is growing and with it, the demand for clean water. Changes to the climate and a dietary shift towards more meat products will exacerbate that demand, as well. Some of the increased demand will be met through more efficient management. Water reuse must also be a part of the solution, but reusing water introduces treatment challenges, especially in waters which have been contaminated. Traditional treatment techniques are capable of handling a number of biological and chemical contaminants. However, these techniques are inadequate for some emerging contaminants. One of the most difficult to treat of these emerging contaminants is the solvent and stabilizer 1,4-dioxane, which is the reason it was chosen for this study.

Dioxane contamination in surface and ground water has been detected throughout the world. In the United States, it can be found in 6.9% of public water systems, including detectable levels in the drinking water used for this study (US-EPA, 2016) (Philadelphia Water Department, 2014). Air-stripping is ineffective and it is miscible in water. It is resistant to oxidation from chlorine and oxygen (Zenker, Borden, & Barlaz, 2003). It is not removed by traditional sand or mixed media filtration and is only partially removed by reverse osmosis. In this and other studies, it has been shown that the removal of 1,4-dioxane requires hydroxyl radicals. This dissertation investigated an advanced oxidation process, combined ozone/ultrasound, which was evaluated for its ability to treat drinking water contaminated with environmentally relevant concentration of 1,4-dioxane.

From the scavenger experiments conducted for this study, the removal of 1,4-dioxane was determined to be dependent upon the generation of hydroxyl radicals. The addition of bicarbonate to the matrix was found to progressively shunt the removal of dioxane, resulting in negligible removal at 100mM of added bicarbonate. By combining that piece of information with the results of the ultrasonic intensity study, the relationship between hydroxyl radical formation and aqueous ozone becomes clearer.

In the ultrasonic intensity study, it was found that more intense sonication led to more dioxane removal. Since dioxane removal was shown to be predicated on hydroxyl radicals, this suggests that greater ultrasonic intensity yields more hydroxyl radicals. Since ultrasound alone showed little removal of dioxane, it is hypothesized that the additional hydroxyl radicals in the combined ozone/ultrasound system are the result of ultrasonic decomposition of ozone. The pH study further supports the hypothesis that the observed dioxane removal was mediated by ozone decomposition hypothesis. It was shown that dioxane removal in the combined ozone/ultrasound system was relatively pH independent, while dioxane removal in the ozone system was highly dependent on the pH of the matrix. This makes sense for the ozone system, since ozone stability is dependent on the presence of hydroxide ions (Staehelin & Hoigne, 1982). At pH 10, dioxane removal from ozone alone occurred 630% faster than at pH 4 ( $0.1846 \text{ min}^{-1}$  vs  $0.0293 \text{ min}^{-1}$ ). However, for the combined ozone/ultrasound process, only a 33% improvement was noted. It would appear from these results that ultrasound is capable of causing the breakdown of ozone, and the concurrent formation of hydroxyl radicals, in the absence of hydroxide ions.

In the deionized water tests, the effect of organic carbon as a promoter was observed. Dioxane removal from ozone alone was found to be more effective in a spiked drinking water matrix than a spiked deionized water matrix. Organic carbon has been shown to promote the decomposition of ozone (Staelin & Hoigne, 1985), so the organic carbon naturally present in the drinking water matrix ( $1.95 \pm 0.32$  ppm organic carbon) is believed to be responsible. The addition of ultrasound to the deionized matrix was found to cause the rate of dioxane removal to increase by 830% ( $0.39 \text{ min}^{-1}$  vs  $0.047 \text{ min}^{-1}$ ). The addition of ultrasound to the drinking water matrix caused the rate of dioxane removal to increase by only 240% ( $0.24 \text{ min}^{-1}$  vs  $0.010 \text{ min}^{-1}$ ). Considering treatment by ozone alone, the lack of organic carbon in deionized matrix was found to be more of a hindrance to production of hydroxyl radicals than the presence of natural scavengers ( $7.85 \pm 1.22$  ppm inorganic carbon) was in the drinking water matrix. However, in the combined ozone/ultrasound system, the ultrasound appears to be driving adequate ozone decomposition and the lack of scavenging inorganic carbon means greater dioxane removal is achieved in deionized water.

The key to removing 1,4-dioxane is the generation of hydroxyl radicals, and this study has shown that the decomposition of ozone is the key to generating hydroxyl radicals. This study has shown that there are a number of ways that ozone decomposition can occur: from interaction with hydroxide ions, from sonication, or from interaction with promoters.

The Chick & Watson style model created in this study was found to give predictive results for a wide range of ozone dosages, treatment times, and ultrasonic intensities. While comparisons were only possible for ozone alone, preliminary work

suggests that this model is scalable. The model was found to provide reasonably good, albeit conservative, estimates of dioxane removal by ozone alone over a 50x span of water flow rates and a 10x span of reactor volume.

Combined ozone/ultrasound was shown to not only remove 1,4-dioxane, it was shown to do so at a significantly faster rate than the only other published study on the subject (Xu, Mochida, Naito, & Yasuda, 2012). There were key differences between this study and the previous study: the previous was a batch study utilizing 490 kHz ultrasound and was likely conducted using deionized water, while this study was done in a continuous flow reactor using drinking water and 20 kHz sonication. Additionally, the reactor used in this study was closer in performance to a plug flow reactor than the continuous mixed flow reactor that employed in Xu et al. The ozone kinetics in a continuous mixed flow reactor are dependent on the final/in-tank ozone concentration. However, the kinetics for an ideal plug flow reactor are dependent on the greater initial ozone concentration, giving an advantage to the reactor employed in this study. Each of these factors is believed to be the cause of the improved performance noted in this study versus the previous batch study. Because the drinking water matrix used in this study is believed to be more representative of a water reuse treatment scenario, the combined ozone/ultrasound process might be a better candidate for the treatment of dioxane-contaminated waters than previously published results would indicate.

Advanced water treatment solutions are needed to address the water scarcity challenges. As an AOP capable of removing a recalcitrant and widespread contaminant like 1,4-dioxane, combined ozone/ultrasound process holds promise as a treatment option for water reuse situations. This process doesn't require additional chemical inputs, only

electricity is needed. As such, it also holds promise as a treatment option to increase access to safe water in remote areas where recalcitrant contaminants may be present, but access to chemical oxidants is challenging or impossible. The world of the future will need more water, and the combined ozone/ultrasound process is one of many AOPs that could help provide it.

## BIBLIOGRAPHY

Abe, A. (1999). Distribution of 1,4-Dioxane in Relation to Possible Sources in the Water Environment. *The Science of the Total Environment*, 227, 41-47.

Acero, J. L., & Von Gunten, U. (2001). Characterization of Oxidation Processes: Ozonation and the AOP O<sub>3</sub>/H<sub>2</sub>O<sub>2</sub>. *Journal American Water Works Association*, 93(10), 90-100.

Acero, J. L., Stemmler, K., & Von Gunten, U. (2000). Degradation Kinetics of Atrazine and Its Degradation Products with Ozone and OH Radicals: A Predictive Tool for Drinking Water Treatment. *Environmental Science & Technology*, 34, 591-597.

Adams, C. D., Scanlan, P. A., & Secrist, N. D. (1994). Oxidation and Biodegradability Enhancement of 1,4-Dioxane using Hydrogen Peroxide and Ozone. *Environmental Science & Technology*, 28, 1812-1818.

Agency for Toxic Substances and Disease Registry. (2008). *Public Health Statement - Formaldehyde*. Bethesda, MD: US Department of Health and Human Services. Retrieved December 18, 2015, from [http://www.atsdr.cdc.gov/toxprofiles/formaldehyde\\_fig\\_1-2.jpg](http://www.atsdr.cdc.gov/toxprofiles/formaldehyde_fig_1-2.jpg)

Agency for Toxic Substances and Disease Registry. (2012). *Public Health Statement - 1,4-Dioxane*. Bethesda, MD: US Department of Health and Human Services. Retrieved December 18, 2015, from <http://www.atsdr.cdc.gov/ToxProfiles/tp187-c1-b.pdf>

- Agriculture, U. S. (2015, December 18). *Agricultural Research Service*. Retrieved from  
USDA National Nutrient Database for Standard Reference:  
<http://www.ars.usda.gov/Main/docs.htm?docid=9444>
- Aitchison, E. W., Kelley, S. L., Alvarez, P. J., & Schnoor, J. L. (2000). Phytoremediation  
of 1,4-Dioxane by Hybrid Poplar Trees. *Water Environment Research*, 72(3),  
313-321.
- Al-Hashimi, A. M., Mason, T. J., & Joyce, E. M. (2015). Combine Effect of Ultrasound  
and Ozone on Bacteria in Water. *Environmental Science & Technology*, 49,  
11697-11702.
- Alliger, H. (1975). Ultrasonic Disruption. *American Laboratory*, 10, 75-85.
- American Public Health Association, A. W. (2012). *Standard Methods for the  
Examination of Water and Wastewater* (22 ed.). (E. W. Rice, R. B. Baird, A. D.  
Eaton, & L. S. Clesceri, Eds.) Washington DC: American Public Health  
Association.
- Andaluri, G. (2011). *Ultrasound Induced Destruction of Emerging Contaminants*.  
Temple University.
- Andaluri, G. (2016, 7 1). Personal Communication Regarding Ozonation of 1,4-Dioxane  
in Pilot-Scale Reactor. (M. Dietrich, Interviewer)
- Andaluri, G., Curran, M., & Suri, R. (2012). Removal of 1, 4-Dioxane and Volatile  
Organics from Contaminated Groundwater Using Ozone Based Advanced

Oxidation Processes. *Abstracts of Papers of the American Chemical Society*. 244.  
Washington, DC: American Chemical Society.

Andaluri, G., Suri, R. P., & Kumar, K. (2012). Occurrence of Estrogen Hormones in Biosolids, Animal Manure and Mushroom Compost. *Environmental Monitoring and Assessment*, 184(2), 1197-1205.

Argus, M. F., Arcos, J. C., & Hoch-Ligeti, C. (1965). Studies on the Carcinogenic Activity of Protein-Denaturing Agents: Hepatocarcinogenicity of Dioxane. *Journal of the National Cancer Institute*, 35(6), 949-958.

Bagenstose, K. (2016, May 30). Water Utilities Talk Cost of Contamination at Second Community Meeting. *Bucks County Courier Times*. Retrieved May 30, 2016, from [http://www.buckscountycouriertimes.com/news/horsham-pfos/water-utilities-talk-cost-of-contamination-at-second-community-meeting/article\\_ae7804f8-22b3-11e6-9a61-37ba7d0aa767.html](http://www.buckscountycouriertimes.com/news/horsham-pfos/water-utilities-talk-cost-of-contamination-at-second-community-meeting/article_ae7804f8-22b3-11e6-9a61-37ba7d0aa767.html)

Barndok, H., Cortijo, L., Hermosilla, D., Negro, C., & Blanco, A. (2014). Removal of 1,4-Dioxane from Industrial Wastewates: Routes of Decomposition Under Different Operational Conditions to Determine Ozone Oxidation Capacity. *Journal of Hazardous Materials*, 280, 340-347.

Barnstead Thermolyne. (2000). *NANOpure Diamond TOC Life Science (UV/UF with TOC)*. Instruction Manual, Dubuque, IA. Retrieved 5 10, 2016

- Beckett, M. A., & Hua, I. (2000). Elucidation of the 1,4-Dioxane Decomposition Pathway at Discrete Ultrasonic Frequencies. *Environmental Science & Technology*, 3944-3953.
- Beckett, M. A., & Hua, I. (2003). Enhanced Sonochemical Decomposition of 1,4-Dioxane by Ferrous Iron. *Water Research*, 37, 2372–2376.
- Bell, A. (2009). *Peak Water; Civilization and the World's Water Crisis*. Edinburgh: Luath Press Limited.
- Beltran, F. J. (2003). Ozone-UV Radiation-Hydrogen Peroxide Oxidation Technologies. In M. A. Tarr, *Chemical Degradation Methods for Wastes and Pollutants; Environmental and Industrial Applications* (pp. 1-71). New York: Marcel Dekker Inc.
- Brennen, C. E. (2014). *Cavitation and Bubble Dynamics*. New York, NY: Cambridge University Press.
- Buxton, G. V., Greenstock, C. L., & Helman, W. P. (1988). Critical Review of Rate Constants for Reactions of Hydrated Electrons, Hydrogen Atoms, and Hydroxyl Radicals in Aqueous Solution. *Journal of Physical and Chemical Reference Data*, 17(513), 513-886.
- California. (2010, September 30). *Senate Bill No. 918*. Retrieved from California Legislative Information:  
[http://leginfo.legislature.ca.gov/faces/billNavClient.xhtml?bill\\_id=200920100SB918](http://leginfo.legislature.ca.gov/faces/billNavClient.xhtml?bill_id=200920100SB918)

California Dept of Public Health. (2014). *Title 22 Code of Regulations, 60320.201.d.*

Retrieved 6 25, 2015, from

[http://www.waterboards.ca.gov/drinking\\_water/certlic/drinkingwater/documents/lawbook/RWregulations\\_20140618.pdf](http://www.waterboards.ca.gov/drinking_water/certlic/drinkingwater/documents/lawbook/RWregulations_20140618.pdf)

California Environmental Protection Agency. (2016, 2 22). *State Water Resources*

*Control Board*. Retrieved from 1,4-Dioxane:

[http://www.waterboards.ca.gov/drinking\\_water/certlic/drinkingwater/14-Dioxane.shtml](http://www.waterboards.ca.gov/drinking_water/certlic/drinkingwater/14-Dioxane.shtml)

Candeias, L. P., Stanford, M. R., & Wardman, P. (1994). Formation of Hydroxyl

Radicals on Reaction of Hypochlorous Acid with Ferrocyanide a Model Iron(II)

Complex. *Free Radical Research*, 20(4), 241-249.

Chakraborti, R. K., Lozier, J. C., Witwer, M., Bays, J. S., Erdal, U. G., & Ortega, K.

(2009). Pilot Study on the Performance of Reverse Osmosis, Microfiltration, and

Wetlands Concentrate Treatment of Wastewater with High Membrane Fouling

Potential. *Proceedings of the Water Environment Federation*, 13, pp. 3610-3630.

Chartres, C., & Varma, S. (2011). *Out of Water; From Abundance to Scarcity and How*

*to Solve the World's Water Problems*. Upper Saddle River, New Jersey: FT Press.

Chitra, S., Paramasivan, K., Cheralathan, M., & Sinha, P. K. (2012). Degradation of 1,4-

Dioxane Using Advanced Oxidation Processes. *Environmental Science and*

*Pollution Research*, 19, 871-878.

- Choi, J. Y., Lee, Y. J., Shin, J., & Yang, J. W. (2010). Anodic Oxidation of 1,4-Dioxane on Boron Doped Diamond Electrodes for Wastewater Treatment. *Journal of Hazardous Materials*, 179(1-3), 762-768.
- Coleman, H. M., Vimonses, G., Leslie, G., & Amal, R. (2007). Degradation of 1,4-Dioxane in Water Using TiO<sub>2</sub> Based Photocatalytic and H<sub>2</sub>O<sub>2</sub>/UV Processes. *Journal of Hazardous Materials*, 146(3), 496-501.
- Cyr, P. J., Paraskewich, M. R., & Suri, R. P. (1999). Sonochemical Destruction of Trichloroethylene in Water. *Water Science and Technology*, 40, 131-136.
- Ecosphere Technologies, I. (2016, February 23). *Patent No. 9266752 B2*. United States of America.
- Elovitz, M. S., & von Gunten, U. (1999). Hydroxyl Radical/Ozone Ratios During Ozonation Processes. *International Ozone Association*, 21, 239-260.
- Elovitz, M. S., von Gunten, U., & Kaiser, H.-P. (2000). Hydroxyl Radical/Ozone Ratios During Ozonation Processes. *Ozone Science & Engineering*, 22, 123-150.
- Environmental Health Analysis Center. (2012, September 4). *PBT Profiler*. Retrieved March 24, 2015, from Persistent, Bioaccumulative, and Toxic Profiles Estimated for Organic Chemicals: <http://www.pbtprofiler.net/ChemDetails.asp?I=0>
- Even-Ezra, I., Mizrahi, A., Gerrity, D., Snyder, S., Salveson, A., & Lahav, O. (2009). Application of novel plasma-based advanced oxidation process for efficient and cost-effective destruction of refractory organics in tertiary effluents and contaminated groundwater. *Desalination and Water Treatment*, 11, 236-244.

- Felix-Navarro, R. M., Lin, S. W., Zizumbo-Lopez, A., Perez-Sicairos, S., Reynoso-Soto, A., & Espinoza-Gomez, J. H. (2013). 1,4-Dioxane Degradation Using Persulfate Ion and Ag(I) Ion. *Journal of the Mexican Chemical Society*, 57(2), 127-132.
- Felix-Navarro, R. M., Lin-Ho, S. W., Barrera-Diaz, N., & Perez-Sicairos, S. (2007). Kinetics of the Degradation of 1,4-Dioxane Using Persulfate. *Journal of the Mexican Chemical Society*, 51(2), 67-71.
- Fishman, C. (2011). *The Big Thirst; the Secret Life and Turbulent Future of Water*. New York, New York: Free Press.
- Florida Department of Environmental Protection. (2011, September 21). *Florida's Reuse Projects*. Retrieved from <http://www.dep.state.fl.us/water/reuse/project.htm>
- Fogler, H. S. (1992). *Elements of Chemical Reaction Engineering* (Second ed.). Upper Saddle River, NJ: Prentice Hall PTR.
- Franc, J.-P., & Michel, J.-M. (2006). *Fundamentals of Cavitation* (Vol. 76). Springer Science & Business Media.
- Fujikawa, S., & Akamatsu, T. (1980). Effects of the Non-Equilibrium Condensation of Vapour on the Pressure Wave Produced by the Collapse of a Bubble in a Liquid. *Journal of Fluid Mechanics*, 97, 481-512.
- Gerrity, D., & Snyder, S. (2011). Review of Ozone for Water Reuse Applications: Toxicity, Regulations, and Trace Organic Contamination Oxidation. *Ozone: Science & Engineering*, 33, 253-266.

- Ghosh, P., Samanta, A. N., & Ray, S. (2010). Oxidation Kinetics of Degradation of 1,4-Dioxane in Aqueous Solution by H<sub>2</sub>O<sub>2</sub>/Fe(II) system. *Journal of Environmental Science and Health, Part A: Toxic/Hazardous Substances and Environmental Engineering*, 45, 395-399.
- Glaze, W. H. (1987). Drinking Water Treatment with Ozone. *Environmental Science & Technology*, 21(3), 224-230.
- Glaze, W. H., & Kang, J.-W. (1989). Advanced Oxidation Processes. Description of a Kinetic Model for the Oxidation of Hazardous Materials in Aqueous Media with Ozone and Hydrogen Peroxide in a Semibatch Reactor. *Industrial and Engineering Chemistry*, 28, 1573-1580.
- Gogate, P. R., Mededovic-Thagard, S., McGuire, D., Chapas, G., Blackmon, J., & Cathey, R. (2014). Hybrid Reactor Based on Combined Cavitation and Ozonation: From Concept to Practical Reality. *Ultrasonics Sonochemistry*, 21, 590-598.
- Gultekin, I., & Ince, N. H. (2006). Degradation of Aryl-Azo-Naphthol Dyes by Ultrasound, Ozone and Their Combination: Effecto of Apha-Substituents. *Ultrasonics Sonochemistry*, 13, 208-214.
- Guo, W.-Q., Yin, R.-L., Zhou, X.-J., Du, J.-S., Cao, H.-O., Yang, S.-S., & Ren, N.-Q. (2015). Sulfamethoxazole Degradation by Ultrasound/Ozone Oxidation Process in Water: Kinetics, Mechanisms, and Pathways. *Ultrasonics Sonochemistry*, 22, 182-187.

- Hach Lange. (2009). *ORBISPHERE Model 410 Analyer User Manual* (Version F ed.). Retrieved March 30, 2015
- Hach Lange. (2010). *Hach Orbisphere C1100 Ozone Sensor with Orbisphere 410 Controller Data Sheet*. Retrieved March 30, 2015
- Halling-Sorensen, B., Nielsen, S. N., Lanzky, P. F., Ingerslev, F., Lutzhoft, H. C., & Jorgensen, S. E. (1998). Occurrence, Fate and Effects of Pharmaceutical Substances in the Environment - A Review. *Chemosphere*, 36(2), 357-394.
- Hart, E. J., & Henglein, A. (1986). Sonolysis of Ozone in Aqueous Solution. *The Journal of Physical Chemistry*, 90(14), 3061-3062.
- Henley, D. V., & Korach, K. S. (2005). Endocrine-Disrupting Chemicals Use Distinct Mechanisms of Action to Modulate Endocrine System Function. *Endocrinology*, 147(6), S25-S32.
- Hoch-Ligeti, C., Argus, M. F., & Arcos, J. C. (1970). Induction of Carcinomas in the Nasal Cavity of Rats by Dioxane. *British Journal of Cancer*, 24(1), 164-167.
- Hoffman, S. J. (2009). *Planet Water; Investing in the World's Most Valuable Resource*. Hoboken: John Wiley & Sons.
- Hoigne, J. (1998). Chemistry of Aqueous Ozone and Transformation of Pollutants by Ozonation and Advanced Oxidation Processes. In J. Hrubec, & J. Hrubec (Ed.), *The Handbook of Environmental Chemistry-Quality and Treatment of Drinking Water II* (Vols. 5-C, pp. 83-143). Berlin, Germany: Springer.

- Hoigne, J., & Bader, H. (1983). Rate Constants of Reactions of Ozone with Organic and Inorganic Compounds in Water. *Water Resources*, 17, 173-183.
- Ince, N. H., & Tezcanli, G. (2001). Reactive Dyestuff Degradation by Combined Sonolysis and Ozonation. *Dyes and Pigments*, 49, 145-153.
- International Association for the Properties of Water and Steam. (2007). *Revised Release of the IAPWS Formulation 1997 for the Thermodynamic Properties of Ordinary Water Substances for General and Scientific Use*. Lucerne, Switzerland: International Association for the Properties of Water and Steam. Retrieved Dec 16, 2015, from <http://www.iapws.org/relguide/IAPWS-95.html>
- Johns, M. M., Marshall, W. E., & Toles, C. A. (1998). Agricultural Byproducts as Granular Activated Carbons for Adsorbing Dissolved Metals and Organics. *Journal of Chemical Technology and Biotechnology*, 71, 131-140.
- Johnson, P. N., & Davis, R. A. (1996). Diffusivity of Ozone in Water. *Journal of Chemical and Engineering Data*, 41, 1485-1487.
- Joyce, E. M., & Mason, T. J. (2008). Sonication Used as a Biocide: A Review: Ultrasound a Greener Alternative to Chemical Biocides? *Chemistry Today*, 26(6), 22-26.
- Joyce, E., Phull, S. S., Lorimer, J. P., & Mason, T. J. (2003). The Development and Evaluation of Ultrasound for the Treatment of Bacterial Suspensions. A study of Frequency, Power, and Sonication Time on Cultured Bacillus Species. *Ultrasonics Sonochemistry*, 10(6), 315-318.

- Kang, J.-W., & Hoffmann, M. R. (1998). Kinetics and Mechanism of the Sonolytic Destruction of Methyl tert-Butyl Ether by Ultrasonic Irradiation in the Presence of Ozone. *Environmental Science & Technology*, 32, 3194-3199.
- Kegel, F. S., Rietman, B. M., & Verliefde, A. R. (2010). Reverse Osmosis Followed by Activated Carbon Filtration for Efficient Removal of Organic Micropollutants from River Bank Filtrate. *Water Science & Technology*, 61(10), 2603-2610.
- Kindak, R., & Ince, N. H. (2007). Catalysis of Advanced Oxidation Reactions by Ultrasound: A Case Study with Phenol. *Journal of Hazardous Materials*, 146, 630-635.
- King, M. E., Shefner, A. M., & Bates, R. R. (1973). Carcinogenesis Bioassay of Chlorinated Dibenzodioxins and Related Chemicals. *Environmental Health Perspectives*, 163-170.
- Kishimoto, N., & Nakamura, E. (2011). Effects of Ozone-Gas Bubble Size and pH on Ozone/UV Treatment. *Ozone Science and Engineering*, 33(5), 396-402.
- Kishimoto, N., & Sugimura, E. (2010). Feasibility of an Electrochemically Assisted Fenton Method Using Fe<sup>2+</sup>/HOCl as an Advanced Oxidation Process. *Water Science & Technology*, 62, 2321-2329.
- Kishimoto, N., Nakagawa, T., Asano, M., Abe, M., Yamada, M., & Ono, Y. (2008). Ozonation Combined with Electrolysis of 1,4-Dioxane Using a Two-Compartment Electrolytic Flow Cell with Solid Electrolyte. *Water Research*, 379-385.

- Kitamura, T., Kishimoto, N., Okura, M., & Otsu, H. (2011). Effects of Several Factors on Operation of an Electro-Advanced Oxidation Process using Fe<sup>2+</sup>/HOCl System. *Journal of Japan Society on Water Environment*, 34, 81-87.
- Klecka, G. M., & Gonsior, S. J. (1986). Removal of 1,4-Dioxane From Wastewater. *Journal of Hazardous Materials*, 13, 161-168.
- Kwon, S. C., Kim, J. Y., Yoon, S. M., Bae, W., Kang, K. S., & Rhee, Y. W. (2012). Treatment Characteristics of 1,4-Dioxane by Ozone-Based Advanced Oxidation Processes. *Journal of Industrial and Engineering Chemistry*, 18, 1951-1955.
- Lall, R., Mutharasan, R., Shah, Y. T., & Dhurjati, P. (2003). Decolorization of the Dye, Reactive Blue 19, Using Ozonation, Ultrasound and Ultrasound Enhanced Ozone. *Water Environment Research*, 75(2), 171-179.
- Laugier, F., Andrianstiferana, C., Wilhelm, A. M., & Delmas, H. (2008). Ultrasound in Gas-Liquid Systems: Effects on Solubility and Mass Transfer. *Ultrasonics Sonochemistry*, 15(6), 965-972.
- Lesko, T., Hoffmann, M., & Colussi, A. (2006). Sonochemical Decomposition of Phenol: Evidence for a Synergistic Effect of Ozone and Ultrasound for the Elimination of Total Organic Carbon from Water. *Environmental Science & Technology*(40), 6818-6823.
- Levenspiel, O. (1999). *Chemical Reaction Engineering* (Third ed.). New York: John Wiley & Sons.

- Linden, K. G., & Darby, J. L. (1997). Estimating Effective Germicidal Dose From Medium Pressure UV Lamps. *Journal of Environmental Engineering*, 123, 1142-1149.
- Lomborg, B. (2001). *The Skeptical Environmentalist: Measuring the Real State of the World*. Cambridge University Press.
- Madge, B. A., & Jensen, J. N. (2002). Disinfection of Wastewater Using a 20-kHz Ultrasound Unit. *Water Environment Federation*, 74(2), 159-169.
- Mahendra, S., Grostern, A., & Alvarez-Cohen, L. (2013). The Impact of Chlorinated Solvent Co-Contaminants on the Biodegradation Kinetics of 1,4-Dioxane. *Chemosphere*, 91, 88-92.
- Mahendra, S., & Alvarez-Cohen, L. (2005). Pseudonocardia dioxanivorans Sp. Nov. A Novel Actinomycete that Grows on 1,4-Dioxane. *International Journal of Systemic and Evolutionary Microbiology*, 55(2), 593-598.
- Maurino, V., Calza, P., Minero, C., Pelizzetti, E., & Vincenti, M. (1997). Light-Assisted 1,4-Dioxane Degradation. *Chemosphere*, 35(11), 2675-2688.
- McGuire, D. (2015). *Patent No. US 9169146 B2*. United States.
- McGuire, M. J., Suffet, I. H., & Radzuil, J. V. (1978). Assessment of Unit Processes for the Removal of Trace Organic Compounds from Drinking Water. *Journal of the American Water Works Association*, 10, 565-572.
- Medvedev, D. D. (2013). *Patent No. WO 2013155283 A1*.

- Mohr, T. K. (2010). *Environmental Investigation and Remediation; 1,4-Dioxane and Other Solvent Stabilizers*. Boca Raton: CRC Press.
- Muruganandham, M., Suri, R. P., Jafari, S., Sillanpaa, M., Lee, G.-J., & Wu, J. J. (2014). Recent Developments in Homogeneous Advanced Oxidation Processes for Water and Wastewater Treatment. *International Journal of Photoenergy*. Retrieved from <http://dx.doi.org/10.1155/2014/821674>
- Nothe, T., Fahlenkamp, H., & Von Sonntag, C. (2009). Ozonation of Wastewater: Rate of Ozone Consumption and Hydroxyl Radical Yield. *Environmental Science & Technology*, 43, 5990–5995.
- Obama, B. (2015). *Executive Order -- Planning for Federal Sustainability in the Next Decade*. Washington D.C.: The White House Office of the Press Secretary.
- OECD, T. O.-o. (2012). *OECD Economic Outlook to 2050: The Consequences of Inaction*. Paris: OECD Publishing.
- Olson, T. M., & Barbier, P. F. (1993). Oxidation Kinetics of Natural Organic Matter by Sonolysis and Ozone. *Water Resources*, 28(6), 1383-1391.
- Orange County Water District. (n.d.). *Water Reuse*. Retrieved May 31, 2016, from Orange County Water District: <http://www.ocwd.com/what-we-do/water-reuse/>
- Parales, R. E., Adamus, J. E., White, N., & May, H. D. (1994). Degradation of 1,4-Dioxane by an Actinomycete in Pure Culture. *Applied and Environmental Microbiology*, 60(12), 4527-4530.

- Pearch, P. J., & Simkins, R. J. (1968). Acid Strengths of Some Substituted Picric Acids. *Canadian Journal of Chemistry*, 46, 241-248.
- Peyton, G. R., & Glaze, W. H. (1988). Destruction of Pollutants in Water with Ozone in Combination with Ultraviolet Radiation. *Environmental Science & Technology*, 22, 761-767.
- Philadelphia Water Department. (2014). *2015 Drinking Water Quality Report*. Water System Identification PA1510001. Retrieved from <http://www.phila.gov/water/wu/Water%20Quality%20Reports/2015WaterQuality.pdf>
- Philadelphia Water Department, <http://www.phila.gov/water/wu/Water%20Quality%20Reports/2015WaterQuality.pdf>. (2014). *2015 Drinking Water Quality Report*. Water System Identification PA1510001.
- Pivetz, B. E. (2001). *Phytoremediation of Contaminated Soil and Ground Water at Hazardous Waste Sites*. US-EPA Office of Research and Development.
- Richardson, K. E. (1973). The Effect of Partial Hepatectomy on the Toxicity of Ethylene Glycol, Glycolic Acid, Glyoxylic Acid, and Glycine. *Toxicology and Applied Pharmacology*, 24, 530-538.
- Roy, D., Anagnostu, G., & Chaphalkar, P. (1995). Analysis of Respirometric Data to Obtain Kinetic Coefficients for Biodegradation of 1,4-Dioxane. *Journal of*

*Environmental Science and Health. Part A: Environmental Science and Engineering and Toxicology*, 30(8), 1775-1790.

Son, H. S., Im, J. K., & Zoh, K. D. (2009). A Fenton-Like Degradation Mechanism for 1,4-Dioxane Using Zero-Valent Iron (Fe-0) and UV Light. *Water Research*, 43(5), 1457-1463.

Son, H.-S., Choi, S.-B., Khan, E., & Zoh, K.-D. (2006). Removal of 1,4-dioxane from water using sonication: Effect of adding oxidants on the degradation kinetics. *Water Research*, 40(4), 692-698.

Stahelin, J., & Hoigne, J. (1982). Decomposition of Ozone in Water: Rate of Initiation by Hydroxide Ions and Hydrogen Peroxide. *Environmental Science and Technology*, 16, 676-681.

Stahelin, J., & Hoigne, J. (1985). Decomposition of Ozone in Water in the Presence of Organic Solutes Acting as Promoters and Inhibitors of Radical Chain Reactions. *Environmental Science & Technology*, 19(12), 1206-1213.

Stefan, M. I., & Bolton, J. R. (1998). Mechanism of the degradation of 1,4-dioxane in dilute aqueous solution using the UV hydrogen peroxide process. *Environmental Science & Technology*, 32(11), 1588-1595.

Steinhart, J. S., & Hart, S. R. (1968). Calibration Curves for Thermistors. *Deep-Sea Research*, 15, 497-503.

- Stepniak, L., Stanczyk-Mazanek, E., & Kusiak, M. (2012). Ultrasonics and Ozone in Removal of Humic Substances From Water. *Inzynieria i Ochrona Srodowiska*, 15(2), 143-154.
- Suh, J. H., & Mohensi, M. (2004). A Study on the Relationship Between Biodegradability Enhancement and Oxidation of 1,4-Dioxane Using Ozone and Hydrogen Peroxide. *Water Research*, 259-2604.
- Suri, R. P., Andaluri, G., Abburi, S., & Velicu, M. (2008). Ultrasound Assisted Removal of Estrogen Hormones. *Waste Management and the Environment IV* (pp. 13-19). Granada, Spain: International Conference on Waste Management and the Environment.
- Suslick, K. S. (1990). Sonochemistry. *Science*, 247(4949), 1439-1445.
- Suthersan, S. S., & Payne, F. C. (2004). *In Situ Remediation Engineering*. Boca Raton, FL: CRC Press. Retrieved May 2015
- Swenson, P. A., & Setlow, R. B. (1962). Kinetics of Dimer Formation and Photohydration in Ultraviolet Irradiated Polyuridylic Acid. *Photochemistry and Photobiology*, 2, 419-434.
- Takahashi, N., Hibino, T., Torii, H., Fujioka, T., Tasaka, S., Sugimoto, K., . . . Ogasawara, H. (2013). Evaluation of O<sub>3</sub>/UV and O<sub>3</sub>/H<sub>2</sub>O<sub>2</sub> as Practical Advanced Oxidation Processes for 1,4-Dioxane. *Ozone Science and Engineering*, 35(5).
- Telsonic AG. (2006). *Operating Instructions Sonoprocessor DG200*. Bronschhofen, Germany.

- Thomas, J. K. (1965). Reaction Rates of the Hydroxyl Radical. *Transactions of the Faraday Society*, 61, 702-707.
- U.S. Department of the Interior. (1998). *Ground Water and Surface Water A Single Resource*. U.S. Department of the Interior. Denver, CO: U.S. Government Printing Office.
- UN General Assemblyl. (2010, July 28). United Nations; Meetings Coverage and Press Releases. *General Assembly Adopts Resolution Recognizing Access to Clean Water, Sanitation as Human Right, by Recorded Vote of 122 in Favour, None against, 41 Abstentions*. New York, New York, USA. Retrieved May 30, 2016, from <http://www.un.org/press/en/2010/ga10967.doc.htm>
- Unluturk, S., Atilgan, M., Baysal, A. H., & Unluluk, M. S. (2010). Modeling Inactivation Kinetics of Liquid Egg White Exposed to UV-C Irradiation. *International Journal of Food Microbiology*, 3(142), 341-347.
- US Army Environmental Command. (2010). *Studies on Metabolism of 1,4-Dioxane*. Aberdeen Proving Ground, MD: US Army Public Health Command.
- US Food and Drug Administration. (2015). *Title 21--Foods and Drugs*. Department of Health and Human Services. Silver Spring, MD: United States Food and Drug Administration. Retrieved December 18, 2015, from <file:///C:/Users/Engineering/OneDrive/scientific%20literature/CFR%20-%20Code%20of%20Federal%20Regulations%20Title%2021.html>

- US National Center for Biotechnology Information. (2015). *1,2-Diformyloxyethane*. Bethesda, MD: National Institute for Health. Retrieved from <https://pubchem.ncbi.nlm.nih.gov/compound/12376>
- US National Center for Biotechnology Information. (2015). *Formaldehyde*. Bethesda, MD: National Institute for Health. Retrieved December 18, 2015, from <https://pubchem.ncbi.nlm.nih.gov/compound/712#section=Top>
- US-DoD. (2014). *Quadrennial Defense Review*. United States Department of Defense.
- US-EPA. (1987). *Air Stripping of Contaminated Water Sources - Air Emissions and Controls*. Triangle Park, NC: Environmental Protection Agency-Control Technology Center.
- US-EPA. (2005). *1,4-Dioxane (CASRN 123-91-1)*. EPA Integrated Risk Information System (IRIS). Retrieved 6 22, 2015, from <http://www.epa.gov/IRIS/subst/0326.htm>
- US-EPA. (2006). *Treatment Technologies for 1,4-Dioxane: Fundamentals and Field Applications*. US EPA.
- US-EPA. (2012). *Guidelines for Water Reuse*. Environmental Protection Agency. Cincinnati: National Risk Management Research Laboratory.
- US-EPA. (2012). *Technical Fact Sheet - 1,4-Dioxane*. Retrieved 5 2015, from [http://www.epa.gov/fedfac/pdf/technical\\_fact\\_sheet\\_14-dioxane.pdf](http://www.epa.gov/fedfac/pdf/technical_fact_sheet_14-dioxane.pdf)
- US-EPA. (2013). *Toxic Release Inventory Explorer*. Retrieved 7 28, 2015, from <http://www.epa.gov/triexplorer>

US-EPA. (2016). *Fact Sheet; PFOA & PFOS Drinking Water Health Advisories*. US-EPA.

US-EPA. (2016, May 25). Lifetime Health Advisories and Health Effects Support Documents for Perfluorooctanoic Acid and Perfluorooctane Sulfonate. *Federal Register*, 81(101), 33250.

US-EPA. (2016). *Third Unregulated Contaminant Monitoring Rule (UCMR 3): Data Summary April 2016*. Office of Water. US-EPA.

Wang, R., & Zimmerman, J. (2016). Hybrid Analysis of Blue Water Consumption and Water Scarcity Implications at the Global, National, and Basin Levels in an Increasingly Globalized World. *Environmental Science & Technology*, A-K.

Wang, S. Y. (1976). *Photochemistry and Photobiology of Nucleic Acids*. New York: Academic Press Inc.

Weavers, L. K., & Hoffmann, M. R. (1998). Sonolytic Decomposition of Ozone in Aqueous Solution: Mass Transfer Effects. *Environmental Science and Technology*, 32, 3941-3947.

Wedeco. (2004). *Installation, Operation and Maintenance Manual for CHI Series Ultraviolet Water Disinfection Unit*. Charlotte, NC.

Westerhoff, P., Song, R., Amy, G., & Minear, R. (1997). Applications of Ozone Decomposition Model. *Ozone: Science & Engineering*, 19(1), 55-73.

- Woo, Y., Neuburger, B. J., Arcos, J. C., Argus, M. F., Nishayama, K., & Giffin, G. W. (1980). Enhancement of Toxicity and Enzyme-Repressing Activity of Para-Dioxane by Chlorination--Stereoselective Effects. *Toxicology Letters*, 5, 69-75.
- World Health Organization. (2012). *Global Costs and Benefits of Drinking-Water Supply and Sanitation Interventions to Reach the MDG Target and Universal Coverage*. Water Sanitation and Health. Geneva: WHO Press.
- Xu, X.-w., Shi, H.-x., & Wang, D.-h. (2005). Ozonation with ultrasonic enhancement of p-nitrophenol wastewater. *Journal of Zhejiang University Science*, 6B(5), 319-323.
- Xu, Z., Mochida, K., Naito, T., & Yasuda, K. (2012). Effects of operational conditions on 1,4-dioxane degradation by combined use of ultrasound and ozone microbubbles. *Japanese Journal of Applied Physics*, 51(7 Part 2).
- Young, J. D., Braun, W. H., Rampy, L. W., & Chenoweth, M. B. (1977). Pharmacokinetics of 1,4-Dioxane in Humans. *Journal of Toxicology and Environmental Health*, 3(3), 507-520.
- Zenker, M. J., Borden, R. C., & Barlaz, M. A. (2000). Mineralization of 1,4-Dioxane in the Presence of a Structural Analog. *Biodegradation*, 11, 239-246.
- Zenker, M. J., Borden, R. C., & Barlaz, M. A. (2003). Occurrence and Treatment of 1,4-Dioxane in Aqueous Environments. *Environmental Engineering Science*, 20(5), 423-432.

Zenker, M. J., Borden, R. C., & Barlaz, M. A. (2004). Biodegradation of 1,4-dioxane using trickling filter. *Journal of Environmental Engineering-Asce*, 130(9), 926-931.

# APPENDICES

## APPENDIX A

### ARDUINO SKETCH

```
[code]
// This sketch is used for a custom data collection and recording module, consisting of an Arduino UNO, an aluminum
// enclosure, a Sreed Studio SD Card Shield V4.0, a 1602 LCD display, a printed circuit board, four 1/8 inch stereo jack
// inputs, and various jumpers, wires, resistors, and potentiometers. The sketch interprets data from a variety of sensors,
// displays them to its screen, and saves the data as a comma-separated value table to both the serial port and an SD card
// (if present). This sketch was created in March 2015 by Major Michael Dietrich, USAF, BSC, while a graduate student
// at Temple University, and utilized various open source example code from Arduino.cc.

// comments begin with "/"
#include <LiquidCrystal.h> // include library for LCD displays
LiquidCrystal lcd(9,3,5,6,7,8); // pins hooked up to LCD (4 is reserved for SD card)
#include <SPI.h> // include SPI library for SD Card Shield (requires pins 11, 12, 13)
#include <SD.h> // include the SD card library that comes with the Arduino (pin 10 used for SD comm)
#include <math.h> // this is included for the Steinhart-Hart thermistor calculations

int chipSelect = 4; // pin 4 is needed for the SD card
int sensor0 = A0; // establish the sensor inputs with their various analog pins (A0-A5) (A0 is US power)
int sensor1 = A1; // UV
int sensor2 = A2; // ozone
int sensor3 = A3; // pressure
int sensor4 = A4; // final temp
int sensor5 = A5; // initial temp

//int sensor6 = 1; // flow meter #1 (pulse width) 1=TX
int sensor7 = 2; // flow meter #2 (pulse width)
//int sensor8 = 0; // ultrasonic frequency (pulse width) 0=RX

// volatile unsigned long duration1a; // USING PULSE WIDTH for flow measurement
// volatile unsigned long duration1b;
volatile unsigned long duration2a;
volatile unsigned long duration2b;
float flowrate1;
float flowrate2;

int sensor0Value = 0; // establish and zero initial sensor variables
int sensor1Value = 0;
int sensor2Value = 0;
int sensor3Value = 0;
int sensor4Value = 0;
int sensor5Value = 0;
int sensor6Value = 0;
int sensor7Value = 0;
int sensor8Value = 0;

// unsigned long hightime; // establish variables
// unsigned long lowtime;
// volatile unsigned long timeperiod;
unsigned long sensorTime;
float minutes;
float pressure;
float uvvolts;
float uv;
float tempfresist;
float tempfvolts;
float tempf;
float watts;
float freq;
```

```

float ozonevolts;
float ozone;
float tempivolts;
float tempi;
float mll;           // Orbisphere tri-linear parameters
float ml;
float mh;
float mhh;
float aoh;
float aol;

void setup()
{
//pinMode(sensor6, INPUT);           //assign digital pin 1 as an input
pinMode(sensor7, INPUT);           //assign digital pin 2 as an input
//pinMode(sensor8, INPUT);           //assign digital pin 0 as an input

  lcd.begin(16,2);           // display initialization screen information
  lcd.setCursor(0, 0);
  lcd.print("Data Montitor +");
  lcd.setCursor(0, 1);
  lcd.print("Recorder V6.0");
  delay(1200);           // delays are set to ensure first measurement is recorded at 0.100 minutes
  lcd.clear();
  lcd.setCursor(0, 0);
  lcd.print("Created by");
  lcd.setCursor(0, 1);
  lcd.print("Mike Dietrich");
  delay(1000);
  lcd.clear();
  lcd.setCursor(0, 0);
  lcd.print("TempleUniversity");
  lcd.setCursor(0, 1);
  lcd.print("WET Center 2015");
  delay(1000);
  lcd.clear();

           // open serial communications and wait for port to open:
  // Serial.begin(9600);
  // NOTE: serial comm was disabled in version 5, because the comm port (pin 1), was needed for second flow meter. The
  // while (!Serial) {
  // flowmeters were programmed and debugged with pin 1 vacant, and flowmeter 1 was plugged in prior to experimentation.
  //;           // wait for serial port to connect. Needed for Leonardo only
  // }
  // Serial.print("Initializing SD card...");
  pinMode(10, OUTPUT);
           // Check if the SD card is present and can be initialized:
  if (!SD.begin(chipSelect)) {
  // Serial.println("Card failed, or not present");
  lcd.begin(16,2);
  lcd.setCursor(0, 0);
  lcd.print("SD card absent.");
  lcd.setCursor(0, 1);
  lcd.print("Insert & reset.");
  delay(60000);           // if SD card isn't detected, wait up to one minute before displaying data
  }
  else {           // create column headers for data on SD card
    File datalog=SD.open("datalog.txt", FILE_WRITE);
    if (datalog)
    {
      datalog.println(", ,");           // insert a line break
      String header = "Time(min),duration2(usec), Flowrate2(mL/min),
Pressure(psi),InitTemp(C),FinalTemp(C),UltrasoundPower(W),Freq(kHz),Ozone(mg/l),UV(mW/cm2)";
      datalog.println(header);
      datalog.close();
      // Serial.println(" ");           // print data header to serial port, as well
      // Serial.println("Time(min),Flowrate 1, Flowrate 2, Pressure(psi),InitTemp(C),FinalTemp(C),UltrasoundPower(W),Freq(
kHz),Ozone(mg/l)");
      return;
    }
  }
}

```

```

}
delay(10); // create custom glyphs to maximize use of the 16 X 2 character display
byte tempinit[8] = { // glyphs are stored as bytes. each line gives the pixel conditions of 8 rows.
  B11100, // 1 means pixel is lit, 0 means it is unlit.
  B01000, // each character has 5 columns and 8 rows of pixels.
  B01000,
  B01010, // corresponds to initial temp, or T sub i, "Ti"
  B01000,
  B01010,
  B01010,
  B00010,
};
  lcd.createChar(0,tempinit);
delay(10);
byte tempfin[8] = {
  B11100,
  B01000,
  B01000, // corresponds to final temp, or T sub f, "Tf"
  B01011,
  B01010,
  B01111,
  B01010,
  B00010
};
  lcd.createChar(1,tempfin);
delay(10);
byte hertz[8] = {
  B10010,
  B11110,
  B10010, // corresponds to H & z, "Hz"
  B00000,
  B01111,
  B00010,
  B00100,
  B01111,
};
  lcd.createChar(2,hertz);
delay(10);
byte gl[8] = {
  B11100,
  B10100,
  B11100,
  B00101, // corresponds to g / l, "g/l", couples with custom mu glyph for "mg/l"
  B11010,
  B00101,
  B01001,
  B10001,
};
  lcd.createChar(4,gl);
delay(10);
byte mu[8] = {
  B11010,
  B10101,
  B10101, // corresponds to mu, "m", couples with custom "gl" glyph for "mg/l"
  B10000,
};
  lcd.createChar(3,mu);
delay(10);
byte celsius[8] = {
  B01000,
  B10100,
  B01000, // corresponds to degrees C, "*C"
  B00110,
  B01001,
  B01000,
  B01001,
  B00110,
};
  lcd.createChar(5,celsius);
delay(10);

```

```

    byte perc[8] = {
    B10001,
    B10101,
    B11111,           // corresponds to "W/c"
    B00010,
    B00100,
    B01011,
    B10100,
    B00011,
    };
    lcd.createChar(6,perc);
    delay(10);

    byte msquare[8] = {
    B01110,
    B00001,
    B00110,           // corresponds to "m2"
    B01111,
    B00000,
    B11010,
    B10101,
    B10101,
    };
    lcd.createChar(7,msquare);
    delay(10);

    // Serial.println("card initialized.");
    }

void loop()
{
    mll = 0;           // settings for orbisphere trilinear ozone analog inputs
    ml = 2.5;
    mh = 12.5;
    mhh = 22.5;
    aoh = 4.0;
    aol = 1.0;
    tempfresist = 2252;

    //duration1a=pulseIn(sensor6,LOW,1000000);
    //measure the time (microsec) between triggers from the Hall-effect flow sensor for later flowrate calculation
    duration2a=pulseIn(sensor7,LOW,1000000);
    //measure the time (microsec) between triggers from the Hall-effect flow sensor for later flowrate calculation

    sensor0Value = analogRead(sensor0); // front top distal pin "ultrasound power in Watts"
    sensor0Value = analogRead(sensor0);
    watts = sensor0Value * 0.0048876; // temporary equation to calculate sensor voltage
    watts = 400.0 * watts;
    // 2000W full scale value, R1/R2 mismatch correction factor based on data output comparion
    sensor1Value = analogRead(sensor1);
    uvvolts = sensor1Value*(0.0048876); // temporary calculation for measured volts
    uv=uvvolts*10.0;
    sensor2Value = analogRead(sensor2); // back top medial pin "ozone in mg/l"
    sensor2Value = analogRead(sensor2);
    ozonevolts = sensor2Value*0.0048876;
    // voltage is given 0-1024, corresponding to 0-5000mV. 5000/1021(corrected)=4.897. Trilinear.
    if (ozonevolts <= aol) {
        ozone = mll + (ml-mll)*(ozonevolts/aol);}
    else if (aoh >= ozonevolts && ozonevolts > aol) {
        ozone = ml + (mh-ml)*(ozonevolts-aol)/(aoh-aol);}
    else if (ozonevolts > aoh) {
        ozone = mh + (mhh-mh)*(ozonevolts-aoh)/(5.0-aoh);}
    else ozone = 99999; // return error reading of "99999" if measurement falls outside of trilinear ranges
    sensor3Value = analogRead(sensor3); // bottom medial pin "pressure in psi"
    sensor3Value = analogRead(sensor3);
    pressure = sensor3Value*(0.0048876); // temporary calculation for measured volts
    pressure = (pressure/0.023)-21.7391;
    // from transducer eq: vout=vin(0.75*p+0.1) from pressure transducer manufacturer's data [psi=(volts-0.45)/0.0402]
    sensor4Value = analogRead(sensor4); // bottom medial pin "final temp in C"
    sensor4Value = analogRead(sensor4);

```

```

tempfvolts = 0.0048828 * sensor4Value; // calculate measured voltage, Vin
tempfresist = (2160 * 5.0)/tempfvolts-2160;
// calculate thermistor value using voltage divider eq [R1=(R2*Vin)/Vout - R2, where R2=2200ohm]
tempf = log(tempfresist); // calculate natural log for Steinhart-Hart equation, store temporarily
tempf = 1/(0.001468 + (0.0002383*tempf) + (0.0000001007*tempf*tempf*tempf));
// Steinhart-Hart equation [1/T = A + B*ln(R) + C*ln(R)^3
tempf = tempf - 273.15; // convert temperature from Kelvin to Celsius
sensor5Value = analogRead(sensor5); // back top distal pin "initial temp in C"
sensor5Value = analogRead(sensor5);
tempivolts = sensor5Value*0.0048876; // voltage is given 0-1023, corresponding to 0-5000mV. 5000/1024=4.8876.
tempi=15.0+(35.0-15.0)*(tempivolts/5);
// given by Orbisphere software: M1 + (Mh - M1)*(V - 1) / 4 for linear analog setup
sensorTime = millis(); // note the current elapsed time
minutes = sensorTime/60000.0;
//sensor8Value = analogRead(sensor8);
//hightime=pulseIn(sensor8,HIGH,50000); // sensor1 measures the waveform frequency output from the sonicator
//lowtime=pulseIn(sensor8,LOW,50000); // first pulseIn measures the duration that sensor1 is HIGH, then LOW
//timeperiod=(hightime+lowtime);
// the period of ultrasound oscillations is the sum of hightime and lowtime (in microseconds)
//if (timeperiod>0) { // frequency is the inverse of the period.
//freq=1000.0/timeperiod; // 1000/us = kHz
//}
//else freq = 0; // this condition is added because the pulseIn command has a timeout period

lcd.begin(16,2); // display the data on the 16 X 2 display
lcd.setCursor(0, 0); // display the first line
lcd.print(watts,0);
lcd.setCursor(4,0);
lcd.print("W ");
lcd.setCursor(6, 0);
lcd.print(ozone,2);
lcd.setCursor(10,0);
lcd.write(byte(3)); // custom glyphs are made using the lcd.write command instead of lcd.print
lcd.setCursor(11,0);
lcd.write(byte(4));
lcd.setCursor(12,0);
lcd.print(" ");
lcd.setCursor(13,0);
lcd.print(minutes,1);
lcd.setCursor(0, 1); // display the second line
lcd.write(byte(0));
lcd.setCursor(2, 1);
lcd.print(tempi,1);
lcd.setCursor(4,1);
lcd.write(byte(5));
lcd.setCursor(5,1);
lcd.print(" ");
lcd.setCursor(6, 1);
lcd.print(pressure,1);
lcd.setCursor(9,1);
lcd.print("psi ");
lcd.setCursor(13,1);
lcd.print("min");
delay(500);

byte tempinit[8] = { //reinitialize glyphs in case they have been corrupted
B11100,
B01000,
B01000,
B01010,
B01000,
B01010,
B01010,
B00010, // corresponds to intial temp, "Ti"
};
lcd.createChar(0,tempinit);
delay(10);

byte tempfin[8] = {
B11100,

```

```

B01000,
B01000,
B01011,
B01010,
B01111,
B01010,
B00010,          // corresponds to final temp, "Tf"
};
lcd.createChar(1,tempfin);
delay(10);

byte hertz[8] = {
B10010,
B11110,
B10010,
B00000,
B01111,
B00010,
B00100,
B01111,          // corresponds to Hertz, "Hz"
};
lcd.createChar(2,hertz);
delay(10);

byte gl[8] = {
B11100,
B10100,
B11100,
B00101,
B11010,
B00101,
B01001,
B10001,          // corresponds to "g/l"
};
lcd.createChar(4,gl);
delay(10);

byte mu[8] = {
B11010,
B10101,
B10101,
// corresponds to mu, "m", couples with custom "gl" glyph "mg/L" and "perc" and "msquare" glyphs for "mW/cm^2"
};
lcd.createChar(3,mu);
delay(10);

byte celsius[8] = {
B01000,
B10100,
B01000,
B00110,
B01001,
B01000,
B01001,
B00110,          // corresponds to Celsius, "*C"
};
lcd.createChar(5,celsius);
delay(10);

byte perc[8] = {
B10001,
B10101,
B11111,          // corresponds to "W/c"
B00010,
B00100,
B01011,
B10100,
B00011,
};
lcd.createChar(6,perc);

```

```

delay(10);

byte msquare[8] = {
  B01110,
  B00001,
  B00110,           // corresponds to "m^2"
  B01111,
  B00000,
  B11010,
  B10101,
  B10101,
};
lcd.createChar(7,msquare);

delay(1500);           // delay to control sample frequency. 2582 for ~6 sec sample rate

sensor0Value = analogRead(sensor0); // front top distal pin "ultrasound power in Watts"
sensor0Value = analogRead(sensor0);
watts = sensor0Value * 0.0048876; // temporary equation to calculate sensor voltage
watts = 400.0 * watts; // 2000W full scale value, R1/R2 mismatch correction factor based on data output comparion
sensor1Value = analogRead(sensor1);
uvvolts = sensor1Value*(0.0048876); // temporary calculation for measured volts
uv=uvvolts*10.0;
sensor2Value = analogRead(sensor2); // back top medial pin "ozone in mg/l"
sensor2Value = analogRead(sensor2);
ozonevolts = sensor2Value*0.0048876;
// voltage is given 0-1024, corresponding to 0-5000mV. 5000/1021(corrected)=4.897. Trilinear.
if (ozonevolts <= aol) {
  ozone = mll + (ml-mll)*(ozonevolts/aol);}
else if (aoh >= ozonevolts && ozonevolts > aol) {
  ozone = ml + (mh-ml)*(ozonevolts-aol)/(aoh-aol);}
else if (ozonevolts > aoh) {
  ozone = mh + (mhh-mh)*(ozonevolts-aoh)/(5.0-aoh);}
else ozone = 99999; // return error reading of "99999" if measurement falls outside of trilinear ranges
sensor3Value = analogRead(sensor3); // bottom medial pin "pressure in psi"
sensor3Value = analogRead(sensor3);
pressure = sensor3Value*(0.0048876); // temporary calculation for measured volts
pressure = (pressure/0.023)-21.7391;
// from transducer eq: vout=vin(0.75*p+0.1) from pressure transducer manufacturer's data [psi=(volts-0.45)/0.0402]
sensor4Value = analogRead(sensor4); // bottom medial pin "final temp in C"
sensor4Value = analogRead(sensor4);
tempfvolts = 0.0048828 * sensor4Value; // calculate measured voltage, Vin
tempfresist = (2160 * 5.0)/tempfvolts-2160;
// calculate thermistor value using voltage divider eq [R1=(R2*Vin)/Vout - R2, where R2=2200ohm]
tempf = log(tempfresist); // calculate natural log for Steinhart-Hart equation, store temporarily
tempf = 1/(0.001468 + (0.0002383*tempf) + (0.0000001007*tempf*tempf*tempf));
// Steinhart-Hart equation [1/T = A + B*ln(R) + C*ln(R)^3
tempf = tempf - 273.15; // convert temperature from Kelvin to Celsius
sensor5Value = analogRead(sensor5); // back top distal pin "initial temp in C"
sensor5Value = analogRead(sensor5);
tempivolts = sensor5Value*0.0048876; // voltage is given 0-1024, corresponding to 0-5000mV. 5000/1024=4.8828.
tempi=15.0+(35.0-15.0)*(tempivolts/5);
// given by Orbisphere software: Ml + (Mh - Ml)*(V - 1) / 4 for linear analog setup
sensorTime = millis(); // note the current elapsed time
minutes = sensorTime/60000.0;
// sensor8Value = analogRead(sensor8);
// hightime=pulseIn(sensor8,HIGH,50000); // sensor1 measures the waveform frequency output from the sonicator
// lowtime=pulseIn(sensor8,LOW,50000); // first pulseIn measures the duration that sensor1 is HIGH, then LOW
// timeperiod=(hightime+lowtime);
// the period of ultrasound oscillations is the sum of hightime and lowtime (in microseconds)
// if (timeperiod>0) { // frequency is the inverse of the period.
// freq=1000.0/timeperiod; // 1000/us = kHz
// }
// else freq = 0; // this condition is added because the pulseIn command has a timeout period

lcd.begin(16,2); // display the data on the 16 X 2 display
lcd.setCursor(0, 0); // display the first line
lcd.print(uv,1);
delay(10);
lcd.setCursor(3,0);

```

```

delay(10);
lcd.write(byte(3));
lcd.setCursor(4,0);
delay(10);
lcd.write(byte(6));
delay(10);
lcd.setCursor(5,0);
delay(10);
lcd.write(byte(7));
delay(10);
lcd.setCursor(7, 0);
lcd.print(ozone,2);
lcd.setCursor(10,0);
lcd.write(byte(3));
lcd.setCursor(11,0);
lcd.write(byte(4));
lcd.setCursor(12,0);
lcd.print(" ");
lcd.setCursor(13,0);
lcd.print(minutes,1);
lcd.setCursor(0, 1); // display the second line
lcd.write(byte(1)); // custom glyphs are made using the lcd.write command instead of lcd.print
lcd.setCursor(2, 1);
lcd.print(tempf,1);
lcd.setCursor(4,1);
lcd.write(byte(5));
lcd.setCursor(5,1);
lcd.print(" ");
lcd.setCursor(6, 1);
lcd.print(freq,1);
lcd.setCursor(10,1);
lcd.print("k");
lcd.setCursor(11,1);
lcd.write(byte(2));
lcd.setCursor(13,1);
lcd.print("min");
delay(1000); // 2582 for ~6 sec sample rate

// duration1b=pulseIn(sensor6,LOW);
// measure the time (microsec) between triggers from the Hall-effect flow sensor
// flowrate1=0.5*(duration1a+duration1b); // average the previous two Hall-effect times
// if (flowrate1>0)
// {flowrate1=(1000000/flowrate1); // divide 10^6 microseconds by the average time in microseconds
// flowrate1=(flowrate1+8.469)/0.1297;} // translate calculated flow value to mL/min using calibration curve equation
// else flowrate1=0

duration2b=pulseIn(sensor7,LOW,1000000);
// measure the time (microsec) between triggers from the Hall-effect flow sensor
flowrate2=0.5*(duration2a+duration2b); // average the previous two Hall-effect times
if (flowrate2>0)
{flowrate2=(1000000/flowrate2); // divide 10^6 microseconds by the average time in microseconds
flowrate2=(flowrate2+8.469)/0.1297;}
else flowrate2=0; // translate calculated flow value to mL/min using calibration curve equation

lcd.begin(16,2); // display the data on the 16 X 2 display
lcd.setCursor(0, 0); // display the first line
// lcd.print(flowrate1,0);
lcd.setCursor(4,0);
// lcd.print("mL/m in");
lcd.setCursor(12,0);
lcd.print(minutes,1);
lcd.setCursor(0, 1); // display the second line
lcd.print(flowrate2,0);
lcd.setCursor(4,1);
lcd.print("mL/min");
lcd.setCursor(13,1);
lcd.print("min");
delay(1000);

String dataString = ""; // make a string for assembling the data to log:

```

```

        // append the current calculated values to the string:
        dataString=String(minutes,2)+String(",")+String(duration2b,0)+String(",")+String(flowrate2,0)+String(",")+String(pressu
re,2)+String(",")+String(tempi,2)+String(",")+String(tempf,2)+String(",")+String(watts,1)+String(",")+String(freq,2)+String(",")+Stri
ng(ozone,2)+String(",")+String(uv)+String(",");
        delay(10);
        File dataFile = SD.open("datalog.txt", FILE_WRITE);
        // if the file is available (on SD card), write to it:
        if (dataFile) {
            dataFile.println(dataString);
            dataFile.close();
            // Serial.println(dataString);    // print the data to the serial port, too:
        }

        // String dataStringdebug = "";
        // dataStringdebug=String(minutes,3)+String("minutes,")+String(sensor0Value)+String(",")+String(sensor1Value)+Strin
g(",")+String(sensor2Value)+String(",")+String(sensor3Value)+String(",")+String(sensor4Value)+String(",")+String(sensor5Value)
+String(",")+String(lowtime);
        // Serial.println(dataStringdebug);
    }

[/code]

```

## APPENDIX B.

### GNUPLOT SCRIPT FOR 3D PLOTS

*(pulls x,y,z data from two .txt files, ozonedata.txt and ozoneusdata.txt)*

```
gnuplot> set xrange [0:16]
gnuplot> set yrange [0:16]
gnuplot> set zrange [0:100]
gnuplot> set cbrange [0:100]
gnuplot> set xyplane at 0
gnuplot> set ztic offset -1
gnuplot> set xtic offset -.5,-.5
gnuplot> set ytic offset -.5,-.5
gnuplot> set colorbox horiz user origin 0.1, .859 size .3, .022
gnuplot> set term wxt size 900,800 font "Times, 14"
gnuplot> set title "Figure 6. Experimental Results with Model Prediction Overlay for
Ozone" ALTERNATIVELY "Figure 7. Experimental Results with Model Prediction
Overlay for Ozone/Ultrasound"
gnuplot> set xlabel "Time (min)"
gnuplot> set ylabel "[O_3]_a_q (mg/L)"
gnuplot> set zlabel "% 1,4-Dioxane Removal" rotate by 90
gnuplot> set pm3d at b
gnuplot> set dgrid 30,30 gauss 1
gnuplot> splot 100*(1-exp(-x*0.17*(y**0.39))) title 'O_3/US Model',"ozoneusdata.txt"
with lines title 'O_3/US Experimental' ALTERNATIVELY splot 100*(1-exp(-
x*0.07*(y**0.39))) title 'O_3 Model',"ozonedata.txt" with lines title 'O_3 Experimental'
```

## B. APPENDIX A

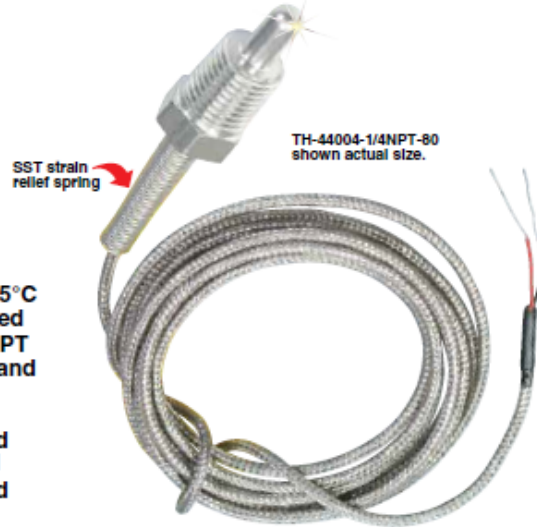
## APPENDIX C

### THERMISTOR MANUFACTURER'S DATA

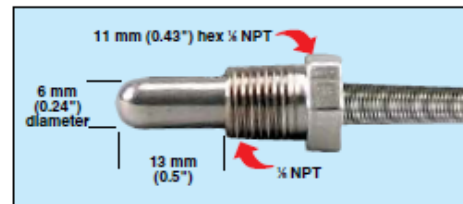
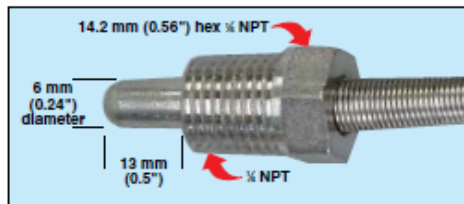
# Pipe-Plug Thermistor Probes

## TH-44004 Series

- ✓ Ideal for Use in Pressure Vessel Applications 2500 psi (172 bar) Maximum
- ✓ Max Temperature 150°C (302°F) or 75°C (167°F) Depending on Option Selected
- ✓ 6 mm Diameter Sheath with ¼ or ½ NPT Mounting Thread Standard; Sheath and Plug are 300 Series Stainless Steel
- ✓ 2 m (80") 26 AWG Stranded, PFA Insulated and Jacketed, SST Braided Cable with Stripped Leads Standard
- ✓ Available in 5 Resistance Values and 2 Tolerances



TH-44004-1/4NPT-80 shown actual size.



#### Standard Dimensions

To Order Visit <a href="http://omega.com/th-44000-npt">omega.com/th-44000-npt</a> for Pricing and Details					
Model Number	Resistance @ 25°C	Tolerance @ 0 to 70°C	Sheath Diameter (mm)	Cable Lgth m (inch)	Cable Termination
TH-44004-1/4NPT-80	2252 Ω	±0.2°C	6	2 (80)	Stripped
TH-44004-1/8NPT-80	2252 Ω	±0.2°C	6	2 (80)	Stripped

*Options: Other thermistor selections are available—select from the table below, insert the thermistor number into the model number and add any additional price shown into the probe price. For phone plug option, add “-PP” to the model number for an additional cost. For leads over 2 m (80”), change model number to required length for an additional cost. For longer cable length, contact Sales.*

*Ordering Examples: TH-44004-1/4NPT-80, ¼ NPT pipe plug sensor, 2252 Ω at 25°C, interchangeability ±0.2°C, 2 m (80”) of cable.  
TH-44033-1/8NPT-120-PP, ⅛ NPT pipe plug sensor, 2252 Ω at 25°C, interchangeability ±0.1°C, 3 m (10’) of cable with phone plug connector.*

#### Thermistor Selection Table

Model Number	Resistance @ 25°C	Tolerance @ 25°C	Max Temperature
44004	2252 Ω	±0.2°C	150°C (302°F)
44005	3000 Ω		
44007	5000 Ω		
44006	10000 Ω		
44008	30000 Ω		
44033	2252 Ω	±0.1°C	75°C (167°F)
44030	3000 Ω		
44034	5000 Ω		
44031	10000 Ω		
44032	30000 Ω		

# APPENDIX D

## PRESSURE TRANSDUCER MANUFACTURER'S DATA

**PART NO.** PS401

TOLERANCES UNLESS SPECIFIED  
THREE PLACE DECIMALS +/- .005

ANGLES +/- 1°

ENGINE OIL PRESSURE  
SENSOR SIGNAL

SENSOR GROUND

5V SUPPLY

27mm HEX

1/8-27 NPT

.17 I.D.

2.20

PRESSURE (PSIG)	SENSOR SIGNAL (VOLTS DC)
80	3.70
60	2.85
40	2.02
20	1.22
0	.45

REPLACES OE #56028807AA, 56028807AB, 5149064AA

(A) (B)

SCALE		NTS		DATE		MATERIAL		MATERIAL		SCALE		DATE		MATERIAL	
ENGINEER	6-19-00	APPROVED	6-19-00	FINISH	N/A	DATE	6-19-00	DATE	6-19-00	DATE	6-19-00	DATE	6-19-00	DATE	6-19-00
BY	DAB	BY	JKS	DL	N/A	BY	DAB	BY	DAB	DATE	6-19-00	DATE	6-19-00	DATE	6-19-00
PURCH.		PROD.		MODEL		CAD REF.		PS401		SCALE		DATE		MATERIAL	
<input type="checkbox"/>		<input type="checkbox"/>		PS401		PS401		PS401		DATE		DATE		MATERIAL	
TITLE		PART NO.		MODEL		CAD REF.		PS401		SCALE		DATE		MATERIAL	
OIL PRESSURE SWITCH		PS401		PS401		PS401		PS401		DATE		DATE		MATERIAL	
WELLS MANUFACTURING L.P.		FOND DU LAC, WISCONSIN		DATE		MATERIAL		PS401		SCALE		DATE		MATERIAL	

## APPENDIX E

### EXPERIMENTAL DATA

*Table E1 Effects of Ozone Dose, Treatment Time, and Ultrasound Intensity*

*Figures 4-1, 4-2, 4-16, 4-17, 4-18, 4-20*

Sample Name	Date	[O <sub>3</sub> ] <sub>in</sub> (mg/L)	Flow Rate (mL/min)	Residence Time (min)	Ultrasound (W)	Dioxane <sub>in</sub> (ppm)	Dioxane <sub>fin</sub> (ppm)	C/C <sub>0</sub>	Reduction (%)	ln (C/C <sub>0</sub> )
Ozone US A1	9/17/14	11.11	1034	2.49	720	19.35	7.33	0.38	62.11	-0.97
Ozone US A2	9/17/14	11.11	1034	2.49	720	19.35	7.99	0.41	58.71	-0.88
Ozone US A3	9/17/14	11.11	1034	2.49	720	19.35	7.23	0.37	62.61	-0.98
Ozone US B1	9/17/14	5.39	1034	2.49	750	19.35	9.40	0.49	51.42	-0.72
Ozone US B2	9/17/14	5.39	1034	2.49	750	19.35	9.49	0.49	50.96	-0.71
Ozone US B3	9/17/14	5.39	1034	2.49	750	19.35	9.27	0.48	52.10	-0.74
Ozone US C1	9/17/14	4.84	1034	2.49	762	19.35	10.40	0.54	46.24	-0.62
Ozone US C2	9/17/14	4.84	1034	2.49	762	19.35	10.87	0.56	43.83	-0.58
Ozone US C3	9/17/14	4.84	1034	2.49	762	19.35	10.16	0.53	47.47	-0.64
ultrasound 1	9/17/14	0.00	1034	2.49	780	19.35	19.29	1.00	0.30	0.00
ultrasound 2	9/17/14	0.00	1034	2.49	780	19.35	19.04	0.98	1.59	-0.02
ultrasound 3	9/17/14	0.00	1034	2.49	780	19.35	18.66	0.96	3.56	-0.04
ozone A1	9/17/14	11.00	1034	2.49	0	19.35	12.28	0.63	36.55	-0.45
ozone A2	9/17/14	11.00	1034	2.49	0	19.35	12.30	0.64	36.41	-0.45
ozone A3	9/17/14	11.00	1034	2.49	0	19.35	11.93	0.62	38.35	-0.48
ozone B1	9/17/14	7.92	1034	2.49	0	19.35	14.15	0.73	26.89	-0.31
ozone B2	9/17/14	7.92	1034	2.49	0	19.35	14.26	0.74	26.32	-0.31
ozone B3	9/17/14	7.92	1034	2.49	0	19.35	14.27	0.74	26.25	-0.30
ozone C1	9/17/14	3.74	1034	2.49	0	19.35	14.91	0.77	22.92	-0.26
ozone C2	9/17/14	3.74	1034	2.49	0	19.35	15.19	0.78	21.50	-0.24
ozone C3	9/17/14	3.74	1034	2.49	0	19.35	14.72	0.76	23.94	-0.27
initial 1	9/17/14	0.00	1034	2.49	0	19.35	18.62	0.96	3.76	-0.04
initial 2	9/17/14	0.00	1034	2.49	0	19.35	19.62	1.01	-1.42	0.01
initial 3	9/17/14	0.00	1034	2.49	0	19.35	19.79	1.02	-2.29	0.02
ozone US A1	9/22/14	10.34	534	4.82	714	19.35	2.51	0.13	87.01	-2.04
ozone US A2	9/22/14	10.34	534	4.82	714	19.35	2.27	0.12	88.25	-2.14
ozone US A3	9/22/14	10.34	534	4.82	714	19.35	2.50	0.13	87.07	-2.05
ultrasound 1	9/22/14	0.00	534	4.82	686	19.35	16.97	0.88	12.27	-0.13
ultrasound 2	9/22/14	0.00	534	4.82	686	19.35	16.80	0.87	13.18	-0.14
ultrasound 3	9/22/14	0.00	534	4.82	686	19.35	17.35	0.90	10.33	-0.11
ozone A 1	9/22/14	9.02	534	4.82	0	19.35	9.09	0.47	53.03	-0.76
ozone A 2	9/22/14	9.02	534	4.82	0	19.35	9.43	0.49	51.27	-0.72
ozone A 3	9/22/14	9.02	534	4.82	0	19.35	8.86	0.46	54.22	-0.78
initial 1	9/17/14	0.00	506	5.08	0	18.89	18.86	1.00	2.53	0.00
initial 2	9/17/14	0.00	506	5.08	0	18.89	19.03	1.01	1.66	0.01
initial 3	9/17/14	0.00	506	5.08	0	18.89	18.79	0.99	2.90	-0.01
ozone US D1	10/1/14	12.87	400.6	6.42	600	18.89	2.49	0.13	87.14	-2.03

ozone US D2	10/1/14	12.87	400.6	6.42	600	18.89	2.70	0.14	86.07	-1.95
ozone US D3	10/1/14	12.87	400.6	6.42	600	18.89	2.56	0.14	86.78	-2.00
ozone D1	10/1/14	10.78	400.6	6.42	0	18.89	9.35	0.50	51.66	-0.70
ozone D2	10/1/14	10.78	400.6	6.42	0	18.89	9.32	0.49	51.81	-0.71
ozone D3	10/1/14	10.78	400.6	6.42	0	18.89	9.51	0.50	50.87	-0.69
ultrasound 1	10/1/14	0.00	400.6	6.42	647	18.89	15.50	0.82	19.89	-0.20
ultrasound 2	10/1/14	0.00	400.6	6.42	647	18.89	15.57	0.82	19.55	-0.19
ultrasound 3	10/1/14	0.00	400.6	6.42	647	18.89	15.29	0.81	20.99	-0.21
ozone US A1	10/8/14	17.66	550	4.68	726	20.45	1.47	0.07	92.82	-2.63
ozone US A2	10/8/14	17.66	550	4.68	726	20.45	1.43	0.07	93.01	-2.66
ozone US A3	10/8/14	17.66	550	4.68	726	20.45	1.47	0.07	92.83	-2.64
ozone US B1	10/8/14	11.33	550	4.68	739	20.45	2.53	0.12	87.61	-2.09
ozone US B2	10/8/14	11.33	550	4.68	739	20.45	2.34	0.11	88.54	-2.17
ozone US B3	10/8/14	11.33	550	4.68	739	20.45	2.51	0.12	87.71	-2.10
ozone US C1	10/8/14	5.67	550	4.68	748	20.45	4.55	0.22	77.72	-1.50
ozone US C2	10/8/14	5.67	550	4.68	748	20.45	4.14	0.20	79.74	-1.60
ozone US C3	10/8/14	5.67	550	4.68	748	20.45	4.51	0.22	77.94	-1.51
ultrasound 1	10/8/14	0.00	550	4.68	737	20.45	20.24	0.99	1.00	-0.01
ultrasound 2	10/8/14	0.00	550	4.68	737	20.45	20.46	1.00	-0.09	0.00
ultrasound 3	10/8/14	0.00	550	4.68	737	20.45	21.44	1.05	-4.88	0.05
ultrasound 4	10/8/14	0.00	550	4.68	737	20.45	22.23	1.09	-8.77	0.08
ultrasound 5	10/8/14	0.00	550	4.68	737	20.45	20.45	1.00	-0.04	0.00
ultrasound 6	10/8/14	0.00	550	4.68	737	20.45	20.69	1.01	-1.20	0.01
ozone A 1	10/8/14	17.03	550	4.68	0	20.45	6.68	0.33	67.34	-1.12
ozone A 2	10/8/14	17.03	550	4.68	0	20.45	6.97	0.34	65.89	-1.08
ozone A 3	10/8/14	17.03	550	4.68	0	20.45	6.82	0.33	66.64	-1.10
ozone B 1	10/8/14	11.48	550	4.68	0	20.45	7.80	0.38	61.85	-0.96
ozone B 2	10/8/14	11.48	550	4.68	0	20.45	8.02	0.39	60.76	-0.94
ozone B 3	10/8/14	11.48	550	4.68	0	20.45	7.43	0.36	63.65	-1.01
ozone C 1	10/8/14	5.79	550	4.68	0	20.45	12.69	0.62	37.92	-0.48
ozone C 2	10/8/14	5.79	550	4.68	0	20.45	13.31	0.65	34.90	-0.43
ozone C 3	10/8/14	5.79	550	4.68	0	20.45	12.85	0.63	37.15	-0.46
initial 1	10/8/14	0.00	550	4.68	0	20.45	20.09	0.98	1.70	-0.02
initial 2	10/8/14	0.00	550	4.68	0	20.45	20.84	1.02	-1.95	0.02
initial 3	10/8/14	0.00	550	4.68	0	20.45	20.43	1.00	0.07	0.00
ozone US A1	10/21/14	16.01	359	7.17	721	20.35	0.67	0.03	96.71	-3.41
ozone US A2	10/21/14	16.01	359	7.17	721	20.35	0.78	0.04	96.16	-3.26
ozone US A3	10/21/14	16.01	359	7.17	721	20.35	0.75	0.04	96.32	-3.30
ozone US B1	10/21/14	11.19	359	7.17	698	20.35	0.91	0.04	95.55	-3.11
ozone US B2	10/21/14	11.19	359	7.17	698	20.35	0.78	0.04	96.19	-3.26
ozone US B3	10/21/14	11.19	359	7.17	698	20.35	0.76	0.04	96.26	-3.28
ozone US C1	10/21/14	5.42	359	7.17	709	20.35	1.65	0.08	91.93	-2.51
ozone US C2	10/21/14	5.42	359	7.17	709	20.35	1.60	0.08	92.16	-2.54
ozone US C3	10/21/14	5.42	359	7.17	709	20.35	1.38	0.07	93.24	-2.69
ultrasound 1	10/21/14	0.00	359	7.17	678	20.35	20.10	0.99	1.68	-0.01
ultrasound 2	10/21/14	0.00	359	7.17	678	20.35	20.31	1.00	0.66	0.00
ultrasound 3	10/21/14	0.00	359	7.17	678	20.35	18.91	0.93	7.47	-0.07
ozone A1	10/21/14	16.06	359	7.17	0	20.35	5.44	0.27	73.39	-1.32
ozone A2	10/21/14	16.06	359	7.17	0	20.35	4.81	0.24	76.47	-1.44
ozone A3	10/21/14	16.06	359	7.17	0	20.35	5.09	0.25	75.11	-1.39
ozone B1	10/21/14	10.82	359	7.17	0	20.35	5.67	0.28	72.28	-1.28

ozone B2	10/21/14	10.82	359	7.17	0	20.35	5.14	0.25	74.83	-1.38
ozone B3	10/21/14	10.82	359	7.17	0	20.35	5.09	0.25	75.11	-1.39
ozone C1	10/21/14	5.51	359	7.17	0	20.35	5.81	0.29	71.59	-1.25
ozone C2	10/21/14	5.51	359	7.17	0	20.35	6.17	0.30	69.81	-1.19
ozone C3	10/21/14	5.51	359	7.17	0	20.35	6.31	0.31	69.14	-1.17
initial 1	10/21/14	0.00	359	7.17	0	20.35	20.66	1.02	-1.08	0.02
initial 2	10/21/14	0.00	359	7.17	0	20.35	19.33	0.95	5.41	-0.05
initial 3	10/21/14	0.00	359	7.17	0	20.35	21.06	1.03	-3.01	0.03
ozone US B1	10/27/14	17.27	1169	2.20	805	21.65	4.32	0.20	78.89	-1.61
ozone US B2	10/27/14	17.27	1169	2.20	805	21.65	4.31	0.20	78.91	-1.61
ozone US B3	10/27/14	17.27	1169	2.20	805	21.65	3.97	0.18	80.57	-1.70
ozone B1	10/27/14	17.42	1169	2.20	0	21.65	9.63	0.44	52.90	-0.81
ozone B2	10/27/14	17.42	1169	2.20	0	21.65	9.28	0.43	54.61	-0.85
ozone B3	10/27/14	17.42	1169	2.20	0	21.65	9.99	0.46	51.13	-0.77
initial 1	10/27/14	0.00	1169	2.20	0	21.65	22.14	1.02	-8.33	0.02
initial 2	10/27/14	0.00	1169	2.20	0	21.65	21.88	1.01	-7.06	0.01
initial 3	10/27/14	0.00	1169	2.20	0	21.65	20.93	0.97	-2.42	-0.03
ozone US A1	11/6/14	2.58	362.9	7.09	730	22.51	3.45	0.15	84.67	-1.88
ozone US A2	11/6/14	2.58	362.9	7.09	730	22.51	3.55	0.16	84.24	-1.85
ozone US A3	11/6/14	2.58	362.9	7.09	730	22.51	2.80	0.12	87.56	-2.08
ozone US B1	11/6/14	2.46	445.5	5.78	754	22.51	7.20	0.32	68.02	-1.14
ozone US B2	11/6/14	2.46	445.5	5.78	754	22.51	6.64	0.29	70.52	-1.22
ozone US B3	11/6/14	2.46	445.5	5.78	754	22.51	6.43	0.29	71.43	-1.25
ozone A1	11/6/14	2.56	362.9	7.09	0	22.51	9.79	0.43	56.52	-0.83
ozone A2	11/6/14	2.56	362.9	7.09	0	22.51	8.21	0.36	63.55	-1.01
ozone A3	11/6/14	2.56	362.9	7.09	0	22.51	9.45	0.42	58.02	-0.87
ozone B1	11/6/14	2.52	445.5	5.78	0	22.51	14.65	0.65	34.92	-0.43
ozone B2	11/6/14	2.52	445.5	5.78	0	22.51	14.87	0.66	33.93	-0.41
ozone B3	11/6/14	2.52	445.5	5.78	0	22.51	20.83	0.93	7.48	-0.08
initial	11/10/14	0.00	919.7	2.80	0	22.51	22.51	1.00	-10.14	0.00
ozone US	11/10/15	2.60	404.5	6.36	614	22.51	5.06	0.22	77.53	-1.49
Ozone	11/10/15	2.60	405	6.35	0	22.51	12.30	0.55	45.35	-0.60
initial	1/20/15	0.00	400	6.43	0	20.00	13.79	0.69	0.00	-0.37
initial	5/8/15	0.00	1018	2.53	0	25.86	26.21	1.01	0.00	0.01
init 2	5/8/15	0.00	1018	2.53	0	25.86	25.51	0.99	2.68	-0.01
us	5/8/15	0.00	1170	2.20	890	25.86	23.61	0.91	9.92	-0.09
us 2	5/8/15	0.00	1170	2.20	890	25.86	23.79	0.92	9.24	-0.08
o3	5/8/15	2.40	826	3.12	0	25.86	20.48	0.79	21.88	-0.23
o3us	5/8/15	2.67	877.8	2.93	848	25.86	15.01	0.58	42.73	-0.54
o3us orig	5/8/15	2.67	878	2.93	848	25.86	13.96	0.54	46.76	-0.62
Initial	11/13/15	0.00	550	4.67	0	20.91	20.91	1.00	0.00	0.00
O3US A 25%	11/13/15	4.68	553.9	4.64	396	20.91	9.64	0.46	53.89	-0.77
O3 A	11/13/15	4.86	569.8	4.51	0	20.91	11.49	0.55	45.02	-0.60
O3US B 25%	11/13/15	2.42	518.1	4.96	424	20.91	10.53	0.50	49.64	-0.69
O3 B	11/13/15	2.43	529.9	4.85	0	20.91	12.83	0.61	38.62	-0.49
US 25%	11/13/15	0.00	518	4.96	334	20.91	19.24	0.92	7.95	-0.08
initial 1	1/15/16	0.00	166.5	15.44	0	16.32	16.16	0.99	0.97	-0.01
initial 2	1/15/16	0.00	166.5	15.44	0	16.32	16.64	1.02	-1.95	0.02
initial 3	1/15/16	0.00	166.5	15.44	0	16.32	16.16	0.99	0.98	-0.01
o3us 1	1/15/16	1.25	159.3	16.13	788	16.32	1.61	0.10	90.13	-2.32

o3us 2	1/15/16	1.25	159.3	16.13	788	16.32	1.48	0.09	90.94	-2.40
o3us 3	1/15/16	1.25	159.3	16.13	788	16.32	1.55	0.10	90.49	-2.35
o3 1	1/15/16	1.04	157.1	16.36	0	16.32	5.83	0.36	64.27	-1.03
o3 2	1/15/16	1.04	157.1	16.36	0	16.32	5.81	0.36	64.43	-1.03
o3 3	1/15/16	1.04	157.1	16.36	0	16.32	6.29	0.39	61.45	-0.95
us 1	1/15/16	0.00	168.5	15.25	831	16.32	14.49	0.89	11.20	-0.12
us 2	1/15/16	0.00	168.5	15.25	831	16.32	13.35	0.82	18.18	-0.20
us 3	1/15/16	0.00	168.5	15.25	831	16.32	12.64	0.77	22.55	-0.26
initial 1	1/18/16	0.00	384.6	6.68	0	15.61	15.75	1.01	-0.90	0.01
initial 2	1/18/16	0.00	384.6	6.68	0	15.61	14.80	0.95	5.20	-0.05
initial 3	1/18/16	0.00	384.6	6.68	0	15.61	16.28	1.04	-4.28	0.04
o3us 1	1/18/16	0.99	407	6.31	869	15.61	6.82	0.44	56.33	-0.83
o3us 2	1/18/16	0.99	407	6.31	869	15.61	7.10	0.45	54.54	-0.79
o3us 3	1/18/16	0.99	407	6.31	869	15.61	5.82	0.37	62.73	-0.99
o3 1	1/18/16	1.10	405.2	6.34	0	15.61	10.30	0.66	34.03	-0.42
o3 2	1/18/16	1.10	405.2	6.34	0	15.61	10.33	0.66	33.82	-0.41
o3 3	1/18/16	1.10	405.2	6.34	0	15.61	10.55	0.68	32.43	-0.39
us 1	1/18/16	0.00	410.2	6.27	892	15.61	14.65	0.94	6.18	-0.06
us 2	1/18/16	0.00	410.2	6.27	892	15.61	13.92	0.89	10.85	-0.11
us 3	1/18/16	0.00	410.2	6.27	892	15.61	15.07	0.97	3.43	-0.03
initial 1	1/20/16	0.00	158.6	16.20	0	16.02	16.13	1.01	-0.70	0.01
initial 2	1/20/16	0.00	158.6	16.20	0	16.02	15.81	0.99	1.32	-0.01
initial 3	1/20/16	0.00	158.6	16.20	0	16.02	16.12	1.01	-0.62	0.01
o3us 1	1/20/16	2.54	167.1	15.38	869	16.02	0.31	0.02	98.04	-3.93
o3us 2	1/20/16	2.54	167.1	15.38	869	16.02	0.22	0.01	98.61	-4.28
o3us 3	1/20/16	2.54	167.1	15.38	869	16.02	0.63	0.04	96.09	-3.24
o3 1	1/20/16	2.53	166.4	15.44	0	16.02	3.05	0.19	80.95	-1.66
o3 2	1/20/16	2.53	166.4	15.44	0	16.02	3.25	0.20	79.70	-1.59
o3 3	1/20/16	2.53	166.4	15.44	0	16.02	4.09	0.26	74.45	-1.36
us 1	1/20/16	0.00	158.9	16.17	892	16.02	14.26	0.89	11.00	-0.12
us 2	1/20/16	0.00	158.9	16.17	892	16.02	12.43	0.78	22.42	-0.25
us 3	1/20/16	0.00	158.9	16.17	892	16.02	12.79	0.80	20.13	-0.22
initial 1	3/7/16	0.00	450	5.71	0	17.01	17.41	1.02	-2.35	0.02
initial 2	3/7/16	0.00	450	5.71	0	17.01	17.32	1.02	-1.85	0.02
initial 3	3/7/16	0.00	450	5.71	0	17.01	16.29	0.96	4.21	-0.04
o3us 1	3/7/16	2.52	363	7.08	940	17.01	3.26	0.19	80.84	-1.65
o3us 2	3/7/16	2.52	363	7.08	940	17.01	2.66	0.16	84.35	-1.85
o3us 3	3/7/16	2.52	363	7.08	940	17.01	3.25	0.19	80.88	-1.65
o3 1	3/7/16	2.52	387	6.85	0	17.01	7.10	0.42	58.27	-0.87
o3 2	3/7/16	2.52	387	6.85	0	17.01	6.70	0.39	60.60	-0.93
o3 3	3/7/16	2.52	387	6.85	0	17.01	7.60	0.45	55.33	-0.81
us 1	3/7/16	0.00	405	6.35	961	17.01	16.69	0.98	1.87	-0.02
us 2	3/7/16	0.00	405	6.35	961	17.01	18.53	1.09	-8.94	0.09
us 3	3/7/16	0.00	405	6.35	961	17.01	17.52	1.03	-2.99	0.03
initial 1	3/10/16	0.00	375	6.85	0	16.52	16.52	1.00	0.00	0.00
initial 2	3/10/16	0.00	375	6.85	0	16.52	16.52	1.00	0.00	0.00
initial 3	3/10/16	0.00	375	6.85	0	16.52	16.52	1.00	0.00	0.00
initial 1 pH 7	3/22/16	0.00	391	6.57	0	13.39	13.39	1.00	0.00	0.00
o3 1 pH 7	3/22/16	2.47	368	6.98	0	13.39	7.58	0.57	43.43	-0.57
o3us 1 pH 7	3/22/16	2.71	376	6.84	801	13.39	2.37	0.18	82.29	-1.73
initial 1	6/22/16	0.00	442	5.81	0	21.29	21.55	1.01	-1.22	0.50

initial 2	6/22/16	0.00	442	5.81	0	21.29	21.27	1.00	0.08	-0.09
initial 3	6/22/16	0.00	442	5.81	0	21.29	21.05	0.99	1.15	0.04
o3 1	6/22/16	16.00	199.8	12.86	0	21.29	3.91	0.18	81.66	-1.70
o3 2	6/22/16	16.00	199.8	12.86	0	21.29	3.10	0.15	85.44	-1.93
o3 3	6/22/16	16.00	199.8	12.86	0	21.29	2.91	0.14	86.32	-1.99

Table E2 Calibration Standards

Figure 3-4

Sample Name	Date	Standard [1,4-Dioxane] (µg/L)	1,4 Dioxane Area (m/z=88)	1,4 Dioxane-d8 Area (m/z=96)	Area <sub>m/z=88</sub> / Area <sub>m/z=96</sub>
20ppb std	11/16/15	20	45607	21885	2.08
5ppb std	11/16/15	5	15788	21976	0.72
1ppb std	11/16/15	1	2632	21857	0.12
blank	1/13/16	0	0	20290	0.00
1ppb std	11/16/15	1	2632	21857	0.12
5ppb std	1/13/16	5	8399	20293	0.41
5 ppb std	11/16/15	5	15788	21976	0.72
50ppb std	1/13/16	50	99431	19918	4.99
25ppb std	3/7/16	25	36435	15426	2.36
50ppb std	3/7/16	50	73792	14731	5.01
5ppb std	3/10/16	5	9713	12706	0.76
1ppb std	3/10/16	1	4574	14202	0.32
5ppb std	3/10/16	5	15048	19947	0.75
1ppb std	3/10/16	1	8983	18105	0.50
50ppb std	3/24/16	50	96164	18185	5.29
25ppb std	3/24/16	25	60865	23790	2.56
50ppb std	3/29/16	50	87087	14084	6.18
50ppb std	3/29/16	50	724729	137502	5.27
25ppb std	3/29/16	25	84833	35598	2.38
5ppb std	3/29/16	5	125086	207065	0.60
50ppb std	3/31/16	50	118160	21990	5.37
25ppb std	3/31/16	25	145838	58011	2.51
5ppb std	4/26/16	5	38101	69835	0.55
25ppb std	4/26/16	25	256599	93466	2.75
5ppb std	4/11/16	5	32984	54765	0.60
25ppb std	4/11/16	25	185327	67058	2.76
5ppb std	4/11/16	5	43535	64220	0.68
25ppb std	4/11/16	25	244102	85371	2.86
5ppb std	4/22/16	5	43583	64220	0.68
25ppb std	4/22/16	25	244102	85371	2.86
5ppb std	4/27/16	5	49936	86114	0.58
25ppb std	4/27/16	25	344685	122114	2.82
5ppb std	5/3/16	5	78276	123165	0.64
25ppb std	5/3/16	25	553344	206054	2.69
25ppb std	5/4/16	25	696869	225281	3.09
5ppb std	5/4/16	5	64709	104497	0.62

Table E3 Effects of Reactor Pressure

Figures 4-5, 4-29

Sample Name	Date	Pressure (PSI)	Weight %	Influent [O <sub>3</sub> ] <sub>bag</sub> (mg/L)	Affluent [O <sub>3</sub> ] <sub>bag</sub> (mg/L)	Flow Rate (mL/min)	Residence Time (min)	Ultrasound Power (W)	1,4 Dioxane Initial (ppm)	1,4 Dioxane Final (ppm)	C/C <sub>0</sub>	Reduction %	ln(C/C <sub>0</sub> )
initial	12/15/14	45		0.00		393	6.55	0	16.73	16.73	1.00	0.00	0.00
ozone us D	12/15/14	75	0.26	2.62		405	6.35	560	16.73	9.22	0.55	44.91	-0.60
ozone us C	12/15/14	45	0.37	2.64		386	6.66	622	16.73	9.42	0.56	43.67	-0.57
ozone D	12/15/14	75	0.26	2.56		386	6.66	0	16.73	9.71	0.58	41.96	-0.54
ozone C	12/15/14	45	0.43	2.72		405	6.36	0	16.73	9.69	0.58	42.08	-0.55
ultrasound	12/15/14	45		0.00		391	6.58	614	16.73	17.65	1.06	-5.51	0.05
ozone US A	3/31/16	8	0.88	2.48	0.49	405	6.36	0	22.51	5.06	0.22	77.53	-1.49
ozone A	3/31/16	8	1.14	2.46	1.69	405	6.35	0	22.51	11.69	0.52	48.08	-0.66
initial	1/8/15	15		0.00		500	5.15	0	19.31	19.31	1.00	0.00	0.00
ozone US B	1/8/15	15	0.57	2.50		500	5.15	755	19.31	7.54	0.39	60.97	-0.94
ozone B	1/8/15	15	0.57	2.50		500	5.15	0	19.31	12.25	0.63	36.56	-0.46
ozone us D	1/20/15	75	0.38	4.99		376	6.85	570	20.00	4.89	0.24	75.53	-1.41
ozone us C	1/20/15	45	0.44	4.97		383	6.73	633	20.00	4.31	0.22	78.47	-1.54
ozone us B	1/20/15	15	0.60	4.95		420	6.13	779	20.00	2.26	0.11	88.68	-2.18
ozone us A	10/21/14	8		5.51		359	7.17	709	20.35	1.54	0.08	92.41	-2.58
ozone D	1/20/15	75	0.36	4.94		400	6.43	0	20.00	6.52	0.33	67.40	-1.12
ozone C	1/20/15	45	0.40	5.07		392	6.57	0	20.00	6.43	0.32	67.87	-1.14
ozone B	1/20/15	15	0.60	4.92		382	6.73	0	20.00	6.31	0.32	68.43	-1.15
ozone A	10/21/14	8		5.51		359	7.17	0	20.00	6.10	0.30	69.52	-1.19
initial 1	3/31/16	8		0.00	0.00	440	5.85	0	18.40	17.61	0.96	4.32	-0.04
initial 2	3/31/16	8		0.00	0.00	440	5.85	0	18.40	21.37	1.16	-16.11	0.15
initial 3	3/31/16	8		0.00	0.00	440	5.85	0	18.40	16.23	0.88	11.79	-0.13
o3us 1	3/31/16	8	0.88	2.48	0.49	399	6.44	745	18.40	4.61	0.25	74.97	-1.38
o3us 2	3/31/16	8	0.88	2.48	0.49	399	6.44	745	18.40	3.70	0.20	79.88	-1.60
o3us 2	3/31/16	8	0.88	2.48	0.49	399	6.44	745	18.40	3.32	0.18	81.97	-1.71
o3 1	3/31/16	8	0.88	2.46	1.69	393	6.54		18.40	11.71	0.64	36.39	-0.45
o3 2	3/31/16	8	0.88	2.46	1.69	393	6.54		18.40	8.85	0.48	51.88	-0.73
o3 3	3/31/16	8	0.88	2.46	1.69	393	6.54		18.40	8.00	0.43	56.51	-0.83
o3 1	3/22/16	8	0.42	2.47	1.97	368	6.98		18.40	8.57	0.47	53.44	-0.76
o3us 1	3/31/16	15	0.88	4.35	0.67	372	6.91	958	18.40	1.40	0.08	92.40	-2.58
o3us 2	3/31/16	15	0.88	4.35	0.67	372	6.91	958	18.40	0.95	0.05	94.83	-2.96
o3us 3	3/31/16	15	0.88	4.35	0.67	372	6.91	958	18.40	0.84	0.05	95.43	-3.08
o3us 4	3/31/16	15	0.88	4.35	0.67	372	6.91	958	18.40	1.58	0.09	91.44	-2.46
o3 1	3/31/16	15	0.88	4.20	3.01	382	6.74		18.40	6.07	0.33	66.99	-1.11
o3 2	3/31/16	15	0.88	4.20	3.01	382	6.74		18.40	5.64	0.31	69.37	-1.18
o3us 1	3/31/16	45	0.88	6.35	2.32	415	6.19	890	18.40	2.35	0.13	87.21	-2.06
o3us 2	3/31/16	45	0.88	6.35	2.32	415	6.19	890	18.40	2.08	0.11	88.68	-2.18
o3us 3	3/31/16	45	0.88	6.35	2.32	415	6.19	890	18.40	2.43	0.13	86.80	-2.03
o3 1	3/31/16	45	0.88	6.52	4.55	427	6.03		18.40	6.24	0.34	66.09	-1.08
o3 2	3/31/16	45	0.88	6.52	4.55	427	6.03		18.40	5.85	0.32	68.20	-1.15

o3 3	3/31/16	45	0.88	6.52	4.55	427	6.03		18.40	6.44	0.35	65.02	-1.05
------	---------	----	------	------	------	-----	------	--	-------	------	------	-------	-------

Table E4 Effects of Matrix

Figures 4-20, 4-21

Sample Name	Matrix	Date	Influent [O <sub>2</sub> ] <sub>bag</sub> (mg/L)	Effluent [O <sub>2</sub> ] <sub>bag</sub> (mg/L)	Flow Rate (mL/min)	Chamber Residence Time (min)	Ultrasound Power (W)	C/C <sub>0</sub>	ln(C/C <sub>0</sub> )
initial 1	100mM HCO <sub>3</sub>	11/4/15	0.00	0.00	381	6.75	0	1.00	0.00
initial 2	100mM HCO <sub>3</sub>	1/5/16	0.00	0.00	381	6.75	0	1.00	0.00
US 1	100mM HCO <sub>3</sub>	11/4/15	0.00	0.00	391	6.57	908	1.19	0.18
US 2	100mM HCO <sub>3</sub>	1/5/16	0.00	0.00	391	6.57	908	0.83	-0.19
US 3	100mM HCO <sub>3</sub>	1/5/16	0.00	0.00	391	6.57	908	0.88	-0.13
O <sub>3</sub> 1	100mM HCO <sub>3</sub>	11/4/15	2.50	1.85	359	7.15	0	1.02	0.02
O <sub>3</sub> 2	100mM HCO <sub>3</sub>	1/5/16	2.50	1.85	359	7.15	0	0.96	-0.04
O <sub>3</sub> 3	100mM HCO <sub>3</sub>	1/5/16	2.50	1.85	359	7.15	0	1.01	0.01
O <sub>3</sub> US 1	100mM HCO <sub>3</sub>	11/4/15	2.50	0.90	382	6.73	905	1.06	0.06
O <sub>3</sub> US 2	100mM HCO <sub>3</sub>	1/5/16	2.50	0.90	382	6.73	905	1.09	0.09
O <sub>3</sub> US 3	100mM HCO <sub>3</sub>	1/5/16	2.50	0.90	382	6.73	905	1.04	0.04
Initial 1	1mM HCO <sub>3</sub>	12/28/15	0.00	0.00	379	6.79	0	1.02	0.02
Initial 2	1mM HCO <sub>3</sub>	12/28/15	0.00	0.00	379	6.79	0	0.91	-0.09
O <sub>3</sub> US 1	1mM HCO <sub>3</sub>	12/28/15	2.55	0.73	386	6.66	953	0.27	-1.30
O <sub>3</sub> US 2	1mM HCO <sub>3</sub>	12/28/15	2.55	0.73	386	6.66	953	0.21	-1.56
O <sub>3</sub> US 3	1mM HCO <sub>3</sub>	12/28/15	2.55	0.73	386	6.66	953	0.28	-1.28
O <sub>3</sub> 1	1mM HCO <sub>3</sub>	12/28/15	2.51	2.18	402	6.39	0	0.60	-0.52
O <sub>3</sub> 2	1mM HCO <sub>3</sub>	12/28/15	2.51	2.18	402	6.39	0	0.44	-0.83
O <sub>3</sub> 3	1mM HCO <sub>3</sub>	12/28/15	2.51	2.18	402	6.39	0	0.43	-0.85
US 1	1mM HCO <sub>3</sub>	12/28/15	0.00	0.00	389	6.60	916	1.03	0.03
US 2	1mM HCO <sub>3</sub>	12/28/15	0.00	0.00	389	6.60	916	0.85	-0.16
US 3	1mM HCO <sub>3</sub>	12/28/15	0.00	0.00	389	6.60	916	0.87	-0.14
Initial	10mM HCO <sub>3</sub>	12/28/15	0.00	0.00	379	6.79	0	1.06	0.06
O <sub>3</sub> 1	10mM HCO <sub>3</sub>	1/5/16	2.58	0.70	377	6.82	904	0.54	-0.61
O <sub>3</sub> 2	10mM HCO <sub>3</sub>	12/28/15	2.58	0.70	377	6.82	904	0.66	-0.42
O <sub>3</sub> 3	10mM HCO <sub>3</sub>	12/28/15	2.58	0.70	377	6.82	904	0.58	-0.55
O <sub>3</sub> 1	10mM HCO <sub>3</sub>	12/28/15	2.61	2.22	402	6.40	0	0.77	-0.26
O <sub>3</sub> 2	10mM HCO <sub>3</sub>	12/28/15	2.61	2.22	402	6.40	0	0.72	-0.33
O <sub>3</sub> 3	10mM HCO <sub>3</sub>	12/28/15	2.61	2.22	402	6.40	0	0.75	-0.29
US 1	10mM HCO <sub>3</sub>	12/28/15	0.00	0.00	0	0.00	1034	1.05	0.05
US 2	10mM HCO <sub>3</sub>	12/28/15	0.00	0.00	0	0.00	1034	0.89	-0.12
US 3	10mM HCO <sub>3</sub>	12/28/15	0.00	0.00	0	0.00	1034	0.87	-0.14
initial 1	deionized	4/22/16	0.00	0.00	407	6.31	0	0.95	-0.06
initial 2	deionized	4/22/16	0.00	0.00	407	6.31	0	1.07	0.07

initial 3	deionized	4/22/16	0.00	0.00	407	6.31	0	0.98	-0.02
US A1	deionized	4/22/16	0.00	0.00	379	6.78	941	0.88	-0.13
US A2	deionized	4/22/16	0.00	0.00	379	6.78	941	0.83	-0.18
US A3	deionized	4/22/16	0.00	0.00	379	6.78	941	0.78	-0.25
US B1	deionized	4/22/16	0.00	0.00	515	4.99	883	0.84	-0.17
US B2	deionized	4/22/16	0.00	0.00	515	4.99	883	0.91	-0.09
US B3	deionized	4/22/16	0.00	0.00	515	4.99	883	0.88	-0.12
O <sub>3</sub> bypass A1	deionized	4/22/16	2.57	n/a	476	5.40	0	0.92	-0.08
O <sub>3</sub> bypass A2	deionized	4/22/16	2.57	n/a	476	5.40	0	0.91	-0.10
O <sub>3</sub> bypass A3	deionized	4/22/16	2.57	n/a	476	5.40	0	0.77	-0.27
O <sub>3</sub> A1	deionized	4/22/16	2.57	2.45	476	5.40	0	0.86	-0.15
O <sub>3</sub> A2	deionized	4/22/16	2.57	2.45	476	5.40	0	0.79	-0.24
O <sub>3</sub> A3	deionized	4/22/16	2.57	2.45	476	5.40	0	0.83	-0.18
O <sub>3</sub> US A1	deionized	4/22/16	2.61	1.13	471	5.46	761	0.10	-2.32
O <sub>3</sub> US A2	deionized	4/22/16	2.61	1.13	471	5.46	761	0.10	-2.35
O <sub>3</sub> US A3	deionized	4/22/16	2.61	1.13	471	5.46	761	0.08	-2.53
O <sub>3</sub> bypass B1	deionized	4/22/16	2.58	n/a	393	6.54	0	0.84	-0.18
O <sub>3</sub> bypass B2	deionized	4/22/16	2.58	n/a	393	6.54	0	0.81	-0.21
O <sub>3</sub> bypass B3	deionized	4/22/16	2.58	n/a	393	6.54	0	0.84	-0.17
O <sub>3</sub> B1	deionized	4/22/16	2.55	2.52	402	6.40	0	0.72	-0.33
O <sub>3</sub> B2	deionized	4/22/16	2.55	2.52	402	6.40	0	0.67	-0.40
O <sub>3</sub> B3	deionized	4/22/16	2.55	2.52	402	6.40	0	0.76	-0.28
O <sub>3</sub> US B1	deionized	4/22/16	2.53	1.00	383	6.71	791	0.09	-2.42
O <sub>3</sub> US B2	deionized	4/22/16	2.53	1.00	383	6.71	791	0.09	-2.44
O <sub>3</sub> US B3	deionized	4/22/16	2.53	1.00	383	6.71	791	0.09	-2.44
O <sub>3</sub> C1	deionized	4/27/16	2.55	2.01	557	4.61	0	0.41	-0.89
O <sub>3</sub> C2	deionized	4/27/16	2.55	2.01	557	4.61	0	0.39	-0.94
O <sub>3</sub> C3	deionized	4/27/16	2.55	2.01	557	4.61	0	0.40	-0.91
O <sub>3</sub> US C1	deionized	4/27/16	2.55	1.04	556	4.62	791	0.05	-2.90
O <sub>3</sub> US C2	deionized	4/27/16	2.55	1.04	556	4.62	791	0.05	-2.92
O <sub>3</sub> US C3	deionized	4/27/16	2.55	1.04	556	4.62	791	0.05	-2.96

Table E5 Ozone Concentration and Partial Pressure

Figure 4-9, 4-29

[O <sub>3</sub> ] <sub>aq</sub> (mg/L)	[O <sub>3</sub> ] <sub>aq</sub> (M)	Partial Pressure (atm)
0	0	0
1	2.08333E-05	0.00213
2.5	5.20833E-05	0.006

2.457	5.11875E-05	0.005866667
4.204	8.75833E-05	0.008661089
5	0.000104167	0.007333333
8	0.000166667	0.010826361
15	0.0003125	0.025297477

Table E6 Effects of Mixing Zone

Figures 4-3, 4-4

Sample Name	Date	[O <sub>3</sub> ] <sub>avg</sub> (mg/L)	Flow Rate (mL/min)	Chamber Residence Time (min)	Amplitude (W)	1,4 Dioxane Initial (ppm)	1,4 Dioxane Final (ppm)	C/C <sub>0</sub>	Reduction %	ln(C/C <sub>0</sub> )
initial 1	4/11/16	0	352	7.30114		12.295	13.1196	1.067028	-6.7	0.06488
initial 2	4/11/16	0	352	7.30114		12.295	12.5384	1.01976	-1.98	0.01957
initial 3	4/11/16	0	352	7.30114		12.295	11.7178	0.953018	4.7	-0.04812
initial 4	4/11/16	0	352	7.30114		12.295	12.2776	0.998546	0.15	-0.00145
initial 5	4/11/16	0	352	7.30114		12.295	11.8239	0.961648	3.84	-0.03911
o3 <sub>bypass</sub> no mix 1	4/11/16	2.498	323	0.27245		12.295	10.6965	0.869952	13	-0.13932
o3 <sub>bypass</sub> no mix 2	4/11/16	2.498	323	0.27245		12.295	10.6573	0.866766	13.3	-0.14299
o3 <sub>bypass</sub> no mix 3	4/11/16	2.498	323	0.27245		12.295	11.6424	0.946885	5.31	-0.05458
o3 no mix 1	4/11/16	2.483231	323	7.95666		12.295	5.36497	0.436337	56.4	-0.82934
o3 no mix 2	4/11/16	2.483231	323	7.95666		12.295	6.30843	0.51307	48.7	-0.66734
o3 no mix 3	4/11/16	2.483231	323	7.95666		12.295	5.5117	0.448271	55.2	-0.80236
o3 <sub>bypass</sub> mix 1	4/11/16	2.4358	336	0.2619		12.295	10.9725	0.892406	10.8	-0.11383
o3 <sub>bypass</sub> mix 2	4/11/16	2.4358	336	0.2619		12.295	10.3737	0.843703	15.6	-0.16995
o3 <sub>bypass</sub> mix 3	4/11/16	2.4358	336	0.2619		12.295	10.4409	0.849171	15.1	-0.1635
o3 mix 1	4/11/16	2.4665	336	7.64881		12.295	6.12041	0.497778	50.2	-0.6976
o3 mix 2	4/11/16	2.4665	336	7.64881		12.295	6.03515	0.490844	50.9	-0.71163
o3 mix 3	4/11/16	2.4665	336	7.64881		12.295	6.29526	0.511999	48.8	-0.66943
initial DI 1	4/22/16	0	407	6.3145		17.892	16.9268	0.946064	5.39	-0.05545
initial DI 2	4/22/16	0	407	6.3145		17.892	19.126	1.068979	-6.9	0.06670
initial DI 3	4/22/16	0	407	6.3145		17.892	17.6227	0.984957	1.5	-0.01516
us DI A1	4/22/16	0	379	6.781	941	17.892	15.7601	0.880853	11.9	-0.12686
us DI A2	4/22/16	0	379	6.781	941	17.892	14.9271	0.834299	16.6	-0.18116
us DI A3	4/22/16	0	379	6.781	941	17.892	13.9638	0.780459	22	-0.24787
us DI B1	4/22/16	0	515	4.99029	883	17.892	15.0503	0.841182	15.9	-0.17295
us DI B2	4/22/16	0	515	4.99029	883	17.892	16.2864	0.910269	8.97	-0.09402
us DI B3	4/22/16	0	515	4.99029	883	17.892	15.7973	0.882935	11.7	-0.1245
o3 <sub>bypass</sub> DI A1	4/22/16	2.574	476.3	0.18474		17.892	16.5442	0.92468	7.53	-0.07831
o3 <sub>bypass</sub> DI A2	4/22/16	2.574	476.3	0.18474		17.892	16.238	0.907566	9.24	-0.09699
o3 <sub>bypass</sub> DI A3	4/22/16	2.574	476.3	0.18474		17.892	13.7132	0.766454	23.4	-0.26598
o3 DI A1	4/22/16	2.568375	476.3	5.39538		17.892	15.4246	0.862106	13.8	-0.14838
o3 DI A2	4/22/16	2.568375	476.3	5.39538		17.892	14.0868	0.78733	21.3	-0.23911
o3 DI A3	4/22/16	2.568375	476.3	5.39538		17.892	14.9084	0.833253	16.7	-0.18242
o3 <sub>us</sub> DI A1	4/22/16	2.60825	470.5	5.46227	761	17.892	1.75069	0.097849	90.2	-2.32433
o3 <sub>us</sub> DI A2	4/22/16	2.60825	470.5	5.46227	761	17.892	1.70826	0.095477	90.5	-2.34887
o3 <sub>us</sub> DI A3	4/22/16	2.60825	470.5	5.46227	761	17.892	1.42539	0.079667	92	-2.5299
o3 <sub>bypass</sub> DI B1	4/22/16	2.577	393	0.22392		17.892	15.0005	0.838403	16.2	-0.17626
o3 <sub>bypass</sub> DI B2	4/22/16	2.577	393	0.22392		17.892	14.5169	0.811369	18.9	-0.20903
o3 <sub>bypass</sub> DI B3	4/22/16	2.577	393	0.22392		17.892	15.0985	0.843879	15.6	-0.16975

o3 DI B1	4/22/16	2.548385	401.5	6.401		17.892	12.8461	0.717987	28.2	-0.3313
o3 DI B1	4/22/16	2.548385	401.5	6.401		17.892	12.0335	0.672571	32.7	-0.39665
o3 DI B1	4/22/16	2.548385	401.5	6.401		17.892	13.5116	0.755184	24.5	-0.28079
o3us DI B1	4/22/16	2.529545	383	6.71018	791	17.892	1.59844	0.089339	91.1	-2.41532
o3us DI B2	4/22/16	2.529545	383	6.71018	791	17.892	1.56114	0.087255	91.3	-2.43893
o3us DI B3	4/22/16	2.529545	383	6.71018	791	17.892	1.56595	0.087523	91.2	-2.43585

Table E7 Effect of pH

Figures 4-12, 4-13, 4-14, 4-15

Sample Name	Date	[O <sub>3</sub> ] <sub>inlet</sub> (mg/L)	Flow Rate (ml/min)	Chamber Residence Time (min)	Amplitude (W)	1,4 Dioxane Initial (ppm)	1,4 Dioxane Final (ppm)	C/C <sub>0</sub>	Reduction %	ln(C/C <sub>0</sub> )
initial 1 pH 10	3/22/16	0.00	330	7.79		17.39	17.78	1.02	-2.25	0.02
initial 2 pH 10	3/22/16	0.00	330	7.79		17.39	17.00	0.98	2.25	-0.02
o3us a1 pH 10	3/22/16	2.56	317	8.11	817	17.39	5.12	0.29	70.55	-1.22
o3us a2 pH 10	3/22/16	2.56	317	8.11	817	17.39	3.90	0.22	77.55	-1.49
o3us a3 pH 10	3/22/16	2.56	317	8.11	817	17.39	2.88	0.17	83.43	-1.80
o3 a1 pH 10	3/22/16	2.50	330	7.79		17.39	4.31	0.25	75.22	-1.40
o3 a2 pH 10	3/22/16	2.50	330	7.79		17.39	4.68	0.27	73.10	-1.31
o3 a3 pH 10	3/22/16	2.50	330	7.79		17.39	4.73	0.27	72.81	-1.30
o3us b1 pH 10	3/22/16	2.48	664.5	3.87	852	17.39	4.66	0.27	73.22	-1.32
o3us b2 pH 10	3/22/16	2.48	664.5	3.87	852	17.39	5.44	0.31	68.72	-1.16
o3us b3 pH 10	3/22/16	2.48	664.5	3.87	852	17.39	4.82	0.28	72.27	-1.28
o3 b1 pH 10	3/22/16	2.45	528	4.87		17.39	6.63	0.38	61.85	-0.96
o3 b2 pH 10	3/22/16	2.45	528	4.87		17.39	6.17	0.35	64.51	-1.04
o3 b3 pH 10	3/22/16	2.45	528	4.87		17.39	6.76	0.39	61.14	-0.95
us a 1 pH 10	3/22/16	0.00	373	6.89	1078	17.39	16.66	0.96	4.23	-0.04
us a 2 pH 10	3/22/16	0.00	373	6.89	1078	17.39	17.13	0.98	1.51	-0.02
us b 1 pH 10	3/22/16	0.00	577	4.45	996	17.39	17.32	1.00	0.43	0.00
us b 2 pH 10	3/22/16	0.00	577	4.45	996	17.39	18.14	1.04	-4.29	0.04
initial 1 pH 7	3/22/16	0.00	391	6.57		13.39	13.39	1.00	0.00	0.00
o3 1 pH 7	3/22/16	2.47	368	6.98		13.39	7.58	0.57	43.43	-0.57
o3us 1 pH 7	3/22/16	2.71	376	6.84	800	13.39	2.37	0.18	82.29	-1.73
initial 1 pH 10	3/24/16	0.00	853	3.01		17.42	17.42	1.00	0.00	0.00
o3us 1 pH 10	3/24/16	3.06	723.5	3.55	834	17.42	4.65	0.27	73.30	-1.32
o3us 2 pH 10	3/24/16	3.06	723.5	3.55	834	17.42	4.56	0.26	73.83	-1.34
o3us 3 pH 10	3/24/16	3.06	723.5	3.55	834	17.42	4.54	0.26	73.96	-1.35
o3 1 pH 10	3/24/16	2.69	853	3.01		17.42	7.07	0.41	59.41	-0.90
o3 2 pH 10	3/24/16	2.69	853	3.01		17.42	7.88	0.45	54.78	-0.79
o3 3 pH 10	3/24/16	2.69	853	3.01		17.42	6.58	0.38	62.21	-0.97
o3 bypass 1 pH 10	3/24/16	2.82	853	0.10		17.42	15.65	0.90	10.16	-0.11
o3 bypass 2 pH 10	3/24/16	2.82	853	0.10		17.42	14.81	0.85	14.96	-0.16
o3 bypass 3 pH 10	3/24/16	2.82	853	0.10		17.42	14.45	0.83	17.05	-0.19
initial ph4 1	3/29/16	0.00	406	6.33		15.82	16.18	1.02	-2.29	0.02
initial ph4 2	3/29/16	0.00	406	6.33		15.82	17.12	1.08	-8.25	0.08
initial ph4 3	3/29/16	0.00	406	6.33		15.82	15.26	0.96	3.52	-0.04
us ph4 a1	3/29/16	0.00	417	6.16	978	15.82	12.85	0.81	18.78	-0.21
us ph4 a2	3/29/16	0.00	417	6.16	978	15.82	16.79	1.06	-6.12	0.06

us ph4 c1	3/29/16	0.00	752	3.42	1120	15.82	16.70	1.06	-5.56	0.05
us ph4 c2	3/29/16	0.00	752	3.42	1120	15.82	14.44	0.91	8.69	-0.09
o3 bypass ph4 c1	3/29/16	2.59	445.3	0.20		15.82	13.69	0.87	13.44	-0.14
o3 bypass ph4 c2	3/29/16	2.59	445.3	0.20		15.82	15.21	0.96	3.83	-0.04
o3 ph4 c1	3/29/16	2.59	445.3	5.77		15.82	12.61	0.80	20.29	-0.23
o3 ph4 c2	3/29/16	2.59	445.3	5.77		15.82	14.02	0.89	11.36	-0.12
o3 ph4 c3	3/29/16	2.59	445.3	5.77		15.82	13.29	0.84	15.98	-0.17
o3us ph4 c1	3/29/16	2.60	448	5.74	894	15.82	5.33	0.34	66.30	-1.09
o3us ph4 c2	3/29/16	2.60	448	5.74	894	15.82	5.62	0.36	64.50	-1.04
o3us ph4 c3	3/29/16	2.60	448	5.74	894	15.82	7.78	0.49	50.79	-0.71
o3 ph4 b1	3/29/16	2.60	563	4.56		15.82	15.97	1.01	-0.95	0.01
o3 ph4 b2	3/29/16	2.60	563	4.56		15.82	13.43	0.85	15.12	-0.16
o3 ph4 b3	3/29/16	2.60	563	4.56		15.82	13.47	0.85	14.82	-0.16
o3us ph4 b1	3/29/16	2.59	568	4.52	862	15.82	7.36	0.47	53.48	-0.77
o3us ph4 b2	3/29/16	2.59	568	4.52	862	15.82	6.41	0.41	59.46	-0.90
o3us ph4 b3	3/29/16	2.59	568	4.52	862	15.82	6.85	0.43	56.72	-0.84
o3 ph4 a1	3/29/16	2.51	821	3.13		15.82	14.35	0.91	9.28	-0.10
o3 ph4 a2	3/29/16	2.51	821	3.13		15.82	15.19	0.96	3.98	-0.04
o3 ph4 a3	3/29/16	2.51	821	3.13		15.82	14.51	0.92	8.30	-0.09
o3us ph4 a1	3/29/16	2.42	775	3.32	880	15.82	8.09	0.51	48.83	-0.67
o3us ph4 a2	3/29/16	2.42	775	3.32	880	15.82	8.21	0.52	48.09	-0.66
o3us ph4 a3	3/29/16	2.42	775	3.32	880	15.82	7.46	0.47	52.87	-0.75

Table E8 Pressure/Flow/Ozone Concentration Data

Figures 4-5, 4-21, 4-29

Sample Name	Date	[O <sub>3</sub> ] <sub>inlet</sub> (mg/L)	[O <sub>3</sub> ] <sub>outlet</sub> (mg/L)	[O <sub>3</sub> ] <sub>inlet</sub> (Ng/m <sup>3</sup> )	[O <sub>3</sub> ] <sub>outlet</sub> (Ng/m <sup>3</sup> )	Flow Rate (mL/min)	Chamber Residence Time (min)	[1,4 Dioxane] Initial (µg/L)	[1,4 Dioxane] Final (µg/L)	C/C <sub>0</sub>
initial 2	4/27/2016	0.00	0.00	0.00	0.00	442	5.81	12.5	12.7	1.02
initial 3	4/27/2016	0.00	0.00	0.00	0.00	442	5.81	12.5	12.3	0.98
o3us 8psi 1	4/27/2016	2.56	0.68	5.87	5.55	420	6.13	12.5	2.2	0.18
o3us 8psi 2	4/27/2016	2.56	0.68	5.87	5.55	420	6.13	12.5	2.4	0.19
o3us 8psi 3	4/27/2016	2.56	0.68	5.87	5.55	420	6.13	12.5	2.0	0.16
o3 8psi 1	4/27/2016	2.55	1.93	6.30	6.60	409	6.28	12.5	5.0	0.40
o3 8psi 2	4/27/2016	2.55	1.93	6.30	6.60	409	6.28	12.5	5.3	0.43
o3 8psi 3	4/27/2016	2.55	1.93	6.30	6.60	409	6.28	12.5	4.7	0.37
o3us 15psi 1	4/27/2016	4.00	0.98	6.03	4.15	400	6.43	12.5	1.1	0.09
o3us 15psi 2	4/27/2016	4.00	0.98	6.03	4.15	400	6.43	12.5	1.6	0.13
o3us 15psi 3	4/27/2016	4.00	0.98	6.03	4.15	400	6.43	12.5	1.5	0.12
o3 15psi 1	4/27/2016	3.57	2.68	6.08	6.03	375	6.85	12.5	4.0	0.32
o3 15psi 2	4/27/2016	3.57	2.68	6.08	6.03	375	6.85	12.5	4.8	0.39
o3 15psi 3	4/27/2016	3.57	2.68	6.08	6.03	375	6.85	12.5	4.5	0.36
o3us 45psi 1	4/27/2016	6.43	2.19	6.55	4.00	405	6.35	12.5	1.2	0.09
o3us 45psi 2	4/27/2016	6.43	2.19	6.55	4.00	405	6.35	12.5	1.8	0.14
o3us 45psi 3	4/27/2016	6.43	2.19	6.55	4.00	405	6.35	12.5	1.5	0.12
o3 45psi 1	4/27/2016	6.25	4.01	6.55	5.00	388	6.62	12.5	3.9	0.31
o3 45psi 2	4/27/2016	6.25	4.01	6.55	5.00	388	6.62	12.5	4.3	0.34

o3 45psi 3	4/27/2016	6.25	4.01	6.55	5.00	388	6.62	12.5	3.5	0.28
initial 1	3/31/2016	0.00	0.00	0.00	0.00	440	5.84	20.0	21.1	1.06
initial 2	3/31/2016	0.00	0.00	0.00	0.00	440	5.84	20.0	26.4	1.32
initial 3	3/31/2016	0.00	0.00	0.00	0.00	440	5.84	20.0	15.9	0.80
initial 4	3/31/2016	0.00	0.00	0.00	0.00	440	5.84	20.0	16.5	0.82
o3us 8psi 1	3/31/2016	2.47	0.49	10.47	4.43	396	6.44	20.0	4.6	0.23
o3us 8psi 2	3/31/2016	2.47	0.49	10.47	4.43	396	6.44	20.0	3.7	0.19
o3us 8psi 3	3/31/2016	2.47	0.49	10.47	4.43	396	6.44	20.0	3.3	0.17
o3 8psi 1	3/31/2016	2.47	1.69	10.47	4.90	396	6.54	20.0	11.7	0.59
o3 8psi 2	3/31/2016	2.47	1.69	10.47	4.90	396	6.54	20.0	8.9	0.44
o3 8psi 3	3/31/2016	2.47	1.69	10.47	4.90	396	6.54	20.0	8.0	0.40
o3 1 pH 7	4/10/2016	2.47	1.97	6.95	10.93	368	6.98	16.3	8.6	0.52
o3us 15psi 1	3/31/2016	4.27	0.67	9.73	4.55	377	6.91	20.0	1.4	0.07
o3us 15psi 2	3/31/2016	4.27	0.67	9.73	4.55	377	6.91	20.0	1.0	0.05
o3us 15psi 3	3/31/2016	4.27	0.67	9.73	4.55	377	6.91	20.0	0.8	0.04
o3us 15psi 4	3/31/2016	4.27	0.67	9.73	4.55	377	6.91	20.0	1.6	0.08
o3 15psi 1	3/31/2016	4.27	3.01	9.73	6.14	377	6.74	20.0	6.1	0.30
o3 15psi 2	3/31/2016	4.27	3.01	9.73	6.14	377	6.74	20.0	5.6	0.28
o3us 45psi 2	3/31/2016	6.43	2.32	10.60	3.23	421	6.19	20.0	2.4	0.12
o3us 45psi 3	3/31/2016	6.43	2.32	10.60	3.23	421	6.19	20.0	2.1	0.10
o3us 45psi 4	3/31/2016	6.43	2.32	10.60	3.23	421	6.19	20.0	2.4	0.12
o3 45psi 1	3/31/2016	6.43	4.55	10.60	5.13	421	6.03	20.0	6.2	0.31
o3 45psi 2	3/31/2016	6.43	4.55	10.60	5.13	421	6.03	20.0	5.9	0.29
initial DI 1	4/22/2016	0.00	0.00	0.00	0.00	407	6.31	17.9	16.9	0.95
initial DI 2	4/22/2016	0.00	0.00	0.00	0.00	407	6.31	17.9	19.1	1.07
initial DI 3	4/22/2016	0.00	0.00	0.00	0.00	407	6.31	17.9	17.6	0.98
us DI a1	4/22/2016	0.00	0.00	0.00	0.00	379	6.78	17.9	15.8	0.88
us DI a2	4/22/2016	0.00	0.00	0.00	0.00	379	6.78	17.9	14.9	0.83
us DI a3	4/22/2016	0.00	0.00	0.00	0.00	379	6.78	17.9	14.0	0.78
us DI b1	4/22/2016	0.00	0.00	0.00	0.00	515	4.99	17.9	15.1	0.84
us DI b2	4/22/2016	0.00	0.00	0.00	0.00	515	4.99	17.9	16.3	0.91
us DI b3	4/22/2016	0.00	0.00	0.00	0.00	515	4.99	17.9	15.8	0.88
o3 bypass DI a1	4/22/2016	2.57	n/a	8.70	7.00	476	5.40	17.9	16.5	0.92
o3 bypass DI a2	4/22/2016	2.57	n/a	8.70	7.00	476	5.40	17.9	16.2	0.91
o3 bypass DI a3	4/22/2016	2.57	n/a	8.70	7.00	476	5.40	17.9	13.7	0.77
o3 DI a1	4/22/2016	2.57	2.45	5.33	5.70	476	5.40	17.9	15.4	0.86
o3 DI a2	4/22/2016	2.57	2.45	5.33	5.70	476	5.40	17.9	14.1	0.79
o3 DI a3	4/22/2016	2.57	2.45	5.33	5.70	476	5.40	17.9	14.9	0.83
o3us DI a1	4/22/2016	2.61	1.13	8.06	5.70	471	5.46	17.9	1.8	0.10
o3us DI a2	4/22/2016	2.61	1.13	8.06	5.70	471	5.46	17.9	1.7	0.10
o3us DI a3	4/22/2016	2.61	1.13	8.06	5.70	471	5.46	17.9	1.4	0.08
o3 bypass DI b1	4/22/2016	2.58	n/a	8.37	6.60	393	0.22	17.9	15.0	0.84
o3 bypass DI b2	4/22/2016	2.58	n/a	8.37	6.60	393	0.22	17.9	14.5	0.81
o3 bypass DI b3	4/22/2016	2.58	n/a	8.37	6.60	393	0.22	17.9	15.1	0.84
o3 DI b1	4/22/2016	2.55	2.52	8.43	6.97	402	6.40	17.9	12.8	0.72
o3 DI b2	4/22/2016	2.55	2.52	8.43	6.97	402	6.40	17.9	12.0	0.67
o3 DI b3	4/22/2016	2.55	2.52	8.43	6.97	402	6.40	17.9	13.5	0.76
o3us DI b1	4/22/2016	2.53	1.00	8.44	5.73	383	6.71	17.9	1.6	0.09
o3us DI b2	4/22/2016	2.53	1.00	8.44	5.73	383	6.71	17.9	1.6	0.09
o3us DI b3	4/22/2016	2.53	1.00	8.44	5.73	383	6.71	17.9	1.6	0.09
o3 DI c1	4/27/2016	2.55	2.01	6.50	5.70	557	4.61	n/a	n/a	n/a

o3 DI c2	4/27/2016	2.55	2.01	6.50	5.70	557	4.61	n/a	n/a	n/a
o3 DI c3	4/27/2016	2.55	2.01	6.50	5.70	557	4.61	n/a	n/a	n/a
o3us DI c1	4/27/2016	2.55	1.04	6.30	4.70	556	4.62	17.9	1.0	0.05
o3us DI c2	4/27/2016	2.55	1.04	6.30	4.70	556	4.62	17.9	1.0	0.05
o3us DI c3	4/27/2016	2.55	1.04	6.30	4.70	556	4.62	17.9	0.9	0.05

Table E9 AOP Comparison Data

Figures 4-5, 4-21, 4-29

Sample Name	Date	[O <sub>3</sub> ] <sub>inlet</sub> (mg/L)	[O <sub>3</sub> ] <sub>inlet</sub> effluent (mg/L)	Ultrasonic Power (W)	UV (mW/cm <sup>2</sup> )	UV (mJ/cm <sup>2</sup> )	H <sub>2</sub> O <sub>2</sub> flow (ml/min)	H <sub>2</sub> O <sub>2</sub> (ppm)	Flow Rate (mL/min)	Chamber Residence Time (min)	[1,4 Dioxane] Initial (µg/L)	[1,4 Dioxane] Final (µg/L)	C/C <sub>0</sub>
Initial	8/25/2015	0.00	0.00	0	0.00	0.00	0.00	0.00	446	4.04	18.30	18.30	1.00
UV	8/25/2015	0.00	0.00	0	11.26	2841.31	0.00	0.00	428	4.21	18.30	12.88	0.70
UV+H <sub>2</sub> O <sub>2</sub>	8/25/2015	0.00	0.00	0	11.26	2745.72	3.50	8.02	443	4.06	18.30	1.09	0.06
H <sub>2</sub> O <sub>2</sub>	8/25/2015	0.00	0.00	0	0.00	0.00	3.50	8.14	436	4.13	18.30	14.96	0.82
O <sub>3</sub> +UV+H <sub>2</sub> O <sub>2</sub>	8/25/2015	2.42	0.30	0	11.26	2745.10	3.50	8.01	443	4.06	18.30	1.09	0.06
O <sub>3</sub> +US+H <sub>2</sub> O <sub>2</sub>	8/25/2015	2.94	0.11	867	0.00	0.00	3.50	7.52	472	5.44	18.30	1.21	0.07
CBD initial	8/28/2015	0.00	0.00	0	0.00	0.00	0.00	0.00	n/a	0.00	10.01	10.01	1.00
CBD+UV+H <sub>2</sub> O <sub>2</sub>	8/28/2015	0.00	0.00	0	n/a	1700.00	0.00	10.00	n/a	7.68	10.01	8.78	0.88
CBD initial	9/9/2015	0.00	0.00	0	0.00	0.00	0.00	0.00	n/a	0.00	19.99	19.99	1.00
CBD UV+H <sub>2</sub> O <sub>2</sub>	9/9/2015	0.00	0.00	0	n/a	1000.00	0.00	10.00	n/a	14.20	19.99	19.66	0.98
initial	9/11/2015	0.00	0.00	0	0.00	0.00	0.00	0.00	1039	1.73	14.90	14.90	1.00
o3 us h2o2	9/11/2015	2.97	0.47	800	0.00	0.00	2.93	11.92	737	3.49	14.90	3.97	0.27
o3 uv h2o2	9/11/2015	1.92	0.11	0	11.26	1618.85	2.93	11.70	751	2.40	14.90	3.24	0.22
uv h2o2	9/11/2015	0.00	0.00	0	11.26	1182.27	3.88	11.32	1029	1.75	14.90	3.51	0.24
uv o3	9/11/2015	1.70	0.11	0	11.26	1376.90	0.00	0.00	883	2.04	14.90	3.38	0.23
init new is	9/11/2015	0.00	0.00	0	0.00	0.00	0.00	0.00	1039	1.73	14.90	14.90	1.00
o3 h2o2 new is	9/11/2015	3.01	0.09	0	0.00	0.00	2.93	11.61	757	2.38	14.90	1.52	0.10
h2o2 new is	9/11/2015	0.00	0.00	0	0.00	0.00	3.88	11.10	1049	2.45	14.90	12.82	0.86
uv new is	9/11/2015	0.00	0.00	0	11.26	1141.22	0.00	0.00	1066	1.69	14.90	12.31	0.83
CBD initial	9/15/2015	0.00	0.00	0	0.00	0.00	0.00	0.00	0	0.00	20.00	20.00	1.00
CBD+H <sub>2</sub> O <sub>2</sub>	9/15/2015	0.00	0.00	0	n/a	1000.00	0.00	10.00	181	14.20	20.00	0.10	0.01
CBD+H <sub>2</sub> O <sub>2</sub>	9/15/2015	0.00	0.00	0	n/a	1000.00	0.00	10.00	181	14.20	20.00	1.24	0.06
CBD+H <sub>2</sub> O <sub>2</sub>	9/15/2015	0.00	0.00	0	n/a	3500.00	0.00	10.00	52	49.60	20.00	0.10	0.01
CBD+H <sub>2</sub> O <sub>2</sub> foil	9/16/2015	0.00	0.00	0	n/a	100.00	0.00	10.00	1810	1.42	20.00	4.18	0.21
CBD+H <sub>2</sub> O <sub>2</sub>	9/16/2015	0.00	0.00	0	n/a	100.00	0.00	10.00	1810	1.42	20.00	15.33	0.77
CBD+H <sub>2</sub> O <sub>2</sub> foil	9/16/2015	0.00	0.00	0	n/a	500.00	0.00	10.00	363	7.08	20.00	2.92	0.15
CBD+H <sub>2</sub> O <sub>2</sub>	9/16/2015	0.00	0.00	0	n/a	500.00	0.00	10.00	363	7.08	20.00	7.97	0.40
CBD+H <sub>2</sub> O <sub>2</sub>	9/17/2015	0.00	0.00	0	n/a	200.00	0.00	10.00	907	2.83	20.00	9.05	0.45

Table E10 Mass Balance Analysis

Figures 4-33

Treatment	Pressure (PSI)	Theoretical O <sub>3</sub> Transfer Rate (mg/min)	Mean ln(C/C <sub>0</sub> )	Aqueous O <sub>3</sub> Consumption Rate (mg/min)	1,4-Dioxane Removal Rate (µg/min)	Predicted Dioxane Removal Rate (µg/min)	Lower Confidence Limit	Upper Confidence Limit
o3 (none)	8	0.00	0.00	0.00	0.00	0.24	0.16	0.32
o3 (none)	15	0.00	0.00	0.00	0.00	0.24	0.16	0.32
o3 (none)	45	0.00	0.00	0.00	0.00	0.24	0.16	0.32
o3us	8	-0.19	-2.36	2.15	2.38	2.19	2.14	2.24
o3	8	0.00	-1.01	1.65	1.64	1.73	1.68	1.79
o3us	8	0.09	-0.87	3.67	3.72	3.57	3.53	3.61
o3	8	0.00	-0.41	2.15	2.18	2.19	2.14	2.24
o3us	8	-0.35	-3.82	2.27	2.64	2.30	2.25	2.35
o3	8	0.00	-1.54	2.16	2.11	2.20	2.15	2.25
o3us	8	0.46	-1.72	5.45	5.12	5.19	5.14	5.24
o3	8	0.00	-0.87	3.84	3.73	3.72	3.68	3.76
o3us	8	0.12	-0.63	4.18	4.29	4.04	3.99	4.08
o3	8	0.00	-0.16	1.50	1.35	1.60	1.54	1.66
o3us	15	0.70	-0.79	5.51	4.72	5.25	5.19	5.30
o3	15	0.00	-0.24	2.00	1.99	2.05	2.00	2.10
o3us	8	0.49	-1.65	6.62	6.50	6.25	6.18	6.32
o3	8	0.00	-0.73	3.25	4.16	3.19	3.15	3.23
o3us	15	0.78	-2.85	7.69	7.07	7.23	7.14	7.31
o3	15	0.00	-1.23	5.30	5.45	5.05	5.00	5.11
o3us	45	1.00	-1.92	8.31	7.43	7.78	7.69	7.88
o3	45	0.00	-1.20	5.86	6.01	5.56	5.50	5.62
o3us	8	0.33	-1.80	4.75	4.56	4.55	4.51	4.60
o3	8	0.00	-0.97	3.26	3.30	3.20	3.16	3.24
o3us	15	0.92	-2.21	5.38	4.61	5.12	5.07	5.17
o3	15	0.00	-1.06	3.20	3.19	3.14	3.10	3.18
o3us	45	0.50	-2.11	5.22	4.62	4.98	4.93	5.03
o3	45	0.00	-1.24	3.83	3.57	3.72	3.67	3.76
o3	8	0.00	-1.88	3.60	3.68	3.51	3.47	3.55

Statistical Analysis

<b>slope</b>	0.908382	0.237206063	<b>intercept</b>	<b>n</b>	28
<b>SE slope</b>	0.028539	0.121331125	<b>SE intercept</b>	<b>Xm</b>	3.67148
<b>RSQ</b>	0.974979	0.323713848	<b>SE y</b>	<b>SSxx</b>	128.6629
<b>F</b>	1013.136	26	<b>d.o.f.</b>	<b>t95</b>	2.055529
<b>SS reg</b>	106.1672	2.724557036	<b>SSres</b>	<b>SE</b>	0.104791

## APPENDIX F

### RAW DATA FROM ARDUINO DATA COLLECTION DEVICE

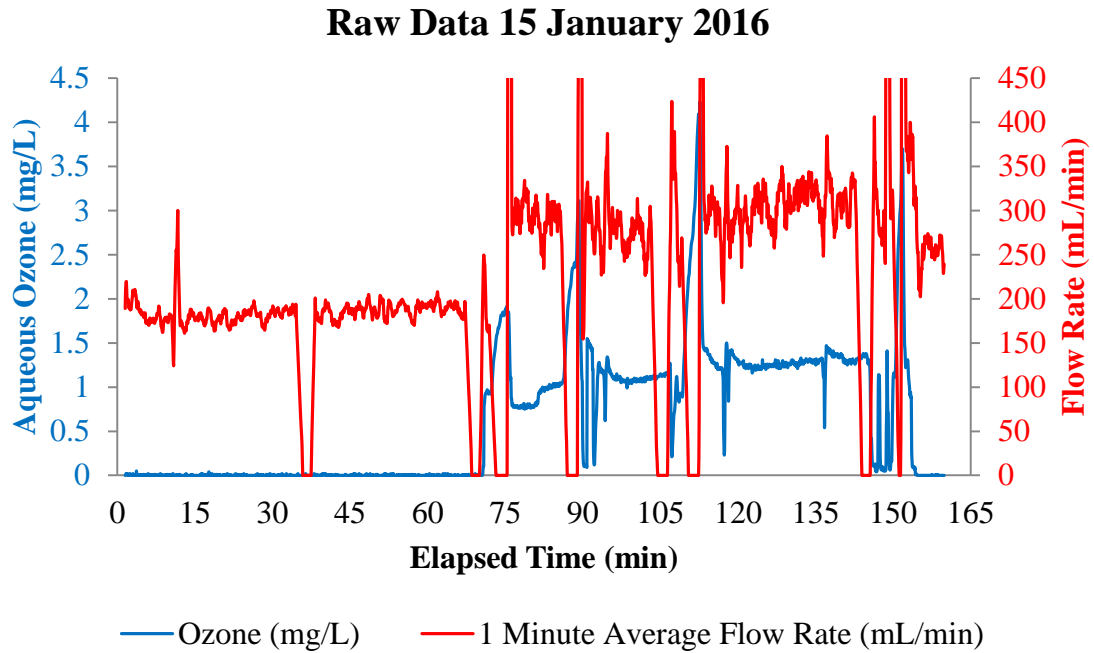


*Figure F1 Ozone and Flow Rate Data from January 2016*

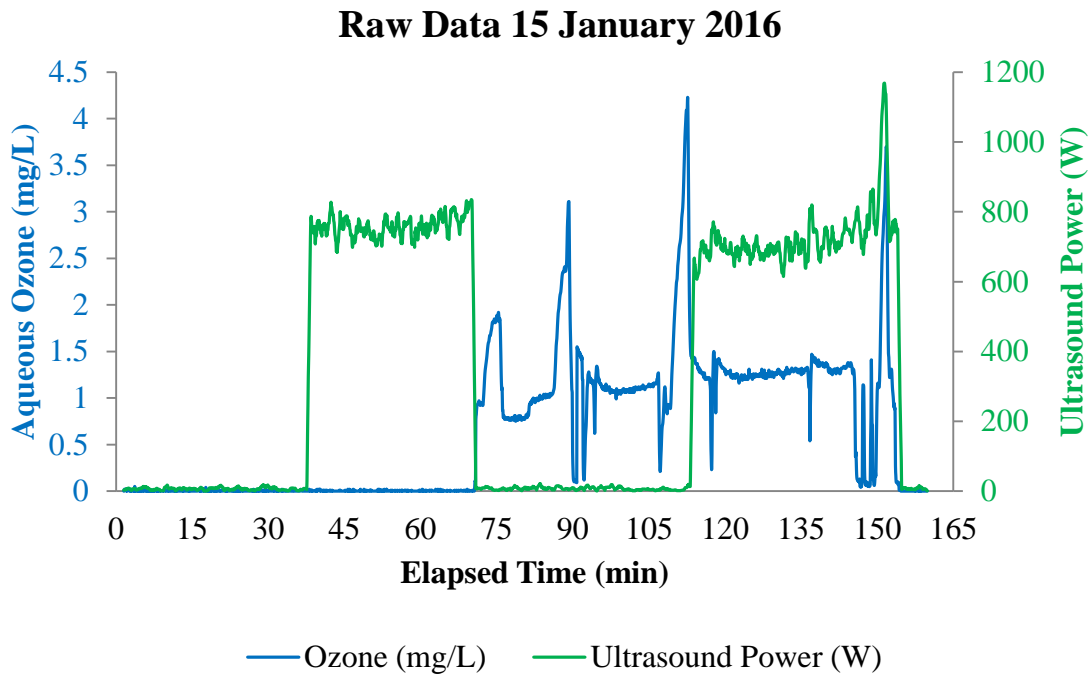


Figure F2 Ozone and Ultrasound Data from January 2016

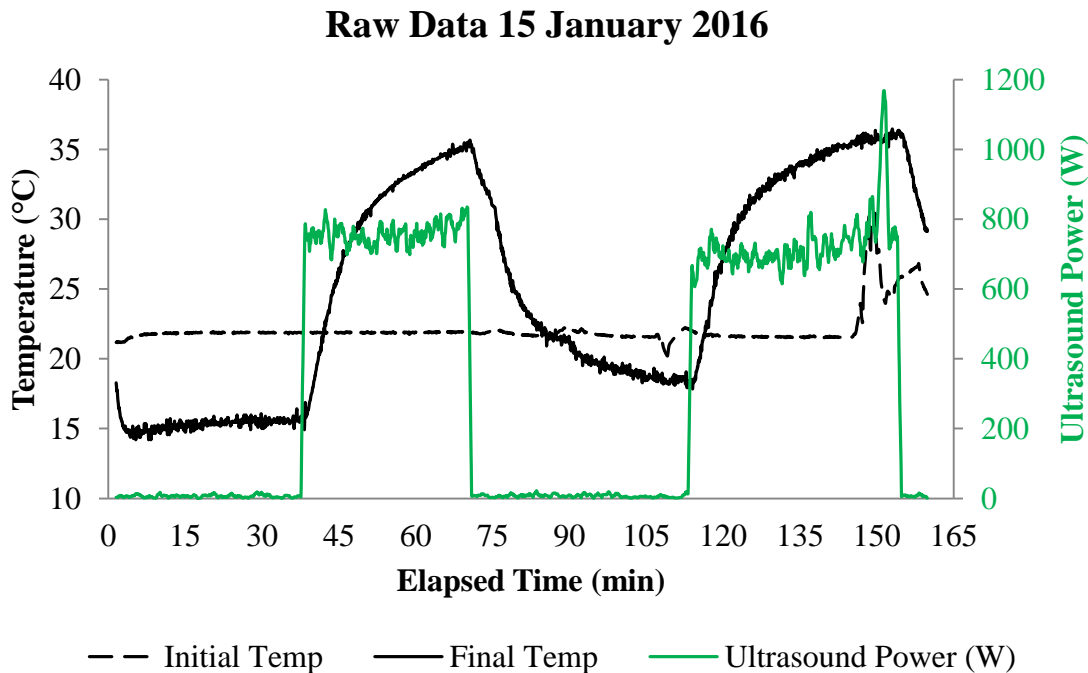


Figure F3 Temperature and Ultrasound Data from January 2016

Figures F1 through F5 show data obtained by the Arduino-based data recorder featured in Appendix A. The data presented in figures F1 to F3 was taken from different sensors during a set of experiments on January 15<sup>th</sup>, 2016, while figures F4 and F5 were from experiments on November 13<sup>th</sup>, 2015. Figure F1 shows a 1 minute timed average flow rate and ozone concentration versus time. The flow rate sensor used a small paddle wheel which rotated in response to flow. The paddle had a magnet and a Hall Effect sensor which was triggered with each rotation. Based on limitations of the Arduino and the demands of the other sensors, the flow rate sensor was set to measure the pulse width of each Hall Effect trigger event, rather than the a timed counter, as is typically used. This system still responded to flow rates, but the software configuration resulted in unacceptable noise and flow rates were measured by weight using effluent captured over 30-60 seconds in a tared beaker.

Figure F2 shows ozone concentration (blue trace) and ultrasonic power (green trace) versus time. The sample events are clear in this figure. In the initial section, both ozone and ultrasound are zero. This corresponds to flushing and the initial sample. The second section shows zero ozone and about 750 W of ultrasound. This section corresponds to the sample for ultrasound alone. In the third section, ozone is approximately 1 mg/L and ultrasound returns to zero. This corresponds to the sample for ozone alone. In the final section, ozone is approximately 1 mg/L and ultrasound is approximately 750 W. This corresponds to the sample for combined ozone/ultrasound.

Figure F3 shows ultrasonic power (green trace), influent (black dashed trace) temperature, and effluent temperatures (black solid trace) versus time. This figure shows how the temperature trace can also signal events in the experimental history. Prior to the

application of ultrasound, the effluent temperature (solid black) is less than the influent temperature (dashed black). This is a result of the reactor being submerged in a chilled water bath held, causing a decrease in temperature as the water flows through the reactor. When the ultrasonic power is applied, the effluent temperature responds in a hyperbolic curve, quickly ramping up and then tapering towards an equilibrium temperature. This equilibrium temperature is the result of the water bath chiller, which was set at 7 °C, absorbing the heat produced by the ultrasound. Once the ultrasound is turned off, the effluent temperature follows another hyperbolic curve, again dropping below the influent temperature.

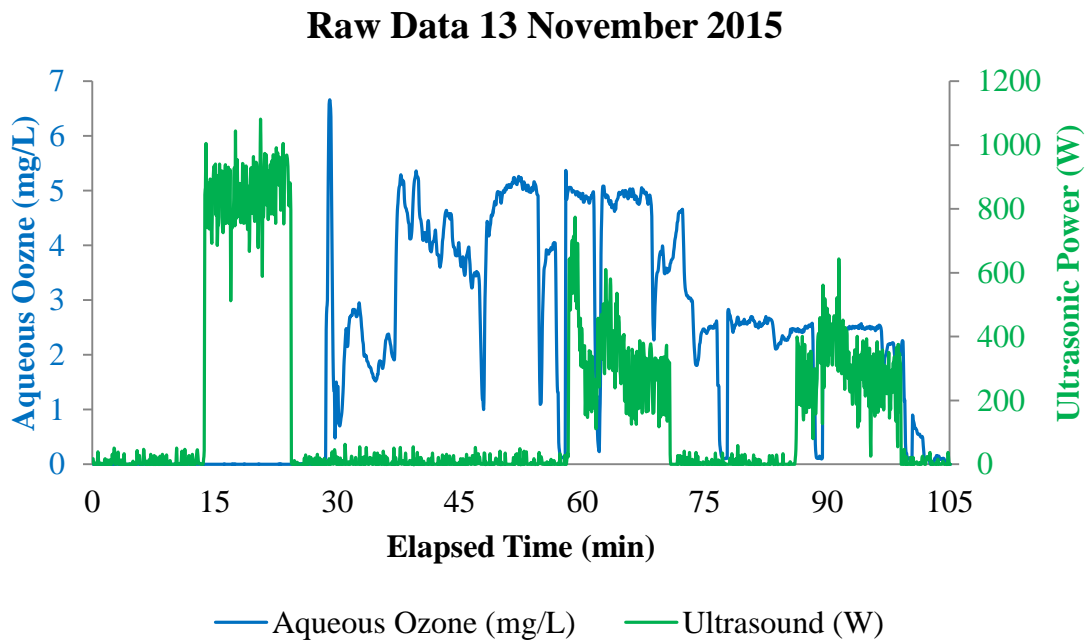


*Figure F4 Ozone and Ultrasound Data from November 2015*

### Raw Data 13 November 2015

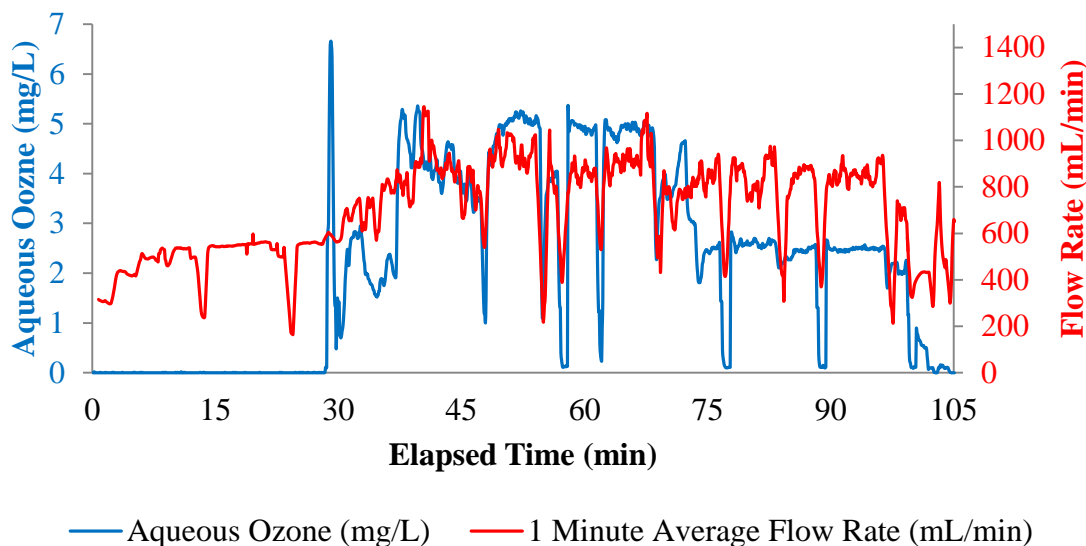


*Figure F5 Ozone and Flow Rate Data from November 2015*

Figure F4 shows ozone and ultrasound versus time from November 13<sup>th</sup>, 2015. This set of experiments shows two different ultrasonic intensities were used. The first section was full power (approximately 850 W @ 15-25 minutes), while the second and third sections were only 25% intensity (approximately 375 W @ 55-70 and 85-100 minutes). There were two aqueous ozone concentrations used as well. From approximately 50-70 minutes, 5 mg/L was used, and after ~70 minutes the ozone was reduced to 2.5 mg/L.

Figure F5 is also from the November 13<sup>th</sup> experiments and shows the flow rate and ozone data. From this figure, it is apparent that the flow rate was maintained at approximately 900 mL/min throughout the experiment set. Additionally, it should be noted that the flow rate reads as zero during sampling or sample line flushing.